УДК 538.971:577.359:57.043

THE INFLUENCE OF SURFACE ALLOYING WITH TANTALUM OR SILICON ON CYTOCOMPATIBILITY OF TITANIUM NIKELID

Andrey Leonidovich MATVEEV[1], Lyudmila Vladimirovna ARTEM'EVA[1], Stanislav Nikolaevich MEISNER[2,3], Vera Aleksandrovna MATVEEVA[1], Lyudmila Leovidovna MEISNER[2,3]

[1] Institute of Chemical Biology and Fundamental Medicine of SB RAS
630090, Novosibirsk, Lavrent'ev's ave., 8

[2] Institute of Strength Physics and Materials Science of SB RAS
634055, Tomsk, Akademicheskiy ave., 2/4
National Research Tomsk State University

[3] 634050, Tomsk, Leniv ave., 36

The influence of physicochemical properties of titanium nikelid with the surface layers modified with silicon or tantalum ions was studied on *in vitro* cultured mesenchymal stem cells of the rats' bone marrow. It was shown by the methods of laser scanning microscopy, light microscopy, MTT test that the ion-plasma modification of the titanium nikelid surface layers with silicon or tantalum ions improves the cytocompatibility of metal alloy.

Keywords: titanium nikelid, ion-plasma modification, silicon, tantalum, cytocompatibility, mesenchymal stem cell,, viability, proliferation, mitochondrial tetrazolium test.

Titanium nikelid (TiNi) alloys are known for their unique properties of shape memory, superelastic [1] that allows their usage in medicine. However, there is a potential risk of toxic, allergic and nickel carcinogenic effect on cells and tissues during the washout from alloy [4]. An effective method of biocompatibility improvement of products from nickel and titanium alloys limiting the washout of nickel from alloy and improving the integration of the implant with the surrounding tissue are the methods of ion-beam modification of the alloy surface [5].

For screening of materials after various kind of treatments the transformed cell lines and mesenchymal stem cells (MSCs) are used. The selection of MSCs is due to the fact that they are cells of normal tissues, differentiate *in vivo* into cells of various organs and the viability, morphology, adhesion, proliferation, directed differentiation of these cells can be studied *in vitro* during the evaluation of the influence of the physicochemical and morphological properties of the metal implant surface onto cells [2, 2].

Thereby, the aim of the work was to study the cytotoxicity of NiTi samples after modification of their surface with silicon or tantalum ion beams on the culture of mesenchymal stem cells of rat bone marrow *in vitro*.

MATERIAL AND METHODS

Materials

The samples of TH1 alloy were tested, which surface was successively exposed to chemical etching, mechanical polishing and electropolishing

Matveev A.L. *– junior researcher of laboratory for molecular microbiology, e-mail: vam@niboch.nsc.ru*
Artem'eva L.V. *– leading engineer of laboratory for stem cells*
Meisner S.N. *– candidate of technical sciences, junior researcher of laboratory for material sciences of shape memory allow, junior researcher of laboratory for medical material sciences*
Matveeva V.A. *– candidate of biological sciences, researcher of laboratory for stem cell*
Meisner L.L. *– doctor of physico-mathematical sciences, professor, chief researcher of laboratory for material sciences of shape memory allow, professor of the chair for metal physics, leading researcher for medical material sciences*

(TiNi samples) and ion-beam modification with monocomponent ion beams of chemically pure tantalum (samples TiNi_Ta) or silicon (samples TiNi_Si). The samples TiNi were comparison samples. For biological experiments the samples were washed with water and sterilized for 90 minutes at 180 °C.

Cells cultivation

Rat bone marrow MSCs were used for experiments. The cells were cultivated in α-MEM medium with 10 % fetal calf serum, 4 mM GlutaMax, 1 % antibiotic/antimycotics (Gibco) at 37 °C in an atmosphere of 5 % CO_2 at saturated humidity conditions. To determine the proliferative activity of the cells in the presence of samples the suspension of MSCs with the density of 5×10^3 cells/cm^2 was placed on sterile samples in wells of 12-well plate. After 14 days of cultivation the cell viability in the wells was investigated by MTT method, the samples were washed, transferred to the new wells and cultivated for another 3 days to estimate the efficiency of colonies formation. After 3 days the samples were removed for MSCs visualization on the samples surface, the cells cultivation was continued and after 11 days the viability of the cells in MTT assay, the number and size of cell colonies on the surface of the wells were determined.

Mitochondrial tetrazolium test (MTT)

The viability of cells cultivated on the surface of the wells was determined using a soluble form of formazan WST1 (Roche, USA) according to manufacturer's instructions. The estimation of MTT assay results was carried out by comparing of the optical density of the solution from control and test wells at wavelength $\lambda = 450$ nm and reference $\lambda = 655$ nm on a plate spectrophotometer BioRad 680 (BioRad, USA).

Visualization of cells on the samples surface

The membranes and nucleus of MSCs cultivated on the surface of the samples were stained with fluorescent dyes Vybrant-CM-Dil and Hoechst (Life Thechnology, USA) according to the manufacturer's instructions. The nuclei and cell membranes visualization were performed on microscope LSM 780 (C. Zeiss, Germany).

Visualization of cells on the surface of wells

MSCs cultivated on the surface of wells were stained with Giemsa (Panreac) solution according to the manufacturer's instructions, then watched in the light microscope «Stemi 2000C» (C. Zeiss, Germany); the number and size of colonies were counted with «Axiovision» software.

Processing of measurement results

The statistical analysis was performed with standard Microsoft Excel software package. The statistical significance of differences between two groups of data was estimated with nonparametric Mann-Whitney U-test at the selected significance level $p \leq 0{,}05$ for $n = 3$ in three independent experiments.

RESULTS AND DISCUSSION

The influence of surface properties of titanium nikelid samples modified with silicon or tantalum ions on MSCs

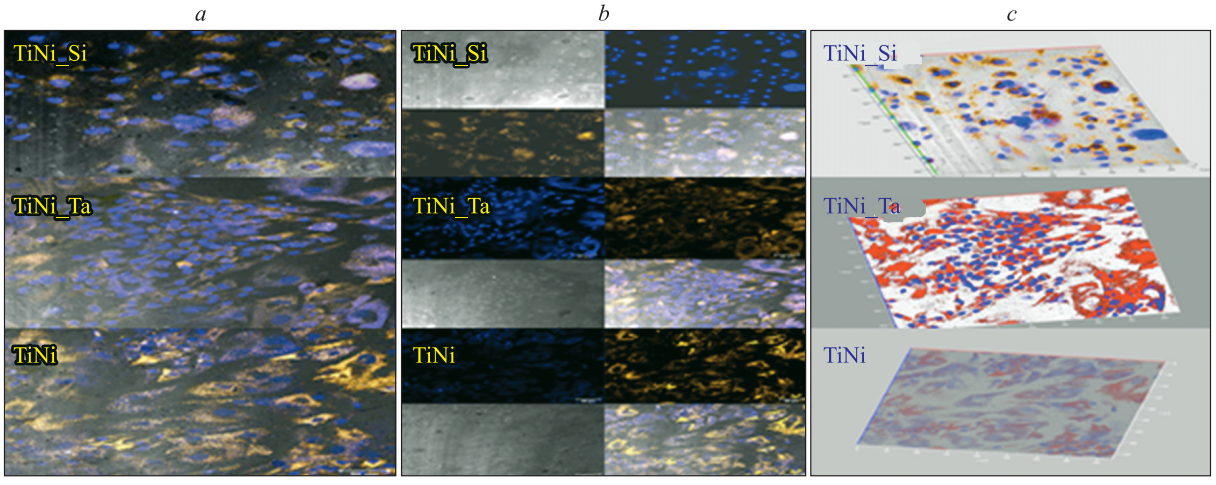

Fig. 1. *The pictures of mesenchymal stem cells of the rat bone marrow on the surface of TiNi samples before and after modification with silicon or tantalum ions; a – micrographs of cells; b – The pictures of cells structures and samples surface in the fluorescence channels; c – 3-D*

Table 1

The influence of titanium nikelid samples on proliferation of rat bone marrow MSCs

The measure unit	Sample		
	TiNi	TiNi_Ta	TiNi_Si
The average value of optical density	0,882 ± 0,231	0,926 ± 0,187	0,956 ± 0,162
The relative optical density in %	100,00 ± 7,06	104,99 ± 5,30	108,39 ± 4,62

The optical density in wells with cells after MSCs application to the surface of samples with surface-unmodified TiNi after 14 days of cultivation was taken as 100 %. For $n = 3$, the most representative data of 3 independent experiments are presented.

According to results of the laser scanning microscopy method (Fig. 1) with fluorescent dyes Vybrant-CM-Dil and Hoechst, the rat bone marrow MSCs were found on the surface of TiNi samples after 17 days of cultivation. The physico-chemical properties of the surface of samples TiNi_Si, TiNi_Ta and TiNi had no an acute toxic effect on cells cultured on their surfaces. The cells colonized the surface of all NiTi samples regardless of the surface modification options.

The influence of titanium nikelid samples modified with silicon or tantalum ions on proliferation of MSCs cultivated in the presence of the samples.

According to MTT assay results no significant differences were found in mitochondrial respiration index of cells colonized the surface of the wells after their application to the surface of NiTi samples and cultivation for 14 days (Table 1).

The samples TiNi_Si, TiNi-Ta and TiNi did not have acute toxic effects on mesenchymal stem cells. During the cells cultivation in the presence of TiNi samples, MSC on the surface of culture wells retained the proliferative activity. The effectiveness of the cells proliferation on the wells surface was not dependent of the variant of alloy surface modification.

According to the results of the light microscopy (Fig. 2), cells migrated from the surface of TiNi_Si, TiNi-Ta and TiNi samples preserved the clonal activity *in vitro*, forming the colonies and colonizing the surface of the plastic cultural wells.

According to MTT assay (Table 2), the relative amount of viable cells migrated from TiNi-Ta and TiNi_Si samples surface did not significantly differ and was nearly 2 times higher in comparison with the number of viable cells migrated from TiNi samples surface.

The average number of colonies (Table 3) formed by cells migrated from TiNi samples surface modified by silicon or tantalum ions did not significantly differ. At the same time, the average number of colonies formed by cells migrated from TiNi samples was more than 2-fold smaller than the number of colonies formed by cells from TiNi_Si and TiNi_Ta samples. The colonies formed by cells migrated from TiNi_Ta or TiNi_Si samples took in average about 50–60 % of the area of the cultural well surface. While the total area of the cells colonies migrated from TiNi samples was in average about 30 % of the area of the wells surface and was approximately 2-fold less in comparison with the cells from TiNi_Ta or TiNi_Si samples.

This cells behavior could be possibly connected with both a decrease of the total number of viable cells and/or decrease of the population of fast pro-

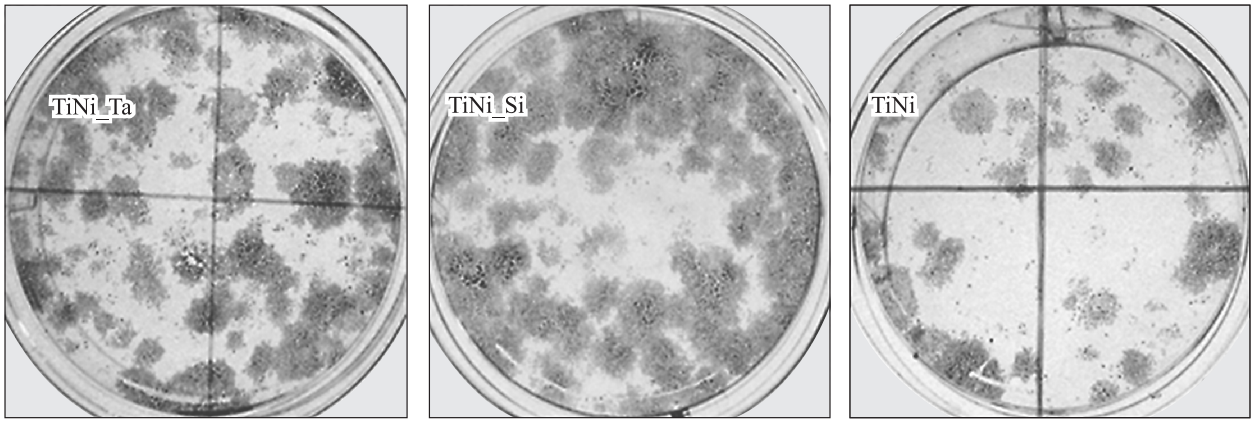

Fig. 2. *Micrograph of mesenchymal stem cells colonies formed on the surface of the plastic cultural wells by cells migrated from TiNi samples; increase × 4*

Table 2

The influence of TiNi sample surface treatment with silicon or tantalum ions on the viability of cells migrated from TiNi samples surface and formed colonies on the cultural wells surface

The measure unit	Sample		
	TiNi	TiNi_Ta	TiNi_Si
The average value of optical density	0,342 ± 0,127	0,786 ± 0,153	0,910 ± 0,134
The relative optical density in %	100,00 ± 6,04	229,82 ± 6,92	266,08 ± 7,30

The content of cells in wells migrated from the surface of unmodified TiNi samples after 14 days of cultivation was taken as 100 %. For $n = 3$, the most representative data of 3 independent experiments are presented.

Table 3

The influence of TiNi samples surface treatment with silicon or tantalum ions on the formation of cells colonies migrated from TiNi samples surface to the surface of cultural plastic wells

The measure unit	Sample		
	TiNi	TiNi_Ta	TiNi_Si
The average number of colonies *	79 ± 10	163 ± 23	154 ± 15
The relative number of colonies, % *	100,00 ± 12,66	206,33 ± 14,11	194,937 ± 9,74
The relative area occupied by colonies on the culture wells surface, % **	26,17 ± 7,54	50,88 ± 13,50	56,29 ± 9,55

* The number of colonies per well containing the cells migrated from unmodified TiNi sample surface after 14 days of cultivation was taken as 100 %.

** The area of the well was taken as 100 %. For $n = 3$, the most representative data of 3 independent experiments are presented.

liferating cells due to cell death because of chemical elements toxicity and/or TiNi samples surface morphology possibly affecting the attachment and/or differentiation of mesenchymal stem cells.

CONCLUSION

Based on the results of laser scanning microscopy, light microscopy and MTT assay the silicon or tantalum ion implantation is not toxic for mesenchymal stem cells and enhances the cytocompatibility of electropolished TiNi alloy.

ACKNOWLEDGMENTS

The authors thank the leading expert in laser scanning microscopy OOO OPTEK Barinov A.A. for the assistance provided under the work on microscope LSM 780 (C. Zeiss, Germany) in the CCU ICG SB RAS (Head of division, Bayborodin S.I., Ph.D.). The study was funded by Russian Science Foundation grant (project N15-13-0023 from 18.05.2015).

REFERENCES

1. *Es-Souni M., Fischer-Brandies H.* On the properties of two binary NiTi shape memory alloys. Effects of surface finish on the corrosion behaviour and in vitro biocompatibility // Biomaterials. 2002. 23. 2887–2894.

2. *Logan N., Brett P.* The control of mesenchymal stromal cell osteogenic differentiation through modified surfaces // Stem Cells Int. 2013. 2013. ID 361637.

3. *Pittenger M.F., Gittens R.A., Olivares-Navarrete R., McLachlan T. et al.* Differential responses of osteoblast lineage cells to nanotopographically-modified, microroughened titanium-aluminum-vanadium alloy surfaces // Biomaterials. 2012. 33. 8986–8994.

4. *Wever D.J., Veldhuizen A.G., Sanders M.M. et al.* Cytotoxic, allergic and genotoxic activity of a nickel-titanium alloy // Biomaterials. 1997. 18. 1115–1120.

5. *Zhao T., Li Y., Zhao X. et al*. Ni ion release, osteoblast-material interactions, and hemocompatibility of hafnium-implanted NiTi alloy // J. Biomed. Mater. Res. B. Appl. Biomater. 2012. 100. 646–659.

ВЛИЯНИЕ ПОВЕРХНОСТНОГО ЛЕГИРОВАНИЯ С ИСПОЛЬЗОВАНИЕМ ТАНТАЛА ИЛИ КРЕМНИЯ НА ЦИТОСОВМЕСТИМОСТЬ НИКЕЛИДА ТИТАНА

Андрей Леонидович МАТВЕЕВ[1], Людмила Владимировна АРТЕМЬЕВА[1], Станислав Николаевич МЕЙСНЕР[2,3], Вера Александровна МАТВЕЕВА[1], Людмила Леонидовна МЕЙСНЕР[2,3]

[1] ФГБУН Институт химической биологии и фундаментальной медицины СО РАН 630090, г. Новосибирск, пр. Лаврентьева, 8

[2] ФГБУН Институт физики прочности и материаловедения СО РАН 634055, г. Томск, пр. Академический, 2/4

[3] Национальный исследовательский Томский государственный университет 634050, г. Томск, пр. Ленина, 36

Влияние физико-химических свойств никелида титана с приповерхностными слоями, модифицированными ионами кремния или тантала, изучали на культивируемых in vitro мезенхимальных стволовых клетках костного мозга крысы. Методами лазерной сканирующей микроскопии, световой микроскопии, теста МТТ показано, что ионно-плазменная модификация приповерхностных слоев никелида титана ионами кремния или тантала улучшает цитосовместимость металического сплава.

Ключевые слова: никелид титана, ионно-плазменная модификация, кремний, тантал, цитосовместимость.

Матвеев А.Л. *– м.н.с. лаборатории молекулярной микробиологии, e-mail: vam@niboch.nsc.ru*
Артемьева Л.В. *– ведущий инженер лаборатории стволовой клетки*
Матвеева В.А. *– к.б.н., научный сотрудник лаборатории стволовой клетки*
Мейснер Л.Л. *– д.ф.-м.н., профессор, главный научный сотрудник лаборатории материаловедения сплавов с памятью формы; профессор кафедры физики металлов, ведущий научный сотрудник лаборатории медицинского материаловедения*
Мейснер С.Н. *– к.т.н., м.н.с. лаборатории материаловедения сплавов с памятью формы; м.н.с. лаборатории медицинского материаловедения*

УДК 612.821

CLUSTERING OF INDEPENDENT COMPONENTS OF EEG IN DETERMINING INDIVIDUAL CHARACTERISTICS OF REACTIONS RELATED TO A MORAL CHOICE

Andrey Viktorovich BOCHAROV[1,2], Sergey Aleksandrovich BOGOMAZ[3], Aleksandr Nikolaevich SAVOSTYANOV[1,2,3], Gennady Georgievich KNYAZEV[1], Anna Vasil'evna BUDAKOVA[3], Mikhail Sergeevich ZALESHIN[3], Tat'yana Nikolaevna ASTAKHOVA[2]

[1] Scientific Research Institute of Physiology and Basic Medicine
630117, Novosibirsk, Timakov's str., 4

[2] National Research Novosibirsk State University
630090, Novosibirsk, Pirogov's str., 2

[3] National Research Tomsk State University
634050, Tomsk, Lenin ave., 36

Moral judgment can be defined as the evaluation of actions with respect to norms and values established in a society. In the modern world, morality is considered as the social capital, which determines a level of society well-being. Participants were showed 24 moral dilemma and 24 control task vignettes represented artist-sketched cartoons of control and dilemma scenarios. For all participants and every experimental condition, the model of localization equivalent dipoles electroencephalogram (EEG) components was made. Individual localization of EEG electrodes was matched with the model of head electrodes localization used for determining the equivalent dipoles. Event-related spectral perturbations were calculated to estimate induced responses via the EEGLAB toolbox. The dataset was prepared for clustering by the original PCA method. The correction for multiple comparisons was made by the False Discovery Rate method. To determine the correlations cortical sources of EEG activity with Social Intellect, sLORETA was applied to the data. Differences between moral dilemmas and control tasks without moral choice were found in delta, theta, alpha and beta diapasons in clusters localized in temporal and frontal lobe. Social intellect positively correlated with difference between the test interval and the baseline during making moral dilemma choice in theta in the left middle temporal gyrus and beta in the left middle frontal gyrus.

Keywords: moral dilemmas, EEG, independent components, source localization, social intellect.

The study of factors that determine social cognition and behavior in humans is an actual problem of modern neuroscience. Social cognition is defined as that mental activity through which we can understand and know the social world [22]. The phenomenon of social cognition concerns morality. Moral judgment can be defined as the evaluation of actions with respect to norms and values established in a society (such as not stealing or being an honest citizen). When judging a behavior as morally good or

Bocharov A.V *– candidate of biological sciences, senior researcher of laboratory for differential psychophysiology, senior researcher of NSU, e-mail: bocharov@physiol.ru*
Bogomaz S.A. *– doctor of psychological sciences, professor of laboratory for psychophysiology of the chair for psychology*
Savostyanov A.N. *– candidate of biological sciences, doctor of medical sciences, leading researcher of laboratory for differential psychophysiology, professor of NSU, senior researcher of NSU, e-mail: a.n.savostyanov@physiol.ru*
Knyazev G.G. *– doctor of biological sciences, head of laboratory for differential psychophysiology, e-mail: knyazev@physiol.ru*
Budakova A.V. *– junior researcher of laboratory for cognitive researches and psycho genetics, postgraduate student of the chair for psychology*
Zaleshin M.S. *– lecturer of the chair for psychology*
Astakhova T.N. *– undergraduate student*

bad, people refer to their internal representations of these norms and values (i.e. emotionally laden internal moral orientations or principles) [27]. In the modern world, morality is considered as the social capital, which determines a level of society well-being.

It is difficult to model real moral situation in laboratory conditions, that is why we used an experimental paradigm was taken from Harrison and collegues (2008) study [10]. Nowadays studies of brain activity during moral choice were made by methods of positron emission tomography (PET) and functional magnetic resonance imaging (fMRI) [3, 7, 8, 27].

These techniques allow to evaluate the level of metabolic activity in different parts of brain using as an indicator consumption of glucose or blood oxygenation. fMRI and PET techniques are extremely important and indispensable for the accurate spatial localization of the processes in brain, but have a number of limitations. Nature of the relationship of the metabolic processes and related neurophysiological activity is not always clear. It is not clear as measured these techniques metabolic changes in neurons reflect the processes taking place in them [4]. Due to the low temporal resolution these techniques, which is limited by the speed of blood flow, they do not give opportunities to investigate the dynamics of the processes of brain on a millisecond time scale. Known to date that brain functioning based on the principle of association structures of brain in functional systems required for the performing current function and inhibition of conflict processes are not required at the current moment. According to modern views, the role of integration in functional systems perform oscillations of bioelectrical activity of brain [2, 25]. The aim of the study was to investigate individual differences in oscillatory dynamics of structures of brain related to decision making during moral dilemma.

MATERIAL AND METHODS

Subjects

The sample included 26 participants (11 men and 15 women; age range from 17 to 22 years). Sample consisted of healthy, right-handed volunteers with normal or corrected-to-normal vision who received a sum equivalent to about $7 (U.S.) for participation. All subject filled out Social Intellect questionnaire [21, 30]. All applicable subject protection guidelines and regulations were followed in conducting the research in accordance with the Declaration of Helsinki. All participants gave informed consent to the study. The study has been approved by the Tomsk State University ethical committee.

Instruments and Procedure

The subjects sat in a soundproof and dimly illuminated room. Participants were showed 24 moral dilemma and 24 control task vignettes represented artist-sketched cartoons of control and dilemma scenarios accompanied by text descriptions. A preliminary instruction was presented at the screen: «You will be presented with different scenarios depicting the hero in a choice situation; please imagine yourself on the hero's place and make the choice pressing 1 for 'yes' and 2 for 'no'». In each trial, the participant viewed a cartoon and accompanying description of a hero in a control or dilemma situation. In the last lines of the description, the participant was asked to press the spacebar when he/she had understood the situation. Next, a prompt appeared that asked: «If you were at hero's place, would you buy the piece of furniture» or «would you push the fat man». For nonmoral dilemmas, response 'yes' implied the choice of an 'active' option (e.g., to purchase something). For moral dilemmas, response 'yes' implied the choice of a utilitarian option (e.g., to sacrifice a fat man in order to save five people).

Moral and control tasks were delivered randomly, and the interstimulus interval randomly varied between 4 and 6 s. For the EEG analysis, 1500 milliseconds from –2000 to –500 before the vignette presentation (vignette presentation was taken as 0) was chosen as the baseline and three seconds before the button-press were chosen as the test interval.

EEG Recording and Analysis

EEG record was collected using 128-channels according to the extended International 10–5 system with sampling rate 1000 Hz. The signals were amplified using BrainVision actiCHamp hardware. In contrast to PET and fMRI, EEG is a two-dimensional time-frequency distribution electric signal. EEG registered from scalp is a bioelectric activity of different areas of whole brain. Independent component analysis was applied to separate this activity. Artifact components connected with eye movements, muscle movements, pulse, artifact local activity of channels were removed. For all participants and every experimental condition, the model of localization equivalent dipoles EEG components was made with DIPFIT function. Individual localization of EEG electrodes was matched with a model of localization of electrodes of head, which was used for determining the equivalent dipoles. The analysis included only those EEG components whose models of equivalent dipole have residual dispersion of cortical maps that is no more than 15 % as compared with the most appropriate projection model of equivalent dipole of the head electrodes. Event-re-

lated spectral perturbations (ERSP) were calculated to estimate induced responses using timef function of EEGLAB toolbox (http://www.sccn.ucsd.edu/eeglab/). The ERSP [20] shows mean log event-locked deviations from baseline-mean power at each frequency. Method of ERSP calculation realized in EEGLAB toolbox is described in Delorme and Makeig [5].

Time-frequency decomposition of the signal produced by wavelet transform version of Morlet, overlap time window started from 3-cycle wavelet, the number of cycles increased linearly when reached a half of the number of cycles with the high frequency. This method allowed to obtain better frequency resolution at higher frequencies than the conventional wavelet which used a constant amount of cycles [5]. The dataset was prepared for clustering by the original PCA method [5]. The time-frequency differences between groups and conditions had been estimated with using nonparametric permutation statistic method. The correction for multiple comparisons was made by the False Discovery Rate method [11]. This method is used instead of the Bonferroni correction if variables are highly correlated with each other [32]. Reliable effects were effects which had significance level $p < 0.05$ after False Discovery Rate method was applied.

To determine the correlations cortical sources of EEG activity with Social Intellect, sLORETA [26] was applied to the data. The sLORETA is a linearly distributed solution that is based on standardized values of the current density estimates given by the minimum norm solution. The sLORETA uses a three-shell spherical head model registered to the digitized Talairach and Tournoux (1988) atlas. The solution space is restricted to cortical gray matter and parahippocampal areas. The sLORETA yields images of standardized current source density of 6430 voxels at 5 mm spatial resolution. Statistical analysis of sources of induced oscillations in sLORETA was performed using regression of current source density estimates on Social Intellect scores. Statistical significance was assessed using a randomization test which corrects for multiple comparisons [26]. For this study, the significance level was set to $p < 0.05$.

RESULTS

We got 12 clusters and six of them had significant differences. The first cluster showed significant effect during three seconds before the button-press when making a choice. Delta synchronization was observed for moral condition, in contrast for control condition delta desynchronization was obtained. Central dipole was located in the right superior temporal gyrus (Brodmann area (BA) 22). The second cluster showed significant effect during last 2 sec but one before making a choice. Delta desynchronization was more pronounced for control task. Theta synchronization was more pronounced for moral condition. Central dipole had symmetric localization to first cluster in the left temporal gyrus (BA 22). The third cluster had localization in the right middle temporal gyrus (BA 37). Alpha desynchronization was more pronounced for moral condition during three seconds before making a choice. The fourth cluster localized near rectal gyrus in the right frontal lobe (BA 11). Delta synchronization and alpha desynchronization was more pronounced for moral condition during three seconds before making a choice. Central dipole of the fifth cluster localized near the middle frontal gyrus (BA 6). Delta synchronization was more pronounced for moral condition during last 2 sec but one before making a choice. Beta desynchronization was less pronounced for moral condition during 3 sec before making a choice. The sixth cluster included the posterior cingulate cortex (PCC). Delta and theta synchronization was obtained for moral condition, delta and theta desynchronization was obtained for control task during last 2 sec but one before making a choice. Beta desynchronization was less pronounced for moral condition during last 2 sec but one before making a choice.

sLoreta regression analysis of Social intellect on the difference between the test interval and the baseline during making moral dilemma choice yielded positive correlations for theta and beta2 diapasons (Figure).

For theta, the strongest effect is observed in the left middle temporal gyrus, BA 21 (MNI coordinates $X = –60$, $Y = 0$, $Z = –15$) $r = 0.587$, Extreme $p = 0.007$, for beta2 in the middle frontal gyrus, BA 10 (MNI coordinates $X = –25$, $Y = 50$, $Z = 0$) $r = 0.602$, Extreme $p = 0.007$ (Figure).

DISSCUSSION

The long-standing rationalist tradition in moral psychology emphasizes the role of reason in moral judgment. A more recent trend places increased emphasis on emotion [8]. Results of this study show that oscillatory responses in the moral condition differ significantly from ones in the nonmoral condition. The difference is most strong in delta and theta bands, which are known to be involved in emotion processing, and in brain regions associated with emotion. Many studies show that delta and theta bands are associated with emotional and motivational processes [13, 15]. Cluster 1 and cluster 3 are found in the right (‘emotional’) hemisphere and

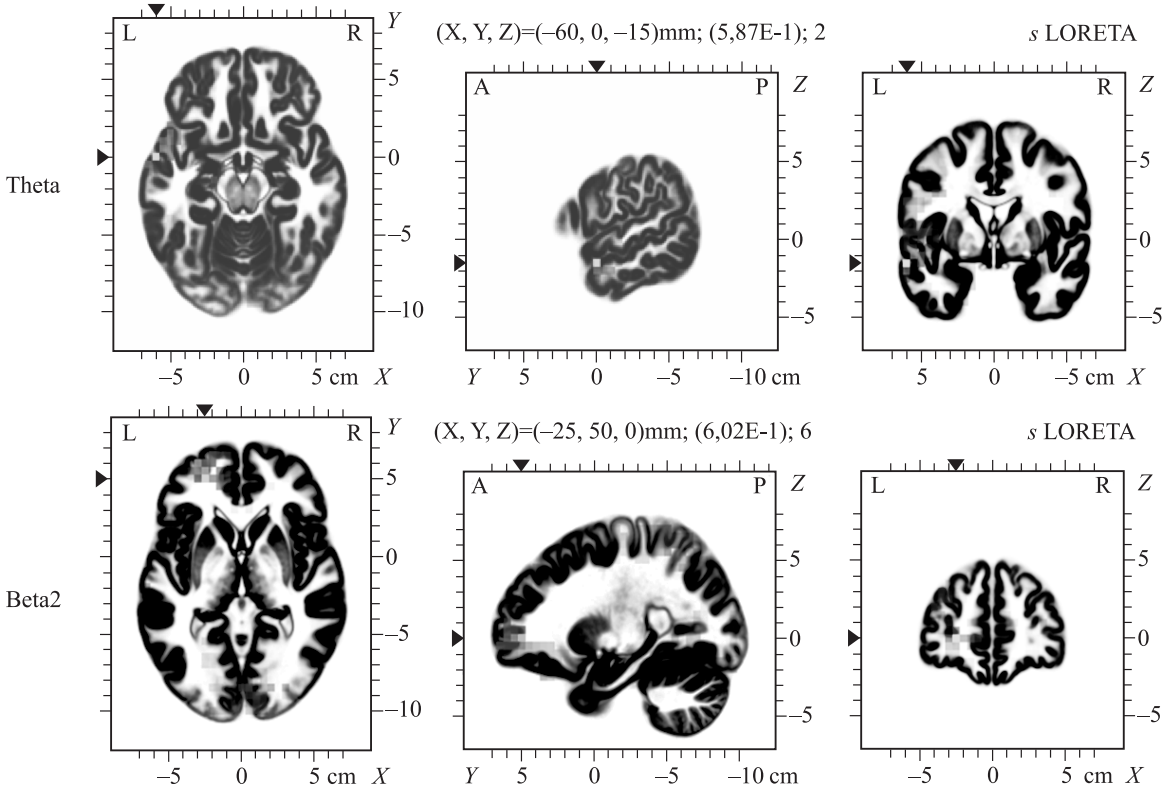

Fig. *sLORETA results of a regression analysis of Social intellect scores on the difference between the test interval and the baseline during making moral dilemma choice. The strongest effect is observed in the left middle temporal gyrus, brodmann area 21, X = –60, Y = 0, Z = –15 for theta, for beta2 in the middle frontal gyrus, brodmann area 10, X = –25, Y = 50, Z = 0*

in its temporal lobe, which undoubtedly is involved in emotion processing [19]. Our results are in line with Greene and colleagues [7, 8] and Knyazev and colleagues findings [17]. Also higher Social intellect was associated with larger theta synchronization (difference between the test interval and the baseline) in temporal lobe in moral condition. This implies that higher sensitivity to moral issues and it might be essential for understanding the implications choices in moral dilemmas.

Other significant effects were also found in the alpha frequency band (cluster 3 and 4), but they were in the opposite direction. In this case, the difference between the test interval and the baseline was lower (i.e., more negative) in moral than in nonmoral condition. It could be suggested that is related with difficulty of making a decision in moral condition because the degree of desynchronization of alpha correlates with the complexity of the task and reflects the amount resources included in the task [6].

Another clusters (4 and 6) localized in the orbitofrontal prefrontal cortex (OFB) and the PCC. The OFC represents the affective value of primary reinforcers and it learns to associate other stimuli with these to produce representations of the expected reward value, thus, playing a key role in emotion [28]. The OFC activation during moral decision-making has been shown [1, 31]. In this study subject were asked to report his/her prospective behavior in respective situation. This aspect of the task might be responsible for the involvement of the cortical midline structure such as the PCC, because this structure is included in self-processing and social cognition [16, 24].

In our study, higher Social intellect was associated with larger difference between the test interval and the baseline during moral condition in theta in the left temporal lobe and beta2 diapason in the left OFC. The right OFC was found to be activated during passive viewing of moral stimuli compared with nonmoral stimuli [9], while the activation of the left OFC has been related to processing of emotionally salient statements with moral value [23]. In recent years, we have witnessed a surge of interest to the question of so-called cross-frequency coupling of brain oscillations. It has been repeatedly shown that low-frequency oscillations of mostly delta and theta bands are able to affect high-frequency oscillations of beta and gamma bands [12]. This coupling is functionally relevant [33] and some evidence shows that it might increase in emotionally engaging states [14, 18, 29].

In this study, more effects were found in low delta, theta and were located in emotional areas

such as temporal cortex, while more higher frequency (alpha and beta) effects were located in frontal cortex which related with decision making. Overall, the pattern of results is in line with the idea that in moral condition, the subject appears to be in a state of higher emotional engagement and perceives this situation as more self-related than in nonmoral conditions.

ACKNOWLEDGMENTS

Contribution to this work of A.V. Bocharov, A.N. Savostyanov and G.G. Knyazev was supported by the Russian Science Foundation (RSCF) under Grant № 14-15-00202; contribution to this research of S.A. Bogomaz, A.V. Budakova and M.S. Zaleshin was carried out on the instructions N 2014/233 to perform public works in the framework of the basic tasks of the State Ministry of Education of Russia, the project «Psychotechnological ensuring the process of the development of cognitive and communicative potential».

REFERENCES

1. *Bechara A., Damasio H., Damasio A.R.* Emotion, decision making and the orbitofrontal cortex // Cereb. Cortex. 2000. 10. 295–307.

2. *Buzsaki G., Draguhn A.* Neuronal oscillations in cortical networks // Science. 2004. 304. 1926–1929.

3. *Ciaramelli E., Muccioli M., Ladavas E., di Pellegrino G.* Selective deficit in personal moral judgment following damage to ventromedial prefrontal cortex // Soc. Cogn. Affect. Neurosci. 2007. 2. 84–92.

4. *Debener S., Ullsperger M., Siegel M., Engel A.K.* Single-trial EEG-fMRI reveals the dynamics of cognitive function // Trends Cogn. Sci. 2006. 10. 558–563.

5. *Delorme A., Makeig S.* EEGLAB: an open source toolbox for analysis of single-trial EEG dynamics including independent component analysis // J. Neurosci. Methods. 2004. 134. 9–21.

6. *Gevins A., Smith M.E., McEvoy L., Yu D.* High-resolution EEG mapping of cortical activation related to working memory: effects of task difficulty, type of processing, and practice // Cereb. Cortex. 1997. 7. 374–385.

7. *Greene J.D., Nystrom L.E., Engell A.D. et al.* The neural bases of cognitive conflict and control in moral judgment // Neuron. 2004. 44. 389–400.

8. *Greene J.D., Sommerville R.B., Nystrom L.E. et al.* An fMRI investigation of emotional engagement in moral judgment // Science. 2001. 293. 2105–2108.

9. *Harenski C.L., Hamann S.* Neural correlates of regulating negative emotions related to moral violations // Neuroimage. 2006. 30. 313–324.

10. *Harrison B.J., Pujol J., Lopez-Sola M. et al.* Consistency and functional specialization in the default mode brain network // Proc. Natl. Acad. Sci. USA. 2008. 105. 9781–9786.

11. *Holm S.* A simple sequentially rejective multiple test procedure // Scand. J. Stat. 1979. 6. 65–70.

12. *Jensen O., Colgin L.L.* Cross-frequency coupling between neuronal oscillations // Trends Cogn. Sci. 2007. 11. 267–269.

13. *Knyazev G.G.* Motivation, emotion, and their inhibitory control mirrored in brain oscillations // Neurosci. Biobehav. Rev. 2007. 31. 377–395.

14. *Knyazev G.G.* Cross-frequency coupling of brain oscillations: an impact of state anxiety // Int. J. Psychophysiol. 2011. 80. 236–245.

15. *Knyazev G.G.* EEG delta oscillations as a correlate of basic homeostatic and motivational processes // Neurosci. Biobehav. Rev. 2012. 36. 677–695.

16. *Knyazev G.G.* EEG correlates of self-referential processing // Front. Hum. Neurosci. 2013. 7. 264.

17. *Knyazev G. G., Savostyanov A. N., Bocharov A. V. et al.* Oscillatory correlates of moral decision-making: Effect of personality // Soc. Neurosci. 2015. 1–16.

18. *Knyazev G. G., Slobodskoj-Plusnin J. Y.* Behavioural approach system as a moderator of emotional arousal elicited by reward and punishment cues // Pers. Indiv. Differ. 2007. 42. 49–59.

19. *Lang P.J.* Emotion and motivation: Toward consensus definitions and a common research purpose // Emot. Rev. 2010. 2. 229–233.

20. *Makeig S.* Auditory event-related dynamics of the EEG spectrum and effects of exposure to tones // Electroencephalogr. Clin. Neurophysiol. 1993. 86. 283–293.

21. *Matsuta V.V., Bogomaz S.A., Sudneva O.Y.* The role of intellectual and personal factors in achieving high performance in the use in mathematics // Sibirskiy zhurnal psikhologii = Siberian Journal of Psychology. 2014. 52. 52–66. [In Russian].

22. *Mitchell J.P.* Mentalizing and Marr: an information processing approach to the study of social cognition // Brain Res. 2006. 1079. 66–75.

23. *Moll J., de Oliveira-Souza R., Eslinger P.J. et al.* The neural correlates of moral sensitivity: a functional magnetic resonance imaging investigation of basic and moral emotions // J. Neurosci. 2002. 22. 2730–2736.

24. *Northoff G., Bermpohl F.* Cortical midline structures and the self // Trends Cogn. Sci. 2004. 8. 102–107.

25. *Nunez P.L.* Toward a quantitative description of large-scale neocortical dynamic function and EEG // Behav. Brain Sci. 2000. 23. 371–398.

26. *Pascual-Marqui R.D.* Standardized low-resolution brain electromagnetic tomography (sLORETA): technical details // Methods Find. Exp. Clin. Pharmacol. 2002. 24 (Suppl. D). 5–12.

27. *Prehn K., Wartenburger I., Meriau K. et al.* Individual differences in moral judgment competence influence neural correlates of socio-normative judgments // Soc. Cogn. Affect. Neurosci. 2008. 3. 33–46.

28. Rolls E.T., Grabenhorst F. The orbitofrontal cortex and beyond: from affect to decision-making // Prog. Neurobiol. 2008. 86. 216–244.

29. *Schutter D.J., van Honk J.* Decoupling of midfrontal delta-beta oscillations after testosterone administration // Int. J. Psychophysiol. 2004. 53. 71–73.

30. *Shcherbakov S.V.* Diagnostics of student social intellect // Actualnye voprosy fiziologii, psihofiziologii i psikhologii = Actual questions of physiology, psychophysiology and psychology. Ufa: RIC Bash-IFC, 2010. 122–126. [In Russian].

31. *Shenhav A., Greene J.D.* Moral judgments recruit domain-general valuation mechanisms to integrate representations of probability and magnitude // Neuron. 2010. 67. 667–677.

32. *Tanji K., Suzuki K., Delorme A. et al.* High-frequency g-band activity in the basal temporal cortex during picture-naming and lexical-decision tasks // J. Neurosci. 2005. 25. 3287–3293.

33. *Tort A.B., Kramer M.A., Thorn C. et al.* Dynamic cross-frequency couplings of local field potential oscillations in rat striatum and hippocampus during performance of a T-maze task // Proc. Natl. Acad. Sci. USA. 2008. 105. 20517–20522.

КЛАСТЕРИЗАЦИЯ НЕЗАВИСИМЫХ КОМПОНЕНТОВ ЭЭГ ДЛЯ ОПРЕДЕЛЕНИЯ ИНДИВИДУАЛЬНЫХ ОСОБЕННОСТЕЙ РЕАКЦИЙ, СВЯЗАННЫХ С МОРАЛЬНЫМ ВЫБОРОМ

Андрей Викторович БОЧАРОВ[1,2], Сергей Александрович БОГОМАЗ[3], Александр Николаевич САВОСТЬЯНОВ[1,2,3], Геннадий Георгиевич КНЯЗЕВ[1], Анна Васильевна БУДАКОВА[3], Михаил Сергеевич ЗАЛЕШИН[3], Татьяна Николаевна АСТАХОВА[2]

[1] НИИ физиологии и фундаментальной медицины
630117, г. Новосибирск, ул. Тимакова, д. 4

[2] Новосибирский государственный университет
630090, г. Новосибирск, ул. Пирогова, д. 2

[3] Томский государственный университет
634050, г. Томск, ул. Ленина, д. 36

Моральное суждение может быть определено как оценка действий в соответствии с нормами и ценностями, установленными в обществе. В современном мире мораль рассматривается как социальный капитал, который определяет степень жизнеспособности общества. Участникам были показаны нарисованные художником изображения 24 моральных дилемм и 24 контрольных заданий, с описанием представленных на них ситуаций. Для всех участников и для каждого экспериментального условия сделана модель локализации эквивалентных диполей компонентов электроэнцефалограммы (ЭЭГ). Индивидуальная локализация ЭЭГ электродов была совмещена с моделью локализации электродов головы, которую использовали для определения эквивалентных диполей. Связанные с событием спектральные пертурбации рассчитаны для оценки индуцированных ответов с помощью программы EEGLAB. Кластеризация произведена методом главных компонент, поправка на множественные сравнения – методом контроля ложных эффектов. Для определения корреляции активности ЭЭГ участков мозга с социальным интеллектом использован анализ sLORETA. Различия между моральными дилеммами и контрольными заданиями без морального выбора найдены в дельта-, тета-, альфа- и бета-диапазонах в кластерах, локализованных в височной и лобной долях. Социальный интеллект положительно коррелировал с разницей между тестовым интервалом и фоном во время принятия выбора в ситуации моральной дилеммы в тета-диапазоне в левой средней височной извилине и в бета-диапазоне в левой средней лобной извилине.

Ключевые слова: моральные дилеммы; ЭЭГ; независимые компоненты; локализация источников; социальный интеллект.

Бочаров А.В. *– к.б.н., старший научный сотрудник лаборатории дифференциальной психофизиологии», старший научный сотрудник, e-mail: bocharov@physiol.ru*
Богомаз С.А. *– доктор психологических наук, проф. зав. лабораторией психофизиологии факультета психологии*
Савостьянов А.Н. *– к.б.н., д.ф.н., ведущий научный сотрудник лаборатории дифференциальной психофизиологии; профессор, старший научный сотрудник, e-mail: a.n.savostyanov@physiol.ru*
Князев Г.Г. *– д.б.н, зав. лабораторией дифференциальной психофизиологии, e-mail: knyazev@physiol.ru*
Будакова А.В. *– м.н.с. лаборатории когнитивных исследований и психогенетики, аспирант факультета психологии*
Залешин М.С. *– преподаватель факультета психологии*
Астахова Т.Н. *– студент бакалавриата.*

УДК 537.523/527; 533.9.004.14

DEVELOPMENT OF MICROBICIDE EQUIPMENT AND RESEARCH IN PATHOGEN INACTIVATION BY COLD ARGON PLASMA

Aleksandr Petrovich SEMENOV[1], Bair Batoevich BALDANOV[1], Cyrempil Valerevich RANZHUROV[1], Erdem Olegovich NIKOLAEV[1], Sayana Vladimirovna GOMBOEVA[2]

[1] *Institute of Physical Material Science of SB RAS*
670047, Ulan-Ude, Sakhyanova's str., 6

[2] *East Siberia State University of Technology and Management*
670013, Ulan-Ude, Klyuchevskaya str., 40B, bldg. 1

The high bactericidal effect of cold argon plasma generated by low-current spark discharge plasma jets at atmospheric pressure has been revealed. It has been found that the direct contact of low-current spark plasma jets helps perform effective inactivation of bacteria.

Keywords: argon plasma, microorganisms, low-current spark, plasma jets, plasma inactivation, atmospheric pressure glow discharge.

Currently, an increasing focus rests on the researches in the gas-discharge process properties that determine their sterilizing and disinfecting abilities for protection of industrial materials, equipment and electronics from biodegradation and microbiologically induced corrosion [5, 12]. Plasma treatment of living tissues has the desired therapeutic sterilization, wound healing, hemostasis, and skin disease curing effects [4, 6]. This area has become of particular importance in recent years due to the increasing demand for new low-temperature efficient, reliable and high-performance sterilization and decontamination technologies.

A special place among plasma methods is occupied by the study of discharges generating the low-temperature (cold) non-equilibrium plasma at atmospheric pressure [1, 7–11, 13]. As the sources of low-temperature non-equilibrium atmospheric pressure plasma various types of gas discharges are viewed, among which the atmospheric pressure creeping, corona, barrier and pulsed discharges should be noted. Despite the broad range of works [9, 10], dedicated to the study of different discharge characteristics, and proven high efficiency of discharges in biomedical laboratory applications, the atmospheric pressure cold plasma antiseptic treatment has not been practiced widely. This is due, firstly, to the fact that the cold plasma sources currently represent technically sophisticated equipment with low economic efficiency. Secondly, for the treatment of bioobjects, living tissues of animals and humans atmospheric pressure discharges are used at high voltage of 10–40 kV, which requires a high security level. Therefore, the choice of discharge parameters under which a safe and non-destructive effect is observed, is one of the main physical problems of plasma medicine.

The aim of this paper is the study of bactericidal properties of low-temperature non-equilibrium argon plasma generated by high-voltage low-current discharges.

EXPERIMENTAL PROCEDURE

To generate low-temperature (cold) argon plasma two types of non-equilibrium plasma generators have been developed on the basis of low-current high-voltage discharges.

Semyonov A.P. *– doctor of technical sciences, professor, director, e-mail: semenov@ipms.bscnet.ru*
Baldanov B.B. *– candidate of technical sciences, senior researcher of laboratory for plasma power processes and technologies, mail: baibat@mail.ru*
Ranzhurov Ts.V. *– junior researcher of laboratory for plasma power processes and technologies*
Nikolaev E.O. *– postgraduate student*
Gomboeva S.V. *– candidate of biological sciences, docent of the chair for biotechnology*

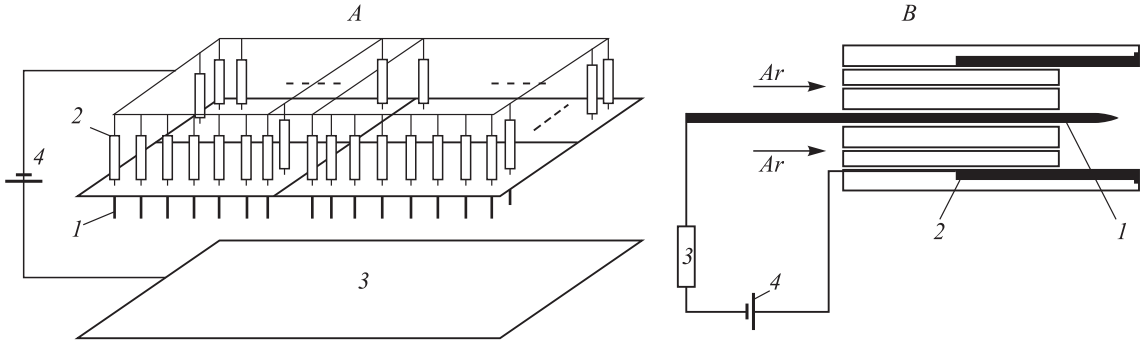

Fig. 1. *Schematic representation of electrode structure. A: 1 – cathode; 3 – ballast resistances; 3 – anode; 4 – power supply; B: 1 – point cathode; 2 – cylindrical anode; 3 – ballast resistance; 4 – power supply*

An approach is based on the use of atmospheric pressure glow discharge. A discharge is generated in a special electrode construction (Fig. 1A) with a multipoint divided cathode and flat metal anode [2]. The stability of discharge in the transition of negative corona to discharge gap spark breakdown is achieved via low gas flow through the discharge gap.

The other approach (Fig. 1B) is based on the use of atmospheric pressure low-current spark discharge plasma jets formed in an argon flux [11]. Cathode 1 (point with a radius of curvature $r = 30$ μm) is placed in a cylindrical nonconducting housing $R =$ $= 2$ cm. Anode 2 is a metal cylinder 1.5 cm long and 2 cm in diameter. To stabilize the discharge the point was loaded with adjustable ballast resistance 3 $R_b > 1$MΩ. The housing has through holes for argon flux supply arranged so that cold argon plasma formed by a system of low-current spark plasma jets is spread via the argon flux in a direction away from the interelectrode spacing, like a flame. Argon consumption $G = 5 \times 10^{-5}$ kg/s was measured using a flowmeter PM – A – 0,16 GUZ.

The study involved the *Escherichia coli* M17 strains in the natural association and vegetative form. The microbial treatment efficiency in an atmospheric pressure glow gas-discharge chamber was evaluated using metal wafers (test strips). The decontamination completeness was determined by placing the test strips in an indicator medium.

To evaluate the sensitivity of microorganisms to cold argon plasma generated by low-current spark discharge plasma jets a method was used based on measuring the diameter of the microbial environment affected areas. Therefore, a medium was inoculated with test microorganisms. 100 μ*l* of working suspension were added into a Petri dish with nutrient medium Agar GRM or RPA, and carefully rubbed with a spreader. The plates with medium inoculated with microorganisms were placed in a discharge chamber under plasma jets. Plasma-treated media were incubated in an incubator within 24 hours at 37 °C, and then the diameters of formed affected areas were measured.

RESULTS AND DISCUSSION

The bactericidal efficacy of diffuse argon plasma formed in the repetitively pulsed negative corona and atmospheric pressure glow discharge mode (Fig. 1A) was tested in the bacteria of natural association of microorganisms. Test strips with microorganisms were placed on a flat anode, the plasma treatment time of wafers ranged from 2 to 5 min.

The study of bacterial survival in the repetitively-pulsed negative corona plasma showed that after treating the wafers for 2 and 5 min (discharge current $I = 250$ μA) bacteria perish totally (tubes 1, 2 Fig. 2). In the atmospheric pressure glow discharge mode (discharge current $I = 700$ μA, treatment time $t = 2$ and 5 min), where the discharge is homogeneous self-sustained discharges covering the

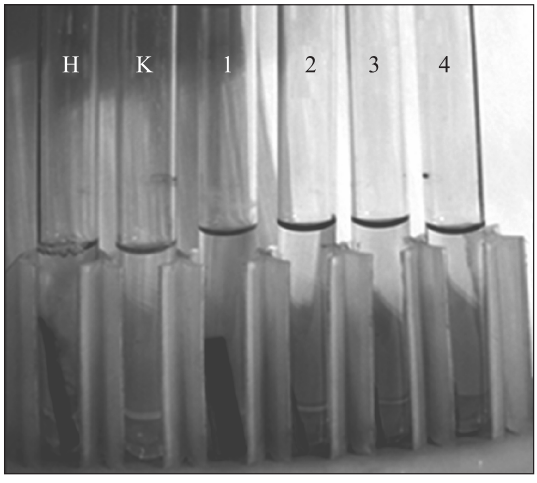

Fig. 2. *Results of bactericidal effect of cold argon plasma. N – untreated wafer; K – control; 1, 2 – pulsed corona treatment, t = 5 and 2 min, respectively; 3, 4 – atmospheric pressure glow discharge treatment, t = 5 and 2 min, respectively*

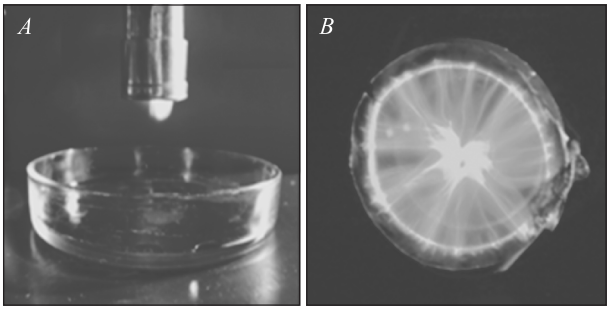

Fig. 3. *Cold argon plasma generator based on low-current spark plasma jets: A – microorganism inactivation in a Petri dish, B – side view of discharge*

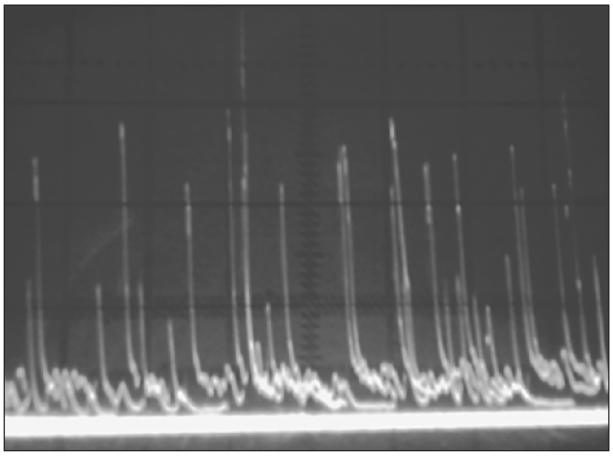

Fig. 4. *Low-voltage spark discharge current pulses. Interelectrode spacing d = 1,25 cm, amperage I = 500 μA, $R_б$ = 21 MΩ; [I] = 100 μA/div, [t] = = 0.2 ms/div*

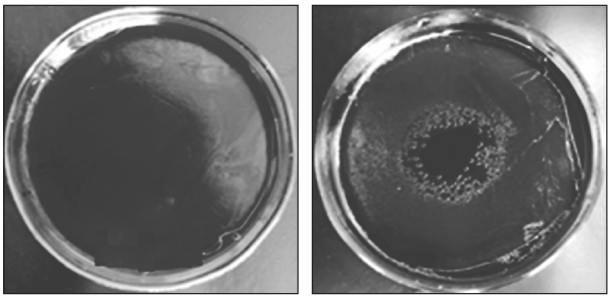

Fig. 5. *Cold argon plasma influence on the vegetative form of the Escherichia coli strain. Exposure time = 30 s. Test medium on the left*

entire interelectrode spacing, bacteria perish totally as well (tubes 3, 4 Fig. 2). Microbial growth after cold argon plasma treatment is absent for the seven days of test strips cultivation in the liquid medium.

The bactericidal properties of low-current spark discharge plasma jets were studied for their effects on the vegetative form of the *Escherichia coli* strains. Fig. 3 shows a picture of low-current spark discharge cold argon plasma jet generator. Low-current spark discharge plasma jetting time ranged from 5 to 60 s. Distance *h* from the plasma source to the surface of microorganism growth ranged from 0.5 to 3 cm.

The current-voltage characteristic of discharge is dropping, and the nature of current flow in the plasma channel is an established mode of periodical current pulses (Fig. 4). In the formation of discharge current pulse two specific areas can be marked out: the initial narrow peak with amplitude $I_m \sim 280$ μA (area 1) and the second longer area ($T \sim 70$ μs) that essentially determines the period *T* of discharge current pulse. The low-current spark plasma jetting influence on microorganisms is registered as round transparent areas, which are the microorganism growth inactivation zones (Fig. 5).

The bactericidal properties of low-temperature non-equilibrium argon plasma generated by plasma jets have been studied for the influence on the *Escherichia coli* strain vegetative forms compared to antibiotics of various inhibitory effect.

It has been shown that the effect of different antibiotics on the *Escherichia coli* bacteria for 18 h results in different affected areas depending on the toxicity of antibiotic. In the case of plasma inactivation, a 30-second treatment causes complete destruction of bacteria on an area ($S = 2$ cm^2) substantially equal to that referring to the most toxic antibiotics.

The data obtained show high sensitivity of microorganisms to cold argon plasma treatment (Fig. 6) [11]. Minimal plasma inactivation time of the *E. coli* cells is 5 s at 0.5 cm from the side section of electrode structure. At a distance increased to 3 cm the number of survived microorganism macrocolonies is considerably greater. Increasing the plasma treatment time up to 40 s at a distance of 3 cm causes a considerable reduction (by 74 %) of survived microorganisms (Fig. 7, *2*). The determination of argon plasma inactivation ability carried out by counting the colonies shows that after a minute of treatment only a few grown-up microorganism macrocolonies survive.

It should be noted that the inactivation area is not restricted by the anode diameter, within which low-current spark plasma jet are formed. As it can be seen in Fig. 8, increasing the time of microbial environment treatment with low-current spark plasma jets allows efficient inactivation of a much larger area. At that, the diameter of inactivation area in direct contact of plasma jets with the surface of microbial environment increases more than in remote exposure. The results obtained correspond with the results shown in [3]. So the diameter of inactivation area increases with increasing time of treatment of

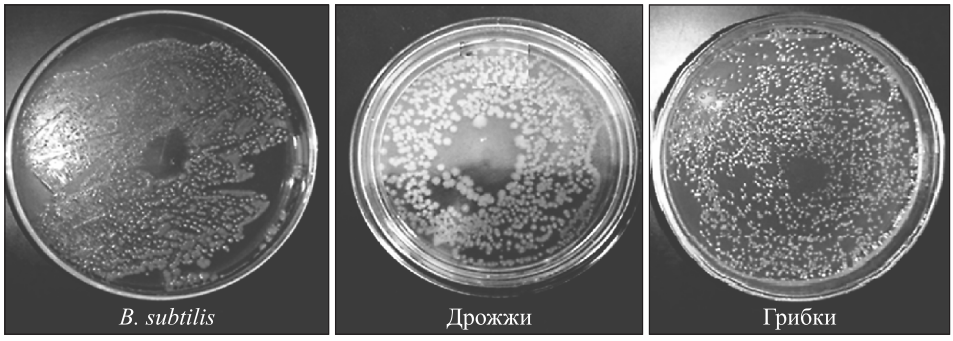

Fig. 6. *Bacterial growth inactivation areas Treatment time t = 4 min, distance h = 0.5 cm*

Pseudomonas aeruginosa bacteria on solid agar with atmospheric pressure cold plasma jets (99.5 % helium and 0.5 % oxygen).

CONCLUSION

The high bactericidal efficiency of low-current high-voltage discharge cold argon plasma is displayed. The study of bacterial survival in the repetitively-pulsed negative corona plasma and atmospheric pressure glow discharge showed that after treating the wafers for 2 min in each mode the microorganisms are totally inactivated. It has been found, that increasing the time of microbial environment treatment with low-current spark plasma jets allows efficient inactivation of a much larger area than the anode electrode cross section.

This work was supported by the Russian Foundation for Basic Research (project no. 15-44-04209 r_sibir_a).

REFERENCES

1. *Arkhipenko V.I., Kirillov A.A., Safronau Y.A., Simonchik L.V.* DC atmospheric pressure glow microdischarges in the current range from microamps up to amperes // Eur. Phys. J. D. 2010. 60. (3). 455.

2. *Baldanov B.B., Ranzhurov T.V.* On the increase in the limiting current of an atmospheric-pressure glow discharge in an argon flow // Technical Physics. Rus. J. Appl. Phys. 2014. 59. (4). 621–623.

3. *Cabiscol E., Tamarit J., Ros J.* Oxidative stress in bacteria and protein damage by reactive oxygen species // Int. Microbiol. 2000. 3. (1). 3–8.

4. *Fridman G., Vasilets V., Gutsol A. et al.* Applied plasma medicine // Plasma Processes Polym. 2008. 5. (6). 503–533.

5. *Heinlin J., Isbary G., Stolz W. et al.* Plasma applications in medicine with a special focus on dermatology // J. Eur. Acad. Dermatol. Venereol. 2011. 25. (1). 1–11.

6. *Kalghatgi S.U., Fridman G., Cooper M. et al.* Mechanism of blood coagulation by nonthermal atmospheric pressure dielectric barrier discharge plasma // IEEE Trans. Plasma Sci. 2007. 35. (5, Pt. 2). 1559–1566.

7. *Kirillov A.A., Pavlova A.V., Safronov E.A. et al.* DC atmospheric pressure glow discharge plasma jet application for *Staphylococcus aureus* inactivation // Prikladnaya fizika = Applied physics. 2013. (5). 52–55. [In Russian].

8. *Lu X., Laroussi M., Puech V.* On atmospheric-pressure non-equilibrium plasma jets and plasma bullets // Plasma Sources Sci. Technol. 2012. 21. (3). ID 034005.

9. *Morent R., Geyter N.D.* Inactivation of bacteria by non-thermal plasmas, biomedical engineering – frontiers and challenges // InTech. Ed. R. Fazel. 2011. DOI: 10.5772/18610.

10. *Plasma* for Bio-Decontamination, Medicine and Food Security // NATO Science for Peace and Security Series A: Chemistry and Biology. Eds. Z. Machala, K. Hensel, Y. Akishev. Dordrecht: Springer, 2012. 479 p.

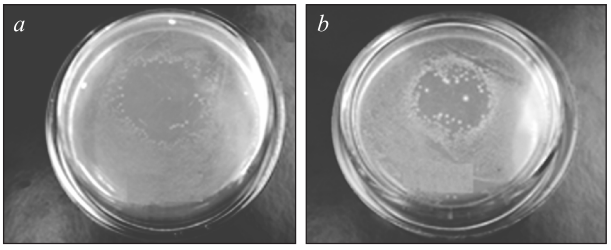

Fig. 7. *E. coli growth inactivation areas in relation to h: a – h = 0.5 cm, t = 30 s; b – h = 3 cm, t = 40 s*

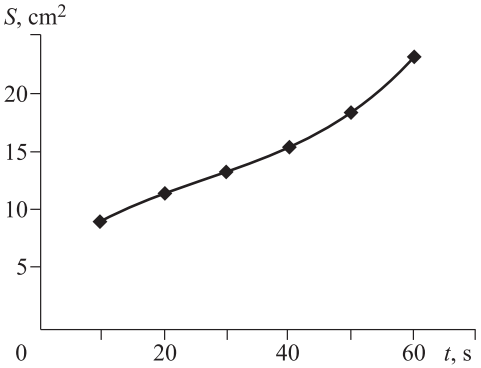

Fig. 8. *The relationship of inactivation area and exposure time, h = 0.5 cm*

11. *Semenov A.P., Baldanov B.B., Ranzhurov T.V., et. al.* Inactivation of microorganisms in cold argon plasma at the atmospheric pressure // Uspekhi prikladnoi fiziki = Advances in Applied Physics. 2014. 2. (3). 229–233 [In Russian].

12. *Sohbatzadeh F., Hosseinzadeh Colagar A., Mirzanejhad S., Mahmodi S. E. coli, P. aeruginosa*, and *B. cereus* bacteria sterilization using afterglow of non-thermal plasma at atmospheric pressure // Appl. Biochem. Biotechnol. 2010. 160. (7). 1978–1984.

13. *Weltmannm K.D., Kindell E., Woedtke T. et al.* Atmospheric-pressure plasma sources: Prospective tools for plasma medicine // Pure Appl. Chem. 2010. 82. (6). 1223.

РАЗРАБОТКА БАКТЕРИЦИДНОГО ОБОРУДОВАНИЯ И ИССЛЕДОВАНИЕ ПРОЦЕССОВ ОБЕЗЗАРАЖИВАНИЯ ПАТОГЕННЫХ МИКРООРГАНИЗМОВ ХОЛОДНОЙ АРГОНОВОЙ ПЛАЗМОЙ

Александр Петрович СЕМЕНОВ[1], Баир Батоевич БАЛДАНОВ[1], Цыремпил Валерьевич РАНЖУРОВ[1], Эрдэм Олегович НИКОЛАЕВ[1], Саяна Владимировна ГОМБОЕВА[2]

[1] Институт физического материаловедения СО РАН
670047, г. Улан-Удэ, ул. Сахъяновой, д. 6

[2] Восточно-Сибирский государственный университет технологий и управления
670013, г.Улан-Удэ, ул. Ключевская, д. 40В, стр. 1

Показана высокая эффективность бактерицидного действия холодной аргоновой плазмы генерируемой плазменными струями слаботочного искрового разряда при атмосферном давлении. Установлено, что прямой контакт плазменных струй слаботочной искры позволяет проводить эффективную инактивацию бактерий микроорганизмов.

Ключевые слова: аргоновая плазма, микроорганизмы, слаботочная искра, плазменные струи, плазменная инактивация, тлеющий разряд атмосферного давления.

Семенов А.П. *– д.т.н., профессор, директор, e-mail: semenov@ipms.bscnet.ru*
Балданов Б.Б. *– к.т.н., с.н.с. лаборатории плазменно-энергетических процессов и технологий, e-mail: baibat@mail.ru*
Ранжуров Ц.В. *– м.н.с. лаборатории плазменно-энергетических процессов и технологий*
Николаев Э.О. *– аспирант*
Гомбоева С.В. *– к.б.н., доцент, кафедра биотехнологии*

УДК 519.6; 519.8; 51-7; 616

MATHEMATICAL MODELLING OF THE TUMOR MARKERS NETWORK

Olga Falaleevna VOROPAEVA[1], Yurij Ivanovich SHOKIN[1], Lev Moiseevich NEPOMNYASHCHIKH[2], Svetlana Robertovna SENCHUKOVA[2]

[1] *Institute of Computational Technologies* of SB RAS
630090, Novosibirsk, Lavrent'ev ave., 6

[2] *Institute of Molecular Pathology and Pathomorphology*
630117, Novosibirsk, Timakov str., 2

This paper is devoted to a numerical analysis of the solutions of the equations system describing the dynamics of the concentration of p53 and Mdm2 proteins in their interaction. The detailed study of the solutions was made when the mathematical model parameters deviated from the basal values. The system states in which the threat of the cell uncontrolled apoptotic death accelerated the organisms aging processes or the excessive suppression of p53-induced apoptosis increased the tumors risk have been investigated within the numerical experiments. The mechanism of the system managing under stress conditions has been studied.

Keywords: tumor markers; p53-Mdm2-network; time delay equations; numerical modelling.

The p53 protein (tumor necrosis factor), involved in many life and death processes, including the formation of tumors and aging, is expressed in all the cells of the organism. Mdm2 protein is considered to be the key negative p53 regulator. The mechanism for the functioning of the p53–Mdm2 system is very complex, so the answers to questions that are important in clinical practice are often found to be mutually exclusive. In particular, it has been found that the imbalance in the p53 and Mdm2 interaction can be the cause for serious pathological changes in organs and tissues. Thus, the consequences of the faults, caused by the excessive production of p53 and the superactivation of the p53-dependent apoptosis, are often serious diseases such as neurodegeneration (Alzheimer's, Parkinson's, multiple sclerosis, epilepsy), osteoporosis, growth arrest, and premature aging of the internal organs. At the same time, the loss of the p53 protein's function is found in approximately 50 % of human malignant tumors. Therefore, the inactivation of p53 is also conventionally seen as an undesired and dangerous event, while in antitumor therapy the restoration of an active p53, including as a result of the artificial break of the interaction between p53 and Mdm2, is thought of as one of the key elements ensuring the normal passage of signals stopping growth stop and/or apoptosis in cancer cells. It is necessary also to take into account that p53-dependent apoptosis induced in normal tissues can become the cause for serious side effects, thus limiting the efficiency of the antitumor therapy. In this connection, the artificial inhibition of p53 in certain tumors, especially in those without functional p53, can have a protective effect, supporting the normal functioning of the tissue in the process of regeneration.

Thus, the investigation of the function of the p53 and Mdm2 proteins and of the mechanism of their interaction is paramount both for developing new approaches to cancer treatment and determining the prevention strategy for many diseases, including measures to slow the aging processes. Many aspects of this problem have so far remained little known and thus are now at the center of attention among researchers [1–3, 5] (these works contain detailed bibliographies). Under these conditions, the mathematical simulation of the interaction of the p53 and Mdm2 proteins is one of the effective and accessible methods of analysis of the development of the p53–Mdm2 system and of exits from peak situations.

Voropaeva O.F. *– doctor of physical mathematical sciences, senior researcher, e-mail: vorop@ict.nsc.ru*
Shokin Yu.I. *– academician of RAS, director*
Nepomnyaschchikh L.M. *– corresponding member of RAS, director*
Senchukova S.R. *– doctor of medical sciences, leading researcher*

MATHEMATICAL MODELS AND NUMERICAL TECHNOLOGIES

We consider in this work two interrelated mathematical models of the p53–Mdm2 network. The first (basic) model of the proteins concentrations dynamics includes the system of two nonlinear equations with the retarded argument [4] (see also [5, 6]):

$$dy_1/dt = s - a f(y_1(t), y_2(t), k_f) - by_1(t), \quad (1)$$
$$dy_2/dt = c_1 g(y_1(t-\tau), y_2(t-\tau), f, k_g) - c_2 y_2(t), \quad (2)$$

where the interaction of the proteins is determined by nonlinear functions f and g. Here y_1 and y_2 are concentrations of the p53 and Mdm2, respectively; s is the rate of p53 production; a is the rate of p53 degradation by means of ubiquitination; b is the rate of p53 spontaneous degradation; c_1 is the rate of Mdm2 production, including that by its interaction with p53; c_2 is the rate of Mdm2 protein degradation; k_f is the constant of the p53–Mdm2 complex dissociation constant; and k_g is the p53 protein and Mdm2 gene dissociation constant (a more detailed biological description of the parameters is found in [4]). The initial data for system (1)–(2) are given as the functions of «history» $\varphi_k(\theta)$: $y_k(\theta) = \varphi_k(\theta)$, $\theta \in [-\tau, 0]$, $k = 1,2$. The basal values of the parameters [4] are coordinated with the data from different laboratory studies. The time delay parameter τ determines in the Mdm2 reaction to a change in the state of the p53 protein (more detail see in [1–3]).

The second model describes hypothetical stages of process and uses the simplest ODE system of sufficiently higher dimension. We show numerically that in the passage to the limit in which the second model has infinitely many stages we obtain model based equation with retarded argument.

The characteristic features of the present model are nonlinearity, time delay, and the possible rigidity of the system and bifurcation of solution under some combinations of parameters. A sufficiently detailed description of the algorithm's testing procedure is present in [6]. The solution of problem (1)–(2) is based on the widely known method of steps. From considerations of the simplicity of the numerical implementation, in all the calculations the delay value τ was taken as a multiple of the step of the computational grid (on condition that the grid step is a rather small value, this limitation avoids having a substantial effect on the character of the solution). At each time step, the problem's solution is found by numerical methods with the attraction of iterations by nonlinearity. For the sake of convenience of the numerical implementation, the system of equations (1)–(2) can be nondimensionalized with the use of the delay value τ as the time scale. This procedure is equivalent to compressing the time axis τ times. In doing this, one should take into account that in transition to a fairly high τ the accumulation of errors caused apparently by rigidity is typical for the system in the transformed form. To exclude undesirable computational effects, the choice of the numerical method and controlling the influence of the grid step on the solution have been given the closest attention. The methodical calculations of system (1)–(2) were performed on a sequence of grids with a resolution ranging from 1 to 10000 points per second. Based on these tests, in the numerical experiments, the grid with a resolution of not more than 100 points per second was acknowledged as optimal.

Based on the results of the test calculations and comparison of a sufficiently high number of known numerical methods for the solution of problem, the explicit Adams method with iterations by nonlinearity was used. In doing this, the defect of the multistep methods related to the need for a special approach to the simulation of the solution at the first points, in case of equations with delay, is compensated by calculations on sufficiently high time intervals.

In [4–6] it is shown that under basal conditions system (1)–(2) has stationary solution only as immovable limit point $(y_1^{basal}, y_2^{basal})$ at any values of delay, including $\tau = 0$, and in the disturbance of the basal state points the Andronov-Hopf bifurcations can be observed. All the approximated coordinates of the immovable points are with sufficiently high precision in keeping with the analytical stationary solution [4].

Attention was given to the question of the influence of the choice of the initial data on the solution of the problem (1)–(2). A series of numerical experiments were made, in which either zero values or constant stationary basal values of concentrations y_1 and y_2 with the introduction of stress perturbations in them ranging from 10 % to 4 orders (both decreasing and increasing, alternately for each component of solution y_1 and y_2 or simultaneously for both) were used as the «history» functions $\varphi_k(\theta)$. In doing this, the time delay parameter was also varied, and the values of the parameters of the system s, a, b, c_1, c_2, k_f and k_g were taken as basal. In addition, the numerical experiments, in which as the initial data on interval $[-\tau, 0]$ the periodic solutions of this problem were used, and hereinafter at all the calculations were made under basal conditions. The calculations show that in all $t > 0$ the considered stress situations caused by the change of the initial level of protein concentration, the character of the solution of system (1)–(2) does not practically change independent of the value of the delay and the initial concentration levels: $y_1(t)$ and $y_2(t)$ returns to the earlier found limit y_1^{basal}, y_2^{basal}; i.e., the solution of the problem has a stable focus. In using as the initial data the

stationary values of concentrations y_1^{basal} and y_2^{basal} with the introduction in them of stress perturbations ranging from 20 % to 2 orders (towards a decrease and increase, alternately for each component and simultaneously for both, the delay parameters also varied) similar results were obtained.

In addition, numerical experiments were performed, in which different numerical methods were used for the reproduction of a periodic solution (delay τ reached the bifurcation value τ^{bif}). The stationary solution is the focus corresponding to a rather small $\tau < \tau^{bif}$ was used as the initial data. The comparison of the solutions obtained with the use of the predictor--corrector method with iterations by nonlinearity and the Runge-Kutta method of order 4 has shown that both numerical methods yield rather close solutions, and the introduction of the iterations allows a considerable increase in the accuracy of the calculation by using of the predictor-corrector method. The solutions obtained by use of the Adams method of order 4 and those by the Runge-Kutta method of the same order were found to be the closest. In the calculations, where the obtained periodic solutions were used as the initial data, a comparison of the methods yields similar results. Then the real order of accuracy of the method on such solutions ranges from 1 to 2.83.

DEPENDENCE OF THE SOLUTIONS ON THE CHANGE OF THE MODEL PARAMETERS

We have carried out a numerical study of the reaction of system to stresses in the form of a deviation of the parameters from the basal values. The numerical experiments were made in a sufficiently large interval of the delay values ranging from a few seconds to many hours, which is characteristic of the given biological system (see, for example, [1–3]).

Fig. 1 provides some data on the obtained solutions that correspond to the alternatively deviation of the parameters from the basal values. It has been found that the basic part of the solutions are immovable points (focuses). Moreover, the calculated coordinates of the immovable points in the phase plane agree, with a rather high degree of accuracy, with the analytical stationary solution of problem [4], i.e., with the solution of system (1)–(2) at the corresponding values s, a, b, c_1, c_2, k_f and k_g. In the course of these numerical experiments, it has been found that the dissociation constants k_f and k_g become bifurcation parameters, providing the start of periodic oscillations in the p53–Mdm2 network, at the time of delay typical of real conditions.

The analysis of the numerical data shows that within the accepted model, in the deviation of one of the parameters of the system from the basal value, there may appear the following typical situations: *a*) a considerable accumulation of p53 at a rather low level of its inhibitor Mdm2; *b*) a considerable accumulation of Mdm2 at a lower level of p53; *c*) rapid attenuation of the oscillations of protein concentrations with the achievement of constant stationary values close to the basal ones; and *d*) periodic oscillations. The calculations show that time delay is one of the key parameters affecting the state of the p53–Mdm2 system. The attenuating solutions are typical for most of the arising situations, which testifies to the stable reaction of the system to the deviation of the parameters from the normal values. We note that although the periodic oscillations of the concentrations in the p53–Mdm2 system, with regard to some characteristic constant values, which are often rather close to the basal values; however, the maximum values of the concentrations achieved in this may become critical for the normal functioning of the system and the organism as a whole.

Note that the obtained data do not conflict with the known ideas on the phenomenon being simulated and allow the conclusion on the adequacy of the considered mathematical model of the p53–Mdm2 grid. In particular, the presence of oscillations of the p53 and Mdm2 concentrations taking place almost in the counterphase are in correspondence with the known data of the laboratory experiments (see, for example, [1–3] and references in [5]).

RESTORATION OF THE P53−MDM2 FEEDBACK

The analysis of the data presented in the previous section shows that a considerable part of the

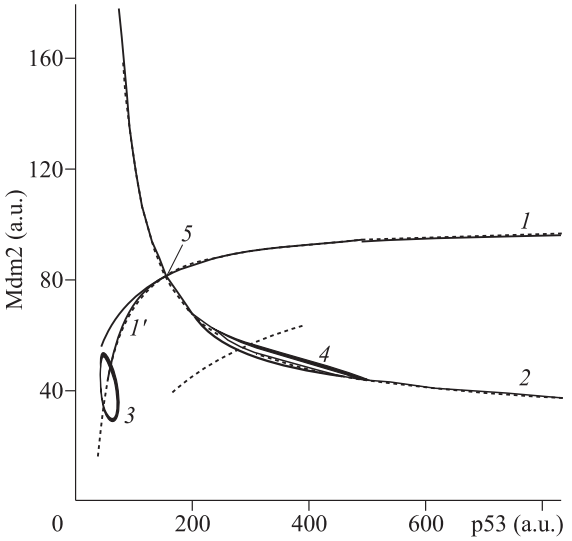

Fig. 1. *The stationary solutions of the problem with the alternating variation of parameters: solid lines – immovable points (1, 1′, 2) and the limit cycles (3, 4) of the numerical solutions; dashed lines – analytical stationary solutions [2]; 5 – the stationary solution under basal conditions*

solutions of system (1)–(2) (including solutions with an immovable point) correspond to situations in which the disturbance of the feedback of proteins p53 and Mdm2 is characteristic. The negative and positive consequences of these disturbances in real medico-biological processes have been discussed above. In this section we will consider in greater detail the most characteristic of the noted situations and present the results of the numerical experiments aimed at finding solutions that are more favorable for the live organism–understood as the achievement of the basal values of the levels of concentration of proteins.

The methodology of the numerical experiments in this section is as follows: we will try to compensated disturbances of the feedback in the p53–Mdm2 network that are the result of a stress for some parameter of system (1)–(2) by the repeated stress for one of the remaining parameters. This methodological technique is fairly well known in medico-biological studies as suppression, i.e., total or partial suppression of the first (direct) mutation by the second (suppressor) mutation, which may lead to the partial or total restoration of the normal phenotype. Our purpose is to find that parameter of the mathematical model, whose change will lead to the restoration of the basal state of the p53–Mdm2 system. As the considered states of the system are characterized by solutions with an immovable limit point, for which earlier stability relative to the initial data was found, for simplicity of the calculation procedure, all the numerical experiments are made at zero initial conditions. All the calculations have been continued down to the delay values of 30 000 s and the duration of the observed processes were not less than 120 days.

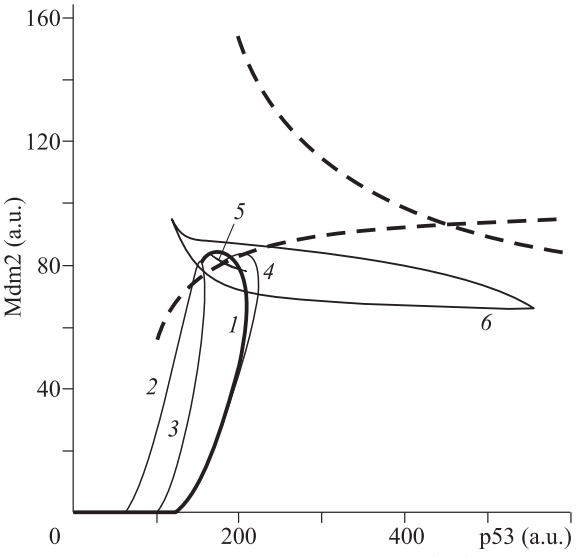

Fig. 2. *Problem solutions at $a = 0.5a^{basal}$: 1 – basal state, 2 – $s = 0.5s^{basal}$, 3 – $b = 35b^{basal}$, 4 – $k_f = 0.13k_f^{basal}$ (τ = 120 s); 5 – $k_f = 0.15k_f^{basal}$ (fragment of the curve in the vicinity of immovable point), 6 – limit cycle at $k_f = 0.13k_f^{basal}$ and τ = 25000 s; the dashed lines show the analytical stationary solution [5] at basal values of s, b, k_f, k_g, c_1, c_2*

Excessive p53 level

Within the considered mathematical model, the excessive p53 level threatening excessive p53 dependent apoptosis can be caused by the lack of balance in the rate of p53 generation and Mdm2 degradation, as well as by disturbances in the mechanism of the interaction of proteins, which is regulated through the introduction of the dissociation constants.

For example, a considerable excess in the value of the rate of p53 generation (parameter s) leading to threatening increase of the p53 level can be, according to the calculations, compensated by increasing the rate of the p53 degradation through ubiquination a or of the rate of p53 spontaneous decomposition b, as well as by a lower dissociation constant of the p53–Mdm2 complex k_f. When a decreases more than by one order, the situation is complicated with a further decrease of p53, and the upper boundary of the Mdm2 concentration is very close to the basal value. The increase of k_f also leads to the further growth of p53. The decrease of b will not change the situation. The decline of the rate of the p53 degradation through ubiquitination (parameter a), which is able to cause the disturbance of the feedback of p53 and Mdm2, can be compensated within the considered model mostly due to the variation of the parameters s, b, k_f (see fig. 2). Variation of the parameters c_1, c_2, and k_g can compensate the negative situation only partially, since in this case the levels of protein concentrations exceeding the basal values by a factor of at least 1.5 to 2 are installed.

Thus, in order to remove the threat of the uncontrolled apoptotic death of cells, first of all it is possible to apply the connection of two pairs of parameters – the rate of p53 generation and the rate of this protein degradation through ubiquitination or the Mdm2 degradation rate and the rate of its generation: an undesirable increase or decrease of one of the parameters in each of these pairs is compensated by a similar (by the same factor) change of the second parameter of this pair. In this situation, the system is considerably less sensitive to both the regulation through the rate of the spontaneous p53 decomposition and also to the strengthening of the p53 and Mdm2 bond through dissociation constants. At sufficiently large values of the τ delay (close to the observed ones), it is not easy to remove the

negative consequences caused by the increased rate of p53 generation by the control of the dissociation constants.

Excessive Mdm2 level

In the course of the numerical experiments, there was a situation in which there was an increased risk of a decrease of the p53 function, when the interaction of p53 and its inhibitor Mdm2 is attenuated, and as a result the p53 level is found to be very low and the level of Mdm2 itself is too high. Within the considered mathematical model, this state arises when the rate of Mdm2 degradation is low or the rate of its generation is too high. We are considered the ways to compensate these disturbances.

The damping of the interaction in the p53–Mdm2 network, accompanied by the fast growth of the Mdm2 concentration, can be compensated within the considered model only through controlling the rates of Mdm2 generation or degradation, and at very moderate delay values it can be also done by a significant increase of the dissociation constant of the p53 protein and the Mdm2 gene. The studies described in this section allow us to answer important questions for the clinical practice on the functioning and regulation of the p53–Mdm2 grid, including those associated with the artificial break of the p53–Mdm2-interaction for therapeutic purposes and with the actions for the restoration of the basal state of the system.

CONCLUSIONS

Balancing the rates of cellular proliferation and apoptosis is an important tool for maintaining the homeostasis of the normal tissue. Disturbance of this balance can become a cause of serious pathological changes in organs and tissues. In this work, a numerical investigation of the disturbances in the system of p53 and Mdm2 proteins, which participate in the correction of DNA defects and are involved in many vital processes, including oncogenesis, neurodegenerative diseases, and aging, was carried out. We are considered two interrelated mathematical models of the p53–Mdm2 network. The basic model of the proteins concentrations dynamics includes the system of two nonlinear equations with the retarded argument. The second model describes hypothetical stages of process and uses the simplest ODE of higher dimension. We show numerically that in the passage to the limit in which the second model has infinitely many stages we obtain model based equation with retarded argument.

All obtained numerical solutions have a sufficiently clear biomedical meaning. The adopted mathematical models describe the functioning of the p53–Mdm2 network in normal conditions and predict possible dangerous situations for the organism. Stress situations associated with the emergence of an imbalance in the rates of p53 and Mdm2 generation and degradation and also with disturbances in the mechanism of interaction of proteins regulated within the considered models through the constants of dissociation have been studied. The variants of the compensation of the considered disturbances by repeated stress for the system parameters have been numerically investigated.

ACKNOWLEDGEMENTS

The work was performed with the financial support of the Council on Grants (grant NSh 5006.2014.9) of the President of the Russian Federation.

REFERENCES

1. *Batchelor E., Loewer A., Mock C., Lahav G.* Stimulus-dependent dynamics of p53 in single cells // Mol. Syst. Biol. 2011. 7. ID 488.

2. *Lane D., Levine A.* p53 Research: the past thirty years and the next thirty years // Cold Spring Harb. Perspect. Biol. 2010. 2. (12). ID a000893.

3. *Loewer A., Batchelor E., Gaglia G., Lahav G.* Basal dynamics of p53 reveal transcriptionally attenuated pulses in cycling cells // Cell. 2010. 142. (1). 89–100.

4. *Tiana G., Jensen M., Sneppen K.* Time delay as a key to apoptosis induction in the p53 network // Eur. Phys. J. B. 2002. 29. (1). 135–140.

5. *Voropaeva O.F., Shokin Yu.I., Nepomnyashchikh L.M., Senchukova S.R.* Mathematical model of function and regulation of p53–Mdm2 biological system. Moscow: Publishing House RAMS, 2014 [In Russian].

6. *Voropaeva O.F., Senchukova S.R., Brodt K.V. et al.* Numerical simulation of ultradian oscillations in p53–Mdm2 network under stress conditions // Math. Models Comput. Simul. 2015. 7. (3). 281–293.

УДК 519.6; 519.8; 51-7; 616

МАТЕМАТИЧЕСКОЕ МОДЕЛИРОВАНИЕ СЕТИ ОНКОМАРКЕРОВ

Ольга Фалалеевна ВОРОПАЕВА[1], Юрий Иванович ШОКИН[1],
Лев Моисеевич НЕПОМНЯЩИХ[2], Светлана Робертовна СЕНЧУКОВА[2]

[1] ФГБУН Институт вычислительных технологий СО РАН
630090, г. Новосибирск, пр. Академика Лаврентьева, 6

[2] ФГБНУ Институт молекулярной патологии и патоморфологии
630117, г. Новосибирск, ул. Тимакова, 2

В работе выполнен численный анализ решений системы уравнений, описывающих динамику концентраций белков p53 и Mdm2 при их взаимодействии. Проведено детальное численное исследование решений при отклонении параметров математической модели от базальных значений. В рамках численных экспериментов получены состояния сети p53-Mdm2, соответствующие как угрозе неуправляемой апоптотической гибели клеток, ускоряющей процессы старения организма, так и ситуации чрезмерного подавления апоптоза, когда увеличивается риск онкологических заболеваний. Исследованы механизмы управления системой p53-Mdm2 в условиях стрессов.

Ключевые слова: онкомаркеры, сеть p53-Mdm2, уравнения с запаздывающим аргументом, численное моделирование.

Воропаева О.Ф. *– д. ф.-м.н., старший научный сотрудник, e-mail: vorop@ict.nsc.ru*
Шокин Ю.И. *– академик РАН, директор*
Непомнящих Л.М. *– член-кор. РАН, директор*
Сенчукова С.Р*. – д.м.н., ведущий научный сотрудник*

УДК 519.622.2, 004.942

A NUMERICAL ALGORITHM OF PARAMETER ESTIMATION FOR DYNAMIC MODEL FOR HIV INFECTION OF CD4+ T CELLS

Sergey Igorevich KABANIKHIN[1,2], Olga Igorevna KRIVOROTKO[1,2], Adele MORTIER[3], Dmitriy Andreevich VORONOV[2], Darya Vladimirovna YERMOLENKO[2]

[1] *Institute of Computational Mathematics and Mathematical Geophysics of SB RAS*
630090, Novosibirsk, Lavrent'ev ave., 6

[2] *Novosibirsk State University*
630090, Novosibirsk, Pirogov str., 2

[3] *Telecom ParisTech*
75013, Paris, 46 rue Barrault

The problem of the values approximation of 6 coefficients of the HIV infection basic model – so-called the inverse problem has been computationally investigated by the complementary measurements of viremia and target cells blood concentrations through the fixed timing. The inverse problem for HIV dynamic model has been reduced to the problem of objective functional minimization. The 6-dimensional Nelder-Mead algorithm has been implemented to the minimization task realization. The proposed algorithm demonstrates the good convergence with probability of 17 % for the fairly small interval range of unknown coefficients relating to average mean (about 33% of the total bandwidth between experimental extreme coefficients values). The numerical experiment results has been performed and discussed.

Keywords: HIV infection, parameter estimation, inverse problem, optimization algorithm, Nelder-Mead method.

The human immunodeficiency virus (HIV), by causing a progressive failure of the human immune system, allows life-threatening opportunistic infections and cancers to thrive. Within blood, HIV includes as both free virus particles and virus within infected immune cells, specifically CD4+ T cells.

HIV infection leads to low levels of CD4+ T cells through a number of mechanisms, including apoptosis of uninfected bystander cells, direct viral killing of infected cells, and killing of infected CD4+ T cells by CD8 cytotoxic lymphocytes that recognize infected cells.

The research in the within-host dynamics of HIV infections focuses on these mechanisms, and especially the spread of the virus *in vivo*. The latest models take into account virus's cell-to-cell interactions, *T cell* activation, and immune exhaustion [19]. However, a simpler model involving ordinary non-linear equations also provides satisfying results for early times, with a limited parameter set.

Since the direct problem remains quite easy to solve, it lends itself well to the study of HIV inverse problem. With this basic model and regular data of viremia and T cells loads over time after infection, we propose an algorithm which characterizes individual parameters in HIV modeling. The knowledge of these parameters could open the way to more personalized (and more efficient) treatments.

The paper organized as follows. In a second section, the different parameters and the model of the problem are presented in order to justify the inverse problem approach.

Then, in a third section, some results and plots of the outputs are shown and analysed, which leads to a concluding paragraph reviewing the global performance of the approach and the accuracy of the

Kabanikhin S.I. *– doctor of physical and mathematical sciences, corresponding member of RAS, professor, director, e-mail: kabanikhin@sscc.ru*
Krivorotko O.I. *– candidate of physical and mathematical sciences, junior researcher, senior lecturer of the chair for advanced mathematics, e-mail: olga.krivorotko@sscc.ru*
Mortier Adele *– student, e-mail: adele.mortier@telecom-paristech.fr*
Voronov D.A. *– senior lecturer of the chair for advanced mathematics, e-mail: dmitriy.voronov.89@gmail.com*
Yermolenko D.V. *– student, e-mail: ermolenko.dasha@mail.ru*

approximate solution. Finally, we will consider future perspectives which could enhance the model or the solving program.

STATEMENT OF THE PROBLEM

A basic model of HIV dynamics involves only three determining variables: uninfected and infected target cells (mostly CD4+ T cell), and free HIV viruses within blood. Their concentrations are respectively noted $T(t)$, $I(t)$, $V(t)$. We can also build the vector quantity $X(t)$, which characterizes the whole immune response to the infection:

$$X(t) = (T(t), I(t), V(t))^T.$$

In practice, it is relatively easy to measure this vector variable, and thus access to the solution of the direct problem of HIV dynamics with an acceptable level of precision: we simply need daily blood samples from HIV-positive patients. Besides, interactions between the three blood concentrations $T(t)$, $I(t)$, $V(t)$ can be modeled quite simply by a *SIR model with vital dynamics and constant population* [5, 13, 15]. It is a basic compartmental model that involves *Susceptible cells* $I(t)$, *Infectious virions* $V(t)$, and *Recovered immune cells* $T(t)$:

$$\frac{dX}{dt} = \begin{cases} \dfrac{dT}{dt} = \lambda - d_T T - \beta VT, \\ \dfrac{dI}{dt} = \beta VT - \delta I, \\ \dfrac{dV}{dt} = pI - cV, \end{cases} \quad (1)$$

with initial conditions at time t_0

$$T(t_0) = T_0, I(t_0) = I_0, V(t_0) = V_0. \quad (2)$$

The description of the parameters and its possible value interval are given in Table 1. These six coefficients may vary according to the metabolism of each individual. But contrary to the variable $X(t)$, they remain quite difficult to measure experimentally. That is the reason why tackling the HIV dynamics modeling with an inverse problem approach seems appropriate [8]. So let q^{ex} be the 6-dimensional vector that contains all information about the immune features of a given individual:

$$q^{\text{ex}} = [\lambda, d_T, \beta, \delta, p, c]^T. \quad (3)$$

The exact solution q^{ex} will be the unknown element of the inverse problem; its components shall be in the ranges specified above. The goal of the *inverse problem* modeling is to approximate these coefficients only by knowing the behaviour of the function $X^{q^{ex}}(t)$ through blood samples of a given individual (*i.e.*, a given q^{ex}) in a given time interval. These baseline data can be written as follows:

$$\left\{ X^{q^{ex}}(t_k) \right\}_{t_k \in [t_0, t_f)}. \quad (4)$$

Henceforth, we will note (4) the sampled solution of (1)–(2) for a given q. A realistic time sampling cannot exceed for instance 5 measurements a day (exhaustion caused by blood taking, equipments required). A frequency of 2 blood samples per day during 5 days was chosen to solve the inverse problem. As a result, sampled times are:

$$\{t_k\}_{k \in [0,9]}, \ \forall k \in [0,9], \ t_k = k/2. \quad (5)$$

As for the *SIR* model, it allows a relatively easy solving of the direct problem for all q we may consider. Moreover, we can assume that the solution q^{ex} of the inverse problem is the value of q which minimizes the following misfit function, based on the *method of Least Squares*:

$$J : q \in R^6 \mapsto \sum_{t_k \in [t_0, t_f)} \left| X^q(t_k) - X^{q^{ex}}(t_k) \right|^2. \quad (6)$$

Consequently, the HIV dynamics inverse problem can be reduced to a problem of optimization (6) and ordinary differential equation (*ODE*) solving. The first step will be carried out through the *Nelder-Mead method* [12], while a fifth-order *Runge-Kutta method* [4] will handle the second step. We will now explain in details the running of these two methods and their implementation.

NUMERICAL METHODS FOR SOLVING DIRECT AND INVERSE PROBLEMS

Direct problem solving

The solving of the direct problem relies on a *Runge-Kutta method* for non-stiff ordinary differential equations, inspired by the Matlab solver ode45.m [3], which gave satisfying results in other studies [14]. The default method of ode45.m is the Dormand-Prince [4] embedded method, designed to produce an estimate of the local truncation error of a single *Runge-Kutta* step. It allows to control the error with adaptive stepsize [18] by managing two methods, one with order 5 and one with order 4.

Minimization of the misfit function

By definition, the solution of the inverse problem is the only q for which $J(q) = 0$. And since J is a positive function:

$$J(q) = 0 \Longleftrightarrow q = \text{argmin}(J). \quad (7)$$

In papers [1, 6] the gradient algorithm was proposed to find the minimum of the misfit function J. In this paper, to find the minimum of the misfit function, the *Nelder-Mead method* [12] was implemented for a 6-dimensional space. The method uses the concept of a simplex, which is a special polytope. In our case, it is made up of 7 different q from the interval described in Table 1. At each steps, $q \in R^6$ is updated using one of these four transformations:

$$\text{reflection } q^* = \overline{q} + \alpha \cdot \overrightarrow{q_h \overline{q}},$$
$$\text{contraction } q^{**} = \overline{q} - \beta \cdot \overrightarrow{q_h \overline{q}},$$
$$\text{expansion } q^{***} = \overline{q} - \gamma \cdot \overrightarrow{q^* \overline{q}},$$
$$\text{reduction } q = q + \frac{1}{2} \cdot \overrightarrow{q q_l}.$$

Here $\overline{q} = \text{centroid}_{q \setminus \{q_h\}} J(q)$, $q_h = \arg\max_q (J(q))$, $q_l = \arg\min_q (J(q))$, $\alpha = 1$, $\beta = 1/2$, $\gamma = 2$.

However, the *Nelder-Mead method* is a heuristic search method that can converge to non-stationary points, i.e., local minima. In this case, we can obtain a wrong solution of inverse problem (1)–(2), (4). This is all the more probable as the initial random set of points q_0 is dispersed around the expected solution. That is why, without the use of an auxiliary method, the initial random generation of the array of the zeros approximation remains a key issue.

Besides, the *Nelder-Mead method* does not take into account the unrealistic character of the q_n it returns. Indeed, the standard stopping condition of this algorithm is:

$$\sqrt{\sum_{q \in R^6} |J(q_n) - J(\overline{q})|^2} \le 10^{-3}.$$

It only quantifies how close to each other are the misfit function's values at the vertices of the simplex. Thus, a subsidiary method should check if the found minimum belongs to Table 1, and if it actually makes the function J converge towards 0. If these two conditions are actually fulfilled, the program can stop. If not, the *NelderMead method* has to be launched once again, with an other random set of points q_n.

Generation of synthetic data

In practice, the blood samples (4) come from experimental measurements (which can, by the way, be erroneous in a certain extent). But here, synthetic exact data have to be generated from a fixed q^{ex}, in order to check the good convergence of the algorithm, which should be able to recalculate this value by itself.

For getting the synthetic data (4) we solve of the direct problem for a fixed q^{ex} by the Runge-Kutta method. Afterwards, the value of q^{ex} should not be reused by the program.

NUMERICAL RESULTS

In this section we demonstrate the numerical results of solving inverse problem (1)–(2), (4) with synthetic data.

Initial settings

We set the time interval $[t_0, t_f)$ as [0, 5) and the time sampling frequency $h = 0.5$: $t_0 \le t_k = kh < t_f$. The value of the exact solution q^{ex} used to generate synthetic data was equal to the mean values of Table 1 (column 3).

The plots of synthetic data generated with the set of coefficients q^{ex} are demonstrated at Figure 1.

As for the generation of the set of initial points q_0, a uniform random distribution over an adjustable interval around the expected solution was chosen. Considering each coefficient, this interval represents a given percentage of the total bandwidth between extrema of Table 1. For a given coefficient, e.g. λ, it can thus be written:

$$\left[\lambda_{\min}^{rel}, \lambda_{\max}^{rel}\right] \text{ with } \begin{cases} \lambda_{\min}^{rel} = \lambda^{ex} - 2(\lambda^{ex} - \lambda_{\min}^{abs})/3, \\ \lambda_{\max}^{rel} = \lambda^{ex} + 2(\lambda_{\max}^{abs} - \lambda^{ex})/3. \end{cases}$$

B. Convergence in the Nelder-Mead Algorithm

The *Nelder-Mead method* does not always converge to a global minimum for the function J, and may be launched several times before giving a relevant solution of the inverse problem. In this section, we focus on the results of the *Nelder-Mead method* when it has been run successfully, so as to estimate the accuracy of the convergence. The behaviours of eight random set were analyzed step-by-step during the *Nelder-Mead method*, by plotting the changing coordinates of the simplex's centroid. Three sets used initial random points from a "2/3-adjusted in-

Table 1

Extreme and mean values of immune coefficients [7]

Parameter	Minimum	Mean	Maximum	Units
λ	4.3×10^{-2}	1.089×10^{-1}	2×10^{-1}	$\mu L^{-1}\ day^{-1}$
d_T	4.3×10^{-3}	1.089×10^{-2}	2×10^{-2}	day^{-1}
β	1.9×10^{-4}	1.179×10^{-3}	4.8×10^{-3}	$\mu L\ day^{-1}$
δ	1.3×10^{-1}	3.660×10^{-1}	8×10^{-1}	day^{-1}
p	9.8×10^{1}	1.427×10^{3}	7.1×10^{3}	day^{-1}
c	3	3	3	day^{-1}

Here: λ and d_T are respectively the birth rate and the dying rate of target cells; β quantifies the infection by free virus; δ is the dying rate of infected cells; p and c are respectively the production rate and the clearing rate of the virions.

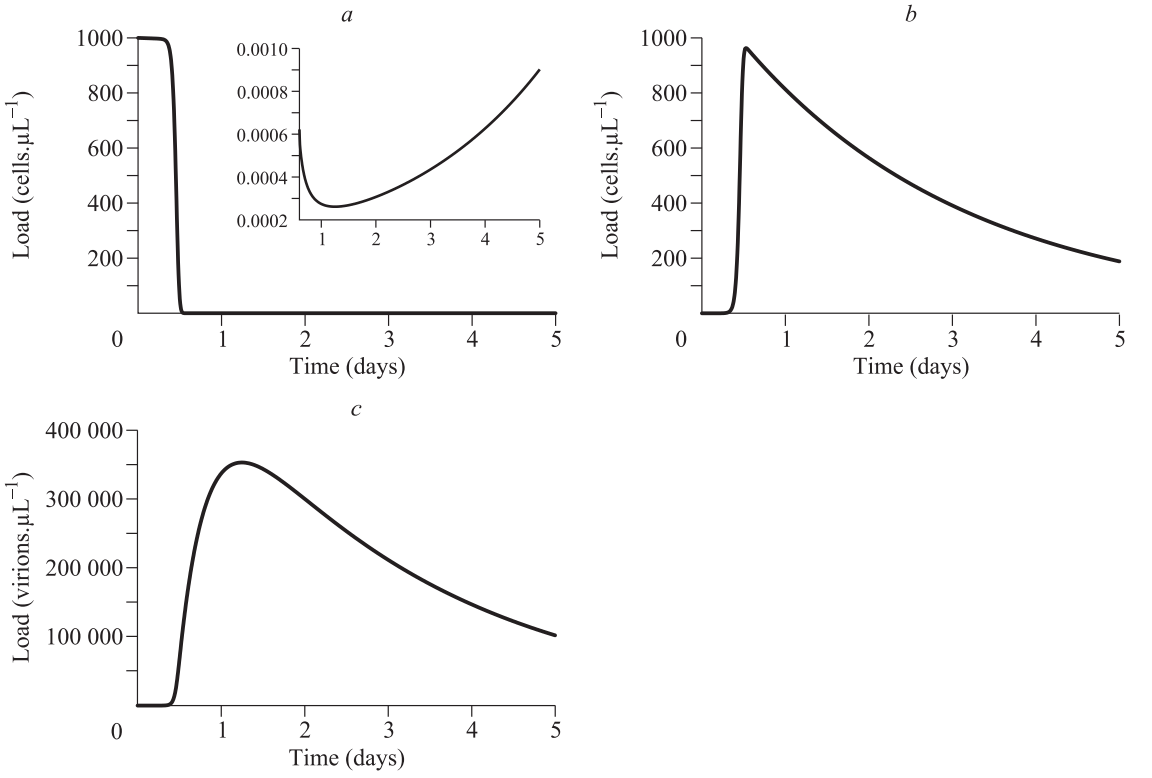

Fig. 1. *Concentration of uninfected target cells* $T^{q^{ex}}(t)$ *(a), of infected target cells* $I^{q^{ex}}(t)$ *(b), and of free HIV viruses* $V^{q^{ex}}(t)$ *(c).*

Table 2

Coefficients of the simplex's centroid $\overline{q}$ *at different steps of the* Nelder-Mead method

Step number	λ		d_T	
	Value	Relative error (%)	Value	Relative error (%)
1	0.120758863	10.89	0.011395613	4.64
10	0.115669636	6.22	0.008978078	–17.56
30	0.114106539	4.78	0.008449692	–22.41
60	0.113997897	4.68	0.008368867	–23.15
100	0.113992729	4.68	0.008364289	–23.19
	β		δ	
Step number	Value	Relative error (%)	Value	Relative error (%)
1	0.001814283	53.88	0.42271688	15.50
10	0.001305623	10.74	0.379353123	3.65
30	0.001185291	0.53	0.368954912	0.81
60	0.001178254	-0.06	0.36633236	0.09
100	0.001179676	0.06	0.366008649	0.00
	p		*c*	
Step number	Value	Relative error (%)	Value	Relative error (%)
1	1984.812433	39.09	3	0.00
10	1447.04152	1.40	3	0.00
30	1429.956621	0.21	3	0.00
60	1426.260772	–0.05	3	0.00
100	1425.38208	–0.11	3	0.00

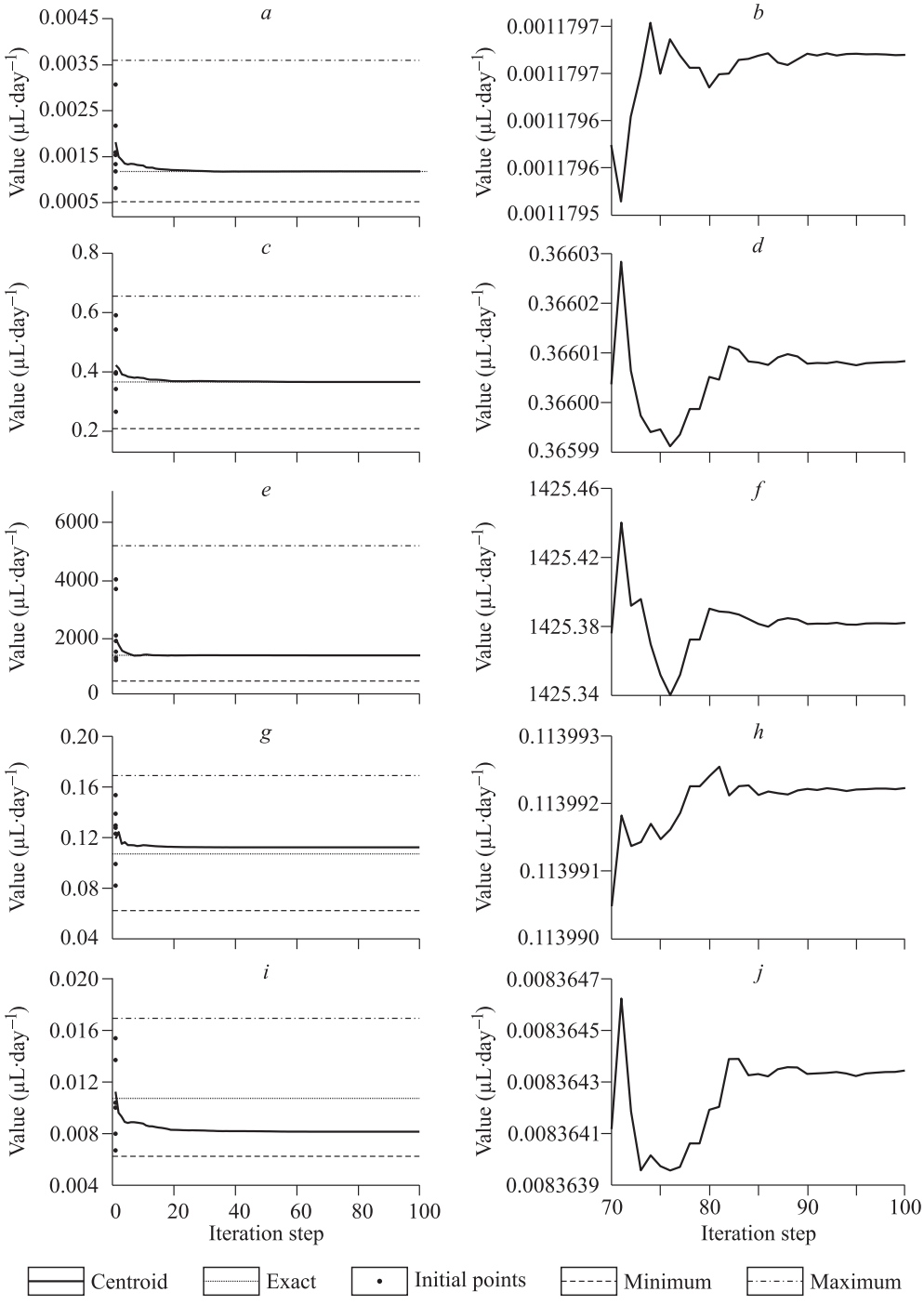

Fig. 2. *Convergence of the coefficients β (a, b), δ (c, d), p (e, f), λ (g, h) and d_T (i, j) using an initial "2/3-adjusted interval"; a, c, e, g, i – global convergence, b, d, f, h, j – later behaviour*

terval". The 5 recovered coefficients of problem (1) by using the *Nelder-Mead method* are demonstrated on Figure 2. Note, that the coefficient c has the exact value at Step 0 (see Table 2 for details).

Overall, we can note a good convergence of the different coefficients towards their exact value, with a final relative error lower than 0.05 %. The only exception seems to be d_T, whose values become apparently further from the exact one.

Besides, the final relative errors seemed to be all the more dispersed that the initial interval allowed for the random points generation is wide.

Another way to estimate the convergence of the algorithm is to focus on the behavior of the misfit function for each computation step. With the initial data form «2/3-adjusted interval», we obtain the behaviour of the misfit function at each computation step (see Fig. 3).

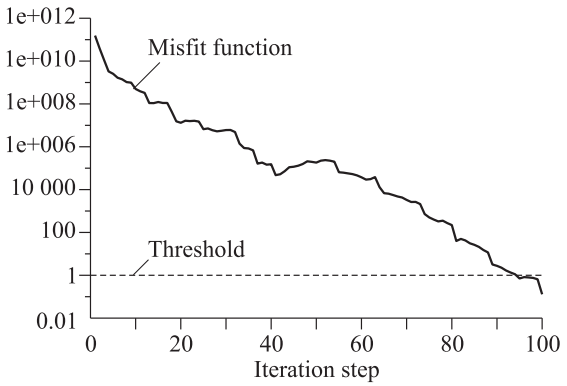

Fig. 3. *The global behaviour of the misfit function at each computation step (base 10 logarithm)*

Most of the time, the simplex algorithm stopped at the 100th iteration step (maximum preset number of allowed iterations). However, we can assume that a hundred step provides a quite satisfying accuracy insofar as the misfit function seems to reach a stationary state, with a value close to unity.

CONCLUSION

The *Nelder-Mead method* has managed to find the coefficients of the initial differential system with a good precision. Nevertheless, its performance remains quite low, because of a total random choice of initial conditions, and a heuristic method that is also too sensible to these conditions. Finally, the trials using synthetic data (which do not include the possible errors caused by experimental measurement) can only give an overview of the operating effectiveness of the whole program.

Future Perspective

A certain number of improvements of the algorithm could be examined, in order to increase its performance in the search of extrema, or its ability to take into account the later fluctuations of viral loads and T-cell blood concentrations.

First of all, the *SIR* simple model does not integrate the influence of latency in human body, which is yet an important long-term factor during the infection. Some studies [9] aimed to deal with this effects, by considering for instance the long-term role of peripheral virion reservoirs. As a result, the time becomes an explicit variable of the global differential system; nevertheless, the solving method does not have to change a lot, since the *Runge-Kutta* complete algorithm is precisely designed for this eventuality.

Furthermore, the *Nelder-Mead method* could be optimized in itself. In this regard, some methods are best suited for constrained optimization [2, 17]; at each step, the points out of preset limits are reset in the good interval. This could be of great advantage, insofar as it prevents the program from looping a long time around unrealistic minima.

Besides, some auxiliary loops including *Monte-Carlo method* could be able to increase the probability of success during the *Nelder-Mead* algorithm, by presetting the more favorable initial conditions. Some of these techniques are based on the *Metropolis algorithm* [10, 11, 16], which samples the probability distribution of the *model space* (ie, the possible solutions of inverse problem) by using of modified random walk. Combining this statistical approach with the classic simplex search could provide a more realistic model, with a better performance and a reasonable complexity (*Monte Carlo* all alone remains time-consuming).

ACKNOWLEDGMENT

The authors would like to thank Prof. A.I. Ilyin for problem statement and fruitful discussions. This work was partially supported by the Ministry of Education and Science of Russian Federation and the project No. 107 with Republic of Kazakhstan ”Development of software for research and numerical solving of direct and inverse problems of pharmacokinetics and epidemiology”.

REFERENCES

1. *Afraites L., Atlas A.* Parameters identification in the mathematical model of immune competition cells // J. Inverse Ill-Posed Probl. 2015. 23. (4). 323–337.

2. *Box M. J.* A new method of constrained optimization and a comparison with other methods // Comput. J. 1965. 8. (1). 42–52.

3. *Compere M.* ODE Solvers for Octave and Matlab. 1999. https://sites.google.com/site/comperem/home/ode solvers.

4. *Dormand J.R., Prince P.J.* A family of embedded Runge-Kutta formulae // J. Comput. Appl. Math. 1980. 6. (1). 19–26.

5. *Hethcote H.W.* Three basic epidemiological models // *Applied Mathematical Ecology*. Eds. S.A. Levin, T.G. Hallam, L.J. Gross. Berlin; Heidelberg: Springer-Verlag, 1989. 18. 119–144.

6. *Ilyin A., Kabanikhin S.I., Nurseitov D.B. et al.* Analysis of ill-posedness and numerical methods of solving a nonlinear inverse problem in pharmacokinetics for the two-compartmental model with extravascular drug administration // J. Inverse Ill-Posed Probl. 2012. 20. (1). 39–64.

7. *Jones E., Roemer P., Raghupathi M., Pankavich S.* Analysis and simulation of the three-component model of HIV dynamics // SIAM Undergrad. Res. Online. 2014. 7. 89–106.

8. *Kabanikhin S.I.* Inverse and Ill-Posed Problems. Theory and Applications. Berlin: de Gruyter, 2011.

9. *Mbogo W.R., Luboobi L.S., Odhiambo J.W.* Stochastic model for Langerhans cells and HIV dynamics in vivo // ISRN Appl. Math. 2014. 2014. ID 594617.

10. Metropolis N., Ulam S. The Monte Carlo method // J. Am. Stat. Assoc. 1949. 44. (247). 335-341.

11. Mosegaard K., Tarantola A. Monte Carlo sampling of solutions to inverse problems // J. Geophys. Res. 1995. 100. (B7). 12431–12447.

12. Nelder J.A., Mead R. A simplex method for function minimization // Comput. J. 1965. 7. (4). 308–313.

13. Perelson A.S., Ribeiro R.M. Modeling the within-host dynamics of HIV infection // BMC Biol. 2013. 11. 96.

14. Roemer P. Stochastic modeling of the persistence of HIV: early population dynamics // Trident Scholar Project Report. 2013. (420). 64 p.

15. Stafford M.A., Corey L., Cao Y. et al. Modeling plasma virus concentration during primary HIV infection // J. Theor. Biol. 2000. 203. (3). 285–301.

16. Tarantola A. Inverse problem theory and methods for model parameter estimation // Society for Industrial and Applied Mathematics. Philadelphia, 2005. 41–54.

17. Tauler R., Brown S.D., Walczak B. Three basic epidemiological models // Comprehensive Chemometrics: Chemical and Biochemical Data Analysis. Eds. S.D. Brown, R. Tauler, B. Walczak. Elsevier Science: 2009. 18. 556–557.

18. Van Der Houwen P.J., Sommeijer B.P. Parallel iteration of high-order Runge-Kutta methods with stepsize control // J. Comput. Appl. Math. 1990. 29. (1). 111–127.

19. Zhang C., Zhou S., Groppelli E. et al. Hybrid spreading mechanisms and T cell activation shape the dynamics of HIV-1 infection // PLoS Comput. Biol. 2015. 11. (4). e1004179.

ЧИСЛЕННЫЙ АЛГОРИТМ ОЦЕНКИ ПАРАМЕТРОВ МАТЕМАТИЧЕСКОЙ МОДЕЛИ ДИНАМИКИ ВИЧ ИНФЕКЦИИ CD4+ Т-КЛЕТОК

Сергей Игоревич КАБАНИХИН[1], Ольга Игоревна КРИВОРОТЬКО[1,2], Адель МОРТЬЕ[3], Дмитрий Андреевич ВОРОНОВ[2], Дарья Владимировна ЕРМОЛЕНКО[2]

[1] Институт вычислительной математики и математической геофизики СО РАН
630090, Новосибирск, пр. Академика Лаврентьева, 6

[2] Новосибирский государственный университет
630090, г. Новосибирск, ул. Пирогова, 2

[3] Telecom ParisTech
75013, Paris, 46 rue Barrault

Численно исследована задача аппроксимации значений шести коэффициентов базовой модели ВИЧ-инфекции по дополнительным измерениям концентраций виремии и целевых клеток крови в фиксированные моменты времени, называемая обратной задачей. Обратная задача для динамической модели ВИЧ сводится к задаче минимизации целевого функционала. Реализован шестимерный алгоритм Нелдера–Мида для решения задачи минимизации. Для достаточно небольшого интервала значений неизвестных коэффициентов относительно некоторой средней величины (около 33 % от общего интервала между экспериментальными значениями крайних коэффициентов), предлагаемый алгоритм демонстрирует хорошую сходимость с вероятностью 17 %. Приведены и обсуждены результаты численного эксперимента.

Ключевые слова: простейшая математическая модель внутриклеточной динамики ВИЧ-инфекции, оценка параметров, обратная задача, оптимизационный алгоритм, метод Нелдера–Мида.

Кабанихин С.И. *– д.ф.-м.н., член-корреспондент РАН, профессор, ВРИО директора, e-mail: kabanikhin@sscc.ru*
Криворотько О.И. *– к.ф.-м.н., младший научный сотрудник, старший преподаватель кафедры высшей математики физического факультета, e-mail: olga.krivorotko@sscc.ru*
Мортье Адель *– студент, e-mail: adele.mortier@telecom-paristech.fr*
Воронов Д.А. *– старший преподаватель кафедры высшей математики физического факультета, e-mail: dmitriy.voronov.89@gmail.com*
Ермоленко Д.В. *– студент 1 курса магистратуры, e-mail: ermolenko.dasha@mail.ru*

УДК: 617.3:[678.09+678.011]

EFFECT OF ELECTRON-BEAM IRRADIATION ON ELECTROSPINNING PRODUCED SCAFFOLDS

Alena Olegovna STEPANOVA[1,2], Mikhail Vasilevich KOROBEYNIKOV[3], Aleksandr Sergeevich YUNOSHEV[4], Pavel Petrovich LAKTIONOV[1,2]

[1] *Novosibirsk Research Institute of Circulation Pathology of Academician E.N. Meshalkinцa Minzdrav of Russia*
630055, Novosibirsk, Rechkunovskaya str., 15

[2] *Institute of Chemical Biology and Fundamental Medicine of SB RAS, Novosibirsk, Russia*
630090, Novosibirsk, Lavrent'ev ave., 8

[3] *Institute of Nuclear Physics, Novosibirsk, Russia*
630090, Novosibirsk, Lavrent'ev ave., 11

[4] *Insitute of Hydrodynamics, Novosibirsk, Russia*
630090, Novosibirsk, Lavrent'ev ave., 15

The influence of electron beam irradiation on the stiffness, stability and biocompatibility of electrospun scaffolds, produced from Nylon 6, polycaprolactone (PCL) and poly(DL-lactic-co-glicolic acid) (PLGA) was investigated. It was shown that irradiation of the matrices with the electron beam generated by the electron beam accelerator ILA-6 (2.2 MeV, 400 mA, 10 Hz, «Radiochemical technologies Ltd») can potentially be used for sterilization of the matrices (irradiation by the dose of 25 kGy does not interfere with the mechanical properties of all studied matrices). Irradiation of the matrices produced from PCL by the dose of 100 kGy increases the proportional limit of the material and allowed us to introduce durable regions into the vascular grafts by irradiating the graft through the template with open areas. Electron beam irradiation of the matrices does not influence over the capacity of the matrices to support adhesion and viability of primary human endotheliocytes at the surfaces of these matrices, as it was shown using Alamar Blue assay.

Keywords: electron beam irradiation, electrospinning, PCL, PLGA, Nylon 6.

One of the promising technologies nowadays for production scaffolds for tissue engineering is electrospinning. The method is based on stretching of the thin and ultrathin fibers from the polymer solution in a strong electric field. Thus, nonwoven 3D matrices of different types of fibers with different fiber orientations are easily been obtained. The method allows the production of different variants of fibers, including fibers from two or more solutions, coaxial fibers, fibers containing a variety of low and high molecular weight biologically active substances [2]. Electrospinning produced scaffolds have been shown to be used for different tissues displacement [4], but modification of their properties, such as stiffness, stability, sterilization, is still needed.

The cross-linking of polymers through electron beam irradiation (EBI) in technology changes a thermoplastic material into a thermoset. This technology is widely used also for modification of mechanical properties of plastic products, by generating free radicals, which lead to polymer chain degradation, or intermolecular crosslink formation [5]. So far, this technology suggests treatment of the end

Stepanova A.O. *– junior researcher of laboratory for molecular medicine and laboratory of biomedical technologies, e-mail: lebedeva@niboch.nsc.ru*
Korobeinikov M.V. *– candidate of technical sciences*
Yunoshev A.S. *– candidate of physical mathematical sciences, head of laboratory for high speed processes of the department for explosive processes*
Laktionov P.P. *– candidate of biological sciences, leading researcher, head of laboratory for molecular medicine, head of laboratory for biomedical technologies, e-mail: lakt@niboch.nsc.ru*

product, widely used for sterilization of medical products in a simple and low-cost way.

We evaluated potentialities of electron beam irradiation for the modification of scaffolds produced by electrospinning that are intended to be used for tissue engineering.

MATERIAL AND METHODS

Materials

Poly(ε-caprolactone) (PCL), Nylon 6 and 1,1,1,3,3,3-Hexafluoro-2-propanol (HFP), Phosphate buffer saline (PBS), gelatine were obtained from Sigma-Aldrich Co. (USA), 50:50 poly(DL-lactide-co--glicolide) (PLGA, inherent viscosity 1.11 dL/g in HFIP) was purchased from Lactel Asorbable Polymers (Pelham, AL, USA). Isolve's Modified Dulbecco's medium (IMDM) (phenol red free), Fetal bovine serum (FBS), penicillin/streptomycin antibiotics, were obtained from Gibco, Life Technologies Co (USA).

Scaffold preparation

Electrospun scaffolds were fabricated using Nylon 6, as the nonbiodegradable polymer, PCL, as the slowly biodegradable polymer and PLGA, as the rapidly biodegradable polymer. Briefly, each polymer Nylon 6, PCL and PLGA was dissolved in HFIP at total concentrations of 10 %, 7 % and 15 % respectively. The polymer solutions were individually electrospun using electrospinning setup NF-103 (MECC, Japan). The solutions were delivered through a 22G blunt tip needle connected to a 5 mL syringe. The spinning conditions for Nylon 6 were 1.5 mL/hour flow rate, 20 kV applied voltage, 190 mm air gap; for PCL – 1.5 mL/hour flow rate, 23 kV applied voltage, 190 mm air gap; for PLGA – 1.5 mL/hour flow rate, 18.4 kV applied voltage, 200 mm air gap. The samples were collected on a custom-designed mandrill collector with an outer diameter of 6 cm. The rotation speed of the collector was 300 rpm. The thickness of all samples was 150 μm. After electrospinning all scaffolds were additionally dried in room conditions for day. Additionally, tubes with inner diameter 1.7 mm and wall thickness 150 μm were prepared using a stainless steel 180 mm rod collector rotating 300 rpm.

Electron beam irradiation

All samples were irradiated by electron beam accelerator ILA-6 (2.2 MeV, 400 mA, 10 Hz, «Radiochemical technologies Ltd») in the Institute of nuclear physic SB RAS (Novosibirsk, Russia) at doses 25, 50, 100, 150 and 200 kGy. Before irradiation, every sample was cut in rectangular specimens 1 × 4 cm, suitable for tensile strength testing, and packaged in a polyethylene zip-lock bag.

Tensile test

The tensile strength of electrospun nonirradiated and irradiated polymer scaffolds was characterized using the Zwick/Roell Z100 (Gemany) testing machine in Institute of hydrodynamic SB RAS (Novosibirsk, Russia) with a deformation speed of 10 mm/min. The mechanical characteristics of the samples were obtained from the stress-strain diagram.

Scanning electron microscopy

Fiber morphologies of irradiated and nonirradiated Nylon 6, PCL and PLGA electrospun samples were examined by scanning electron microscopy (SEM; Model JSM-6460 LV, Jeol, Japan) at acceleration voltages of 20 kV and 25 kV. The samples were sputter coated with gold to achieve the layer 10 Å. The average diameters and standard deviations were calculated from 20 separate fibers per image. The pore size was calculated from 20 separate holes between fibers on the image.

Differential scanning calorimetry (DSC)

DSC data were obtained with Calorimeter setup DSC 550 (Russia) in the Institute of solid state chemistry and mechanochemistry SB RAS (Novosibirsk, Russia) in a nitrogen atmosphere.

Degradation rate of matrices in PBS solution 10 mm diameter discs were prepared with cutting from nonirradiated and irradiated with a dose 100 kGy scaffolds. The discs were replaced into the well with 250 μl of phosphate buffer saline (PBS) of 48 well microplate and incubated at 37°C for 5, 7, 14, 21, and 28 days. After the incubation, the discs were removed from the well, rinsed with water, dried and examined by SEM.

In vitro cell culture analysis

10 mm diameter discs were obtained from nonirradiated and irradiated with dose from 0 to 150 kGy scaffolds. Discs were wetted in PBS and placed into the well of 48 well microplates. Every disc was fixed close to the bottom by a special plastic ring with outer diameter 10 mm and wall thickness 2 mm. After that, 100 μl of IMDM culture medium with 10 % serum was added. Human umbilical vein endothelial cells (HUVEC) were obtained and cultured as described previously [1]. The matrices were incubated at 37°C for 2 hours, after that 2 x 10^4 of HUVEC cells in 100 μl of IMDM culture medium with 10 % serum were added and incubated in 37°C, 6 % CO_2 for next 24 hours. Control cells were incubated in wells of 48 well microplates equipped with plastic rings. After the incubation 20 μl of AlamarBlue reagent was added into the each well.

Table

Average diameter and pore size of electrospun scaffolds

Polymer	Fiber diameter, μm	Pore size, μm
PLGA	2.05 ± 0.12	6.6 ± 0.22
PCL	1.6 ± 0.40	7.0 ± 0.57
Nylon 6	0.8 ± 0.21	3.0 ± 0.37

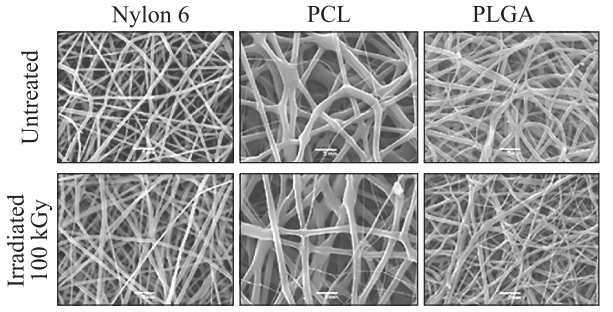

Fig. 1. *SEM Scaffolds morphology before and after irradiation*

After the incubation in CO_2 incubator for 6 hours, OD of the culture medium was assessed at 570/620 nm.

RESULTS AND DISCUSSION

Characterization of morphology of Nylon 6, PCL and PLGA scaffolds

The structure of the obtained scaffolds was investigated by scanning electron microscopy. All samples consist of uniform fibers (Fig. 1). The average diameters for Nylon 6, PCL and PLGA fibers are presented in the Table.

The matrices were irradiated at doses from 0–250 kGy with irradiation increment 25 kGy Considering heat capacity of PCL as 1600 J/kg·°C, and its melting temperature as 60 °C (other polymers have higher Tm) the irradiation power necessary to melt PCL could be estimated as $C \times m \times dT = Q$, $C \times \times dT = Q/m$ ($J/kg = C$). To melt PCL the material should be irradiated with the energy $Q/m = 1.6 \times \times 10^3 \times 0.6 \times 10^2 = 96$ kGy. As far as we treated the scaffolds with discrete dose (~1 min intervals and in a ventilation box) the scaffolds are not apt to be melted at least at irradiation dozes lower than 200 kGy. Actually, SEM demonstrated that scaffolds do not change their morphology and microstructure after irradiation (Fig. 1).

Tensile strength

Before and after irradiation the samples were cut into rectangular specimens of size 10 × 40 mm, and tested on a mechanical testing machine. Stress-strain diagrams demonstrate that EBI scaffolds made of Nylon 6 and PLGA decrease elastic region and strength in plastic region. On the contrary, EBI increased the strength in the area of elastic region for PCL scaffolds along with irradiation dose. At the dose of 100 kGy, the stiffness in the area of elastic region (proportional limit) increased almost twice from 1.2 ± 0.2 MPa to 2.1 ± 0.3 MPa. It

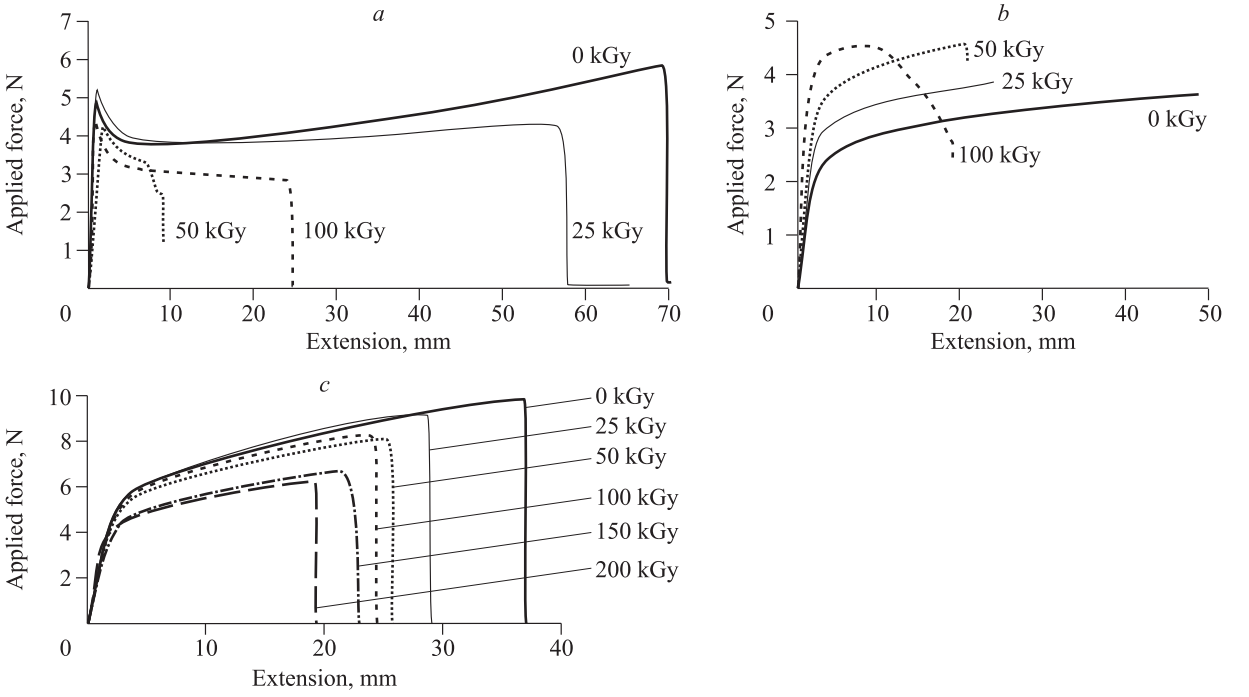

Fig. 2. *Typical stress-strain diagrams of 3D matrices PLGA (a), PCL (b), and Nylon 6 (c). All matrices were tested in the fiber laying direction in triplicate*

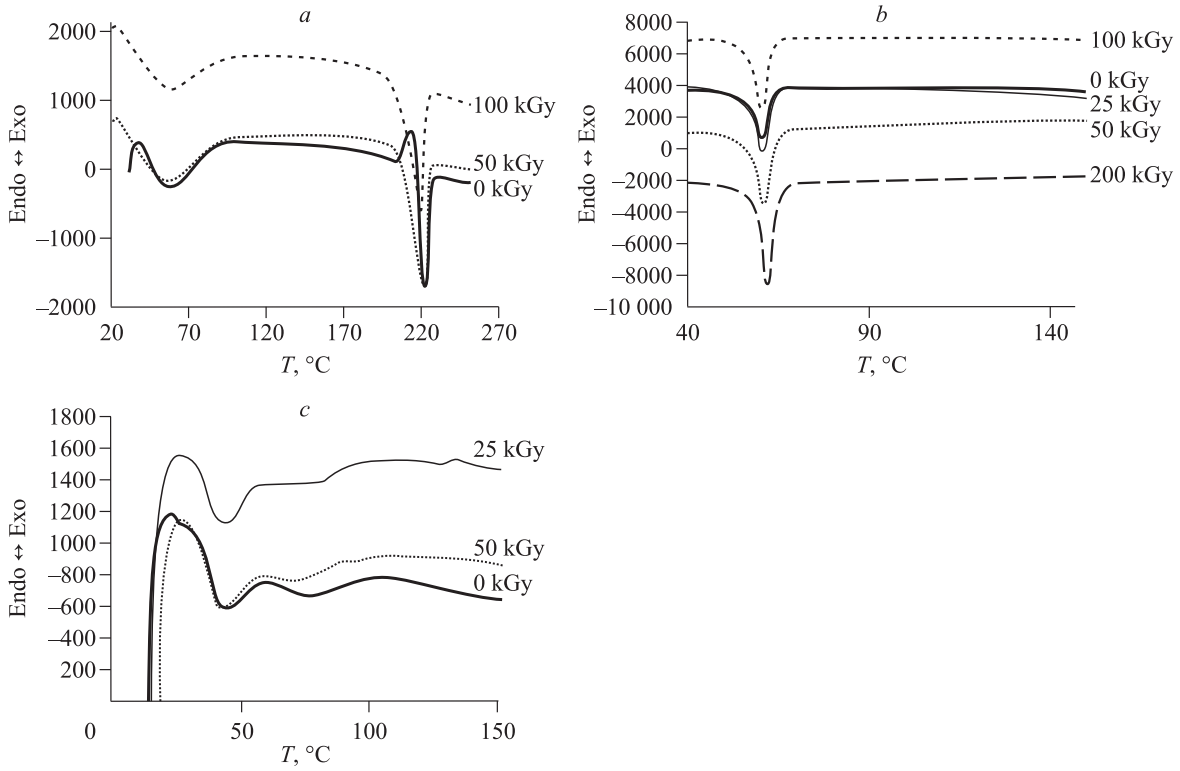

Fig. 3. *Differential scanning spectroscopy of irradiated and nonirradiated electrospun scaffolds, produced from Nylon 6 (a), PCL (b) and PLGA (c)*

should be also noted that the EBI in a dose 25 kGy, which is used for sterilization of medical products, does not interfere with stiffness of the matrices and can be used also for sterilization of electrospinning produced scaffolds (Fig. 2).

Differential scanning spectroscopy

We considered that irradiation would interfere with the crystallinity of polymers, but the data of Differential Scanning Calorimetry did not demonstrate strong effects. It is possible to form interconnections between polymer aggregates that can be generated during electrospinning due to spinodal decomposition of polymer solution [3] (Fig. 3).

Introducing the stiffness zones into tubular electrospun construction.

The illumination of the material through the perforating template allowed us to obtain more stiffness areas in vascular grafts produced by electrospinning from PCL. Tubular structures with inner diameter 1.7 mm and wall thickness 200 μm were irradiated through a steel grid as shown on Figure 4 (a, b). After incubation of the tube in the solution of fluorescently labeled albumin, protein adsorption occurred mainly in the irradiated areas. Thus, irradiation led to modification of the irradiated surfaces. Vascular grafts with stiffeners have twice as great elastic deformation limit and kinked resistance, ~1.5 times lower bend radius. Cyclic hydrodynamic load (10^6 cycles of 0/200 mmHg) (data not shown) did not interfere with the mechanical properties and did not lead to disaggregation of the vascular graft in the interzone areas, demonstrating the efficacy of the approach for the introduction of webbings into electrospun produced goods.

In vitro degradation of irradiated and nonirradiated electrospun matrices

It was shown that EBI decreased the stiffness of the PLGA and Nylon 6 matrices. Therefore, we evaluated the influence of EBI on the degradation rate of the matrices in vitro. The structure of PCL

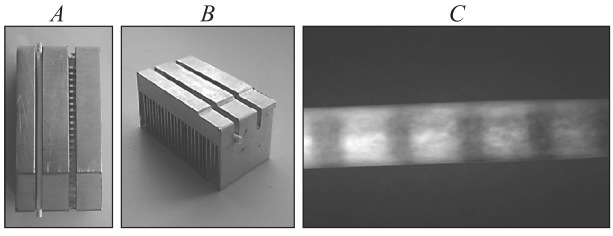

Fig. 4. *Introduction of the stiffeners into the small diameter vascular graft. Bottom (A) and side (B) views of the duralumin templates used for the production of the electron beam irradiated regions in the vascular grafts. (C) Irradiated (light) and not irradiated (dark) areas of the graft, obtained after its incubation with the solution of the fluorescein labeled BSA (fluorescent image obtained using the SteReo Discovery V12)*

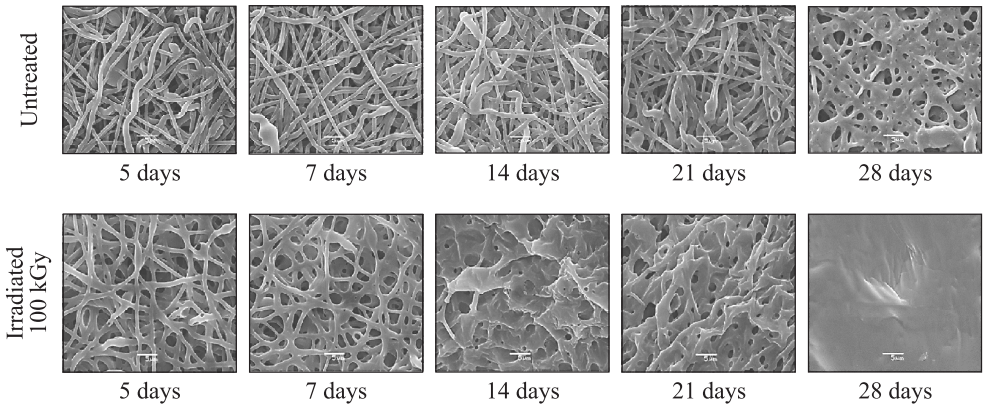

Fig. 5. *Degradation rate of the untreated and irradiated PLGA matrix*

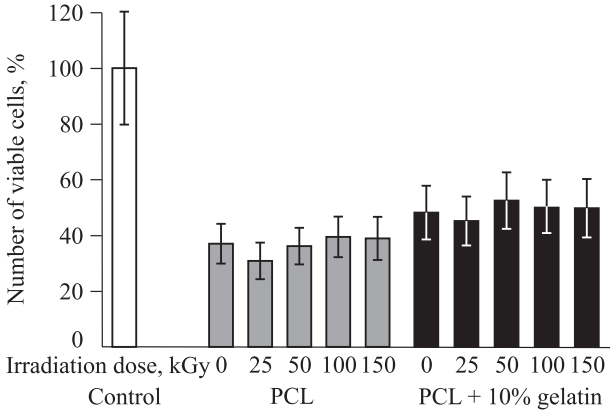

Fig. 6. *Viability of endothelial cells cultivated on the surface of different irradiated and nonirradiated matrices*

and nylon matrices was not significantly changed after incubation in PBS at 37 °C for 7 weeks (data not shown). However, PLGA matrices were shown to degrade faster in compared to non-irradiated scaffold (Fig. 5). Thus, EBI could be used for decreasing the degradation rate, not only for PLGA but also for other similar polymers.

Cell viability test

To evaluate the cell viability, HUVEC cells were cultivated on the surface of tissue culture plastic as a control and on the surface of irradiated matrices of PCL and PCL with 10% of gelatin in fiber. The cell viability was measured by cell viability reagent Alamar Blue (Life Technology production). It was noticed that the cells that were grown on the surface of the irradiated and nonirradiated matrices had no significance (Fig. 6).

CONCLUSIONS

Using electrospinning nonwoven scaffolds from Nylon 6, PCL and PLGA were fabricated. It was shown that EBI of the matrices produced from PCL by a dose of 100 kGy increases the proportional limit of the material and allowed us to introduce a durable region into the vascular grafts by irradiating the graft through the template with open areas. In contrast, EBI decreases the stability of PLGA scaffolds and could be used for increasing the degradation rate of polyester scaffolds. Electron beam irradiation was not shown to interfere with biocompatibility of scaffolds and could be used for scaffold sterilization.

ACKNOWLEDGMENTS

This work was supported by a Russian Science Foundation grant (№ 14-15-00493).

REFERENCES

1. *Cherepanova A.V., Bushuev A.V., Vlassov V.V., Laktionov P.P.* Cell-surface-bound DNA inhibits poly(I:C)-activated IL-6 and IL-8 production in human primary endothelial cells and fibroblasts // Circulating Nucleic Acids in Plasma and Serum. Ed. P.B. Gahan. Springer, 2011. 207–211.

2. *Khorshidi S., Solouk A., Mirzadeh H. et al.* A review of key challenges of electrospun scaffolds for tissue-engineering applications // J. Tissue Eng. Regen. Med. 2015. [Epub ahead of print].

3. *Madurantakam P.A., Cost C.P., Simpson D.G., Bowlin G.L.* Science of nanofibrous scaffold fabrica-

tion: strategies for next generation tissue-engineering scaffolds // Nanomedicine. 2009. 4. (2). 193–206.

4. *Pham Q.P., Sharma U., Mikos A.G.* Electrospinning of polymeric nanofibers for tissue engineering applications: a review // Tissue Eng. 2006. 12. (5). 1197–1211.

5. *Wu J., Soucek M.D., Cakmak M*. Effect of electron beam radiation on tensile and viscoelastic properties of styrenic block copolymers // Polym. Eng. Sci. 2014. 54. (12). 2979–2988.

ВЛИЯНИЕ ОБЛУЧЕНИЯ ПУЧКОМ ЭЛЕКТРОНОВ НА ФИЗИКО-ХИМИЧЕСКИЕ ХАРАКТЕРИСТИКИ МАТРИЦ, ИЗГОТОВЛЕННЫХ МЕТОДОМ ЭЛЕКТРОСПИННИНГА

Алёна Олеговна СТЕПАНОВА[1,2], Михаил Васильевич КОРОБЕЙНИКОВ[3], Александр Сергеевич ЮНОШЕВ[4], Павел Петрович ЛАКТИОНОВ[1,2]

[1] Новосибирский НИИ патологии кровообращения им. академика Е.Н. Мешалкина Минздрава России
630055, г. Новосибирск, ул. Речкуновская, 15

[2] ФГБУН Институт химической биологии и фундаментальной медицины СО РАН
630090, г. Новосибирск, пр. Академика Лаврентьева, 8

[3] ФГБУН Институт ядерной физики им. Г.И. Будкера СО РАН
630090, г. Новосибирск, пр. Академика Лаврентьева, 11

[4] ФГБУН Институт гидродинамики им. М.А. Лаврентьева СО РАН
630090, г. Новосибирск, пр. Академика Лаврентьева, 15

Исследовано влияние облучения пучком электронов на прочность, стабильность и биосовместимость матриц, изготовленных методом электроспиннинга, из нейлона 6, поликапролактона (PCL) и сополимера молочной и гликолевой кислот (PLGA). Показано, что облучение матриц электронным пучком, генерируемым ускорителем электронов ИЛУ-6 (2,2 МэВ, 400 мА, 10 Гц, ФГБУН Институт ядерной физики СО РАН) потенциально может быть использовано для их стерилизации (доза облучения 25 кГр не влияет на механические свойства всех исследованных матриц). Облучение матриц, изготовленных из PCL, в дозе 100 кГр увеличивает предел упругой деформации материала и позволяет ввести прочные участки в структуру протезов сосудов, облучая трансплантаты через шаблон с открытыми участками. Электронно-лучевое облучение матриц не влияет на их способность поддерживать адгезию и жизнеспособность первичных эндотелиальных клеток человека на поверхности этих матриц, как это было показано с помощью анализа на жизнеспособность Alamar Blue.

Ключевые слова: облучение пучком электронов, электроспиннинг, PCL, PLGA, Nylon 6.

Степанова А.О. *– младший научный сотрудник лаборатории молекулярной медицины, лаборатории биомедицинских технологий центра новых технологий, e-mail: lebedeva@niboch.nsc.ru*
Коробейников М.В. *– к.тех.н.*
Юношев А.С. *– к.ф.-м.н., зав. лабораторией высокоскоростных процессов отдела взрывных процессов.*
Лактионов П.П. *– к.б.н., в.н.с., зав. лабораторией молекулярной медицины, зав. лабораторией биомедицинских технологий центра новых технологий, e-mail: lakt@niboch.nsc.ru*

УДК 004.942

THE INFORMATION COMPUTATION SYSTEM FOR GENETIC DATA ANALYSIS ON THE BASIS OF A PERMUTATION TEST

Valeriy Viktorovich KOVALEVSKY[1], Marat Samatovich KHAIRETDINOV[1,2], Aleksandr Aleksandrovich YAKIMENKO[1,2], Mikhail Vladimirovich GRISHCHENKO[2]

[1] *Institute Computational Mathematics and Mathematical Geophysics of SB RAS*
630090, Novosibirsk, Lavrent'ev's ave., 6

[2] *Novosibirsk State Technical University*
630073, Novosibirsk, Karl Marks ave., 20

The genetic data analysis using the hybrid supercomputer has been performed. The architecture of the information computation system of search for traits of genes statistically significant overrepresented characteristics from the given set has been presented. The capabilities of one-level paralleling are demonstrated, and methods of modernization of the developed software are proposed. Modern technologies of paralleling are used.

Keywords: genetic hypotheses, multiple testing, permutation test, GPU, computer technology, information system.

Genetic analysis relates to the branch of genetics dealing with mechanisms of genetic determination of traits. Here problems of formal genetics associated with formalization of inheritance models and testing of genetic hypotheses on specific empirical material occupy an important place. Resampling methods are widely used to solve such problems [1, 3]. These methods were chosen, since they do not need any information about the data distribution law in the general population, but investigate sample data in various combinations, as if considering them from different angles. When using resampling methods there is no need to correct the statistical significance level for simultaneous testing of many statistical hypotheses reflecting, in the case of biological data analysis, the contribution of many factors to the formation of one hereditary trait. In most biological investigations, resampling methods are more correct than analytical methods, but require much computer power.

To apply the above-mentioned methods, the authors developed a parallel computer information technology of search for statistically overrepresented traits of genes under various external or internal conditions implementing the permutation test algorithm [6] using graphic processors. However, the number of requirements to the earlier created technology increases: First of all, the set of genetic hypotheses tested simultaneously, as well as the calculation efficiency, increase. There also emerged new requirements to the organization of remote access to the permutation test program and delivery of results to the user, to the creation of a medium for exchange of experience, and bibliographical data on this subject. This stimulates further development of this technology on a hybrid supercomputer, which is the goal of this paper.

ARCHITECTURE OF THE COMPUTER INFORMATION SYSTEM

The general structure of the program is presented in Fig. 1. The program is implemented at the following three major stages: 1) reading of the input file and formation of data arrays in a form convenient for further calculations; 2) calculation of the sums (or any other quantities, for instance, means, variances, etc.) of measured values of a gene for its

Kovalevsky V.V. *– doctor of technical sciences, deputy director for science, head of laboratory for geophysical informatics, e-mail: kovalevsky@sscc.ru*
Khairetdinov M.S. *– doctor technical sciences, professor, head of the chair for network information technologies, e-mail: marat@opg.sscc.ru*
Yakimenko A.A. *– candidate of technical sciences, associate professor, e-mail: yakimenko@corp.nstu.ru*
Grishchenko M.V. *– student, e-mail: mikhail.grishch@gmail.com*

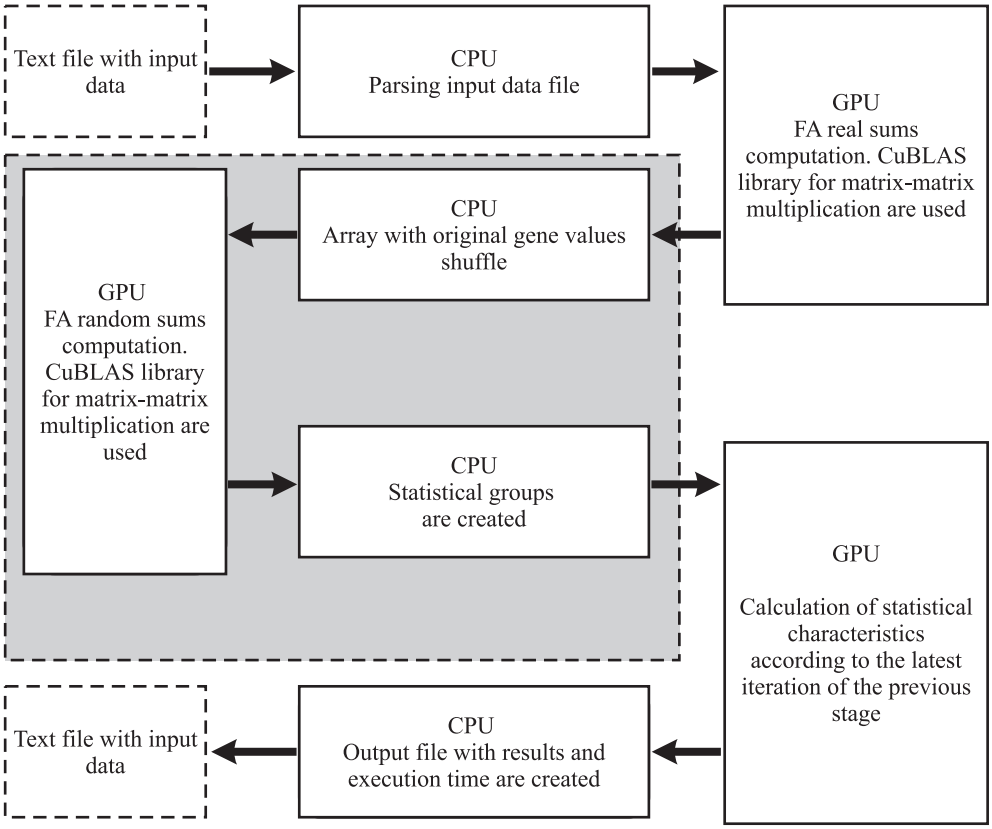

Fig. 1. *Program execution structure*

various properties (for instance, functional annotations, FAs), the cycle with mixing of array elements and obtaining of quantities necessary for statistics; 3) calculation of p-values and formation of a file with the results.

At the first stage, there are two text files at the input: one file with the parameters of a permutation test (the number of iterations and the number of permutations in an iteration), and the other with the input data. The input data file must be read into the main memory and represented as data structures convenient for work. The file format is shown in Fig. 2. Here informative data are the identifiers of functional annotations and characteristics of a gene. Their representation plays an important role in increasing the program speed. For this it is reasonable to present the data in the form of two arrays (instead of the structure std::map) to store information about genes: a two-dimensional array reflecting FA inputs into the gene, and a one-dimensional one containing measured characteristics of the gene. This approach makes it possible to decrease the number of data transmitted to the graphic processor memory and use the standard library CuBLAS for matrix-vector multiplication.

Due to some peculiarities of calculations on the GPU [2, 5], paralleling of a large part of the code is not possible. Therefore, only the algorithm for calculating the sums of values of measured characteristics of genes for each of the available FA was implemented on the GPU. This algorithm is in the following: a set of functional annotations is represented in the form of a two-dimensional array with zeroes and unities. The available genes are in the rows, and the FAs constituting them, in the columns. Thus, unity will be at the corresponding place of a FA included in a gene, and zero otherwise. Then matrix-vector multiplication of this transposed MxN array (where M is the number of rows, and N is the number of columns) by a one-dimensional N array containing the values of gene characteristics will result in an array with the sums of FAs of all genes.

FURTHER DEVELOPMENT OF THE SYSTEM

Several hypotheses with the same set of functional annotations should be verified. In this case, the values of gene characteristics are represented not by a vector, but by an MxK matrix (where M is the number of genes, and K is the number of hypotheses) in which every column is a hypothesis. As a result, we have a two-dimensional NxK array, in which N is the number of FAs [7]. The following changes were made in the existing algorithm to simultaneously verify several hypotheses:

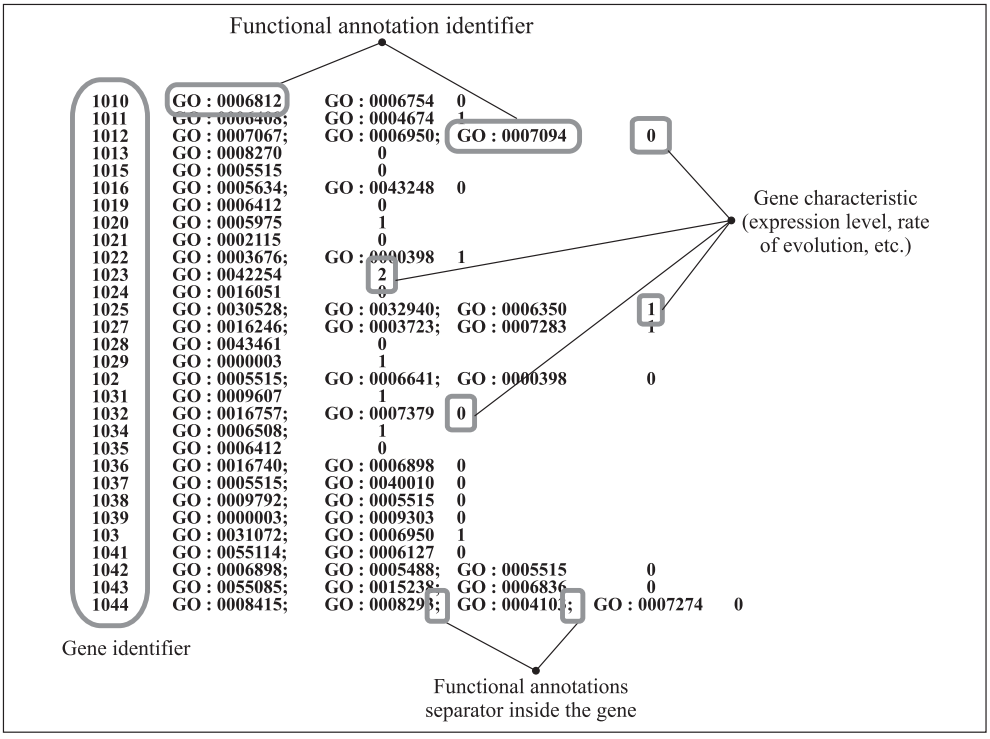

Fig. 2. *Representation of a gene in the input file*

- Multiple testing of hypotheses by replacing matrix-vector multiplication with matrix-matrix multiplication (Fig. 3) was added. The resulting matrix contains a set of arrays with the sums of FAs of all genes for the hypotheses in question.
- Element-by-element permutations of gene characteristics were replaced by permutations of arrays of gene characteristics. This is admissible, because in the general case all hypotheses are independent and independent permutations of the values of gene characteristics are not needed.

Fig. 4 shows how introducing multiple testing of hypotheses affects the total time of the program execution. The program execution time without multiple testing of hypotheses using matrix-vector multiplication is shown by a thin line. It can be interpreted as successive program start a certain number of times. The time spent for simultaneous testing of a certain number of hypotheses using matrix-matrix multiplication is denoted by a heavy line. Thus, for one experiment an advantage of matrix-vector multiplication is evident. This is due to the fact that the function for matrix-vector multiplication is somewhat simpler than that for matrix-matrix multiplication. The larger is the number of hypotheses being tested, the greater is the advantage (as can be expected).

The next step in the program development was to develop architecture of the computer information system (CIS) for organization of remote access to the permutation test program. The CIS includes a

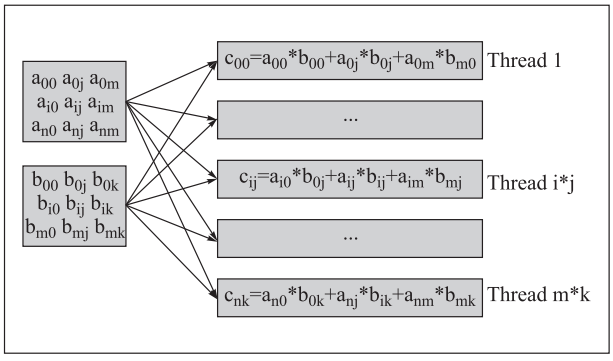

Fig. 3. *Representation of matrix-matrix multiplication*

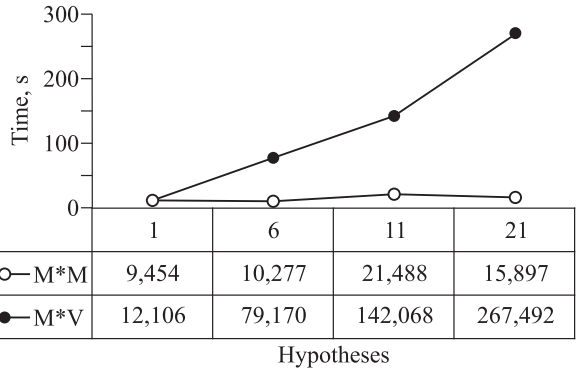

Fig. 4. *Comparison of the execution times of single and multiple testing of hypotheses (M*M – matrix-matrix multiplication, M*V – matrix-vector multiplication)*

medium for exchange of experience and bibliographical data on the subject, organization of efficient remote calculations, and delivery of the results to the user. The system must be well protected against unauthorized access and based on modern technologies. It can be represented as a set of the following components:

- Web server;
- Internet portal;
- Database.

The web server is responsible for the CIS operation logic, that is, for acquisition and processing of users' personal data and compilation of a configuration file to start the permutation test program on the GPU.

The Internet portal allows the users to work with the permutation test in the self-service mode. For this, the site has a system of authorization and registration of users.

The framework Django for the programming language Python was taken for the web server. It was chosen because of its modular character, cross-platform type, and free distribution. Django uses the object approach to work with the database, which greatly simplifies the process of data storage and processing.

The use of the Python makes it possible to maximally simplify user data processing, in particular, the configuration file formation to perform the permutation test.

To store data it was decided to use the database SQLite3 built in the Python. Since SQLite is not an individually operating process but only a library, calls of functions (API) are used as the exchange protocol, which decreases the burden and response time, and simplifies the program. SQLite stores the entire database in one file, which simplifies operation with transactions. During the execution of a transaction the database file is simply blocked. The structure of the developed database is shown in Fig. 5.

At registration of a new user, a name directory to store the configuration and job files is created on the server.

To increase the efficiency of CIS operation, the server has a function of choosing a method for the permutation test execution. If the number of iterations in the configuration file exceeds 100000, the problem must be sent to the hybrid supercomputer; otherwise it is executed by the server itself.

Providing wide access to the computational resources brings up the question of organizing safety. The simplest preventive measure of protection is hiding the reference to the problem execution for unauthorized users.

To protect the internet portal forms, protection against cross site request forgery (CSRF) built in Django is used. For this, a unique hash key is created on the server when a form is initialized, and a new hash key is created when data from the form are sent, which is then sent to the server for verification. If the keys coincide, the form was not changed and the data can be processed; otherwise the server issues an error message.

To increase the efficiency, the program algorithm of the system must be optimized. This can be achieved in different ways.

Primary processing of input data is performed in several stages: 1) reading of the file with initial data; 2) isolation of groups: FA set, gene identifier, gene characteristic; 3) formation of a matrix with FA inputs into the gene and a matrix with measured gene characteristics. Stages 2 and 3 can be paralleled on the CPU. Since genes are independent, the

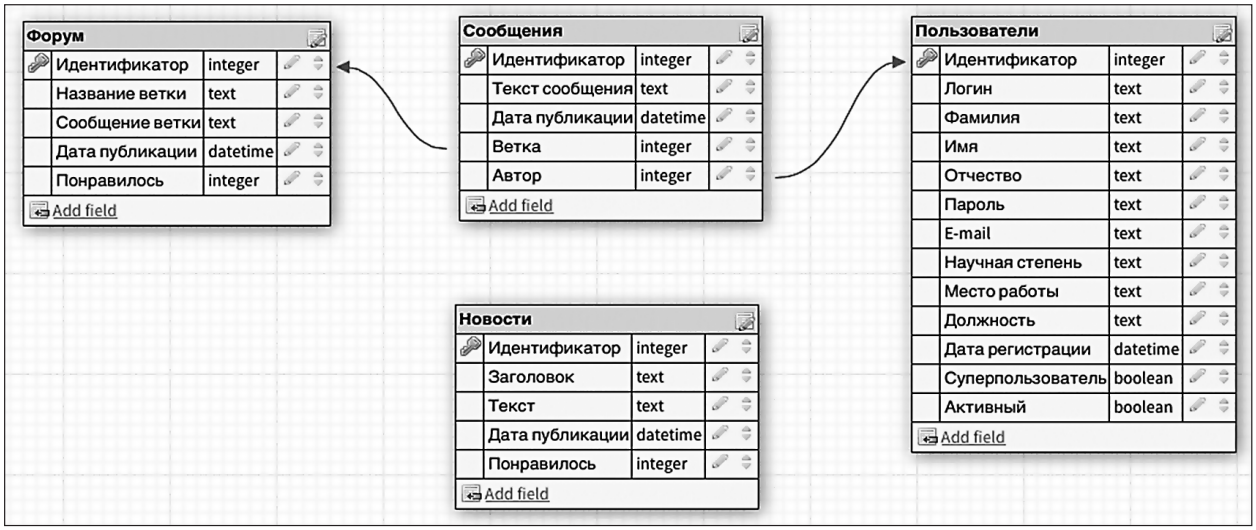

Fig. 5. *Database structure*

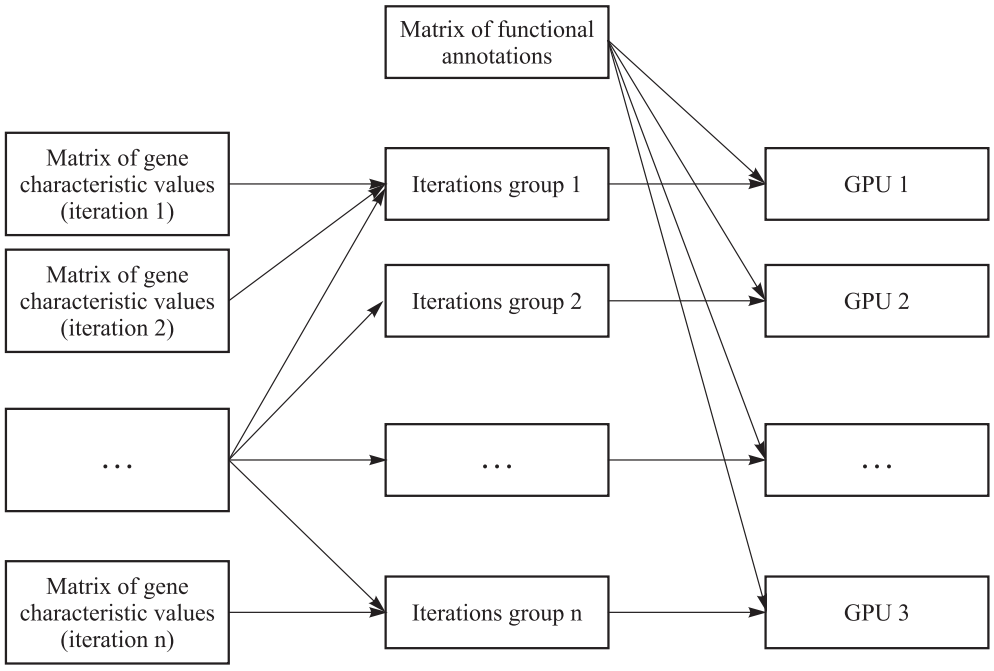

Fig. 6. *Paralleling of permutation cycle iterations*

isolation of groups and formation of matrices with FA inputs in the gene and measured characteristics of the gene can be done independently for each gene.

Iterations of the permutation test are also independent of each other. Therefore, they can be performed simultaneously on several GPUs, which will provide a multiple increase in the efficiency of the system being described (Fig. 6).

CONCLUSIONS

Some results of further development of the computer information technology of a permutation test for genetic data analysis on a hybrid supercomputer are presented, including the function of multiple testing of genetic hypotheses using matrix-matrix multiplication on graphic processors and increasing the calculation speed. The methods of analysis and representation of the input data file in the main computer memory have been improved. The requirements to the software for its introduction into the information system are described.

An information system including a webserver forming a basis for the internet portal operation and a database have been developed and created. Within the framework of the internet portal, mechanisms of registration and authorization of the users have been implemented. A forum to communicate within the internet portal and support feedback between the users and developers has been created. Access to the permutation test program by means of the created information system has been provided.

This work was supported by the grant RFBR 16-37-00240mol_a.

REFERENCES

1. *Ashburner M., Ball C.A., Blake J.A. et al.* Gene ontology: tool for the unification of biology. The Gene Ontology Consortium // Nat Genet. 2000. 25. 25–29.

2. *Boreskov A.V., Kharlamov A.A., Markovkiy N.D. et al.* Parallel computations on the GPU. CUDA architecture and software model. Moscow: Publ. House of Moscow Univ., 2012. 336 p.

3. *Efron B.* Nontraditional methods of statistical analysis. Moscow: Finansy i statistika, 1988. 263 p.

4. *Good P.* Permutation, parametric and bootstrap tests of hypotheses. New York: Springer Verlag, 2005. 315 p.

5. *Van Hemert J.L., Dickerson J.A.* Monte Carlo randomization tests for large-scale abundance datasets on the GPU // Comput Methods Programs Biomed. 2011. 101. 80–86.

6. *Yakimenko A.A., Gunbin K.V., Khairetdinov M.S.* Search for the overrepresented gene characteristics: The experience of implementation of permutation tests using GPU // Optoelectronics, Instrumentation and Data Processing. 2014. 50. (1). 123–129.

7. *Yakimenko A.A., Khairetdinov M.S., Avrorov S.A.* Development of a parallel program to perform a permutation test with the use of GPU // Actual problems of electronic instrument engineering APEIE-2014: abstracts of 12th Int. Conf., Novosibirsk, 2–4 Oct. 2014. Novosibirsk: NSTU, 2014. 1. 723–727.

ИНФОРМАЦИОННО-ВЫЧИСЛИТЕЛЬНАЯ СИСТЕМА ДЛЯ АНАЛИЗА ГЕНЕТИЧЕСКИХ ДАННЫХ НА ОСНОВЕ ПЕРЕСТАНОВОЧНОГО ТЕСТА

Валерий Викторович КОВАЛЕВСКИЙ[1], Марат Саматович ХАЙРЕТДИНОВ[1,2], Александр Александрович ЯКИМЕНКО[1,2], Михаил Владимирович ГРИЩЕНКО[2]

[1] ФГБУН Институт вычислительной математики и математической геофизики СО РАН 630090, г. Новосибирск, пр. Лаврентьева, 6

[2] ФГБОУ ВПО Новосибирский государственный технический университет 630073, г. Новосибирск, пр. Карла Маркса, 20

В статье представлена архитектура информационно-вычислительной системы для поиска признаков статистически значимых перепредставленных характеристик генов из заданного множества. Показаны возможности одноуровнего распараллеливания и предложены пути модернизации разработанного программного обеспечения. Использованы современные технологии распараллеливания.

Ключевые слова: генетические гипотезы, множественное тестирование, перестановочный тест, GPU, вычислительная технология, информационная система.

Ковалевский В.В. *– д.т.н., зам. директора по научной работе, зав. лабораторией геофизической информатики, e-mail: kovalevsky@sscc.ru*
Хайретдинов М.С. *– д.т.н., профессор, зав.кафедрой сетевых информационных технологий e-mail: marat@opg.sscc.ru*
Якименко А.А. *– к.т.н., доцент каф. ВТ, e-mail: yakimenko@corp.nstu.ru*
Грищенко М.В. *– студент, e-mail: mikhail.grishch@gmail.com*

УДК 57.084.1

PROBLEMS OF INVESTIGATIONS IN SPHERE OF ELECTROMAGNETIC FIELDS IMPACT ON BIOLOGICAL OBJECTS

Anna Vladimirovna BUSYGINA, Maxim Evgenyevich KOMNATNOV, Olga Albertovna MATVEYENKO

Tomsk State University of Control Systems and Radioelectronics
634050, Tomsk, Lenin av., 40

Problems of the investigations in the sphere of electromagnetic fields impact on biological objects in the TEM-cell have been considered. Researches on biological objects exposed to electromagnetic fields (cell cultures, plants, worms, insects, animals) have been systematized. Features of devices for climatic (temperature, humidity, CO_2 and nutrients) and electromagnetic exposure needed for research of specific biological objects have been described. The need for temperature control and video monitoring during the research on biological objects exposed to electromagnetic fields has been justified. The results presented may be useful for development of research methods for investigation of the electromagnetic fields impact on specific biological objects, as well as for the development of technical requirements in order to provide devices useful for such studies.

Keywords: biological objects, electromagnetic fields, TEM-cell.

Nowadays, people are exposed to various technogenic factors, one of which is the electromagnetic radiation (EMR). As a result of technological development in the recent decades, the prevalence of this factor increases. It has been found that the EMR impacts molecular genetics, biochemical, and physiological processes in living organisms, so it is impossible to overestimate the importance of this factor for human [4, 6, 20, 27].

Electromagnetic fields (EMF) are still widely used in medicine. For example, magnetic resonance imaging (MRI) is one of the safest methods of diagnostics. Pulsed magnetic fields are used to treat fractures, as they increase the rate of accretion of bone tissue [25]. However, there is an opinion that EMF has negative effects, for example, it increases the risk of neoplasia. At the same time, there are no definitive results showing the carcinogenic nature of EMR. The experimental evidence being not sufficient, the radiofrequency (RF) EMF has been classified as «possibly carcinogenic to humans» [2].

Trends in the development of modern electronic devices (increase of the signal frequency spectrum; growth of computational performance and etc.) cause the increase in the intensity of the human exposure to the EMF. People use devices with wireless communication systems (mobile communication, Bluetooth, Wi-Fi, 3G) in everyday life, thus, their impact on the body should be studied carefully.

The abovementioned highlights the need for a thorough study of the mechanisms of the biological effects of EMF [26], and, therefore, it is necessary to develop methods and devices for the study of EMF impact on the living tissue [11].

Purpose of this article is to highlight important topics in the area of electromagnetic fields impact on biological objects (BO), identify main issues of research and their possible solutions.

EXPOSURE DEVICE

A transversal electromagnetic mode (TEM) cell is one of the most common devices for research on the effect of EMF. This device was originally developed for the research and testing in the area of electromagnetic compatibility (EMC) [3]. The TEM-cell consists of the central conductor and three volumetric parts of rectangular cross-section, two of which have a linear expansion of the cross sections

Busygina A.V. *– postgraduate student of department of television and control, e-mail: bav-tusur@mail.ru*
Komnatnov M.E. *– junior researcher of scientific research laboratory of safety electromagnetic compatibility, e-mail: maxmek@mail.ru*
Matveyenko O.A. *– candidate of biological sciences, researcher of scientific research laboratory of safety electro–magnetic compatibility, e-mail: alterra@inbox.ru*

in the shape of a pyramidal horn, and the third part is shaped as a cube with a regular cross section along the cell, in which the object of the study is placed (Fig. 1). EMF excited by the high-frequency generator inside the TEM-cell affects the equipment under test (EUT).

Nowadays, the construction of the TEM-cell is being improved, which allows the researchers to conduct a wider range of tests on interference immunity and interference emission of various radioelectronic devices, and also to conduct the research in biophysics and biomedicine.

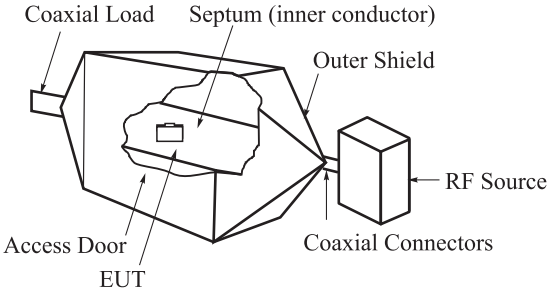

Fig. 1. *Standard construction of the TEM-cell*

BIOLOGICAL OBJECTS AND RESEARCH FACTORS

As various BO are exposed to EMF during the experiments, the establishment of specific conditions typical for a particular object is required. Special design solutions are also required in order to place a BO inside the TEM-cell and ensure its correct positioning and fixation.

Cell cultures

To investigate the EMF impact on living tissues, the human cells were used (promyelocytes [27], fibroblasts [5, 26], leucocytes [18], amnion epithelial cells [15, 16, 29]) and animal cells as well (rat myocytes, guinea-pig myocytes [19], neuronal cells [22]).

Cells can be cultured as monolayers [19, 26], using the artificial substrate in a Petri dish, or they can be grown in suspension [26]. In paper [26] the uniformity of electromagnetic energy absorption was provided for the area of the monolayer less than 50 cm^2 and the volume of the suspension less than 10 ml. The cell monolayer was divided into several Petri dishes, which were placed in the TEM-cell, and the suspension was also divided into several dishes. To investigate these objects, a special system of holders has been developed in order to place the Petri dishes inside the TEM-cell (Fig. 2).

Linz *et al.* [19] used round acrylic chamber (inner diameter 10 mm, height 6 mm) for experiments on the effects of radio frequency fields (RF) on the membrane potential; action potential and on the work of the L-type calcium channels of ventricular myocytes in suspension (total volume of 200 ml). It was found that the RF fields do not affect the resting potential and the action potential of the cell membranes. However, the authors note that other types of Ca^{2+} channels, such as N-type, which can be found in neurons only, might be susceptible to RF fields.

Research is conducted to identify the level of DNA damage caused by the EMF exposure. Thus, in paper [5] the human fibroblasts and rat granulosa cells were used as biological material, they were placed in the Petri dish with a diameter of 35 mm. Six Petri dishes were exposed to the EMF at the same time. The experimental results showed that RF EMF exposure causes single- and double-strand DNA breaks. The researchers emphasize that DNA damage can't be caused by thermal effects.

Several researches are conducted to investigate the impact of EMR on the protein structure. For example, [30] during the analysis of the impact of pulsed electric field and temperature on the structure of chicken egg lysozyme, Zhao and Yang have found changes in the conformation of the active site of the protein, inhibiting the binding of substrate to the protein and destabilizing the protein structure.

Plants

Much attention is given to research on the impact of EMF on plants, as they are an essential element of the Earth's ecosystem. For example, plant *Lemna minor* is the object of study in [20]. Plants of experimental and control groups were grown in the laboratory in a growth chamber and then were moved into the TEM-cell for the experiment, afterwards they were returned to the starting position. Such movements are stressful for the plants and affect the reliability of the results of the experiment, so it is necessary to exclude the movement of the objects during the experiments. Du-

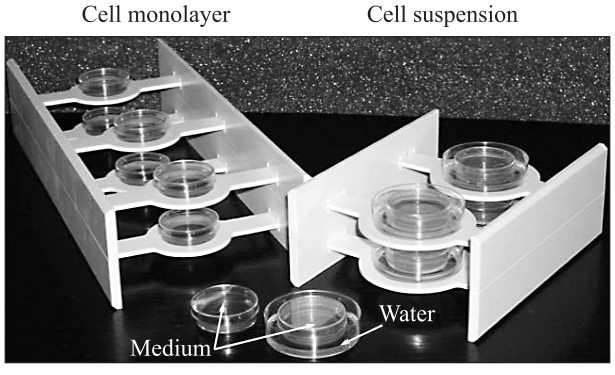

Fig. 2. *Petri dish holders for cell monolayer and cell suspension [26]*

ring the investigation, the negative impact of electromagnetic fields on growth of the *Lemna minor* was revealed (reduction in the number of leaves in the second week of the experiment comparing to the control plants).

Worms

In the paper [4] devoted to the impact of continuous microwave fields on the nematode *Caenorhabditis elegans*, De Pomerai *et al.* have found that the heat shock proteins are generated, and the nematodes are growing in the accelerating rates.

To track a possible temperature rise associated with microwave radiation, the small volumes (0.2 ml) of concentrated suspension with nutrient medium and worms (in ratio of 1 to 2) were exposed to the radiation. In order to check the results of the experiment, identical, but shielded, control samples were placed nearby the experimental ones.

Animals

Researches on the impact of EMF on the whole body are carried out using laboratory animals, and this represents new challenges to developers. The animal is placed in the TEM-cell, so the field will be greatly distorted due to inhomogeneity. In paper [21] it has been shown that theoretical modeling can be used to determine the field distortion in the TEM-cell caused by the presence of structures with losses. It has also been shown that the distribution of field and the power absorbed in the structure depends on the size and the position of an object in a TEM-cell. Images obtained from magnetic resonance or computed tomography can be used as a realistic three-dimensional model of an animal.

For example, experiments on animals have been implemented in the paper of Gatta *et al.* [7], who investigated the impact of EMF on the proliferation of mouse spleen lymphocytes. During the exposure the mice were placed into the individual transparent boxes with holes for air circulation. To increase the uniformity of the field exposure, the mice inside the cell were rotated clockwise all the time. The control group of mice was also placed in the TEM-cell (under similar conditions), but not exposed to the electromagnetic field. The results of this study did not show statistically significant differences in the rate of lymphocyte proliferation neither in the experimental, nor in the control groups exposed to the EMF of various power.

In paper [1] the system which can place up to 12 adult mice has been demonstrated, the length of the TEM-cell in this case is 120 cm. The mice were placed into the in groups of two. To ensure the proper location in the cell, the adult mice were placed inside the cylindrical devices fitted with small holes for evaporation, which were made of materials that do not affect the parameters of exposure, newborn mice were wrapped in the gauze and were placed in the polystyrene blocks.

Insects

Panagopoulos *et al.* [23] investigated the impact of the EMR in the near field antenna of a cell phone on the fertility of the *Drosoplila melanogaster*. Insects were placed in a glass flask in groups of 10. Investigations have been carried out by theopen method (using the unshielded construction), which provided a controlled impact on the object. In the future, in order to achieve accurate dosimetry, systems of shielded exposure should be used. The modulated RF radiation reduces reproductive ability of insects to 50–60 %, while not modulated RF radiation reduces it to 15–20 % only.

PROLONGED STUDIES

According to [15], the scale of the biological impact of EMF exposure depends on the exposure time, and the maximum effect is achieved by prolonged exposure. During the researches devoted to the identification of the biological effects of prolonged exposure of BO to EMF, it is necessary to maintain optimal environmental conditions in the TEM-cell.

Maintenance of the conditions needed for the BO includes some basic aspects:

- Breathing. Particular level of oxygen determines vital functions of BO, so it is important to ensure unhindered access of oxygen to the BO.
- Nutrients. During the prolonged studies, BO need appropriate nutrients that provide their normal functioning. At the same time, nutrients should be delivered to the object periodically, without removing the object from the exposure.
- Temperature. Temperature level comfortable for a BO will eliminate additional stress, which can affect the results.

For example, in the studies concerning fertility of insects, it is necessary to take into account factors that affect the oviposition (temperature, humidity, the amount of nutrients and population size). Studies [23] created the following conditions: temperature 25 °C, 12 hours of light and darkness, humidity of 70 %, nutrient medium was placed on the bottom of the flask.

During the studies of the impact of EMF on the body's cells, the climatic conditions should be maintained in an incubator: temperature of 37°C and certain atmospheric conditions (95 % air / 5 % CO_2) [5, 9, 17, 18, 27, 29]. In the papers of Diem *et al.* [5]

and Merla *et al.* [22] the required level of humidity of 95 % was maintained. In paper [4], for worms the temperature 24–25 °C was maintained.

In the paper of Ardoino *et al.* [1] in order to supply air to the animals, the removable grid-wall was built into one side of the outer conductor of the TEM-cell.

The exposure system developed by Komnatnov and Gazizov [10] provided a tube through which nutrients are delivered directly to the object under exposure.

TEMPERATURE CONTROL

Previously, it was thought that the EMF has only thermal impact, but some studies have shown that there are non-thermal effects of the EMF exposure [27, 29]. Therefore, during the experiments on the EMF impact on living objects, special attention must be paid to temperature control.

- This will evaluate the role of temperature in the possible biological effects associated with EMF exposure [1, 14-16, 18].
- Maintenance of the physiological temperature level will eliminate the thermal effect, so it will provide a thorough examination of non-thermal effects.

Temperature measurements

In the study [4] the temperature of the suspension was measured after the EMF exposure: plates with samples were sequentially extracted from the incubator, the temperature was measured immediately (8 measurements per minute). Such measuring caused a decrease in the temperature of the subsequent samples comparing to the first ones.

During the experiment in the study [1] the temperature sensor was placed under the belly of the mouse for temperature control.

In [9] Kohler *et al.* used a temperature-sensitive fluorescent markers (rhodamin) for temperature control, which do not disturb cellular functions and can be used for visualization of the cellular and subcellular structures for a long period of time (up to several hours). Fluorescent lighting of the cells was performed using the light diode, which was connected to the microscope with the 1 mm quartz fiber. Besides, they used the fiber optic temperature probe for monitoring and evaluating changes in temperature inside the Petri dish, the probe was placed vertically in the cell suspension through the holes in the upper wall of the TEM-cell and the Petri dish lid [18] The other experiments also used the temperature probe, it was introduced into the device through a hole (diameter from 5 mm to 10 mm) in the structure of the TEM-cell [19, 22].

In the experiments of Ticaud *et al.* [28] and Jarrige *et al.* [8] the temperature in the Petri dish was measured by means of the electrooptical sensor. In the study [8] the sensor can simultaneously measure the temperature and a component of the electric field in a continuous wave mode or in a pulsed mode.

Cooling and heating in exposing system

Paper [26] presents the cooling mechanism, based on the rapid exchange of air by fans, when the air flows through the air intake, located in the wall of the incubator.

In the study [1] adult mice were placed in the environment at a temperature of 20 °C, while newborn mice require a temperature of about 30 °C. The system of required temperature used in this paper consists of two outer metal jackets which are connected with the upper and lower cell plates. Jackets were filled with circulating water and connected with a thermo cryostat. This system allows cooling and heating of the internal environment of the cell in accordance with the requirements of the experiment.

VISUAL CONTROL

Nowadays, constructions of TEM-cells are divided into two groups: providing the blind exposure or real time monitoring. In the blind exposure systems, the changes in the test object are measured after the EMF exposure, so it is quite difficult to track the changes in the BO. Visual control systems in real time allow to determine changes in the object exposed to the analyzed factors, avoiding extraction of the object [20, 27] and, therefore, providing continuous exposure, monitoring and evaluation of exposure.

Example of visual control was presented in the paper of Komnatnov [10]. Presented module of visual control provides the opportunity to observe real-time changes that occur in the object of research and to carry out recordings of the received data in the video format. A disadvantage of this module is that it does not have the possibility of multiple image magnification needed for experiments at the cellular level. Work in this direction is being continued.

Paper [19] also represents the exposure system with the visual control. The bottom of the experimental chamber (bottom consisted of a cover glass) in the device is located under the hole in the bottom of the plate. It allows monitoring of cells using an inverted microscope. The holes were covered with copper mesh to prevent irregularities in the device field.

In the study [9] Petri dishes containing a culture medium were placed on the microscope stage of an

inverted microscope. A small hole was made in the center of the bottom panel of the TEM-cell to observe the samples via a microscope with a long lens.

JOINT IMPACT OF THE CLIMATIC AND ELECTROMAGNETIC FACTORS

In a real life human exists in a heterogeneous environment, undergoing various factors, which together form complex interactions. It determines the necessity for a comprehensive study of exposure combinations of different factors (temperature, humidity, EMF) [14, 18, 24, 30].

As discussed in Section IV, it is necessary to maintain certain atmospheric conditions for normal physiological activity of BO. A large number of studies were carried out at 37°C, humidity 95%, it provides a purity effects of EMF exposure. The combined effects of various factors and their simultaneous impact remains unknown.

Nowadays, a device for the EMC tests («Environmental shielded TEM chamber») is being developed. This camera allows carrying out joint tests on climatic and electromagnetic immunity and emissions of small radio electronic devices [12, 13]. Due to the combination of climatic and electromagnetic factors, its application to biomedical research is actual [11].

CONCLUSION

The impact of electromagnetic radiation on biological objects is still ambiguous. Various studies have shown contradictory results. It is probably explained by the experimental methods. Various BO require specific experimental conditions, which should be considered at the stage of planning, design of the exposing device, dosimetry calculations and methods for assessing the effect of EMF. The use of shielded systems provides controlled impact on the object, it improves the accuracy and reproducibility of the results. Video monitoring in real time with multiple zoom is also needed, it allows evaluation of prolonged exposure of the microscopic biological objects to EMF. The need for continuous research emphasizes the importance of maintaining the proper life conditions for BO during the experiment. Thus, there is a necessity to develop new exposure systems and standardized methods for experiments devoted to the EMF impact on living objects.

ACKNOWLEDGMENTS

Review of biological research was supported by RFBR grant 14-29-0925, construction of environmental shielding TEM chamber was supported the state contract 8.1802.2014/K of the Russian Ministry of Education and Science, review of joint impact climatic and electromagnetic factors were carried out at the expense of RSF grant 14-19-01232 in TUSUR.

REFERENCES

1. *Ardoino L., Lopresto V., Mancini S. et al.* A radio-frequency system for in vivo pilot experiments aimed at the studies on biological effects of electromagnetic fields // Phys. Med. Biol. 2005. 50. (15). 3643–3654.

2. *Baan R., Grosse Y., Lauby-Secretan B. et al.* Carcinogenicity of radiofrequency electromagnetic fields // Lancet Oncol. 2011. 12. (7). 624–626.

3. *Crawford M.L.* Generation of standard EM fields using TEM transmission cells // IEEE Trans. Electromagn. Compatibility. 1974. EMC-16. 189–195.

4. *De Pomerai D., Daniells C., David H. et al.* Microwave radiation induces a heat-shock response and enhances growth in the nematode Caenorhabditis elegans // IEEE Trans. Microw. Theory Techn. 2000. 48. 2076–2081.

5. *Diem E., Schwarz C., Adlkofer F. et al.* Non-thermal DNA breakage by mobile-phone radiation (1800 MHz) in human fibroblasts and in transformed GFSH-R17 rat granulosa cells in vitro // Mutat. Res. 2005. 583. (2). 178–183.

6. *Ganatara V., Yadav K., Senjaliya C. et al.* Health hazards due to electromagnetic radiation in the workplace // Int. J. Innov. Res. Sci. Technol. 2015. 1. (8). 138–145.

7. *Gatta L., Pinto R., Ubaldi V. et al.* Effects of in vivo exposure to GSM-modulated 900 MHz radiation on mouse peripheral lymphocytes // Radiat. Res. 2003. 160. (5). 600–605.

8. *Jarrige P., Ticaud N., Kohler S. et al.* Electrooptic probe adapted for bioelectromagnetic experimental investigations // IEEE Trans. Instrum. Meas. 2012. 61. (7). 2051–2058.

9. *Kohler S., O'Connor R.P., Vu T.D.T. et al.* Experimental microdosimetry techniques for biological cells exposed to nanosecond pulsed electric fields using microfluorimetry // IEEE Trans. Microw. Theory Techn. 2013. 61. (5). 2015–2022.

10. *Komnatnov M.E., Busygina A.V.* Module for visual control of in vitro results of the joint impact of climatic and electromagnetic factors on living tissue // EDM: Proc. 16th Int. conf. Erlagol, 2015. 576–579.

11. *Komnatnov M.E., Gazizov T.R.* Environmental shielded TEM chamber for biomedical testing // IMWS-BIO: Proc. IEEE MTT-S Int. Microwave Workshop Series. London, 2014. 1–4.

12. *Komnatnov M.E., Gazizov T.R.* Chamber for joint environmental and electromagetic testing of elec-

tronic components // Tekhnika radiocvyazi = Technology of Radio Communication. 2014. 23. (3). 84–91. [In Russian].

13. *Komnatnov M.E., Gazizov T.R.* On joint climatic and electromagetic testing of radioelectronic equipment // Doklady Tomskogo gosudarstvennogo universiteta sistem upravleniya i radioelektroniki = Proceedings of Tomsk State University of Control Systems and Radioelectronics. 2014. 34. (4). 39–45. [In Russian].

14. *Kwee S., Raskmark P.* Changes in cell proliferation due to environmental non-ionizing radiation 1. ELF electromagnetic fields // Bioelectrochem. Bioenerg. 1995. 36. (2). 109–114.

15. *Kwee S., Raskmark P.* Changes in cell proliferation due to environmental non-ionizing radiation 2. Microwave radiation // Bioelectrochem. Bioenerg. 1998. 44. (2). 251–255.

16. *Kwee S., Raskmark P., Velizarov S.* Changes in cellular proteins due to environmental non-ionizing radiation. I. Heat-shock proteins // Electromagn. Biol. Med. 2001. 20. (2). 141–152.

17. *Lallechere S., Girard S., Roux D. et al.* Mode stirred reverberation chamber (MSRC): a large and efficient tool tolead high frequency bioelectromagnetic in vitro experimentation // Prog. Electromagn. Res. B. 2010. 26. 257–290.

18. *Lim H.B., Cook G.G., Barker A.T., Coulton L.A.* Effect of 900 MHz electromagnetic fields on nonthermal induction of heat-shock proteins in human leukocytes // Radiat. Res. 2005. 163. (1). 45–52.

19. *Linz K.W., von Westphalen C., Streckert J.* et al. Membrane potential and currents of isolated heart muscle cells exposed to pulsed radio frequency fields // Bioelectromagnetics. 1999. 20. (8). 497–511.

20. *Malaric K., Tkalec M., Bartolic J.* Use of GTEM-Cell in Biomedical Experiments // TEMI-2001: Proc. 11th IMEKO TC-4 Symposium, 2001. 394–396.

21. *Martens L., Van Hese J., De Zutter D. et al.* Electromagnetic field calculations used for exposure experiments on small animals in TEM-cells // Bioelectrochem.Bioenerg. 1993. 30. 73–81.

22. *Merla C., Ticaud N., Arnaud-Cormos D. et al.* Real-time RF exposure setup based on a multiple electrode array (MEA) for electrophysiological recording of neuronal networks // IEEE Trans. Microw. Theory Techn. 2011. 59. (3). 755–762.

23. *Panagopoulos D.J., Karabarbounis A., Margaritis L.H.* Effect of GSM 900-MHz mobile phone radiation on the reproductive capacity of Drosophila melanogaster // Electromagn. Biol. Med. 2015. 23. (1). 29–43.

24. *Salovarda M., Malaric K.* Use of GTEM-cell and wire patch cell in calculating thermal and non-thermal biological effects of electromagnetic fields // Advanced Microwave and Millimeter Wave Technologies Semiconductor Devices Circuits and Systems. Ed. M. Mukherjee, 2010. Doi: 10.5772/8748.

25. *Savost'yanik S.A., Spas V.V., Yakubtsevich R.E. et al.* Magnetic fields and modern medicine // Meditsinskie novosti = Medicinal news. 2010 (12). 11–18. [In Belorussian].

26. *Schuderer J., Samaras T., Oesch W. et al.* High Peak SAR Exposure Unit With Tight Exposure and Environmental Control for In Vitro Experiments at 1800 MHz // IEEE Trans. Microw. Theory Techn. 2004. 52. (8). 2057–2066.

27. *Teodori L., Grabarek J., Smolewski P. et al.* Exposure of cells to static magnetic field accelerates loss of integrity of plasma membrane during apoptosis // Cytometry. 2002. 49. (3). 113–118.

28. *Ticaud N., Kohler S., Jarrige P. et al.* Specific absorption rate assessment using simultaneous electric field and temperature measurements // IEEE Antennas Waireless Propag. Lett. 2012. 11. 252–255.

29. *Velizarov S., Raskmark P., Kwee S.* The effects of radiofrequency fields on cell proliferation are non-thermal // Bioelectrochem. Bioenerg. 1999. 48. (1). 177–180.

30. *Zhao W., Yang R.* Experimental study on conformational changes of lysozyme in solution induced by pulsed electric field and thermal stresses // J. Phys. Chem. B. 2010. 114. (1). 503–510.

АКТУАЛЬНЫЕ ВОПРОСЫ ИССЛЕДОВАНИЙ ВЛИЯНИЯ ЭЛЕКТРОМАГНИТНЫХ ПОЛЕЙ НА БИОЛОГИЧЕСКИЕ ОБЪЕКТЫ

Анна Владимировна БУСЫГИНА, Максим Евгеньевич КОМНАТНОВ, Ольга Альбертовна МАТВЕЕНКО

ФГБОУ ВПО Томский государственный университет систем управления и радиоэлектроники 634050, г. Томск, пр. Ленина, 40

Рассмотрены актуальные вопросы исследований влияния электромагнитных полей на биологические объекты в ТЕМ-ячейке. Проведена систематизация исследований биологических объектов (клеточные культуры, растения, черви, насекомые, животные), подвергающихся воздействию электромагнитных полей. Описаны особенности устройств для климатических (температура, влажность, CO_2 и питательные вещества) и электромагнитных воздействий, необходимых для исследования конкретных биологических объектов. Обоснована необходимость температурного контроля и видеонаблюдения во время исследований биологических объектов под воздействием электромагнитных полей. Представленные результаты могут быть полезны при создании методик исследований по воздействию электромагнитных полей на конкретные биологические объекты, а также разработки технических требований к созданию устройств для подобных исследований.

Ключевые слова: биологические объекты, электромагнитные поля, ТЕМ-ячейка.

Бусыгина А.В. *– аспирант кафедры телевидения и управления, e-mail: bav-tusur@mail.ru*
Комнатнов М.Е. *– младший научный сотрудник научно-исследовательской лаборатории «Безопасность и электромагнитная совместимость радиоэлектронных средств», e-mail: maxmek@mail.ru*
Матвеенко О.А. *– к.б.н., научный сотрудник научно-исследовательской лаборатории «Безопасность и электромагнитная совместимость радиоэлектронных средств», e-mail: alterra@inbox.ru*

УДК 542.816:615.47

DEVELOPMENT OF PRODUCTION TECHNOLOGY OF ELECTRODES FOR ELECTRICAL NEUROSTIMULATION BY USING TRACK MEMBRANES

Vladimir Valentinovich TROFIMOV[1], Dmitriy Yurevich KUKUSHKIN[1], Aleksandr Mikhaylovich VASILEV[1], Ivan Aleksandrovich ARKHIPUSHKIN[2], Vladimir Semenovich KUBLANOV[3], Mikhail Vladimirovich BABICH[3], Anton Yurevich DOLGANOV[3], Vadim Maratovich GADELSHIN[3]

[1] MATI – Russian State Technological University named after K.E. Tsiolkovsky 121552, Moscow, Orhanskaya str., 3

[2] Institute of Physical chemistry and Electrochemistry named after A.N. Frumkin of RAS 119071, Moscow, Leninky av., 31, bldg. 4

[3] Ural Federal University named after the first President of Russia B.N. Yeltsin 620002, Ekaterinburg, Mira str., 19

The original technology of electrode production with track membrane materials for electrical neurostimulation has been described. It has been shown that the technology allows one to produce conducting structures with gas- and water-permeability in places of unfilled pores by metal. The created electrodes also have antiseptic properties.

Keywords: track membranes, electrical stimulation electrode, electrical neurostimulation, antiseptic.

Nowadays, multielectrode systems are applied in promising devices for transcutaneous electrical neurostimulation. These systems can be installed in the neck region [4] and on the language [7]. The electrodes in these systems must ensure the reliability and convenience of their fixation on the patient skin during the whole period of the treatment process.

It is necessary that the base material for the electrode have the following properties: it must be biologically neutral; it must be able to conduct air; it should be durable and resistant to sterilization techniques used in healthcare; it must provide an electrochemical resistance to current flow and have mechanical stability. Electrodes may be wetted with a conductive gel to ensure long-term therapy. The cost of the electrodes required for electrical neurostimulation should be reduced as the tightening of the requirements for the sanitary hygiene leads to the transition to the disposable electrode system.

Thus, the next task occurs: a mass production of multi-electrode system with narrow-width electrically conductive bands with a width from 0.1 to 0.5 mm and a length up to several tens of mm, which provide resistance not greater than 100 Ohm and stability of electrical parameters. The topological structure of such system may be quite difficult. The requirements to geometrical stability depend on geometry of neural paths and may be expressed by deviation from bits of mm.

PROBLEM AND METHODS ANALYSIS FOR ITS SOLUTION

Obtaining of conductive structures for different applications on materials, fastened on human body

Trofimov V.V. *– engineer, e-mail: tvv@jinr.ru*
Kukushkin D.Yu. *– assistant, e-mail: skyline34@nxt.ru*
Vasilev A.M. *– docent, e-mail: vasal2@yandex.ru*
Arhipushkin I.A. *– researcher, e-mail: arhi90@mail.ru*
Kublanov V.S. *– professor, e-mail: kublanov@mail.ru*
Babich M.V. *– assistant, e-mail: m.v.babich@urfu.ru*
Dolganov A.Yu. *– junior researche, e-mail: anton.dolganov@urfu.ru*
Gadelshin V.M. *– junior researcher, e-mail: gadelshinvm@mail.ru*

or on dress, is considered as a goal of many strategies like «smart textile». Processes of cloth metallizing and a field of their applicability are offered in a number of papers [8]. Actually, it is impossible to form electrodes on this base and with presented above characteristics because of high surface resistance. The complexity of electrode production, based on woven or not-woven materials via spraying, is caused by shading of fiber pieces. This fact is noted in [2], however, with the proposed technology it is not possible to get contact points with prescribed geometry. That has been examined as a part of current work. Titanium coating was applied by magnetron spraying on different cotton and synthetic clothes, not-woven materials included. The obtained coatings have had a resistance about 10 kOhm. One more possibility is the technology based on carbon nanotubes [3, 8], but this technology is not available for us.

RESULTS AND DISCUSSION

It seems that it is necessary to find a material for the electrodes formation that would be porous, has a smooth surface, has small coefficient of elongation. Such properties are combined in track membranes. [6]. In experiment the PETF membrane with a thickness of 20 μm, a pore diameter of 1 μm and a density about 10^7 pores per cm^2 were used. This membrane characteristics were chosen from consideration of balance between the porosity of 10 % and a mechanical robustness. As a basic material, two types of conductive layers were investigated: titanium nitride and copper. Titanium was deposited by magnetron (or arc) sputtering in the uncooled drums. The thickness of spaying varied from 0.05 to 1 μm. The total direct-current resistance of samples, with sizes of 120 × 30 mm and 50 × 50 mm, was monitored. Values of resistance were in a range from 10^1 to 10^2 Ohm. The surface resistance was measured by four-point method on the booth and by averaging of value over the sample surface. Four modes of spraying were investigated. In Table we present data of minimal and maximal resistances for different spraying modes.

Table

Resistance of samples for different spraying modes

Spraying mode	Resistance, Ohm	
	min	max
1	170.384	191.219
2	73.617	86.581
3	53.245	61.116
4	12.501	13.427

Presented in Table characteristics are satisfactory for the area of the electrode, but are insufficient for lead wires. In addition, it is complex to provide transition from the contacts of sputtered titanium to conductive lines, that are associated with the source of the current pulse field of the electrical neurostimulator, in the mask technology of the electrode formation. On the one hand, the usage of materials with high conductivity (such as noble metals) is precluded by economic considerations. On the other hand, the formation of conductors with copper is unacceptable for hygienic reasons. Therefore, two-layer base material is proposed that has the conductive layer of deposited copper, with a coating of titanium, which provides biocompatibility.

The methodology of copper plating on a porous track membrane consists of several stages: preparation, sensitization, activation, metallizing. At preparation stage, the coated material strip degreased in acetone and washed with twice-distilled water in an ultrasonic bath. Sensitization of surface was carried out in an acid solution of tin chloride $SnCl_2$. Material withstood a few minutes in the solution. After that, material was washed with warm water for the acceleration of the hydrolysis of the adsorbed salt. Activation of non-conductive surfaces was carried out in solution of palladium chloride $PdCl_2$. This was followed by the stage of metal application. In this case, a tartaric solution of electroless copper was used, which is composed of copper sulfate, sodium potassium tartrate, potassium hydroxide. The electrolyte solution is made of recrystallized salt $CuSO_4 \cdot 5H_2O$ then tartrate $KNaC_4H_4O_6 \cdot 4H_2O$ and KOH were inputted. Formaldehyde solution was used as the reducing agent. During the reduction, bubbles of hydrogen is extracting, therefore, solution was being intermixed quietly to reach a coating uniformity. After precipitation of the coating, samples were washed off by water and were dried off in a chamber drier for one hour under temperature of 55 °C.

Standard adhesion test (the «scotch tape»-test) has showed that the coating is durable. The measurement of electric resistance has given values lower than 10^{-2} Ohm between randomly chosen points on the sample. Resistance values are of the same order between two sides of the sample. To understand a mechanism of adhesion and closure between layers, a microscopy of the sample via the electron microscope Hitachi TM 3000 has been carried out. In Fig. 1 front image of electrodes contact surfaces is shown. One can note that pores are not closed. The copper layer does not have cracks and spaces, thus, the attainment of steady electrical contact is ensured.

In Fig. 2 image of a side surface for sliced up sample by cutting edge is presented. Fig. 2 explains

a nature of adhesion. It is caused by the molecular force of coupling. On the other hand, it can be seen that individual pores are filled with metal. Their quantity is not too big; therefore, they cannot be a reason of adhesion. They are links between layers. As two metal-filled pores out of dozen can be clearly noticeable on the presented image, than among 10^7 pores per 1 cm^2 there will be significant number of filled pores to ensure an electrical contact.

The proposed process can be favorably distinguished from tries of develop a multi-stage technology [1, 5], where a glue-free mounting of metallic layer by means of a forming of «anchors» is used. «Anchors» are obtained by filling of intersectional channels of tracks.

Track membrane material remain gas- and water-permeable if in the process of precipitation, a metal does not fill pores. The material with such properties may be interesting not only for production of the electrical neurostimulation electrodes, but also for production of elastic cables, as the crack on the one side of path does not lead to contact breaking. Copper samples have given a resistance in a range of 10^{-2}–10^{-3} Ohm. These values are sufficient for the stated applications.

It is proposed to use a process of laser engraving the material to form the electrode geometry. Prior to the engraving it is advised to glue material to the fabric substrate. This provides mechanical strength.

Also, it seems appropriate to impregnated the fabric which is attached to the electrode with the silver nanoparticles.

Silver nanoparticles have sustained bacteriostatic effect on more than 650 kinds of bacteria and viruses, while maintaining the DNA structure integrity. As it is known, the nanometer-sized particles have several unique properties. They carry a positive charge, and their electrical and physicochemical properties are determined by the size of the nanocluster. Therefore, nanoparticles positioning on the electrode surface is possible by electrophoresis. Reaching the electrode, the particles coalesce and lose their charge, resulting in a colloidal solution coagulates on the surface of the material. The unit and the process of electrophoresis impregnation was also trialed on test material – carboxylic tissue. This choice has been made for reasons of control of the deposition process by electron microscopy. The image of carboxylic tissue with impregnated silver nanoparticles is presented of Fig. 3.

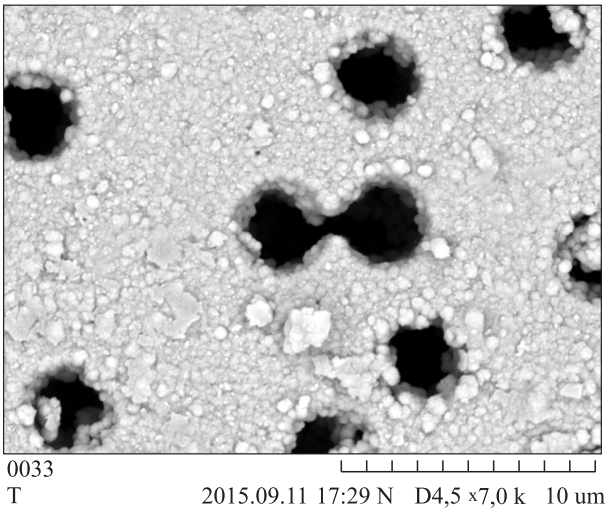

Fig. 1. *Microphotography of front view from the side of contact surface of electrodes*

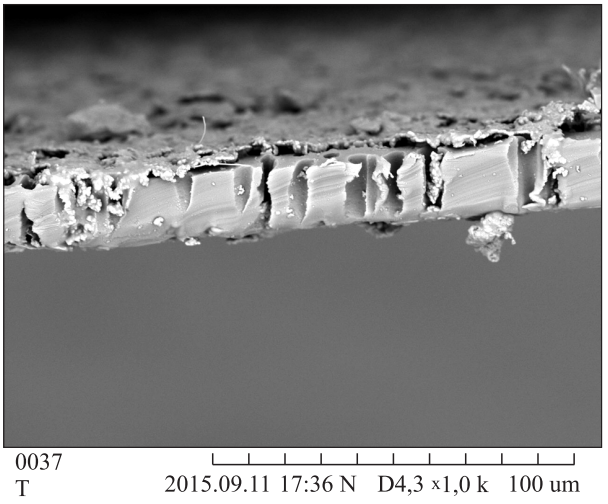

Fig. 2. *Microphotography of cross-sectional view of the slited sample*

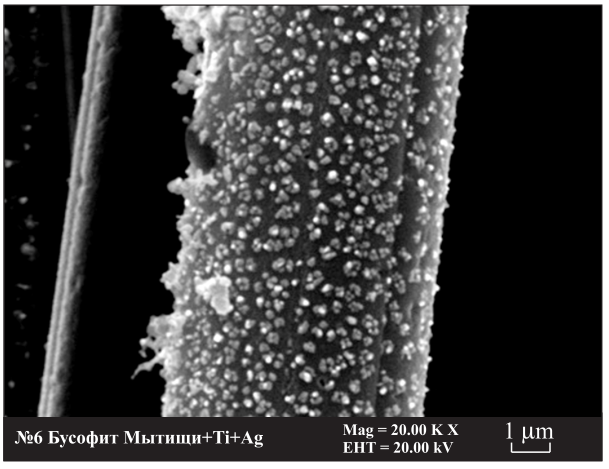

Fig. 3. *Modified carbon fiber with an Ag nanoclusters*

CONCLUSION

Presented in the paper results describe features and peculiarities of the electrical neurostimulation electrodes production technology. The track membrane material application allows one to produce

industrial technologies of manufacturing conducting structures for different spheres of application.

REFERENCES

1. *Danziger M., Voitus W.* Herstellung haftfester Metall-Polymer-Verbunde mit Hilfe der Nanotechnologie // Galvanotechnik. 2008. 1. 70–73.

2. *Hegemann D., Amberg M., Ritter A., Heuberger M.* Recent developments in Ag metallised textiles using plasma sputtering // Materials Technol. 2009. 24. (1). 41–45.

3. *Hu L., Pasta M., Mantia F.L. et al.* Stretchable, porous, and conductive energy textiles // Nano Lett. 2010. 10. (2). 708–714.

4. *Kublanov V.S., Petrenko T.S., Babich M.V.* Multi-electrode neurostimulation system for treatment of cognitive impairments // Engineering in Medicine and Biology Society (EMBC): 37th Annu. Int. Conf. Milan, 2015. 2091–2094.

5. *Patent 7 955 697 U.S.A.* Haftfester verbund und verfahren zur herstellung / M. Danziger, published 02.03. 2004.

6. *Reutov V.F., Dmitriev S.N.* Ion-tracking nanotecnology // Rus. Chem. J. 2002. 46. (5). 74–80.

7. *Wildenberg J.C., Tyler M.E., Danilov Y.P. et al.* Electrical tongue stimulation normalizes activity within the motion-sensitive brain network in balance-impaired subjects as revealed by group independent component analysis // Brain Connect. 2011. 1. (3). 255–265.

8. *Zhou H., Lu Y., Chen W. et al.* Stimulating the comfort of textile electrodes in wearable neuromuscular electrical stimulation // Sensors. 2015. 15. (7). 17241–17257.

РАЗРАБОТКА ТЕХНОЛОГИИ ИЗГОТОВЛЕНИЯ ЭЛЕКТРОДОВ ДЛЯ НЕЙРОЭЛЕКТРОСТИМУЛЯЦИИ С ИСПОЛЬЗОВАНИЕМ ТРЕКОВЫХ МЕМБРАН

Владимир Валентинович ТРОФИМОВ[1], Дмитрий Юрьевич КУКУШКИН[1], Александр Михайлович ВАСИЛЬЕВ[1], Иван Александрович АРХИПУШКИН[2], Владимир Семенович КУБЛАНОВ[3], Михаил Владимирович БАБИЧ[3], Антон Юрьевич ДОЛГАНОВ[3], Вадим Маратович ГАДЕЛЬШИН[3]

[1] *МАТИ – Российский государственный технологический университет им. К.Э. Циолковского 121552, г. Москва, ул. Оршанская, д. 3*

[2] *ФГБУН Институт физической химии и электрохимии* имени А.Н. Фрумкина *РАН 119071, г. Москва, Ленинский пр., 31, корп. 4*

[3] *Уральский федеральный университет им. первого Президента России Б.Н. Ельцина 620002, г. Екатеринбург, ул. Мира, 19*

Описывается оригинальная технология изготовления электродов для нейроэлектростимуляции с применением материалов на основе трековых мембран. Показано, что технология позволяет создавать проводящие структуры и обеспечивать газо- и водопроницаемость в местах, в которых металл не закрывает поры, а также иметь антисептические свойства.

Ключевые слова: трековые мембраны, электроды для электростимуляции, нейроэлектростимуляция, антисептик.

Трофимов В.В. *– инженер, e-mail: tvv@jinr.ru*
Кукушкин Д.Ю. *– ассистент, e-mail: skyline34@nxt.ru*
Васильев А.М. *– доцент, e-mail: vasal2@yandex.ru*
Архипушкин И.А. *– научный сотрудник, e-mail: arhi90@mail.ru*
Кублanов *В.С. – профессор, e-mail: kublanov@mail.ru*
Бабич М.В. *– ассистент e-mail: m.v.babich@urfu.ru*
Долганов А.Ю. *– младший научный сотрудник, e-mail: anton.dolganov@urfu.ru*
Гадельшин В.М. *– младший научный сотрудник, e-mail: gadelshinvm@mail.ru*

УДК 81.342.2(1.571-81)

INNOVATIVE TECHNOLOGIES IN THE STUDY OF ARTICULATORY-ACOUSTIC BASES OF INDIGENOUS ETHNOSES OF SIBERIA: MRI, DIGITAL RADIOGRAPHY AND LARYNGOGRAPHY

Iraida Yakovlevna SELYUTINA[1], Tatyana Raisovna RYZHIKOVA[1], Nikolay Sergeevich URTEGESHEV[1], Albina Albertovna DOBRININA[1], Andrey Ivanovich SHEVELA[2], Andrey Yur'evich LETYAGIN[3]

[1] *Institute of Philology of SB RAS*
630090, Novosibirsk, Nikolaev str., 8

[2] *Institute of Chemical Biology and Fundamental Medicine of SB RAS*
630090, Novosibirsk, Lavrent'ev str., 8

[3] *Institute of Physiology and Fundamental Medicine*
630117, Novosibirsk, Timakov str., 8

The study of the sound systems of the minority languages of the peoples of Siberia and the adjacent regions is based on the supposition that the articulatory-acoustic database being an attribute of ethnicity is a potential historical and linguistic source in the reconstruction of ethno-genetic processes. Instrumental methods have been used by the Novosibirsk phoneticians in the study of sound systems since the late 1960s. Since 2009, researchers from the three institutes of the Siberian branch of the Russian Academy of Sciences both of a philological and medical profile have been conducting a comprehensive interdisciplinary study of articulatory-acoustic bases of indigenous Siberian populations, using magnetic-resonance imaging, digital radiography and laryngography. An electronic database including somatic material on 46 idioms (languages, dialects and sub-dialects) has been created. The results of the study made adjustments to the traditional view of scientists about the Genesis of the autochthonous minority ethnic groups and their languages.

Keywords: languages of Siberian peoples, phonology, instrumental-phonetic methods, magnetic-resonance imaging, digital radiography, laryngography.

Phonology as a science considering speech sounds from the point of view of their distinctive functions originated in Russia. Its founder is a Russian scientist of a Polish origin I.A. Baudouin de Courtenay (1845–1929). He developed a theory of phonemes [1] and was the first to apply mathematical models to linguistics and to lay foundations to a new direction in linguistics – the experimental phonetics.

Instrumental methods in the study of the sound systems of the world languages have been used in linguistics since the mid-nineteenth century. But the active use of hardware methods in phonetic researches have begun in the 1950s, when it became clear that it was necessary to utilize objective data eliminating a subjectivity factor inherent to an auditory phonetics. The researchers perceive a new language through the prism of phonetic and phonological systems of their native language and other languages known to them, because even the most sophisticated ear hears what it is used to hear. For this reason, the descriptions of sound systems of unstudied languages of Siberia, made in the XIX–XX centuries on the auditory level, has been influenced by both the traditions of Indoeuropean and Russian studies. Further development of phonetics was im-

***Selyutina I. Y.** – doctor of philological sciences, professor, chief researcher, e-mail: siya_irina@mail.ru*
***Ryzhikova T. R.** – candidate of philological sciences, senior researcher, e-mal: redtanya@inbox.ru*
***Urtegeshen N. S.** – candidate of philological sciences, researcher, e-mal: urtegeshev@mail.ru*
***Dobrinina A. A.** – candidate of philological sciences, researcher, e-mail: ekinur@mail.ru*
***Shevela A. Yu.** – doctor of medical sciences, professor, deputy director, e-mail: letyagin-andrey@yandex.ru*
***Letyagin A. I.** – doctor of medical sciences, professor, deputy director, e-mail: ashevela@mail.ru*

possible without the use of objective methods ensuring the adequacy of a recorded and interpreted linguistic material.

In Novosibirsk experimental phonetic study of the languages of the peoples of Siberia, the Russian North and Far East has started in the late 1960s under the leadership of V.M. Nadelyaev, who established the laboratory of experimental-phonetic researches at the former Institute of History, Philology and Philosophy, Siberian Branch of the USSR Academy of Sciences (since 1990 – the Institute of Philology, Siberian Branch of the Russian Academy of Sciences).

Frontal experimental phonetic study of the languages of Siberia and the adjacent regions is carried out for the first time both in Russia and abroad. In line with the common theoretical concepts and methodological framework established by the founder of LEPR, various aspects of the sound systems of about 50 languages, dialects and subdialects – Turkic, Mongolian, Tungus-Manchu, Samoyedic, Ob-Ugric, Yenisei and Paleoasiatic have been and are being examined. The results have been published in fifty books and more than 700 articles in various scientific journals and collections.

MATERIALS AND METHODS

A complex procedure used by the Siberian phoneticians includes both the linguistic methods of phonological analysis, and hardware methods of static radiography, dental-palatography, labiography, linguography, spectrography, pneumo-oscillography, as well as computer programs for sound files creating and processing.

At the beginning of XXI century, with the development of innovative technologies, the instrumental studies of the sound systems are conducted in the majority of the leading world laboratories by using the latest techniques of magnetic-resonance imaging (MRI), digital radiography (DRG), laryngography (DLG), electromiography, etc. The English language is examined in the USA in Haskins Laboratories at the Yale University, Connecticut, at the Universities of Brown, Southern California, French in Grenoble, Japanese in Tokyo, the Korean language in Seoul. In Russia such studies are carried out on the material of the Russian language in the center of the magnetic-resonance imaging and spectrography of the Moscow State University.

In Siberia, to foster the research of the endangered minority languages at the current level was made possible thanks to the financial support of the Presidium of SB RAS within the fundamental interdisciplinary studies. Since 2009, researchers from the three institutions of SB RAS – the Institute of Philology, the International Tomography Center (ITC) and the Institute of Chemical Biology and Fundamental Medicine have carried out a comprehensive multidisciplinary investigation of articulatory settings peculiar to the speakers of the endangered Siberian languages.

An innovative paradigm for the study of speech sounds has been developed. Scientists of ITC and ACBFM have done the necessary work for medical programs adaptation of MRI, DRG and DLG in agreement with the goals and objectives of an experimental phonetic research–data acquisition, processing, analysis and interpretation.

Tomographic studies were conducted in ITC on high field MRI Philips Achieva Nova Dual 1.5 T tomograph (Philips medical systems; Eindhoven, Netherlands). Graphical post-processing, archiving and morphometry of MRI was performed on a workstation Philips ViewForum RS.1 (Dell). T2-weighed images (T2W TSE SENSE) in three projections with parameters: FOV – 250 mm, FOV reduction – 90 %, Reconstruction 256 × 256, Scan% – 80, Slice thickness 6 mm, Flip angle = 90, TR/TE = = 1000/80.0 were obtained.

Digital radiography was performed in the Center of New Medical Technologies of ACBFM on a low-dose digital X-ray installation «Siberia-N» (produced by the Institute of Nuclear Physics SB RAS). Shooting of the vocal apparatus of each of the speakers was carried out in a lateral projection in the sitting position at the moment of pronouncing certain phonetic stimulus in accordance with a predesigned program of the experiment. The range of study is from VI cervical vertebra to the upper edge of the orbit.

When performing direct digital laryngoscopy, two devices with the smallest diameter of fiberoptic and superior imaging capacity: Pentax Bronchoscope FB-18V (Japan) and the Bronchofiberscope OLYMPUS BF-S (Japan) were used for visual control of the experiment and subsequent documentation of the received data, a video device EVIS EXERA II Video System Center Olympus CV-180 is used with parallel recording to a video file utilizing AVER Media software. The communication channel of the bronchoscope is connected to the computer. During the research IT specialist performs the digital recording of the process of articulation and provides parallel broadcast of a live video from the bronchoscope on the monitor screen.

For the first time in Russian and foreign linguistics an electronic database was formed including an experimental phonetic somatic material of a unique scientific value, collected in 46 languages and dialects of autochthonous minority ethnic groups. High-resolution MRI scans, digital X-ray images and la-

ryngograms showing articulatory settings of vocal and consonant components of speech were received from 110 informants.

RESULTS AND DISCUSSION

The study of the sound systems of the minority languages of the peoples of Siberia and adjacent regions, performed by the phoneticians of Siberia is based on a supposition proposed by V.M. Nadelyaev in 1980s that the articulatory-acoustic base (AAB) as an attribute of ethnicity is a potential historical and linguistic source in the reconstruction of ethno-genetic processes. AAB theory is especially valuable in the study of the history of the peoples of Siberia, who did not leave written documents. AAB as a system of pronunciation skills and related with them acoustic effects is formed at an early stage of an ethnic group genesis and passes from generation to generation saving its essential features provided the ethnic groups preserve their compact place of living in the process of population transformations.

The results of the complex experimental phonetic data analysis, providing a high level visualization of vocal and consonant articulatory processes in the Turkic, Mongolian, Tungus-Manchu and Finno-Ugric languages, allowed the scientists to make corrections in the traditional notions of the phonetic areals of Siberia, about the Genesis of ethnic groups and their languages, about their intersections.

The Turkic languages

The presence on the territory of Siberia of Turkic languages, vocal (Fig. 1–3) and consonant systems of which is structured by the parameters of the larynx movement, regularities of a developed pharyngeal sinharmonism revealed in the Tuvan language and the obligatory pharyngealization of the Russian borrowings by the Tuvinians – all these factors prove the necessity of revising the existing in Turkology point of view that pharyngealization is a disappearing phenomenon, a relict and witness the

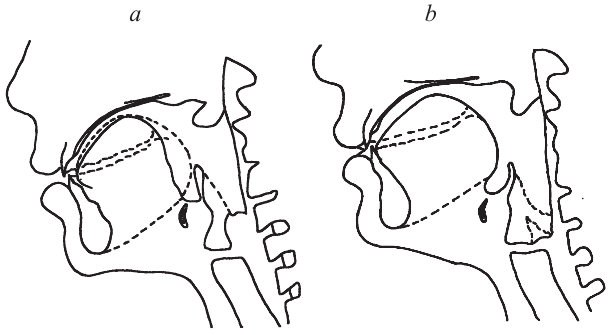

Fig. 1. *X-ray images of the Tuvan vowel sounds: a) non-phayingealized **/i:/** in the word-form **shii** 'the perfomance'; b) pharyngealized **/i'/** in the word-form **irt** 'the castrated sheep'*

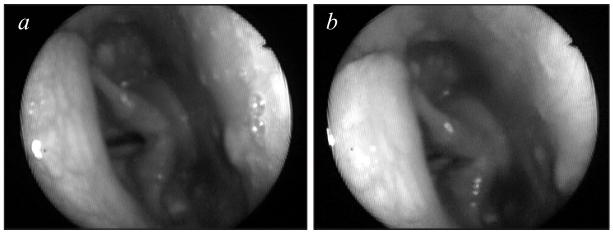

Fig. 2. *Laryngograms of the Tuvan vowel sounds: a) non-pharyngealized **/i:/** in the word-form **shii** 'the perfomance'; b) pharyngealized **/i'/** in the word-form **irt** 'the castrated sheep'*

importance of pharyngo-laryngeal part of a vocal tract for specifying Siberian peoples' AABs and phonological systems of their languages.

The articulatory specificity of the pharyngealized vocal settings is a strong tension of the speech apparatus, the tongue root movement to the back wall of the pharynx and, as a consequence, reduction of a laryngeal-pharyngeal part of the resonator (Fig. 1b), a tight approximation of the vocal cords (Fig. 2b) in comparison with non-pharyngealized vowels (Fig. 1a, 2a). On the waveform, pharyngealization is marked by dramatic falling – smooth falling ~ discontinuous – dramatic rising of the pitch (Fig. 3b) in contrast to the smooth rising pitch when articulating non-pharyngealized vowels (Fig. 3a).

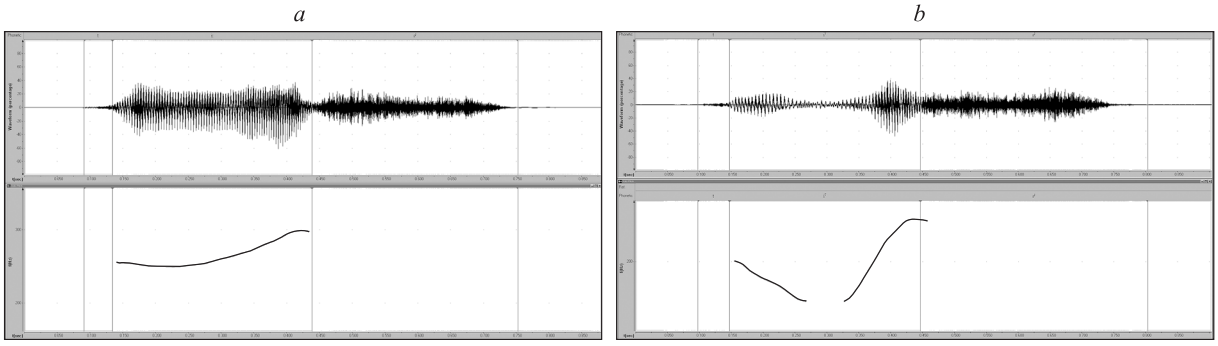

Fig. 3. *Waveforms and pitch movements in the Tuvan vowel sounds: a) non-pharyngealized **/i:/** in the word-form **diis** 'a cat'; b) pharyngealized **/i:/** in the word-form **di's** 'onomatopoeia'*

In Tuvan, consonant phonemes oppose as strong/ week/super-week. The peculiarity of the Tuvan phonetics is that not only vowels but consonants as well are pharyngealized in the pharyngealized word-forms. Glottalization of vowels is a phonemic feature, glottalization of consonants is an allophonic one. Choice of the consonant representant in a monothematic word-forms depends – in full correspondence with Tuvan pharyngeal synharmony – on the quality of a vowel in the first syllable of a stem [2, 6].

Thus, the results of instrumental researches witness the presence of certain correlations between the degree of tenseness and pharyngealization as an additional work of throat walls with the acoustic effect of low resonance when pronouncing pharyngealized consonants. Noteworthy that functional status of pharyngealized consonants in the Southern-Siberian Turkic languages, i.e. pharyngealization of consonants, is a systematizing distinctive feature in Shor and Baraba-Tartars' and allophonic one in Tuvan [10, 13].

The Mongolian languages

Though having a relative proximity, dating back to the period of an original unity in the Circum-Baikal region, the principles of a structural-taxonomical organization of the consonant systems of the Mongolian languages are typologically different. If in the Khalkha Mongolian (Fig. 4) and Kalmyk languages the consonantism is structured by a triple opposition of tension, revealing the similarity with the South Siberian Turkic languages (Tuvan, Tofa) of the Sayan-Baikal ethnoareal, than a Hori Buryat system with binary opposition of weak and superweak consonant phonemes is close to the Altai-Sayan Turkic (Altai, Khakas) and Ural languages for which strong tensed articulation is unacceptable.

A triple opposition of the units by the mode of occlusion is linguistically significant for the Buryat consonantism–phonemes are opposed as stops, fricatives and vibrants. The affricates are absent in the Buryat language, this fact making it stand out among other Mongolian languages, in which complex occlusive consonants are the productive elements of the system.

According to the MRI and DRG data in the phonetic system of Khalkha Mongols, the palatalization (both phonologically moderate and allophonically weak) is accompanied by the forward advancement of the tongue body (more forward at a moderate palatalization). It results in a volumetric back mouth-pharyngeal resonator and simultaneously the area of the contact (with stops) or convergence (with fricatives) of active and passive organs of speech increases. This proves the specificity of the Khalkhas AAB in comparison with the languages of Siberia and adjacent regions, where palatalization is achieved primarily by the additional rise of the front-middle part of the tongue dorsum to the hard palate.

Such significant differences in genetically related languages are caused by different historical development of the ethnic groups, their interactions and mutual influences that resulted in the specifics of the articulatory-acoustic bases of the native speakers of the modern Mongolian languages.

The Tungus-Manchu languages

A comprehensive analysis of instrumental data on the Tungus-Manchu phonetics on the example of the Evenk language showed that the specifics of the Evenk language AAB is determined by more forward localization of the articulatory settings of consonants than in the majority of the surveyed languages of Siberia. The labial, forelingual and forelingual-mediolingual articulations (14 units) prevail, the class of guttural phonemes is represented only by 4 phonemes while no classical uvular realizations have been fixed in the system. The total palatalization of consonant settings when the tongue body moves up-forward thus increasing the volume of the back-oral-pharyngeal part of the resonator and causing the acoustic effect of softness, as well as the absence of velarized, uvularized and nazal-

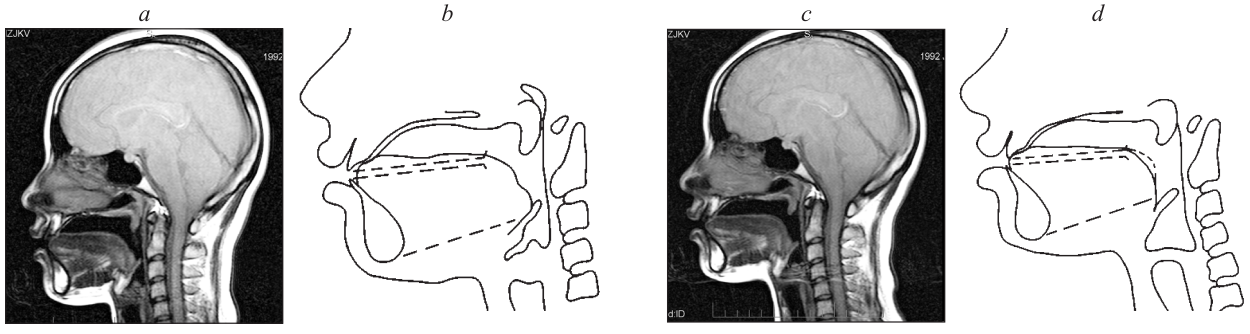

Fig. 4. *MRI image (a, c) and scheme (b, d) of the Khalkha Mongolian strong sound /**t**/ in the word-form **hat** 'a hardening of a steel' (a, b) and week sound /**d**/ in the word-form **had** 'a rock' (c, d)*

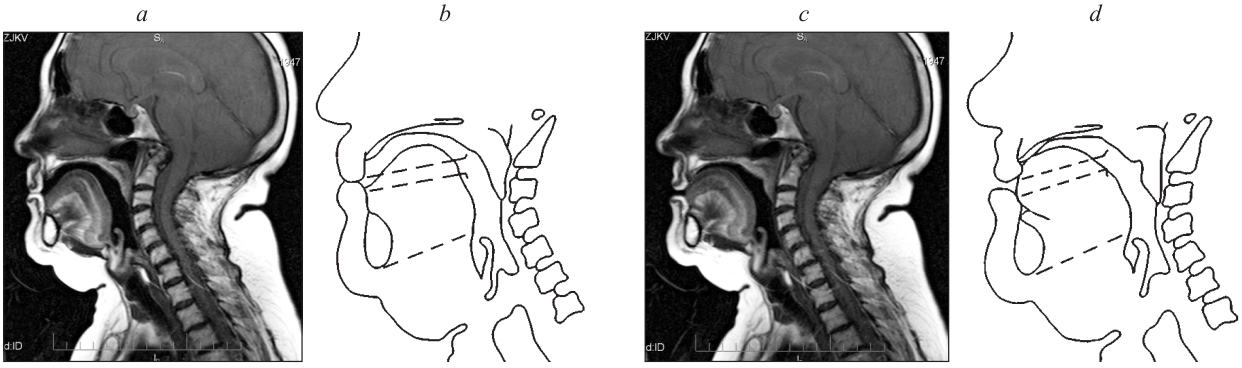

Fig. 5. *MRI image (a, c) and scheme (b, d) of the Evenk moderately palatalized sound /**p**/ in the word-form **chepi** 'to drown' (a, b) and weakly palatalized sound /**t**/ in the word-form **amut** 'the lake' (c, d)*

ized articulations, which seem to be rather productive in the languages of Siberia, also indicate that the movement of the sound producing organs forward is the predominant characteristic of the articulation base of the Evenks (Fig. 5).

For AAB of Selemdzhi Evenks strong tension is unusual: the phoneme manifestations of both noisy and less-noisy consonants are defined as moderately tensed (except labial consonants). Thus, the Evenk language is typologically similar to the Ugro-Samoyedic languages, the Buryat language – one of the languages of the Mongolian family and the Turkic languages of the Altai-Baikal region, which had been formed as a result of turkization of the Ugro-Samoyedic population with unacceptable for them strong articulation. It is this feature that typologically contrasts to the consonant systems of such languages of the Ural-Altaic community as Khalkha Mongolian, Kalmyk, South Siberian Turkic languages of the Sayan-Baikal region (Tuvan, Tofa, Shor, Baraba Tatar).

A specific feature of the Evenk consonantism in its Selemdzhi variant is that stop consonants (11 units) prevail over the fricative ones (4 units) and it makes the Selemdzhi dialect similar to Yakut – one of the contact Turkic languages.

The presence in the system of the pharyngeal sound *h* approximates the Evenk consonantism with Buryat, which includes a similar component but having a phonological status. The Mongolists interpret the consonant *h* as one of the elements of the Evenk phonetic substrate in the Buryat language, which has resulted from the long interaction between the Evenk and Mongolian ethnic groups on the Circum-Baikal territory.

The Ob-Ugric languages

The obtained instrumental data show a high productivity of the laryngeal-pharyngeal part of the vocal apparatus in Khanty – it is fixed not only on auditive-visual level, but also on the MR-images, radiograms and laryngograms.

There is a high frequency localization of the forelingual obstacle of the consonants on the hard palate, and not on the teeth and alveolas as in the Siberian Turkic and Mongolian languages. This feature is most clearly realized in the Surgut dialect. These characteristics of the settings indicate that in the Khanty language forelingual consonant articulations move backward.

Forelingual articulations in the Khanty language are usually apical or cacuminal (Fig. 6) but not dor-

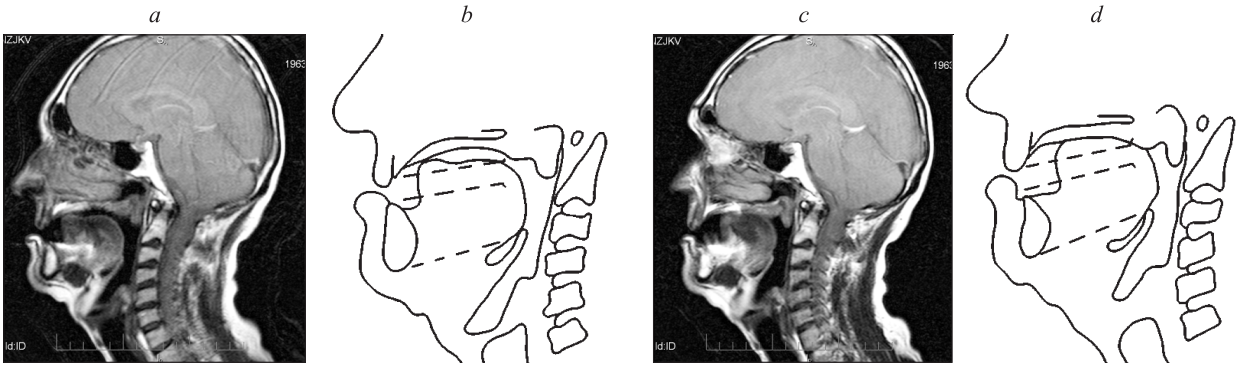

Fig. 6. *MRI image (a, c) and scheme (b, d) of the Khanty sound /ʃ/ in the word-form **hash** 'the willow' (a, b) and sound /**k**/ in the word-form **sak** 'the beads' (c, d)*

sal, as in the majority of the Siberian Turkic and Mongolian languages; dorsality is not, in fact, fixed.

At the same time, the guttural consonants – in preposition to front-raw and back-raw vowels significantly move forward, being realized in mediolingual manifestations. In the Kazym dialect, the uvula settings are revealed neither by X-ray no by MRI.

Experimentally recorded shifts of the Khanty articulations to the center of the oral cavity – the forelingual consonants move backward and guttural settings, on the contrary, move forward, being realized in mediolingual variants, – are similar to the previously identified processes in some vocal systems of the South Siberian Turkic languages, for which an Ugro-Samoyedic substrate is assumed [3, 11].

Further studies using both linguistic and objective experimental-phonetic methods will allow us to determine the specificity of AAB of the ethnic groups of Khanty, the role of laryngeal-pharyngeal part of the resonator in the formation of the vocal and consonant articulations, the functions of ejective and injective settings in phonic and phonological systems. The reasons for the differences should be sought in the historical past of the native speakers of the investigated dialects.

CONCLUSION AND FUTURE WORK

One of the most urgent and priority tasks of modern phonetics is the problem of separation, analysis and identification of speech segments to construct the correlation matrix, in which the variables are articulatory and acoustic parameters of speech sounds. Linguists developed a universal unified classification model of speech sounds in languages of the world, based on the data of the anatomical and physiological features of the vocal apparatus and which take into account both known to science articulatory sound settings and unexplored but theoretically possible articulations in languages [7–9, 12, 14].

Physicists have managed to work in detail an acoustic theory of speech formation [4, 5]. The question of the correlation of the articulatory phases with the corresponding acoustic effects, the problem of the correlation algorithms remain open. The complexity of the problem is in poly-variance of the acoustic signals corresponding to the same articulatory structure. Further improvement of the methodology of integrated synchronous-commit segmentation of sound chains followed by a parallel study of the acoustic and anatomy-physiological components of speech can serve as a basis for constructing a correlation model.

The results obtained are of interest for linguists, teachers and physicians (linguodidactics, speech therapy, neurological practice) and may be used in the automatic recognition and synthesis of speech, the development of computer speech databases, conversion text-to-speech. Innovative paradigm for the study of speech sounds will find application in studies of languages of other typologies, as well as in the solution of the problems of a hardware medicine.

ACKNOWLEDGMENTS

Interdisciplinary integration project № 121 (2012–2014) «The Comparative Investigations of Siberian Indigenous Peoples' Articulatory-acoustic Bases by the Methods of Magnetic-Resonance Imaging, Digital Roentgenography and Laryngoscopy» was financially supported by the Presidium of SB RAS. The authors appreciate the help of the project team members: A.A. Savelov, M.V. Rezakova, E.A. Levshakova, Yu.A. Ganenko. We are also grateful to our subjects for their valuable contribution to the business of the minority languages preservation.

REFERENCES

1. *Baudouin de Courtenay J.* Versuch einer Theorie phonetischer Alternationen. Ein Capitel aus der Psychophonetik. Strassburg: Trübner, 1895.

2. *Dambyra I.D.* The vocalism of the Kaa-Khem sub-dialect in comparison with other sub-dialects and dialects of tuvan language. Novosibirsk: Sova, 2005. [In Russian].

3. Esenbayeva G.A. Vocal systems of South-Siberian Turkic languages and the Kyrgyz language: commonalities and specifics. Novosibirsk: Sova, 2010. [In Russian].

4. *Fant G.* Acoustic theory of speech production. Hague: Mouton, 1960.

5. *Fant G.* Speech acoustics and phonetics. Selected writings. Kluwer Academic Publisher; Springer, 2004.

6. *Kechil-ool S.V.* Typological specificity of consonantism of Syut-Khol sub-dialect in the system of sub-dialects and dialects of the tuvan language. Novosibirsk: Sova, 2006. [In Russian].

7. *Ladefoged P.* IPA and phonetic-phonological interface // Problems of Phonetics. Moscow: Nauka, 1999. 3. 25-37. [In Russian].

8. *Ladefoged P.* Phonetic data analysis: An introduction to fieldwork and instrumental techniques. Oxford: Blackwells, 2003.

9. *Nadelyaev V.M.* The project of the Universal Unified Phonetic Transcription (UUFT). Moscow; Leningrad: Institute of Linguistics of the Academy of Sciences of the USSR, 1960. [In Russian].

10. *Ryzhikova T.R.* The consonantism of the language of the baraba-tatars: a comparative-typological aspect. Novosibirsk, Publishing House of SB RAS, 2005. [In Russian].

11. *Shaldanova A.A.* The vocalism of the dialect of the altai-kizhi (comparative aspect). Novosibirsk: Sova, 2007. [In Russian].

12. *Sherba L.V.* The phonetics of the French language. Essay French pronunciation in comparison with Russian. Leningrad; Moscow: Educational Publishing House, 1937. [In Russian].

13. *Urtegeshev N.S.* Noisy consonantism of the Shor language (on the material of mras dialect. Novosibirsk: Publishing Center of Novosibirsk State University, 2002. [In Russian].

14. *Urtegeshev N.S., Selyutina I.Ya., Esenbaeva G.A. et al.* UUPT and IPA phonetic transcription standards: the system of correlations // Voprosy filologii. Seriya «Uralo-Altayskie issledovaniya» = Questions of philology. Series «Ural-Altaic studies». 2009. (1). 100–115. [In Russian].

УДК 81.342.2(1.571-81)

ИННОВАЦИОННЫЕ ТЕХНОЛОГИИ В ИЗУЧЕНИИ АРТИКУЛЯЦИОННО-АКУСТИЧЕСКИХ БАЗ КОРЕННЫХ ЭТНОСОВ СИБИРИ (ПО ДАННЫМ МРТ, ДИГИТАЛЬНОГО РЕНТГЕНОГРАФИРОВАНИИЯ И ЛАРИНГОГРАФИРОВАНИЯ)

Ираида Яковлевна СЕЛЮТИНА[1], Татьяна Раисовна РЫЖИКОВА[1], Николай Сергеевич УРТЕГЕШЕВ[1], Альбина Альбертовна ДОБРИНИНА[1], Андрей Иванович ШЕВЕЛА[2], Андрей Юрьевич ЛЕТЯГИН[3]

[1] Институт филологии СО РАН
630090, г. Новосибирск, ул. Академика Николаева, 8

[2] Институт химической биологии и фундаментальной медицины СО РАН
630090, г. Новосибирск, пр. Академика Лаврентьева, 8

[3] Институт физиологии и фундаментальной медицины
630117, г. Новосибирск, ул. Тимакова, 4

Исследования звуковых систем миноритарных языков народов Сибири и сопредельных регионов базируются на положении о том, что артикуляционно-акустическая база как атрибут этноса является потенциальным историко-лингвистическим источником при реконструкции этногенетических процессов. Инструментальные методы используются новосибирскими фонетистами при изучении звуковых систем с конца 60-х гг. XX в. С 2009 г. ученые трех институтов Сибирского отделения Российской академии наук филологического и медицинского профиля проводят комплексное междисциплинарное исследование артикуляционно-акустических баз коренных популяций Сибири методами магнитно-резонансного томографирования, дигитального рентгенографирования и ларингографирования. Сформирована электронная база данных, включающая соматический материал по 46 идиомам (языкам, диалектам и говорам). По результатам исследования внесены коррективы в традиционные представления учёных о генезисе автохтонных миноритарных этносов и их языков.

Ключевые слова: языки народов Сибири, фонология, методы инструментальной фонетики, магнитно-резонансная томография, цифровая рентгенография, ларингография.

Селютина И.Я. *– д.ф.н., профессор, главный научный сотрудник, siya_irina@mail.ru*
Уртегешев Н.С. *– к.ф.н., старший научный сотрудник, urtegeshev@mail.ru*
Добринина А.А. *– к.ф.н., научный сотрудник, ekinur@mail.ru*
Рыжикова Т.Р. *– к.ф.н., доцент кафедры иностранных языков, redtanya@inbox.ru*
Шевела А.И. *– д.м.н., проф., зам. директора, ashevela@mail.ru*
Летягин А.Ю. *– д.м.н., проф., зам. директора, letyagin-andrey@yandex.ru*

УДК 535.371+616.9+578.74

MULTIPLEX DETECTION OF IgG CLASS ANTIBODIES TO TOXOPLASMA GONDII, RUBELLA VIRUS, CYTOMEGALOVIRUS AND HERPES SIMPLEX VIRUS USING A NOVEL MULTIPLEX FLOW IMMUNOASSAY

Sergey Anatolievich DOLGUSHIN[1], Ekaterina Mikhaylovna LOSEVA[2], Elena Sergeevna ODINTSOVA[3], Andrey Vladimirovich TRONIN[2], Sergey Vasil'evich SELISHCHEV[1]

[1] *National Research University of Electronic Technology*
124498, Moscow, Zelenograd, Shokin sq., 1

[2] *MBU-Technology, Ltd.*
630090, Novosibirsk, Inzhenernaya str., 16

[3] *Institute of Chemical Biology and Fundamental Medicine of SB RAS*
630090, Novosibirsk, Lavrent'ev av., 8

Preclinical tests of the novel multiplex immunoassay for the detection of TORCH infections in human serum using flow cytometry are presented. The immunoassay is intended for the qualitative detection of specific human IgG class antibodies to *Toxoplasma gondii*, rubella virus, cytomegalovirus and herpes simplex virus in human serum. Multiplex analysis is performed *in vitro* on polystyrene microspheres encoded with organic dye. The diagnostic sensitivity of the kit is evaluated to be not less than 95%.

Keywords: bead-based multiplex immunoassay, immunofluorescence, TORCH complex, immunodiagnostics.

TORCH infections are a group of congenitally transmitted infections that cause significant morbidity and mortality in newborns if untreated [1]. TORCH stands for: T – toxoplasmosis, O – other infections, R – rubella, C – cytomegalovirus, H – herpes simplex virus.

The multiplex kits are based on suspensions of encoded microbeads which are spectrally encoded. Molecular probes (antigens) are attached to their surface [1–4]. Each bead represents a finite element of the biochip, so it can be detected by a unique spectral code and characterized by a unique molecular probe attached to its surface. As a result, it becomes possible to carry out sensitive registration of an identifiable chemical compound. The assay is carried out on fully automated high-performance devices that use the principles of a flow cytometry [2–5]. The multiplex analysis if compared with ELISA requires several times less runtime for analysis; besides, reagent consumption and staff employment time are reduced significantly. Flow cytometry is based on the registration of optical radiation that is scattered on a single particle. This method requires a relatively simple optical system for the registration of the scattered radiation in contrast to the optical systems for the registration of diffusively scattered radiation in time domain [5].

In the present work preclinical tests of a novel multiplex immunoassay for the detection of TORCH infections in human serum using flow cytometry are presented. The kit is based on organic dye-labeled polystyrene beads and is intended to use in clinics for the in vitro detection of blood serum immunoglobulin G (IgG) to *Toxoplasma gondii*, rubella virus, cytomegalovirus (CMV) and herpes simplex virus (HSV).

Dolgushin S.A. *– candidate of physical and mathematical sciences, senior researcher of the chair for biomedical systems, e-mail: dolgushin.sergey@gmail.com*
Selishchev S.I. *– doctor of physical and mathematical sciences, professor, headr of the chair for biomedical systems, e-mail: sersel@miee.ru*
Tronin A.V. *– director, e-mail: tronin@mbu-tech.com*
Loseva E.M. *– researcher, e-mail: losevaem@gmail.com*
Odintsova E.S. *– candidate of biological sciences, junior researcher, e-mail: odintsoval@ngs.ru*

MATERIALS AND METODS

The assay is based on the the following principles.

(i) An investigated sample (diluted serum at the volume of 20 µl) is mixed with 20 µl of polystyrene beads suspension (QuantumPlex™ 5.5 µm COOH Kit, Bangs Labs, USA). Initial polystyrene beads were at a concentration of ~1×10^8 beads/mL and were encoded by different concentrations of IR organic dye (emission wavelength is 685 nm). The initial beads were chemically bound to antigens of pathogens employing DEPC-Carbodiimide (EDAC) linker and standard binding protocol provided by the beads' supplier. If the serum had IgG that are specific to the antigens of *T. gondii*, rubella virus, HSV or CMV, in a sample the binding reaction of on the microspheres surface immobilized antigen and specific antibody was occurred. There was not detected any cross reaction among the antigens in the developed multiplex immunoassay.

(ii) The microspheres suspension is washed at the second step. Then, a conjugate is added to the suspension. The conjugate is specific to human IgG antibodies that labeled by phycoerythrin (PE). Thus, the antigen/IgG-specific antibody/conjugate – complex is formed on the beads' surface.

The control microspheres are present in the mixture, which are intended to control the reaction status of the conjugate. These spheres are loaded with human monoclonal IgG. If control microspheres are mixed with conjugate, then the IgG/conjugate complex is formed on the surface. An absence of the fluorescence from the control microspheres indicates a failure in the test, so the investigated sample should be tested again. Thus, all stages of the reaction can be easily controlled.

The presence of the TORCH infections in the serum sample is indicated by the PE emission peak (575 nm) in a spectrum of fluorescent light emitted from the beads.

RESULTS AND DISCUSSION

The assay of the microspheres was carried out using a flow cytometer BD FACS Canto II. A fluores-

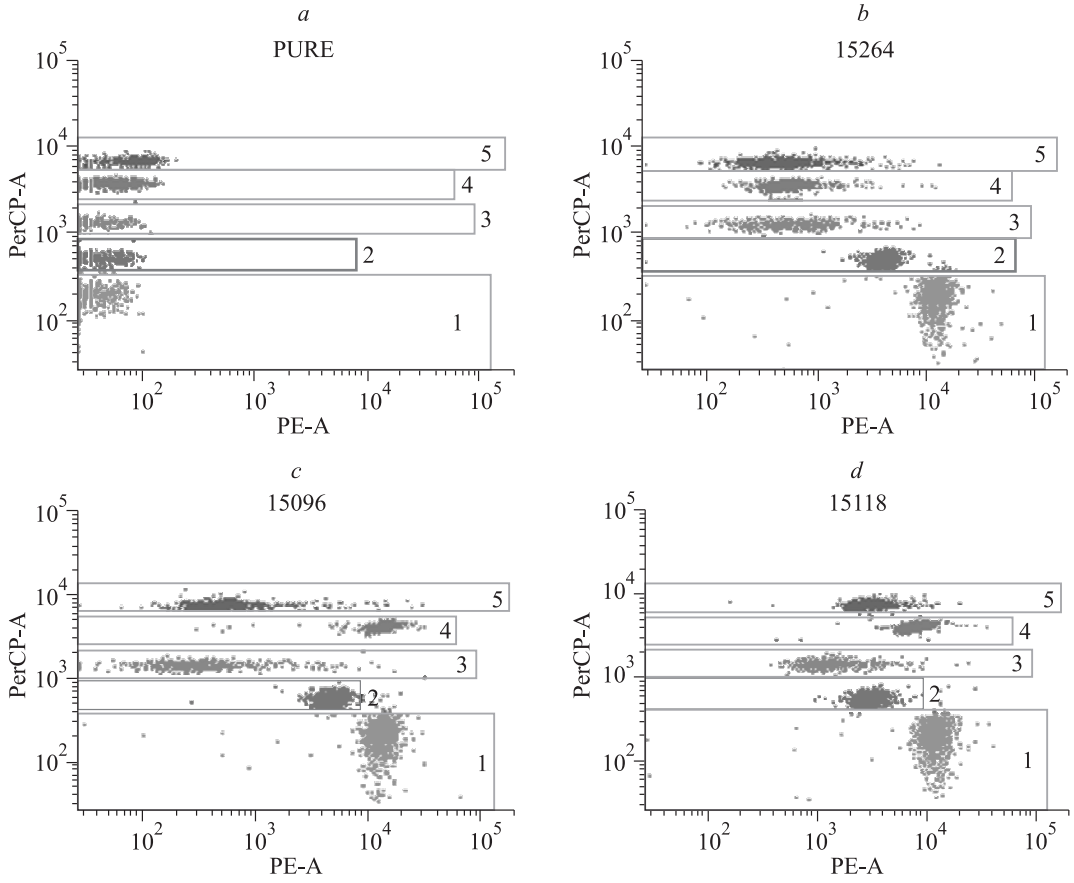

Fig. *Multiplex assay of negative (–) and positive (+) serum samples for HSV (b+, c+, d+), T. gondii (b –, c –, d+), rubella virus (b–, c–, d+) and CMV (b–, c+, d+). The clouds correspond to the following beads populations: 1 – control (K+), 2 – HSV, 3 – rubella virus, 4 – cytomegalovirus, 5 – T. gondii. Results prior to incubation with the serum sample (a) and after the incubation (b, c, d)*

cence excitation is carried out with the argon laser (power 15 mW, wavelength 488 nm). The filter FL-3 (Per-CP-H) was used for detection of microspheres. Fluorescence was recorded for PE and PerCP/PE-Cy5 fluorescence channels by second (FL2) and third (FL3) photomultiplier tube, respectively.

HSV, rubella virus, CMV and *T. gondii* antigen was covalently attached to the microspheres N 2, 3, 4 and 5, respectively. Human monoclonal IgG was covalently attached to the microspheres N 1. All individual sera previously examined on the presence of antibodies to respective antigens using corresponding ELISA kits. As Figure shows, a negative serum cloud of data is located in the first decade of the abscissa (for *T. gondii*, rubella virus (*b*, *c*) and CMV (*b*)). For the analysis of positive samples displacement of clouds in the higher values of the fluorescence channel FL2 PE occurs (for HSV (*b*, *c*, *d*), *T. gondii*, rubella virus (*d*) and CMV(*c*, *d*)). Each serum was analyzed three times and the reproducible results for each infection were obtained.

There were investigated 94 different human serum samples totally. Each serum was tested using a multiplex kit and controlled by corresponding IgG ELISA kit. The results obtained with multiplex kit were in agreement with ELISA for 89 samples and varied for 5 serum samples. Thus, the diagnostic sensitivity of the kit is evaluated to be not less than 95 %. The results of preclinical tests for reagents kit satisfy the requirements for this class of test systems. It was found that a diagnostic sensitivity of the developed reagent kit is close to the sensitivity of commercial products.

ACKNOWLEDGEMENTS

This work was financially supported by the Ministry of Education and Science of the Russian Federation (agreement № 14.575.21.0090, identifier RFMEFI57514X0090).

REFERENCES

1. *Binnicker M.J., Jespersen D.J., Harring J.A.* Evaluation of three multiplex flow immunoassays compared to an enzyme immunoassay for the detection and differentiation of IgG class antibodies to herpes simplex virus types 1 and 2 // Clin. Vaccine Immunol. 2010. 17. 253–257.

2. *Binnicker M.J., Jespersen D.J., Harring J.A.* Multiplex detection of IgM and IgG class antibodies to *Toxoplasma gondii*, rubella virus, and cytomegalovirus using a novel multiplex flow immunoassay // Clin. Vaccine Immunol. 2010. 17. (11). 1734–1738.

3. *Dhiman N., Jespersen D.J., Rollins L.O. et al.* Detection of IgG-class antibodies to measles, mumps, rubella, and varicella-zoster virus using a multiplex bead immunoassay // Diagn. Microbiol. Infect. Dis. 2012. 67. (4). 346–349.

4. *Guigue N., Menotti J., Hamane S. et al.* Performance of the BioPlex 2200 flow immunoassay in critical cases of serodiagnosis of toxoplasmosis // Clin. Vaccine Immunol. 2014. 21. (4). 496–500.

5. *Tereshchenko S.A., Dolgushin S.A., Titenok S.A.* An imperfection of time-dependent diffusion models for a determination of scattering medium optical properties // Opt. Commun. 2013. 306. 26–34.

МНОГОПАРАМЕТРОВАЯ ДЕТЕКЦИЯ IGG АНТИТЕЛ К TOXOPLASMA GONDII, RUBELLA VIRUS, CYTOMEGALOVIRUS И HERPES VIRUS ПРИ ПОМОЩИ НОВОГО МУЛЬТИПЛЕКСНОГО НАБОРА РЕАГЕНТОВ

Сергей Анатольевич ДОЛГУШИН[1], Екатерина Михайловна ЛОСЕВА[2], Елена Сергеевна ОДИНЦОВА[3], Андрей Владимирович ТРОНИН[2], Сергей Васильевич СЕЛИЩЕВ[1]

[1] Национальный исследовательский университет «МИЭТ»
124498, г. Москва, Зеленоград, площадь Шокина, д. 1

[2] ЗАО «МБС-Технология»
630090, г. Новосибирск, ул. Инженерная 16

[3] Институт химической биологии и фундаментальной медицины СО РАН
630090, г. Новосибирск, пр. Ак. Лаврентьева, 8

В работе представлены результаты доклинических испытаний нового мультиплексного набора реагентов для выявления инфекций группы TORCH при помощи метода проточной цитофлуориметрии. Набор предназначен для количественного выявления в сыворотке крови человека иммуноглобулинов класса G, специфичных к антигенам *Toxoplasma gondii*, *Rubella virus, Cytomegalovirus* и *Herpes simplex virus*. Мультиплексный анализ выполняется *in vitro* на полистирольных микросферах, меченных органическим красителем. Установлено, что диагностическая чувствительность разработанного набора реагентов составляет не менее 95 %.

Ключевые слова: мультиплексный иммуноанализ, микросфера, иммунофлуоресцентный анализ, TORCH комплекс, иммунодиагностика

Долгушин С.А. *– к.ф.-м.н., старший научный сотрудник кафедры биомедицинских систем, dolgushin.sergey@gmail.com*
Селищев С.И. *– д.ф.-м.н., профессор, заведующий кафедрой биомедицинских систем, sersel@miee.ru*
Тронин А.В. – *директор, tronin@mbu-tech.com*
Лосева Е.М. – *сотрудник, losevaem@gmail.com*
Одинцова Е.С. – *к.б.н., м.н.с., odintsoval@ngs.ru*

УДК 611.1.001.576: 51-76

PATIENT-SPECIFIC 1D MODEL OF THE HUMAN CARDIOVASCULAR SYSTEM

Ilya Nikolaevich KISELEV[1,2], Fedor Anatol'evich KOLPAKOV[1,2], Elina Arnoldovna BIBERDORF[3,4], Viktor Il'ich BARANOV[5], Tamara Grigor'evna KOMLYAGINA[5], Irina Yurevna SUVOROVA[5], Vladimir Nikolaevich MELNIKOV[5], Sergey Georgievich KRIVOSHCHEKOV[5]

[1] *Institute of Systems Biology Ltd.*
630112, Novosibirsk, Krasin str., 54

[2] *Design Technological Institute of Digital Techniques of SB RAS*
630090, Novosibirsk, Academician Rzhanov str., 6

[3] *Sobolev Institute of Mathematics of SB RAS*
630090, Novosibirsk, Academician Koptyug av., 4

[4] *Novosibirsk State University*
630090, Novosibirsk, Pirogov str., 2

[5] *Institute of Physiology and Basic Medicine*
630117, Novosibirsk, Timakov str., 4

The technique of parameter personalization of 1D hemodynamic model is discussed and validated against physiological data of 1546 examined patients. Different parameter combinations were used, with the quality of prediction of the systolic and diastolic pressures used as the principle validation criterion. It is shown that with an appropriate personalization the model can provide adequate predictions (correlations near 0.9), where the decisive role is played by the total peripheral resistance parameter. Meanwhile parameters of the largest arteries do not play a significant role in the prediction.

Keywords: cardiovascular system, 1D arterial tree model, mathematical modeling, parameters personalization, validation, experimental data.

This work is concerned with the problem of personalization and validation of a one-dimensional model of the human cardiovascular system including the arterial tree. This kind of models is widely known and used in many studies [6, 10, 16, 21, 22]. One-dimensional models are signficiantly simpler than three-dimensional models, which usually describe three-dimensional flow with Navier-Stokes equations in domains with moving boundaries (e.g. [1]). However, they are more complicated than models with lumped parameters (e.g. [15]) and are able to describe particular features of blood flow in separate vessels. Such models are best applicable for global description of arterial systems in order to study propagation of pulse wave or emulating blood loss or zero gravity. The model which we use in the

Kiselev I.N. *– junior researcher, e-mail: axec@developmentontheedge.com*
Kolpakov F.A. *– candidate of biological sciences, director, head of laboratory for bioinformatics*
Biberdorf E.A. *– candidate of physical mathematical sciences, docent, senior researcher, e-mail: biberdorf@ngs.ru*
Baranov V.I. *– candidate of biological sciences, senior researcher of laboratory for organism functional reserves, e-mail: v.i.baranov@physiol.ru*
Komlyagina T.G. *– researcher of laboratory for organism functional reserves, e-mail: KomlyaginaTG@physiol.ru*
Suvorova I.Yu. *– junior researcher of laboratory for organism functional reserves, e-mail: suvorovaiu@physiol.ru*
Melnikov V.N. *– doctor of biological sciences, leading researcher of laboratory for organism functional reserves, e-mail: mvn@physiol.ru*
Krivishchekov S.G. *– candidate of medical sciences, professor, head of laboratory for organism functional reserves, e-mail: krivosch@physiol.ru*

current work was developed by us earlier in the BioUML platform [9].

Model personalization implies calculation of model parameters according to experimental data for a given patient. Wherein it is necessary to validate personalized model against real data and estimate quality of personalization procedure. Most of the studies considering cardiovascular system personalization use models with lumped parameters. Moreover, they usually are restricted to theoretical description of personalization procedure [15] or validate it against small groups (less than 10 subjects) [20] including animals [7]. The work by Kayvanpour et al. [8] should be separately noted as it describes personalization of a three-dimensional heart model including electrophysiological, biological and biomechanical blocks conducted on a group of 46 individuals.

To our best knowledge, there are very few works on personalization of one-dimensional arterial tree models and there is no published validation on significant amount of experimental data. In [14] a smaller model with 24 arteries is validated on data measured using MRT on a single individual. The measured parameters include thickness and length of the most of 24 vessels and input blood flow. In [18] a 1d model with coronary vessels is compared to data collected from a small group of volunteers (6–8 depending on type of data) without personalization. In [17] personalization is conducted but the results are validated on a single subject.

In this work we use results of a clinical study [12] comprising more than 1500 subjects. We restricted ourselves to predicting of systolic (maximal) and diastolic (minimal) pressures.

ARTERIAL TREE MODEL

A detailed mathematical description can be found in [4]. The Equations for the model consisting of one artery are as follows

$$\begin{cases} \partial_1 A + \partial_z Q = 0 \\ \partial_z Q + \alpha \partial_z \left(\dfrac{Q^2}{A} \right) + \dfrac{A}{\rho} \partial_z p + K_r \dfrac{Q}{A} = 0, \end{cases}$$

where $A(t, z)$ – cross-sectional area, $Q(t, z)$ – blood flow through this area, $p(t, z)$ – blood pressure in the artery, α – Coriolis coefficient, ρ – constant blood density, $K_r = 8\pi\nu$ – friction coefficient, ν – constant blood viscosity. For closing of system (1) we use the equation of state based on the Hooke's law

$$p(A, A_0, \beta) = \beta(\sqrt{A} - \sqrt{A_0}) / A_0, \qquad (1)$$

where A_0 – cross-sectional area of artery in relaxed state (external pressure is equal to internal), $\beta = \sqrt{\pi} h_0 E$ – elasticity parameter of the artery, E – Young modulus, h_0 – constant artery wall thickness.

Arteries in the model are organized into binary tree. The model comprising n arteries is described by PDE system

$$\partial_t U_i + B(U_i) \partial_z U_i = S(U_i), \qquad (2)$$

where $U_i = (A_i, Q_i)^T$. Further in the text when it is clear from the context that we speak about a single artery, index *i* will be omitted.

Boundary conditions

Interface conditions at bifurcation points of the arterial tree as well as conditions at the entrance of aorta and ends of terminal arteries (which do not further bifurcate) are formulated as boundary conditions for system (2).

For the aorta entrance it is natural to define input flow Q. Generally speaking, this condition may include aortal and ventricular blood pressures but in the current work we use the explicit form $Q = f(t, SV, HR)$, where t – time, SV – stroke volume, HR – heart rate, f – certain function. At the ends of terminal vessels we use the filtration condition

$$Q = K_f (p - p_v), \qquad (3)$$

where K_f – filtration coefficient, Q – output flow, p – pressure, p_v – pressure in the venous system.

Model parameters

Mathematical modeling of the arterial tree implies numerical solving of initial value boundary problem for hyperbolic system. Model personalization is done by setting individual vessel parameters A_0, h_0 and E, and boundary conditions according to the experimental data for a given individual. To set the boundary condition one should define function f, values of parameters SV, HR, filtration coefficient K_f and pressure p_v.

The data on vessel parameters initially collected by professor A. Noordergraaf [13] have been used for a number of arterial tree models and been modified and adjusted several times. In the work [22] they were extended by data for additional vessels and it was shown that Young modulus is likely to rise along the length of the arterial tree. In [19] it is suggested that the cross-sectional area decreases linearly along each single artery. In [21] cross-sectional areas are adjusted so that reflection coefficients in bifurcation points are minimized. In [10] elastic properties of arteries are also changed. This data is used in the current work and can be found in the supplement materials.

EXPERIMENTAL DATA

As the source of experimental data we use the database [12] including data on common and regional hemodynamics and elasticity of the large arteries of the lower and upper limbs. The Database contains records about 1546 persons examined in a general therapeutic hospital – females and males of different ages, 59 of which are healthy and 1487 have different chronic diseases. Observations were obtained using oscillovasmetry and venous occlusion plethysmography [11].

In total the database contains 127 parameters, including individual and environmental – 17; physiological – 73; clinical – 37. The physiological block contains data on 4 specific arteries in the left and right arms and lower parts of the left and right shins. Particularly the provided data corresponds to brachial arteries in the arms and «generalized» vessels resembling three arteries in the shins [11].

The observations were recorded by the same observer at Scientific Research Institute of Physiology of SB RAMS (currently – Scientific Research Institute of Physiology and Basic Medicine) in the time period from 1993 to 2004. The majority of the examined patients were patients of Clinics of the Institute of Clinical & Experimental Medicine (Novosibirsk). All parameters from the database that were used in the current study are listed in Table 1.

PARAMETERS PERSONALIZATION

The first step in model personalization is creating correspondence between experimental data and model parameters. Particularly for each patient, the personalized model should define properties of the arteries and boundary conditions.

Parameters of limb vessels

In this paragraph we will deal with one artery, so we will omit the artery index. In order to set the modeled vessel properties let's use the equation of state (2). For each model artery we need to define elastic parameter β and cross- sectional area while artery is relaxed A_0.

Equations for elastic resistance K_{in} and characteristic impedance Z_W are taken from [11]. Writing the equation of state separately for systole and diastole we obtain algebraic system with 4 equations and 3 variables (A_S, A_0, β)

$$\begin{cases} P_S = \dfrac{\beta}{c}\dfrac{\sqrt{A_S}-\sqrt{A_0}}{A_0},\ P_D = \dfrac{\beta}{c}\dfrac{\sqrt{A_D}-\sqrt{A_0}}{A_0}, \\ K_{in} = \dfrac{c}{l}\dfrac{P_S - P_D}{A_S - A_D}, \qquad Z_W = \sqrt{\dfrac{\rho\beta}{2\sqrt{A_S}}}\dfrac{1}{A_S}, \end{cases} \tag{4}$$

where V_S – volume of the artery in systole (maximal), V_D – volume of the artery in diastole (minimal), l – artery length, ρ – blood density, coefficient $c \approx 133.32$ serves to translate units from mm hg to dyn/cm2. From the experimental data we know values of A_D, P_S, P_D, K_{in}, Z_W. Variables to be found are A_S, A_0, β System (4) is overdetermined. All its equations are only approximations and the known parameters also contain errors. Therefore magnitude of discrepancy for this system may be considered as measure for compatibility between the database and equation of state used in our model. Let's use the first three equations to calculate unknown variables

Table 1

Parameters from the database used in this study (in total – 31 parameters)

Notation	Description	Units
Individualization parameters		
Age	Age	years
HR	Heart rate	beats/min
H	Height	cm
W	Weight	kg
Physiological parameters (for each of 4 limbs)		
P_D	Blood diastolic pressure	mmHg
P_S	Blood systolic pressure	mmHg
P_P	Pulse pressure	mmHg
r_D	Arterial effective diastolic radius	cm
K_{in}	Arterial elastic resistance	dyn/cm^5
Z_W	Characteristic impedance	(dyn × s)/cm^5

Classification is given according to [12]

and then compare simulated characteristic impedance with given by the fourth equation. Explicit equations for A_0, β can be derived from (4):

$$A_0 = \left(\frac{P_D\sqrt{A_S} - P_S\sqrt{A_D}}{P_S - P_D} \right)^2, \beta = cA_0 \frac{P_S - P_D}{\sqrt{A_S} - \sqrt{A_D}}. \quad (5)$$

These values should be necessarily set to arteries in order to obtain real correspondence between pressures and elastic resistance Kin from the database.

Characteristic impedance can then be calculated from the last equation of (4) and compared to this from the database. It appeared that value $Z_W^{\text{Ratio}} = Z_W^{\text{Sim}} / Z_W$ divides all subjects from the database into two clusters which persist for all 4 vessels. These clusters are not correlated with physiological parameters but are defined by date when observations were taken (Fig. 1). The mean square error of impedance calculation is 0.098 before May 1999 and 0.02 – after. It is reasonable to expect that the overall accuracy of personalization will not exceed accuracy of system (4) solution. We have divided the database into two subgroups according to date when observation were taken. The first group (before 01.05.1999) will be used as a control set. The second group which demonstrates relatively low discrepancy for system (4) will be used as the main dataset for personalization and validation.

Tree structure qualification

Data provided by [10] includes the subclavian artery (a. subclavia), which branches into radial (a. radialis) and ulnar (a. ulnaris) arteries. This indicates that the brachial artery, which is missing, is actually included a. subclavia II which is one of the longest vessels in the model (42,2 cm) and its relaxed cross-sectional area is 0,51 mm^2 which significantly exceeds typical value for a. brachialis in the database (average for left hand is 0.135 mm^2). Probably this is due to a relatively complex structure of the arterial system in the arm, which includes two anastomoses that cannot be correctly modeled with a binary tree, so this structure is described as one vessel, wherein parameters were taken from the main branch and are constant through the vessel.

To make the model and the database compatible, the model was modified as follows. The last 15 centimeters of a. subclavia II were extracted to form a separate artery with an additional branch, which models a. profunda brachii and ensures the binary structure of the tree. The new arterial tree includes 59 arteries. Parameters for the new vessels for each individual from the database were calculated using formulas (5). The elasticity parameter of both added arteries was considered equal. The cross-sectional area of a. profunda brachii was set to 30 % from this of a. brachialis (based on [2]).

Unlike in the upper limbs, in the lower limbs area of measurements covers three arteries with close diameter values (a. tibialis posterior, a. tibialis anterior, a. peronea) while the database records – due to features of measurement techniques – are given for the «generalized» vessel whose volume is equal to the sum of the three arteries. In the model we have only two of these arteries. A. peronea, which in reality is a branch of a. tibialis posterior, is not included. We will consider the model vessel a. tibialis posterior as a «generalized» vessel which resembles real arteries a. tibialis posterior and a. peronea. Elasticity parameters are considered to be equal for both vessels while cross-sectional areas are split in proportion 1 : 2, which agrees with our tabular data and data given in [2].

Reference patient

In this study we consider tabular data from the literature as representative of «average» parameters. Due to the tree extension we need to extend this table as well. We will do it by choosing one patient from the database and using his parameters to extend tabular data. The «reference» patient should satisfy the following criteria.

1. His parameters should be close to mean values of the population. It is checked using the next formula:

$$Dist = \sum_i \left| x_i - \overline{x_i} \right| / \overline{x_i},$$

where $\overline{x_i}$ – mean value of i-th parameter. The next parameters were used: age, height, weight, heart rate, diastolic and systolic pressures.

2. Pressures of the «reference» individual should be close to those produced by the model without changing vessel parameters personalization. We estimate this property by comparison of simulated and expected pressures in the left brachial artery

$$Error = \left| P_S - P_S^{Sim} \right| / P_S + \left| P_D - P_D^{Sim} \right| / P_D,$$

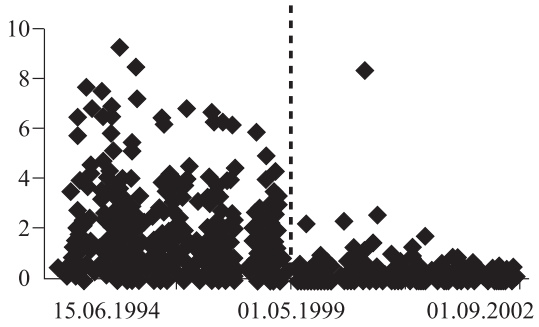

Fig. 1. *Squared error of calculated characteristic impedance*

where P_S, P_D – real pressure values, P_S^{Sim}, P_D^{Sim} – simulated with personalized values of *HR*, *SV* and *TPR*.

3. It should be symmetric in the sense that it minimizes the *Asym* value of

$$\left|1-\frac{A_{0,lh}}{A_{0,rh}}\right|+\left|1-\frac{A_{0,ll}}{A_{0,rl}}\right|+\left|1-\frac{\beta_{0,lh}}{\beta_{0,rh}}\right|+\left|1-\frac{\beta_{0,ll}}{\beta_{0,rl}}\right|,$$

where *lh*, *rh*, *ll*, *rl* – indices of the left and right upper and lower arteries given in the database.

Parameters of the the «reference» patient selected according to these criteria are given in Table 2. We assume that vessel parameters of this patient agree well with the tabular data obtained from the literature.

Extrapolation to the tree

In order to personalize parameters of other arteries we will make the next assumptions. For two subjects, the ratio between cross-sectional areas A0 remains close to constant for all the arteries. Particularly if a. brachialis sinistra of one subject is twice as thick as this artery of another subject then the same can be said about all other arteries of upper part of the body. Analogically, a. tibialis posterior sinistra serves as reference for the lower part (division into two parts was done at the branching point between IV and V segments of a. abdominalis, see the supplement). Thus if we know the parameters of the entire arterial tree of one person and parameters of certain arteries of another then we can restore parameters for all vessels of a second person.

We introduce parameters $A_{F,up}$ and $A_{F,down}$ into the model, which relate to the upper and lower parts of the body. Before simulation starts, all parameters of all vessels are multiplied by the corresponding factor. For the «reference» patient we set $A_{F,up} = A_{F,down} = 1$ (i.e. his parameters are default values presented in the supplement). For arbitrary patient

$$A_{F,up} = A_{o,h} / A^*_{0,h},\ A_{F,down} = A_{o,l} / A^*_{0,l} \qquad (6)$$

where * means parameters of «reference» patient, index *h* means index of a. brachialis sinistra and *l* – a. tibialis posterior sinistra.

For elastic parameter β analogical factors are introduced into the model. In the current work we will not distinguish between left and right parts of tree, i.e. parameters of right part of the tree will be set the same as for the left.

Table 2

Parameters of «referenced» subject

	Value	Min	Max	Median	Mean
Dist	0.37	0.06	1.84	0.64	0.68
Asym	0.405	0.235	4.17	0,87	1.1
Error	0.124	0.048	0.486	0.159	0.183

Parameters of boundary conditions

Natural boundary conditions are blood flow from the heart at the aorta entrance and filtration through porous medium (capillaries) at the terminal arteries ends.

For further calculations we will assume that the systole duration is proportional to the heart cycle duration. Function to model blood flow:

$$Q_{in}(t) = SV(1+\sin(x(t))/T_S,$$

$$x(t) = \begin{cases} \dfrac{s(t)}{a} - 0.5, & s(t) < a, \\ \dfrac{s(t)-a}{T_S^* - a} + 0.5, & s(t) < T_S^*, \\ 1.5, & otherwise, \end{cases}$$

where SV – stroke volume, T_S – systole duration, T_C – heart cycle duration, T_C^* – «reference» heart cycle duration, T_S^* – «reference» systole duration, t – time, % – modulo division, $s(t)$ maps intervals $[\text{NT}_C, (N+1)T_C]$ to $[0, T_C^*]$, where $N = 0, 1, \ldots$ Assuming that the systole duration is proportional to the heart cycle duration, the simulated blood volume for one heart beat will be equal to *SV*. The heart cycle duration is given by formula $T_C = 60/HR$. Parameters $a \approx 0.091$ and $T_S^* \approx 0{,}331$ are fitted to match the desired blood flow profile [3]. The stroke volume can be obtained from the cardiac output and heart rate

$$\text{SV} = \text{CO}/\text{HR}. \qquad (7)$$

To calculate the cardiac output we use the allometric equations from [5]. One particular equation which produces the best results was used (see supplement materials for more details)

$$\text{CO (ml/min)} = 2499\ \text{H (m)}^{1,16}. \qquad (8)$$

To define the output boundary conditions (3) venous pressure P_{veins} and filtration coefficient K_f should be specified. As simulation results show, the total resistance of arterial tree comprising 59 largest vessels is less than 1 % of the normal value of the total peripheral resistance (TPR) which is ≈ 1.1 mmHg/(ml/s). Thus, to compensate for the lack of resistance we should set $K_f = 1/TPR$, which can be calculated from database values:

$$\text{TPR} = 60\ (\text{P}_S/3+2\text{P}_D/3)/\text{CO}. \qquad (8)$$

RESULTS

Numerical simulations were conducted using a specially written Java program using the BioUML

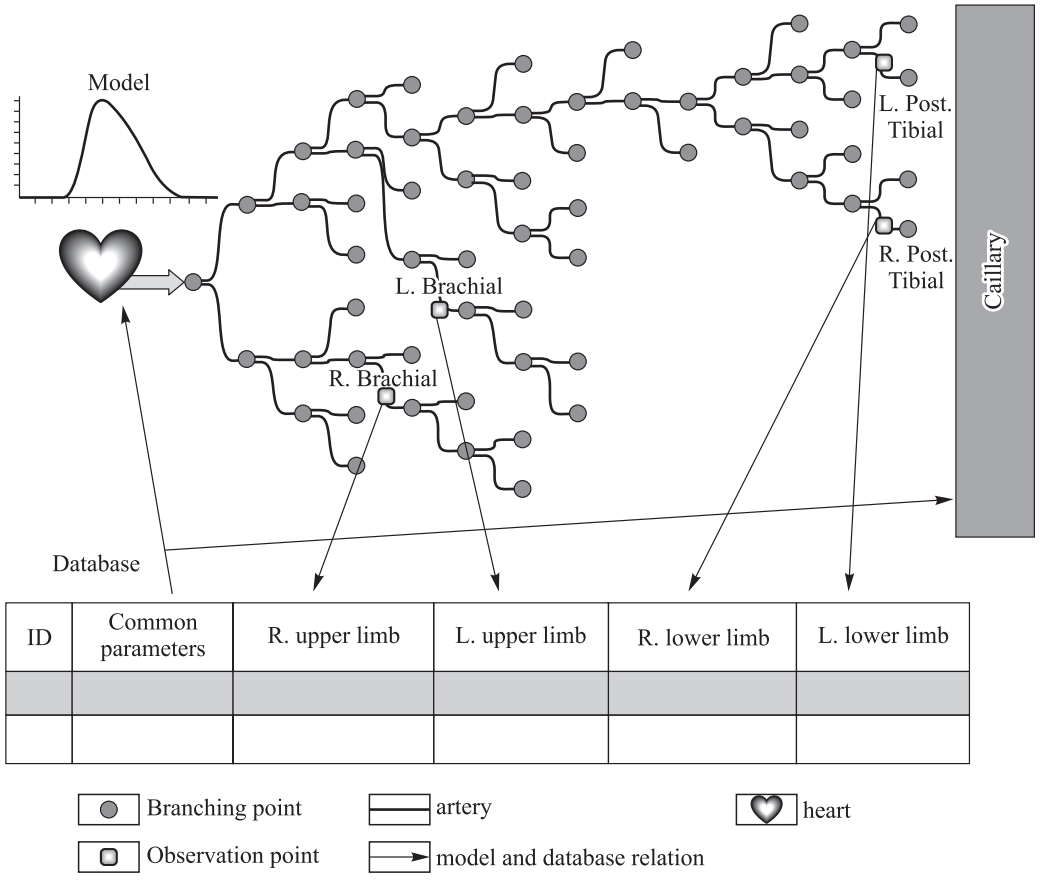

Fig. 2. *Ratio between simulated and expected systolic, diastolic and pulse pressures*

API for model construction and numerical calculations (www.biouml.org).

Before simulation starts, case deletion was performed, reducing the number of patients from 1546 to 1207. To avoid outliers affecting the results, we censored patients by parameters A_0 and β: bottom and upper 5 % were excluded from the groups. In total, there were 556 patients retained in the training group (recorded after 01.05.1999) and 420 in the control group (before 01.05.1999).

For each patient, personal parameters were set to the model and a simulation was performed for 12 seconds of the model time. The last 2 seconds were used to calculate the maximum (systolic) and minimum (diastolic) pressures. As experience has shown, 12 seconds is enough for the model to reach a quasi steady state (see supplement for details).

We have conducted several simulations using different combinations of parameters to personalize. If a parameter is not included to the selected combination, then its default value is used. The total list of personalized parameters is presented below.

Resistance to blood flow from the terminal vessels is set to TPR (8).

Heart rate HR is taken directly from the database. The default value is 72 beats/min.

Stroke volume SV is calculated according to (7). Default value is 75 ml.

Parameters A_0 and β of a. brachialis sinistra, a. brachialis dextra and generalized arteries of lower limbs are calculated with formulas (6). There is no default values, these parameters are personalized in all simulations.

Parameters A_0 and β of all other arteries are obtained multiplying default values by $A_{F,lh}$ and $\beta_{F,lh}$ for upper part of the tree and by $A_{F,ll}$ and $\beta_{F,ll}$ for lower part of the tree. Default values are given in the supplement.

Best simulation results are presented on Fig. 2. Scheme of relations between database and model are given on Fig. 3. Simulated systolic and diastolic pressures were compared to real values utilizing Pearson correlation coefficient and mean relative error. The results for different personalized parameters combinations for a. brachialis dextra are given in Table 3. The first column indicates which parameters were personalized. Additional results can be found in the supplement.

DISCUSSION

The mathematical model helps in revealing of artifacts in experimental data such as unexpected

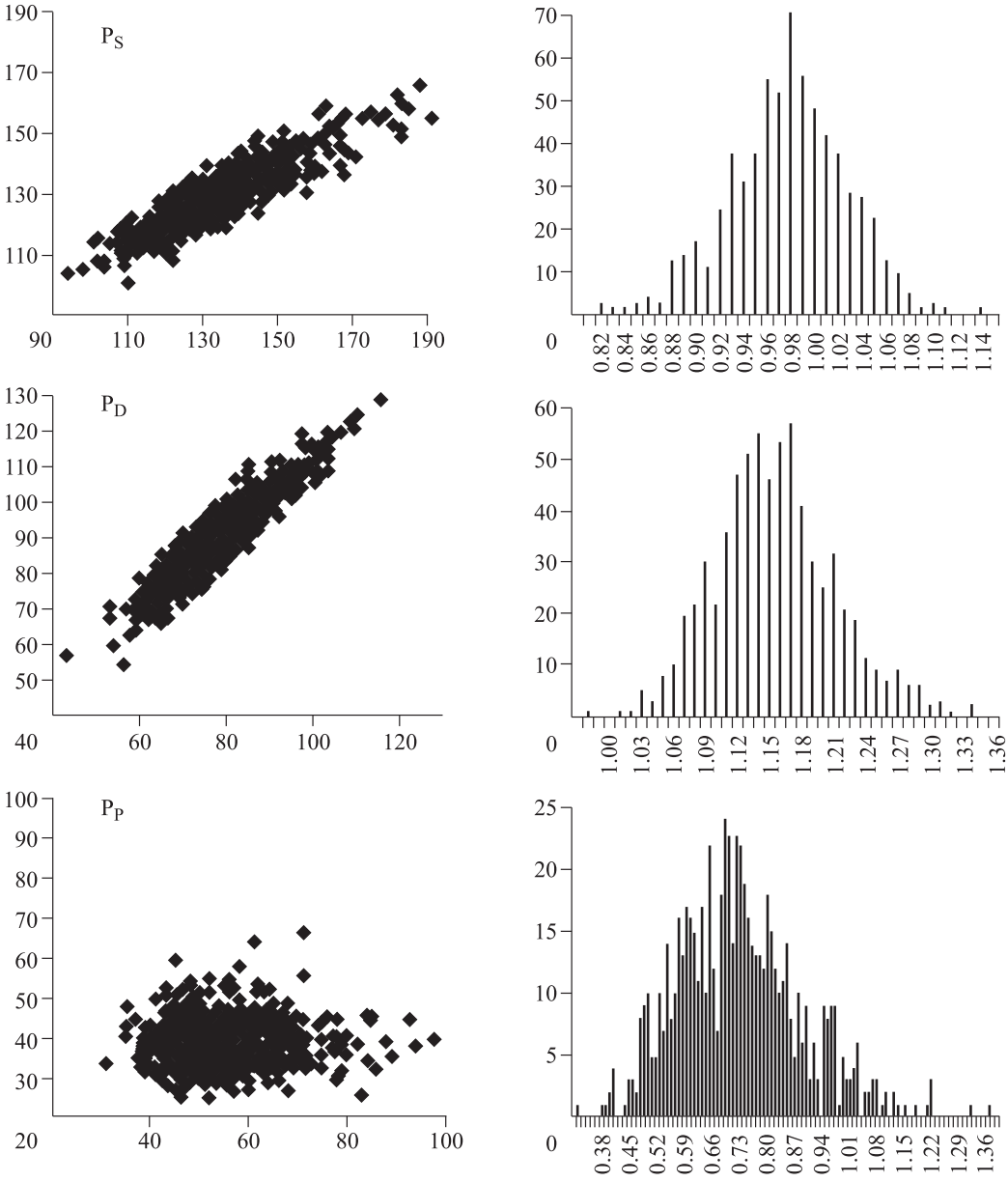

Fig. 3. *Model and database relations scheme*

Table 3

Simulation results for left upper limb

Parameter	Correlations			Mean relative error		
	Ps	Pd	Pp	Ps	Pd	Pp
TPR A_0 β SV HR	0.784[1]	0.864[1]	0.011	0.055	0.208	0.372
A_0 β SV HR	0.007	–0.162[1]	0.046	0.171	0.126	0.342
TPR SV HR	0.897[1]	0.925[1]	–0.070	0.041	0.164	0.283
TPR HR	0.484[1]	0.556[1]	–0.318[2]	0.169	0.391	0.214
TPR SV	0.422[1]	0.530[1]	–0.075	0.119	0.249	0.283
TPR A_0 β	0.693[1]	0.781[1]	0.006	0.158	0.472	0.328
TPR A_0	0.569[1]	0.838[1]	–0.125[2]	0.209	0.385	0.285
TPR β	0.806[1]	0.759[1]	0.085[2]	0.123	0.486	0.400
TPR	0.810[1]	0.838[1]	–0.401[1]	0.164	0.425	0.210

Index 1 denotes P-value< 0.001, index 2 denotes P-value< 0.05.

data clustering, which may be hard or nearly impossible to find by analysis of the database alone (Fig. 1).

The simulation results show that the single parameter – TPR is able to explain up to 70 % of systolic ($r \approx 0{,}838$) and diastolic ($r \approx 0{,}81$) pressures dispersion while other parameters cannot account for more than 10 % of dispersion. The best result is obtained when personalization of the heart rate and stroke volume is added to TPR $r \approx 0{,}897$ and $r \approx$ $\approx 0{,}925$. In comparison to using TPR only it demonstrates a better accuracy with the mean relative error decreasing nearly fourfold. Thus, the structure of the arterial tree and parameters distribution are unlikely to play a significant role in prediction of systolic and diastolic pressures.

It should be kept in mind that the database contains records of people who (in the majority) had suffered from cardiovascular diseases and received medicament treatment for certain periods of time. Their artery properties and relationships between them could have changed as a result.

It was also shown that the model using only *TPR* can predict pressures for different age groups (these results can be found in the supplement).

Meanwhile none of the used personalization parameters could explain the variability of pulse pressure. In the simulated data the pulse pressure is negatively correlated ($r = -0{,}41$) with diastolic pressure while this is not the case in reality ($r = 0{,}13$). This can be a result of inaccurate equation of state (1) with constant parameters A_0 and β. It is possible to improve the model by making the parameters dependent on the pressure.

The error rate in modeling is around 10 %, resulting from a combination of the following factors: observation record error (e.g. heart rate was measured for 10 seconds and multiplied by 6), connection between database and model – equations in system (5) are approximations, the «reference» patient is modeled with ~10% error itself (see Table 2.)

It should be noted that model parameters are personalized in the natural way without a fitting procedure and despite the difference between training and control groups (see Fig. 1.), the model predicts pressures for control group only slightly worse (Table 4).

CONCLUSIONS

We have performed personalization of 1d arterial tree model parameters and consequent validation of this model on a group of 1207 persons (after case deletion from the original 1546). For each subject his own identified parameters were calculated and set to the model and a simulation was performed. The results show good correlations and mean error in the predictions of systolic and diastolic pressures and inability of the model (with used personalized parameters).

Although vessels elasticity and relaxed cross-sectional area do not play a significant role in the predictions, they are expected to be important for the pulse wave profile and velocity prediction. They also can be used for modeling of special states, such as vasoconstriction in certain arteries, stress. Along with model modifications/improvements, this is planned for future work.

The model described in this paper is available as a part of the free open-source platform BioUML at www.biouml.org. One can access the model either through the standalone version of BioUML or using its web-interface. The supplementary materials are available at http://wiki.biouml.org/index.php/Patient-specific cardiovascular model.

ACKNOWLEDGEMENTS

The reported study was supported by RFBR, research project № 16-01-00779 A.

REFERENCES

1. *Appanaboyina S., Mut F., Löhner R. et al.* Computational modelling of blood flow in side arterial branches after stenting of cerebral aneurysms // Int. J. Computat. Fluid Dyn. 2008. 22. 669–676.

2. *Avolio A.P.* Multi-branched model of the human arterial system // Med. Biol. Eng. Comput. 1980. 18. 709–718.

Table 4

Simulation results for main and control groups (depending on observations date)

Date	*n*	Correlations			Mean Error		
		Ps	Pd	Pp	Ps	Pd	Pp
Control	420	0.733[1]	0.801[1]	0.111[2]	0.073	0.199	0.335
Main	556	0.784[1]	0.864[1]	0.011	0.055	0.208	0.372
Any	976	0.754[1]	0.836[1]	0.098	0.062	0.205	0.356

All 5 parameters are personalized. Index 1 denotes P-value< 0.001.

3. *Best C.H., Taylor N.B., West J.B.* Best and Taylor's Physiological basis of medical practice. Baltimore: Williams & Wilkins, 1991. 1170 p.

4. *Biberdorf E.A., Blokhin A.M., Trakhinin Y.L.* Global modeling of the human arterial system // Circulatory System and Arterial Hypertension: Experimental Investigation, Mathematical and Computer Simulation. Eds. L.N. Ivanova, A.L. Markel, A.M. Blokhin, E.V. Mishchenko. N. Y.: Nova Science Publishers Inc., 2012. P. 115–142.

5. *de Simone G., Devereux R.B., Daniels S.R. et al.* Stroke volume and cardiac output in normotensive children and adults. Assessment of relations with body size and impact of overweight // Circulation. 1997. 95. 1837–1843.

6. *Grigoryan S.S., Saakyan Y.S., Tsaturyan A.K.* On the Kortokov method theory // Biomechanics. 1984. 15–16. 54–73. [In Russian].

7. *Hann C.E., Revie J., Stevenson D. et al.* Patient specific identification of the cardiac driver function in a cardiovascular system model // Comput. Methods Programs Biomed. 2011. 101. 201–207.

8. *Kayvanpour E., Mansi T., Sedaghat-Hamedani F. et al.* Towards personalized cardiology: Multiscale modeling of the failing heart // PLoS One. 2015. 10. e0134869.

9. *Kiselev I.N., Semisalov B.V., Biberdorf E.A. et al.* Modular modeling of the human cardiovascular system // Math. Biol. Bioinf. 2012. 7. 703–736. [In Russian].

10. *Lamponi D.* One dimensional and multiscale model for blood flow circulation: Pour l'obtention du grade de docteures sciences. Lausanne, 2004.

11. *Mazhbich B.I.* Oscillowasometry of limb arteries. Novosibirsk: Nauka, 1990. 152 p. [In Russian].

12. *Melnikov V.N., Komlyagina T.G., Rechkina S.Y.* The elasticity of the arteries and hemodynamics in healthy and sick people: the database is registered in the Registry database of the Federal Service for Intellectual Property at June 9, 2012, number 2012620540. [In Russian].

13. *Noordergraaf A.* Physical basis of ballistocardiography: Ph. D. Thesis. Utrecht, 1956.

14. *Olufsen M.S., Peskin C.S., Kim W.Y. et al.* Numerical simulation and experimental validation of blood flow in arteries with structured-tree outflow conditions // Ann. Biomed. Eng. 2000. 28. 1281–1299.

15. *Proshin A.P., Solodyannikov Y.V.* Identification of the parameters of blood circulation system // Autom. Remote Control. 2010. 71. 1629–1647.

16. *Quarteroni A., Formaggia L.* Mathematical modelling and numerical simulation of the cardiovascular system // Handb. Numer. Anal. 2004. 12. 3–127.

17. *Reymond P., Bohraus Y., Perren F. et al.* Validation of a patient-specific one-dimensional model of the systemic arterial tree // Am. J. Physiol. Heart Circ. Physiol. 2011. 301. H1173–1182.

18. *Reymond P., Merenda F., Perren F. et al.* Validation of a one-dimensional model of the systemic arterial tree // Am. J. Physiol. Heart Circ. Physiol. 2009. 297. H208–222.

19. *Stergiopulos N., Tardy Y., Meister J.J.* Nonlinear separation of forward and backward running waves in elastic conduits // J. Biomech. 1993. 26. 201–209.

20. *Vovkodav O., Pasichnyk R.* The method of identification of a mathematical model for the cardiovascular system response dynamics to exercise stress // J. Appl. Comput. Sci. 2014. 22. 91–99.

21. *Wang J.J., Parker K.H.* Wave propagation in a model of the arterial circulation // J. Biomech. 2004. 37. 457–470.

22. *Westerhof N., Bosman F., De Vries C.J., Noordergraaf A.* Analog studies of the human systemic arterial tree // J. Biomech. 1969. 2. 121–143.

ПЕРСОНАЛИЗИРОВАННАЯ ОДНОМЕРНАЯ МОДЕЛЬ СЕРДЕЧНО-СОСУДИСТОЙ СИСТЕМЫ ЧЕЛОВЕКА

Илья Николаевич КИСЕЛЕВ[1,2], Федор Анатольевич КОЛПАКОВ[1,2], Элина Арнольдовна БИБЕРДОРФ[3,4], Виктор Ильич БАРАНОВ[5], Тамара Григорьевна КОМЛЯГИНА[5], Ирина Юрьевна СУВОРОВА[5], Владимир Николаевич МЕЛЬНИКОВ[5], Сергей Георгиевич КРИВОЩЕКОВ[5]

[1] ООО «Институт системной биологии»
630112, г. Новосибирск, ул. Красина, д. 54

[2] Конструкторско-технологический институт вычислительной техники СО РАН
630090, г. Новосибирск, ул. Академика Ржанова, 6

[3] Институт математики им. им. С.Л. Соболева СО РАМН
630090, г. Новосибирск, просп. Академика Коптюга, 4

[4] Новосибирский государственный университет
630090, г. Новосибирск, ул. Пирогова, 2

[5] НИИ физиологии и фундаментальной медицины
630117, г. Новосибирск, ул. Тимакова, 4

В работе обсуждается методика персонализации параметров одномерной модели гемодинамики и ее валидация на основе физиологических данных 1546 пациентов. Использованы различные комбинации параметров, в качестве главного критерия валидации выступало качество прогнозирования систолического и диастолического давления. Показано, что при точной персонализации модель может обеспечить адекватное предсказание давления (коэффициенты корреляции около 0,9), при этом решающую роль играет общее периферического сопротивление, а параметры крупных артерий не играют значительную роль в прогнозировании.

Ключевые слова: сердечно-сосудистая система, одномерная модель артериального дерева, математическое моделирование, персонализация параметров, валидация, экспериментальные данные.

Киселев И.Н. *– младший научный сотрудник, e-mail: axec@developmentontheedge.com*
Колпаков Ф.А. *– к.б.н., директор ООО; зав. лабораторией биоинформатики.*
Бибердорф Э.А. *– к.ф.-м.н., доцент кафедры, старший научный сотрудник, e-mail: biberdorf@ngs.ru*
Баранов В.И. *– к.б.н., старший научный сотрудник лаборатории функциональных резервов организма, e-mail: v.i.baranov@physiol.ru*
Комлягина Т.Г. *– научный сотрудник лаборатории функциональных резервов организма, e-mail: KomlyaginaTG@physiol.ru*
Суворова И.Ю. *– младший научный сотрудник лаборатории функциональных резервов организма, e-mail: suvorovaiu@physiol.ru*
Мельников В.Н. *– д.б.н., ведущий научный сотрудник лаборатории функциональных резервов организма, e-mail: mvn@physiol.ru*
Кривощеков С.Г. *– д.м.н., проф., зав. лабораторией функциональных резервов организма, e-mail: krivosch@physiol.ru*

УДК 611.018.1: 52-17

INDEPENDENCE OF AP PROPAGATION VELOCITY TO TRANSJUNCTIONAL VOLTAGE DEPENDENCE OF GAP JUNCTIONAL COUPLING

Shailesh APPUKUTTAN, Rohit MANCHANDA

Department of Biosciences and Bioengineering, Indian Institute of Technology Bombay 400076, India, Mumbai, Powai

Gap junctions are protein structures that form transmembrane channels between adjacent cells, thereby allowing the direct passage of ions and small molecules. They play an important role in the physiological functioning of the individual cells, and also the tissue. Experimental studies have reported a variety of gap junction subtypes, with differences in their biophysical properties, such as their unitary conductances and sensitivity to transjunctional voltage. Our study aims at computationally exploring the effect of these differences towards the spread of action potentials in syncytial tissues. Results from our simulations suggest that the propagation velocity of action potentials is independent of the transjunctional voltage dependence of the gap junction subtype. The propagation velocity was found to be constant across all subtypes tested, when the maximal conductances were set equal. This was verified using action potentials of widely varying time courses. We attribute this trend to the much slower gating kinetics of gap junctions in comparison to the time course of action potentials, and more specifically the short period where a significant transjunctional voltage is maintained.

Keywords: action potential, propagation velocity, gap junction, transjunctional voltage, syncytium.

Gap junctions are proteins that provide pathways for intercellular communication. They are known to play an important role in the development and functioning of individual cells, as well as of the parent tissue [8]. Experimental studies have revealed the existence of a variety of gap junction subtypes [11]. These subtypes differ in their biophysical properties, such as their unitary conductances and sensitivity to transjunctional voltage, which can potentially influence the functioning of syncytial tissues. The properties are determined by connexins, which are proteins that form the gap junctions.

In this study, we have focused on one of the differing biophysical properties, namely, the transjunctional voltage (V_j) dependence of conductance exhibited by gap junctions. Three connexin subtypes – Cx40, Cx43 and Cx45 – forming homomeric-homotypic gap junctions were explored. These were selected as experimental studies have reported their occurrence in syncytial tissues such as in cardiac and smooth muscle, e.g. the detrusor layer of the urinary bladder wall. Also, these subtypes are known to exhibit markedly different sensitivities to transjunctional voltage, and thus fit the purposes of this study. We have developed models for these subtypes previously [4]. The spread of action potentials (APs) being vital to the functioning of syncytial tissues, the propagation velocity of APs was chosen as the test parameter. To ensure that the study focused solely on the transjunctional voltage dependence of gap junctional coupling, measures were taken to negate other differences. As all the three subtypes were known to exhibit different unitary conductances, the total number of channels for each subtype was adjusted such that the overall maximal conductance between any two cells, expressed for $V_j = 0$ mV, was equal. To assess the generality of our findings, we employed three different AP mechanisms, varying widely in their time courses – from 5 to 500 ms.

The combination of connexins forming each gap junction subtype renders it physiologically unique, and often cannot be adequately replaced by another subtype [4]. For example, in the cardiac tissue, under certain pathological conditions, downregulation of Cx43 is accompanied with the increased expression of Cx40 and Cx45 [5]. Studies such as the one undertaken here would help in identifying the differences between gap junction subtypes that affect physiological functioning.

Appukuttan S. *– Ph.D., Computational NeuroPhysiology Laboratory, e-mai: shailesh.a@iitb.ac.in*
Manchanda R. *– Prof., Ph.D., head of Computational NeuroPhysiology Laboratory, e-mail: rmanch@iitb.ac.in*

MATERIAL AND METHODS

1-D and 3-D models of smooth muscle cells were developed on the NEURON simulation environment, a compartmental modeling platform. Adjacent cells in these models were coupled by means of gap junctions. These have been described in detail in [1]. Separate models were developed for each of the three gap junction subtypes considered in our study, as presented in [4]. The centroid cells in our models were equipped with stimulus via current injection, or synaptic input, to elicit an action potential, which then further propagated to other cells in the electrical syncytium. The active ion channel mechanisms, enabling the generation of action potential, incorporated in each cell is described below.

Obtaining APs of varying time courses

Action potentials of varying time courses were obtained by tweaking the native Hodgkin-Huxley (HH) model in NEURON. The kinetics of the mechanism was altered by adjusting the value of the Q_{10} temperature coefficient parameter. In modeling, the Q_{10} parameter is used to adjust the rate of reaction for changes in temperature. It is formally defined as the change of reaction rate for a 10 °C increase in temperature [6]. The Q10 is calculated as:

$$Q_{10} = \left(\frac{R_2}{R_1}\right)^{10/(T_2 - T_1)}, \quad (1)$$

where R_1 and R_2 are the reaction rates at temperatures T_1 and T_2, respectively. The Q_{10} parameter has no units. It is important to note that our model has no other temperature sensitive parameter. Thus consequences of changing the Q_{10} parameter are restricted to the active ion channel mechanisms, and thereby in the shape of the resultant action potential.

For our current study, we employed action potentials of three widely differing time courses ranging from 5 to 500 ms, as shown in Fig. 1. The Q_{10} values required for arriving at these, and the resultant action potential durations have been summarized in Table 1. The change in the kinetics of the active ion channels also has implications for the excitability of the cell. This is illustrated in Fig. 2 using strength-duration curves for each of the three AP mechanisms evaluated for a single isolated cell.

Setting Equal Maximal Conductances

The various gap junction subtypes are known to have differing levels of unitary conductances [5]. The propagation velocity of action potentials has been shown to depend upon the extent of coupling between cells [4]. Thus, to evaluate the effect of transjunctional voltage dependence of gap junctional coupling on the propagation velocity of APs, it is essential to ensure that the maximal conductance expressed by each of the gap junction subtypes was equal. This was achieved by adjusting the total number of gap junction channels, N_j, at the junction between two cells, as in [4]. This ensured that the total gap junctional conductance, g_j, between two cells, obtained by multiplying the single channel conductance, γ_{main}, with N_j, was equal for $V_j = 0$ mV, i.e. when both cells were at isopotential. Table 2 summarizes this configuration.

$$g_j = \gamma_{main} \times N_j \quad (2)$$

RESULTS

AP Propagation Velocity in a 1-D Model

We began by evaluating the AP propagation velocity in a 1-D arrangement of smooth muscle cells, linked to one another along their longitudinal axis by means of gap junctions. The number of cells was kept large (= 181) to mimic an infinite cable, and thereby eliminate interference due to 'current reflection' from the terminal ends. The central cell was stimulated by means of current injection to elicit an AP, and the propagated action potentials were recorded at each of the cells. The conduction velocity was determined using the time instants at which

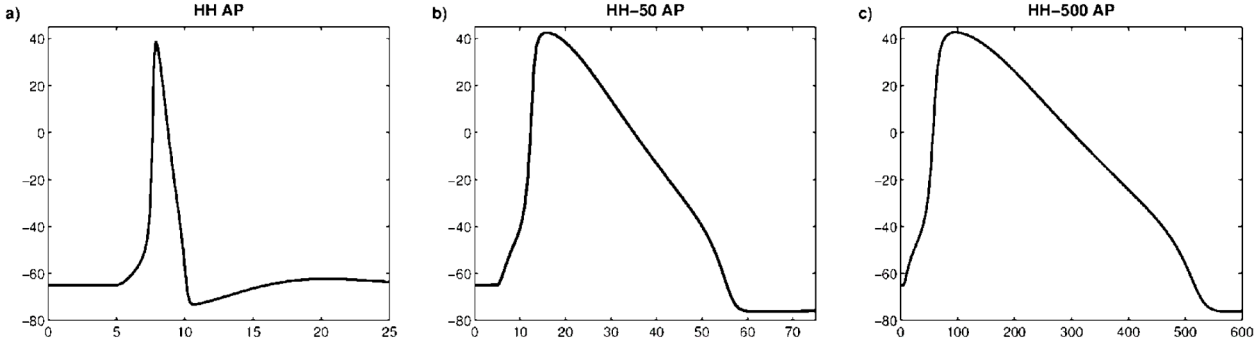

Fig. 1. *Action potentials of varying time courses: (a) HH AP, (b) HH-50 AP, (c) HH-500 AP*

Table 1

Change in Q_{10} parameter to obtain APs of varying time courses

Q_{10}	AP duration (ms)	AP denotation
1	5.1	HH
0.0556	50.4	HH-50
0.00524	511.2	HH-500

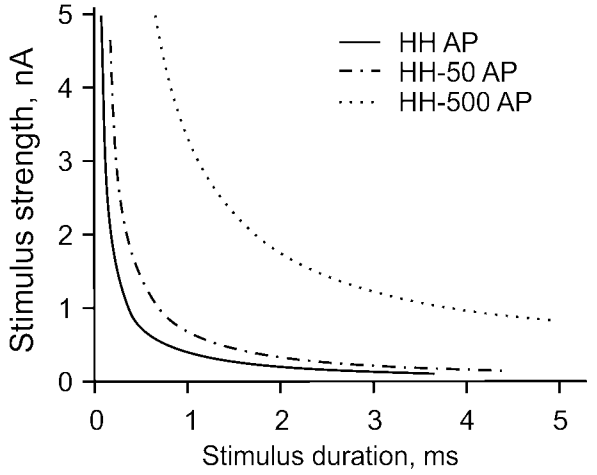

Fig. 2. *Strength-duration curves for each of the three AP mechanisms evaluated from a single isolated cell*

Table 2

Setting equal maximal conductances for all gap junction subtypes

Subtype	γ_{main} (*pS*)	N_j	g_j (*nS*)
Cx40	162	1952	316.2
Cx43	61	5184	316.2
Cx45	32	9882	316.2

these APs peaked. This was repeated using each of the gap junction subtypes, namely, Cx40, Cx43 and Cx45. Table 3 summarizes our findings from these simulations. It was found that the propagation velocity was constant for each of the three gap junction subtypes. This was true irrespective of the AP mechanism employed. Also, as expected, shorter duration APs had a higher propagation velocity when compared to wider APs.

AP Propagation Velocity in a 3-D Model

The above study was extended to a 3-D model of smooth muscle syncytium. The size of the syncytium was set to a 5- cube, as employed in earlier works [2, 3]. The centroid cell was stimulated to elicit an AP, and the propagation velocity was determined as described above. Table 3 lists the propagation velocities measured across cells along the longitudinal axis of the stimulated cell, using each of the three gap junction subtypes. The results were found to be similar to those obtained for the 1-D model, with the propagation velocity remaining constant for all the subtypes, under all three action potential mechanisms.

Analysis of Transjunctional Voltage During an AP

The above findings called for a more detailed investigation of the effect of transjunctional voltage dependence of gap junctional conductance. For each of the three AP mechanisms, we monitored the transjunctional voltage between adjacent cells in the 1-D model. The top panels in Figures 3, 4 and 5 illustrate this for the HH, HH-50, and HH-500 AP mechanisms, respectively. The bottom panels show the change in the conductance of the gap junction connecting the two cells. It is evident that a large transjunctional voltage is maintained for a very short duration. This holds true even for APs with wider temporal profiles, such as HH-500. The lack of change in conductance suggests that the gap junctional gating kinetics is much slower when compared to the time course of action potentials. For all the three subtypes, across all three AP mechanisms, the overall change in conductance is negligible, thereby having no impact on the propagation velocity of APs. This is discussed in more detail below.

DISCUSSION

The above results show that the AP propagation velocity remains constant across the three subtypes

Table 3

AP propagation velocities

AP Type	Propagation velocity (m/s)					
	1-D model			3-D model		
	Cx40	Cx43	Cx45	Cx40	Cx43	Cx45
HH	0.43	0.43	0.43	0.67	0.67	0.67
HH-50	0.12	0.12	0.12	0.30	0.30	0.30
HH-500	0.02	0.02	0.02	0.05	0.05	0.05

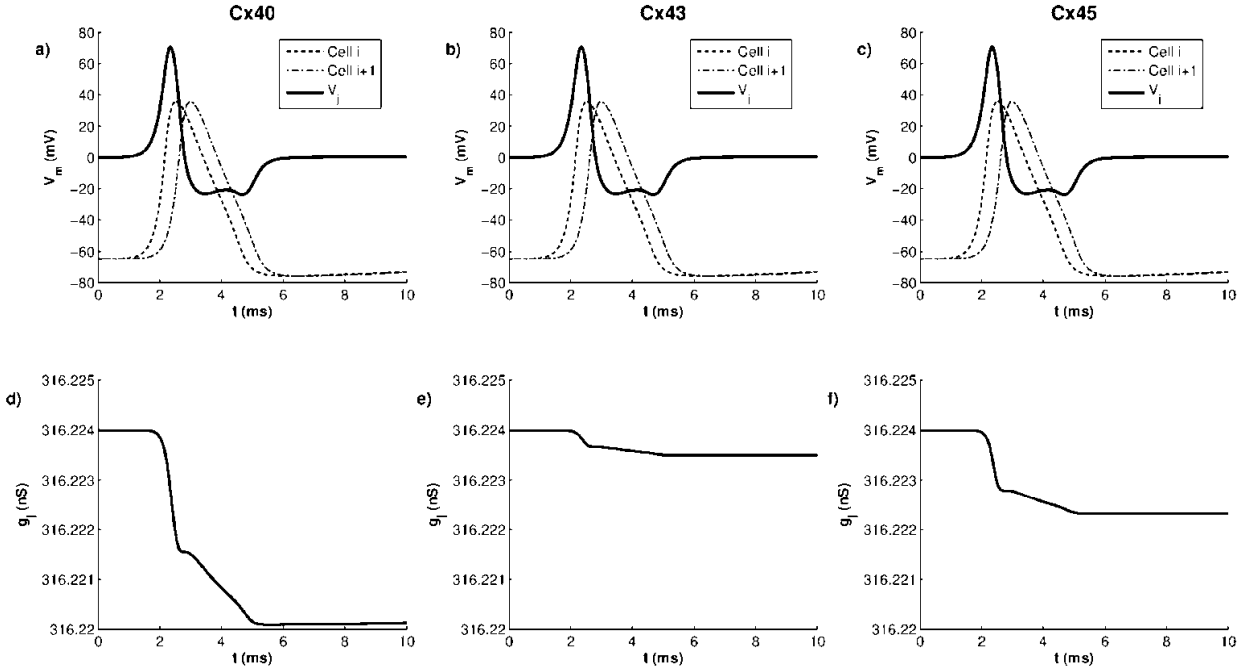

Fig. 3. *(a–c) show the transjunctional voltage between two adjacent cells for each connexin subtype during an action potential using the HH mechanism, and (d-f) show the corresponding change in gap junctional conductance*

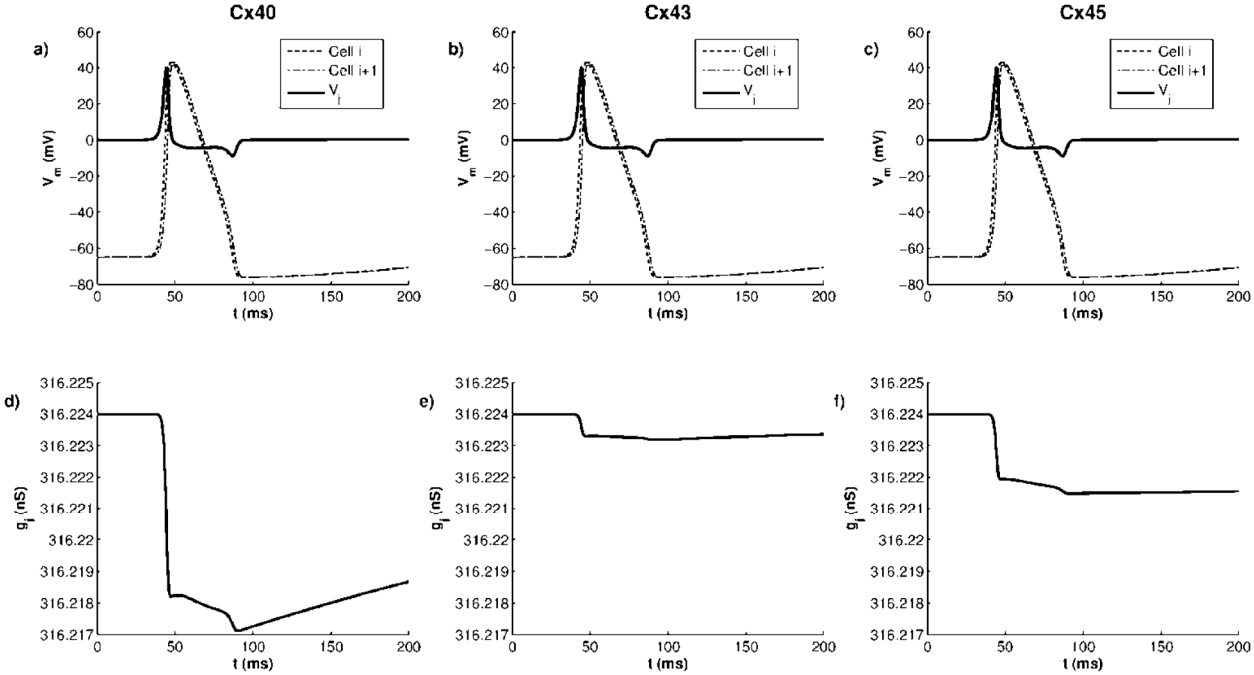

Fig. 4. *(a–c) show the transjunctional voltage between two adjacent cells for each connexin subtype during an action potential using the HH-50 mechanism, and (d-f) show the corresponding change in gap junctional conductance*

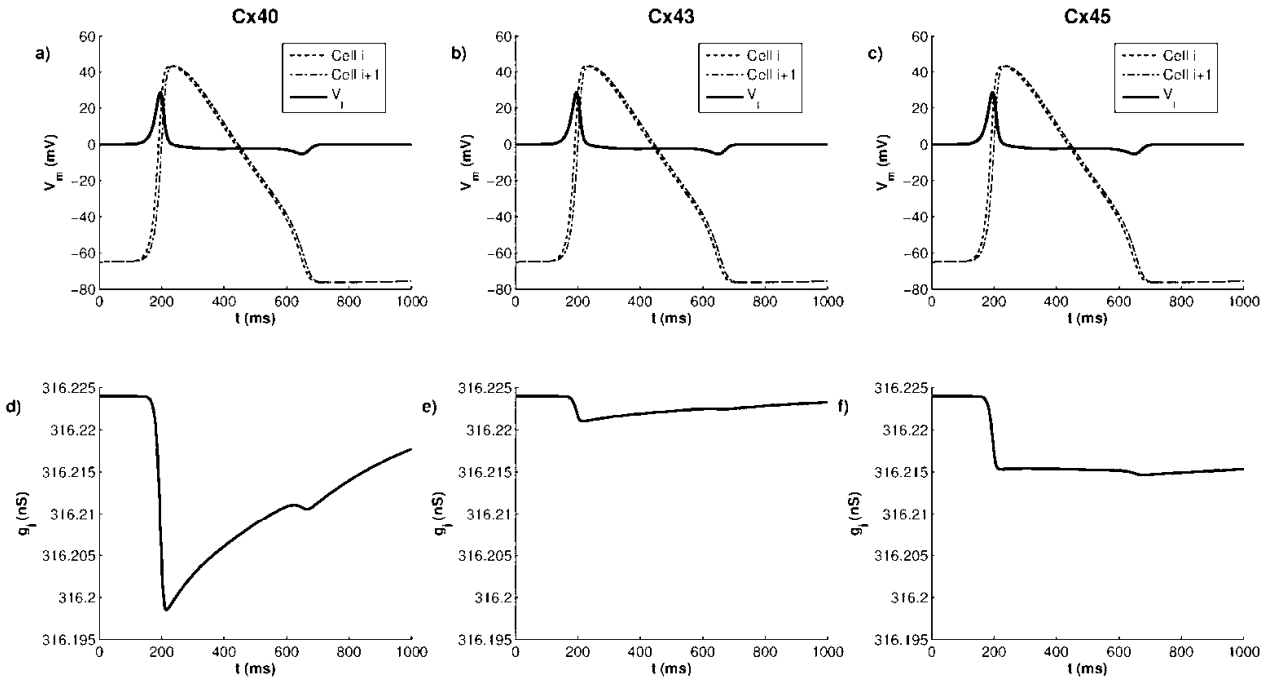

Fig. 5. *(a–c) show the transjunctional voltage between two adjacent cells for each connexin subtype during an action potential using the HH-500 mechanism, and (d-f) show the corresponding change in gap junctional conductance*

for both the 1-D and 3-D models. On further analysis it was found that this correspondence could be attributed to the transjunctional voltage levels emerging during the propagation of APs between adjacent cells. It is found that significant transjunctional voltages (> 5 mV) are maintained for a very short duration of the AP time course, as shown in Table 4. Specifically, only 1.2 ms of the ≈ 5 ms HH-AP, 7.6 ms of the ≈ 50 ms HH-50 AP, and 56 ms of the ≈ 500 ms HH-500 AP, experience a significant transjunctional voltage. These time periods should be considered in view of the gap junctional gating kinetics, which are ~1000-fold slower than most ion channels [10]. The time constants of inactivation are of the order of seconds [7, 9]. Thus, as seen in the bottom panels of Figures 3, 4 and 5, there is negligible change in the conductance offered by gap junctions during the course of an action potential. Further, it can be seen that the Cx43 subtype exhibited the least change in the conductance amongst all three AP mechanisms. Studies have reported that Cx40 and Cx43 possess similar time constants of inactivation, with Cx45 being comparatively slower [5]. Also, Cx43 is least sensitive to transjunctional voltage, followed by Cx40, and Cx45 being most sensitive [5]. Given these, between the three subtypes, it is expected for Cx43 to undergo the least change in conductance during an AP. Cx45, despite being highly sensitive to transjunctional voltage, does not undergo a substantial change in conductance owing to the slower gating kinetics.

Table 4

Analysis of transjunctional voltages during an AP

AP type	Window size (ms)	Total time (ms)	
		$V_j \leq 5$ mV	$V_j > 5$ mV
HH	10	8.8	1.2
HH-50	200	192.4	7.6
HH-500	1000	944.0	56.0

It was seen that shorter APs propagated faster than wider variants. This is easily attributed to the differences in the time required to attain peak of the action potentials. Also, Tables 3 and 4 appear to suggest that the propagation velocity is greater in a 3-D syncytium as compared to a 1-D model. Here, it would be pertinent to mention that the excitability of cells vary depending upon the network layout. Higher intensities of stimuli were required to elicit APs for the 3-D model. The stimuli being different, it would not be appropriate to compare the two cases. In small-sized syncytia, such as that employed here, the stronger stimulus causes significant depolarization even in the neighboring cells, even before an AP peaks in the stimulated cell. This naturally results in faster propagation of APs to the neighboring cells, which have already attained a depolarized membrane potential. This would have lesser effect on syncytia of larger sizes, where the

effect of the stimulus would not be felt at more distant cells. As the focus of the current study was on the effect of transjunctional voltage dependence of gap junctional coupling on action potential propagation, this was not further investigated. A detailed study of syncytial size and AP propagation can be undertaken in future.

To our best knowledge, this is the first study demonstrating the independence of AP propagation velocity to the transjunctional voltage-dependence of gap junctional coupling. We have been able to shown that, irrespective of the gap junction subtype, the spread of action potentials remains unaffected, when the maximal conductance is same. This has been verified for APs of widely varying time courses.

ACKNOWLEDGMENTS

We thank Rohan Sathe (IIT Bombay, India) for his inputs in modeling of the various gap junction subtypes.

REFERENCES

1. *Appukuttan S., Brain K.L., Manchanda R.* A computational model of urinary bladder smooth muscle syncytium // J. Comput. Neurosci. 2015. 38. (1). 167–187.

2. *Appukuttan S., Brain K., Manchanda R.* Syncytial basis for diversity in spike shapes and their propagation in detrusor smooth muscle // Procedia Comput. Sci. 2015. 51. 785–794.

3. *Appukuttan S., Sathe R., Manchanda R.* Mo—dular approach to modeling homotypic and heterotypic gap junctions // ICCABS: Proc. IEEE 5th Int. Conf. Miami, 2015. 1–6.

4. *Appukuttan S., Sathe R., Manchanda R.* Influence of gap junction subtypes on passive and active electrical properties of syncytial tissues // ICSMB: Proc. Int. Conf. Kharagpur, 2016. [in press].

5. *Desplantez T., Dupont E., Severs N.J., Weingart R.* Gap junction channels and cardiac impulse propagation // J. Membr. Biol. 2007. 218. (1–3). 13–28.

6. *Hodgkin A.L., Katz B.* The effect of temperature on the electrical activity of the giant axon of the squid // J. Physiol. 1949. 109. (1-2). 240–249.

7. *Lin X., Crye M., Veenstra R.D.* Regulation of connexin43 gap junctional conductance by ventricular action potentials // Circ. Res. 2003. 93. (6). e63–e73.

8. *Mese G., Richard G., White T.W.* Gap junctions: basic structure and function // J. Invest. Dermatol. 2007. 127. (11). 2516–2524.

9. *Moreno A.P., Laing J.G., Beyer E.C., Spray D.C.* Properties of gap junction channels formed of connexin 45 endogenously expressed in human hepatoma (SKHep1) cells // Am J Physiol. 1995. 268. (2 Pt 1). C356–C365.

10. *Musa H., Veenstra R.D.* Voltage-dependent blockade of connexin40 gap junctions by spermine // Biophys. J. 2003. 84. (1). 205–219.

11. *White T.W., Bruzzone R.* Multiple connexin proteins in single intercellular channels: connexin compatibility and functional consequences // J. Bioenerg. Biomembr. 1996. 28. (4). 339–350.

НЕЗАВИСИМОСТЬ СКОРОСТИ РАСПРОСТРАНЕНИЯ ПОТЕНЦИАЛА ДЕЙСТВИЯ ОТ ВЗАИМОСВЯЗИ МЕЖДУ ТРАНСКОНТАКТНОЙ РАЗНОСТЬЮ ПОТЕНЦИАЛОВ И ПОДТИПОМ ЩЕЛЕВОГО КОНТАКТА

Шайлеш АППУКУТТАН, Рохит МАНЧАНДА

Отдел биологических наук и биоинженерии, Индийский Бомбейский технологический институт 400076, Индия, Мумбаи, Поваи

Щелевые контакты представляют собой белковые структуры, которые формируют трансмембранные каналы между соседними клетками, обеспечивая тем самым прямое прохождение ионов и малых молекул. Они играют важную роль в физиологической активности отдельных клеток, а также тканей. Выявлено множество подтипов щелевых контактов, различающихся по биофизическим свойствам, таким как их унитарная проводимость и чувствительность к трансконтактной разности потенциалов. Наше исследование направлено на вычислительное изучение влияния этих различий на распространение потенциалов действия в синцитии. Результаты нашего моделирования показывают, что скорость распространения потенциалов действия не зависит от взаимосвязи между трансконтактной разностью потенциалов и подтипом щелевого контакта. Установлено, что при равной максимальной проводимости скорость распространения была постоянной для всех исследованных подтипов. Это было подтверждено с использованием потенциалов действия широкого диапазона. Мы связываем данную тенденцию с гораздо более медленной кинетикой функционирования щелевых контактов по сравнению с динамикой потенциалов действия, и, конкретнее, более коротким периодом поддержания значимого трансконтактного потенциала.

Ключевые слова: потенциал действия, скорость распространения, щелевой контакт, трансконтактный потенциал, синцитий.

Аппукуттан Ш. *– к.т.н.*
Манчанда Р. *– к.т.н., проф.*

УДК

AN ONTOLOGICAL-BASED MONITORING SYSTEM FOR PATIENTS WITH BIPOLAR I DISORDER

Chryssa H. THERMOLIA[1], Ekaterini S. BEI[1], Euripides G. M. PETRAKIS[1], Vangelis KRITSOTAKIS[2], Vangelis SAKKALIS[2]

[1] School of Electronic and Computer Engineering, Technical University of Crete 73100, Greece, Chania, Akrotiri Campus

[2] Institute of Computer Science, Foundation for Research and Technology 71110, Greece, Heraklion, N. Plastira, 100

Our aim is to provide a patient monitoring system that integrates a Clinical Decision Support System (CDSS) and an Electronic Health Record (EHR) that assist psychiatrists and primary care physicians to tackle existent health needs of mental illness related to the treatment and management of bipolar I disorder (BDI). Our monitoring system consists of an EHR system based on the Health Level Seven Reference Information Model (HL7-RIM) and an ontological-based CDSS leveraging the Semantic Web capabilities. Based on the evidence-based clinical guidelines and patients' health records, the monitoring system is developed to encode and process this information and subsequently to assign recommendations of choices and alerts to clinicians for improved mental health care. Considering the clinical guidelines germane knowledge, as well as issues of patient's health record, the monitoring system can support a personalized decision-making for bipolar I disorder longitudinal course. We propose AI-CARE as an *online monitoring tool* that may offer useful guidance in clinical practice.

Keywords: clinical decision support system, electronic health record, semantic web, ontology, bipolar disorder.

Optimal health care is a core challenge of several emerging technologies in order to promote the best health care conditions and improved health outcomes for patients living with chronic diseases, such as bipolar disorder. Toward this challenge, the advent of new scientific discoveries in medicine (genetics, epigenetics, pharmaceuticals) along with the technological explosion (medical devices, internet) enable the development of computer-based monitoring systems to aid clinicians in promoting high-quality health care and meeting the goals of «personalized medicine» [10, 12]. Personalized medicine aims to the effective adaptation of biomedical and technological knowledge to the individual features (genetic, anatomical, and physiological characteristics), needs and preferences of each patient mainly considering the difference in patient's susceptibility to a specific disease or patient's response to a particular medical therapy; which does not literally translate in the production of unique drugs or intelligent devices for a specific patient but rather a more targeted therapeutic intervention [12].

In the new era of personalized medicine is highlighted the need to combine «evidence-based medicine» with case based reasoning in order to enhance the health care process [4]. Evidence-based medicine refers to «the conscientious, explicit, and judicious use of current best evidence in making decisions about the care of individual patients», while its practice implies the «integrating individual clinical expertise with the best available external clinical evidence from systematic research» [14]. In this context, CDSS systems are favorable tools to promote the practice of evidence-based medicine and clinical guidelines, in turn is a common method for CDSS [4]. These types of CDS systems, which include documented clinical knowledge, are called knowledge-based systems and provide guidance to clinical decision making [2].

Thermolia Ch.H. *– student, the Intelligent Systems Laboratory, e-mail: cthermolia@ intelligence.tuc.gr*
Bei E.S. *– Ph.D., postdoctoral researcher, the Intelligent Systems Laboratory, e-mail: abei@isc.tuc.gr*
Petrakis E.G.M. *– Ph.D., Professor, laboratory director, the Intelligent Systems Laboratory, e-mail: petrakis@intelligence.tuc.gr*
Kritsotakis V. *– M.Sc., technical staff, Computational BioMedicine Laboratory, e-mail: vkrits@ics.forth.gr*
Sakkalis V. *– Ph.D., principal researcher, Computational BioMedicine Laboratory, e-mail: sakkalis@ics.forth.gr*

In order to interpret information and derive knowledge we use Semantic Web Technologies. The concept of ontology is basic element of Semantic Web, defining a set of primitives containing [11]: concepts, relationships between concepts, described by domain and range restrictions, the taxonomy of concepts with multiple inheritance, axioms describing additional constraints on the ontology that allow to infer new facts from explicitly stated one. Semantic Web Technologies also includes the application of sets of rules that enable us to model knowledge, by inferring new implicit axioms, based on explicitly specified ones, checking for satisfiability of classes, computing hierarchies of classes and properties and checking consistency of the entire ontology.

In our implementation the existence of a domain ontology that supports decision-making is granted and so is the existence of a database supporting the patients' information storage. In order to exploit both the advantages of the existing database and the developed domain ontology we came to develop a mapping mechanism between them, migrating database instances into ontological instances (individuals) (also called ontology population), by a query driven process of transforming the database instances that are the response to a given query.

Bearing in mind the concepts of personalized medicine and evidence-based medicine, section II presents the AI-CARE monitoring system by discussing important issues of the ontological-based CDSS development, and the architecture of the patient-centric EHR (subsection II.A and II.B, respectively), and by focusing on the alignment among Ontology and EHR entities (subsection II.C), as well as test scenarios and validation (subsection II.D). Conclusions and issues for future research are discussed In Section III.

AI-CARE MONITORING SYSTEM FOR PATIENTS WITH BDI

The AI-CARE monitoring system aims to provide an effective monitoring for patients with bipolar disorder.

Bipolar disorder (BD), also known as manic-depressive illness, is a severe mental illness, thought to be caused by an interaction of genetic and environmental factors. BD which is triggered by stressful life events, is often misdiagnosed and/or not sufficiently treated, and is associated with a high risk of suicide. Obviously, considering the important aspects of BD, such as the early onset, natural history, lifetime prevalence (1 to 5 % in general population, estimated in different studies), mental anguish, high rate of recurrence (>90 % of patients who have a single manic episode will have future episodes), and psychiatric/medical morbidity, justify the need to develop an intelligent system in order to longitudinally monitor the evolution of this complex and heterogeneous disease in bipolar patients [17].

The AI-CARE monitoring system utilizes the ontological-based CDSS as part of an electronic health record in order to be beneficial to the bipolar patients, aiming to provide «the right patient with the right drug at the right dose at the right time» and tailoring the medical treatment to the individual characteristics, needs and preferences of a bipolar patient during all stages of care (diagnosis, treatment and follow-up, prevention). Also, is capable of identifying the characteristics of patient-subpopulations that do not benefit from the recommended therapy leading to new expert knowledge, new research and prospectively to new recommendations [12].

DEVELOPMENT OF AN ONTOLOGICAL-BASED CDSS

In order to develop electronic support for clinicians and health care professionals, a knowledge-based system is needed to be developed consisting of a knowledge-base that represents facts about the disorder and an inference engine that can reason about those facts and use rules and other forms of logic to deduce new facts or highlight inconsistencies.

Ontology

The most prominent language for implementing ontologies is Web Ontology Language (OWL). The basic structure of OWL are classes, properties and individuals, which are members of classes. OWL properties are binary relationships and are distinguished in object properties (relate two individuals) and datatype properties (relate an individual with a literal value). Also OWL can define hierarchies of classes and properties, property domain and range restrictions, value restrictions, cardinality, existential and universal quantification restrictions on the individuals of a specific class. Base of OWL is Description Logics (DL) [1].

Ontologies can be distinguished by the subject of the conceptualization, such us knowledge representation, upperlevel, domain and application ontologies [7].

During the definition of a medical domain, achieving formalization of the domain terminology and categorization, is a desired result. In this attempt, formal ontologies such as SNOMED CT [9] or other formal approaches, offer great advantages in formal rigor and inference power. Nonetheless, they limit the expressiveness of the domain representation and design to an upper level description

[8, 15]. Considering these limitations, our attempt to define the bipolar disorder domain integrates: (i) a vocabulary of terms along with concept definition and their inner-relationships, which is offered by formal ontologies, and (ii) a more specialized description that is geared around the concepts related to the patient condition monitoring evolving in time, as presented in Fig. 1.

In order to describe the changing aspects of the disease in terms of states, state transitions and processes, the ontology needs to be dynamic. In our implementation, we design the initial static ontology, describing the main concepts of Bipolar Disorder, using the Protégé ontology editor[1]. The static ontology is converted into dynamic using the CHRONOS plugin of Protégé [13]. The main concepts describing the domain of Bipolar Disorder are distinguished into dynamic entities (entities which evolve in time) and static entities (entities which do not evolve in time).

Ontology is populated with real data collected from 10 patients whose condition is monitored over a period of a few days to a year.

Rules

We derive new knowledge from the assertions in ontology adopting Semantic Web Rule Language rules (SWRL)[2], which is the most prominent language for editing such rule. A SWRL rule presents an implication between an antecedent and a consequent so that the intended meaning is: whenever the condition specified in the antecedent hold, then the conditions specified in the consequent must also hold.

An example of a treatment recommendation rule is presented, resulting into the suggestion of medical treatment. It evaluates the medication the patient is receiving and the type of symptoms the patient presents.

In the case that the patient is first diagnosed, receiving no medication and the symptoms suggest existence of a manic episode then the rule directly suggests medical treatment (Lithium, Li; Valproate, VPA; atypical antipsychotic, AAP). Necessary information for the rule is included in the classes Personal Health Record (PHR), PatientState, Episode, Therapy, and Medicine.

The rule is expressed in DLs [1] as:
PHR∩(∃ PatientState.state = inEpisode)∩
(∃ Episode.type = manic)∩Therapy ∩⊢ ∃ Medicine
→Recommendation (Start Therapy with
Li/VPA/AAP or combination of two medicines)
The rule is expressed in SWRL as:
PHR(?phr), MedicalHistory(?medHist),
Recommendation(?rec),
includesInitialEvaluation(?phr,?ev_medHistory),

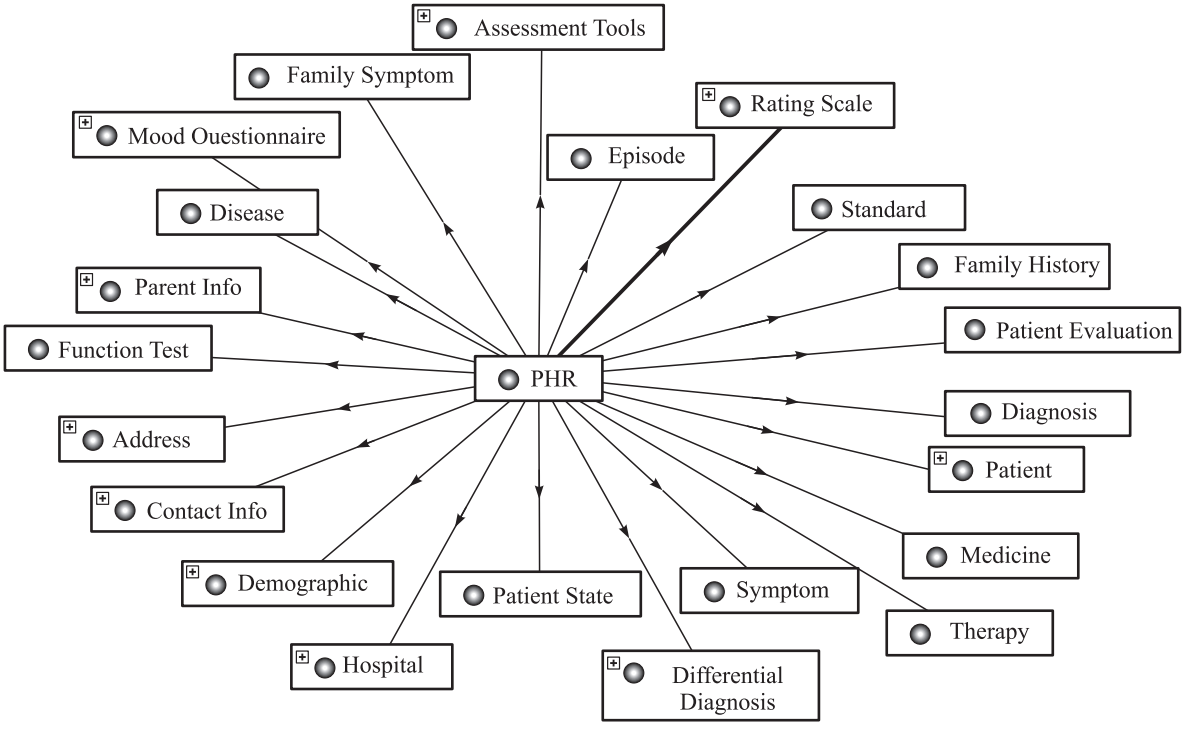

Fig. 1. *Class diagram*

[1] http://protege.stanford.edu/

[2] http://www.w3.org/Submission/SWRL/

includesInitialEvaluation (?ev_medHistory,?medHist), Event(?ev_medHist), Interval(?int_medHist), during(?ev_medHist,int_medHist), evaluationOP(?phr,?ev_eval),evaluation (?ev_eval,?eval),equal(?eval,»mild to severe»), Event(?ev_eval),Interval(?int_eval), during(?ev_eval,?int_eval),interval Before(?int_medHist,?int_eval), text(?rec,?txt), equal(?txt, «Recommend Li/VPA/AAP or 2 drug combination») → recommendationBelongs (?rec,?phr)

DOCUMENTED CLINICAL KNOWLEDGE FOR BDI

Clinical practice guidelines refer to «systematically developed statements to assist practitioner and patient decisions about appropriate health care for specific clinical circumstances» according to the definition of Institute of Medicine (IOM), and are mostly relied on comparative clinical trials [19]. They are commonly utilized by the evidence-based medicine in making clinical decisions to improve the care process [4]. The scope of medication guidelines is to aid the interaction of clinicians and patients in developing the most effective treatment strategy minimizing the side effects.

Clinical guidelines for Bipolar I Disorder (BDI)

We selected evidence-based clinical practice guidelines (e.g. Australian and New Zealand, British Association for Psychopharmacology) related to different aspects of care for BDI, as well as other systematic reviews for BD [5]. Such guidelines utilize evidence-based knowledge for treating and managed patients with BDI defined by specific clinical criteria.

User Scenarios for Bipolar I Disorder

Bipolar Disorder is usually classified within the context of the Diagnostic and Statistical Manual of Mental Disorders (DSM), which differentiates between bipolar I disorder, bipolar II disorder, bipolar disorder not otherwise specified (Bipolar NOS), and cyclothymia.

Presently, we provide user diagnostic and treatment scenarios for the clinical presentation of BDI (at least one manic or mixed episode). Diagnostic scenarios consider specific information of screening and assessment tools and persons' medical/family and past psychiatric history. Diagnosis of bipolar I disorder follows the established criteria of the DSM-IVor DSM-V for a manic or depressive episode along with their severity, considers the psychiatric or/and medical comorbidities and hinders misdiagnosis, especially with unipolar disorder (major depressive disorder).

Based on the aforementioned evidence-based guidelines [5], the diagnostic scenarios are designed to guide the clinicians during the diagnosis procedure (mental state examination, initial evaluation considering the differential diagnosis, assiduous psychiatric examination addressing the different patterns of BD emergence, unobserved comorbidities and related disorders) and the diagnostic accuracy when patients fail to respond to treatment [5]. Also, we developed the user scenarios for BDI treatment options following the dynamic disease course.

The ontology-based CDS system provides diagnosis and treatment recommendations related to the patients' mental state (acute episodes, euthymia), alerts related to crucial mood swings and medication noncompliance, preventive care reminders about monitoring procedures (e.g. extrapyramidal symptoms, lithium serum levels, weight gain, diabetes screening, hyperlipidemia assessment), and warnings related to changes in symptom complex, as well as assists clinicians with decision-making and in developing a personalized disease management.

Longitudinal monitoring of bipolar patients is performed by the developed system to evaluate the presence or absence of symptoms, psychiatric and/or mental comorbidities, medication adherence, and to identify therapeutic drug safety and tolerance. Warnings have been placed in decision nodes with relevant annotation from the literature in order to yield the appropriate hints and alerts to the clinicians on real-time and at the time of care. The monitoring functionality can be further enriched by means of inputs received from biosensors (i.e. biosignals) and smartphone applications (e.g. voice analysis) accompanied by inputs (paper-based and electronic-based data like life charting) from the user's environment (family, carers) or the user himself.

The ontology-based CDS system is highlighted as a crucial component of the patient-centric EHRs for BD. It is implemented using a networked EHR platform, whether the knowledge is available from a repository outside the local site and is accessed, but not incorporated into the local EHR.

ARCHITECTURE OF A PATIENT-CENTRIC EHR

Consistent with the conceptual view of longitudinal monitoring of patients with BD, we created an Electronic Health Record (EHR) for bipolar patients. It encloses five of the essential components of the EHRs: (i) administrative processes, (ii) health information and data, (iii) communication and connectivity, (iv) results management, and (v) decision support [16].

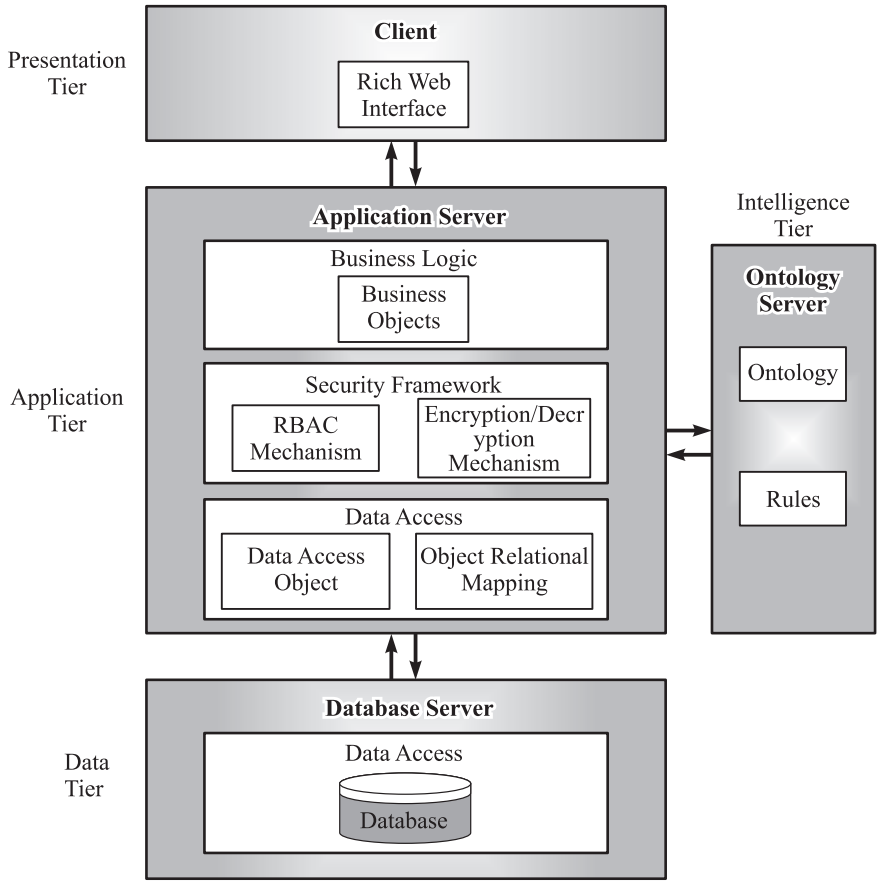

Fig. 2. *Platform architecture – tiers*

The ontology-based CDS system delivered with the EHR as depicted in the platform architecture of Fig. 2 will provide clinicians with suitable tools achieving a better day-to-day clinical decision making.

The architecture of the integrated platform consists of four main tiers (Fig. 2) namely, a) Presentation tier, b) Application tier, c) Intelligence tier, and d) Data tier.

Presentation tier

The first tier, called presentation tier, is the top layer of the integrated platform. This layer is responsible for exchanging information between the general stakeholders and the system. Its main focus is to provide advanced usability and visualization functionality along with a simple and rich graphical

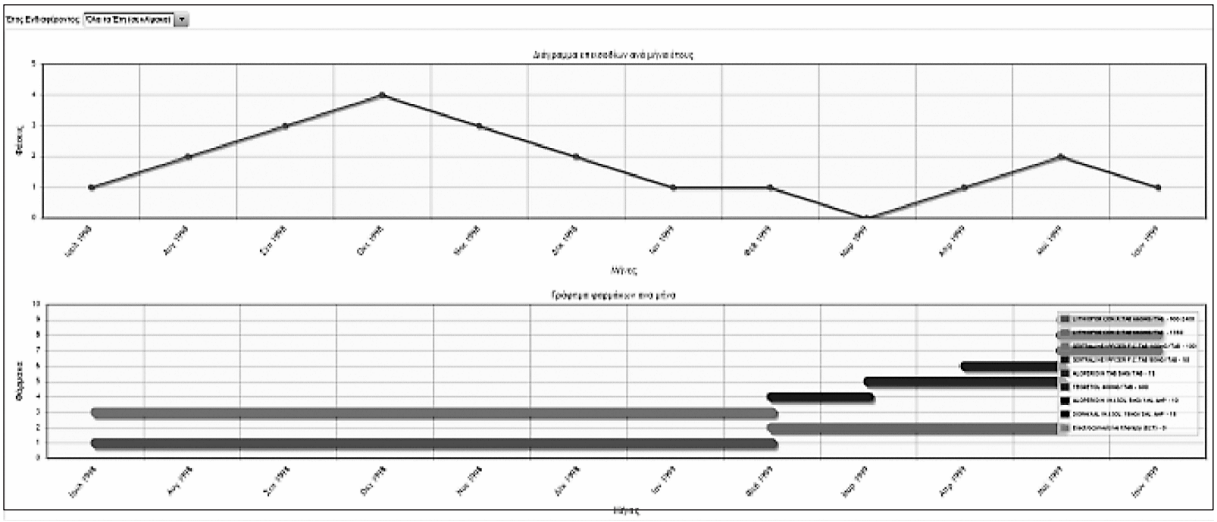

Fig. 3. *Graph presenting patient's episodes with respect to the substance administration over time*

user interface (GUI), in order to present the stored information to the end users. Since it is responsible for the interactions between users and the system, it provides access to the EHR through the web browser and among other useful graphical user interface components it makes statistical graphs available for use for intuitive visualization of the current status of patients in terms of episodes and substance administration over time (Fig. 3).

Application tier

In the middle of the tier platform, there is the application tier. This is in charge of the control of the system's operations, achieved by performing detailed processes. It consists of three sub-tiers: (i) Business logic, (ii) Security and (iii) Data access.

The operations of the business logic sub-tier concern the processing of a heterogeneous information data set. Some of the core functionalities that stand out are the support in retrieving patients' information; exporting patients' data into XLS format file; the dynamic clinical forms generation; the retrieval and process of data for the visualization of diagrams; the comparison of patient's re-examination data and printing capabilities. Furthermore, the business logic sub-tier is responsible for providing a robust working environment, coping with errors during execution and continuing the system's operation despite the potential input inconsistences. That is done mainly by preventing users from entering erroneous input, guiding them towards its proper use and performing in a satisfactory way, such that it does not intercept user's flexibility, agility and operability.

The information to be managed by this tier is patients' clinical and demographic data, users' personal data and access credentials, user's roles, users' access to patients, informed consent documents files, substance administration data and information that concern the dynamic data entry clinical forms. The functionality in this section addresses consistent terminologies/ vocabularies/ standardized transactions, data correctness, and interoperability (i.e. ICD-10, NOM).

The significance of security for the integrated platform is vital since it manages sensitive data when at the same time it is accessed by a variety of users which as stakeholders they have different roles and responsibilities according to their position and skills. The heterogeneity that characterizes those users raises the necessity of utilizing a Role Based Access Control (RBAC) [6] mechanism to regulate user actions within the system. These roles can guarantee that no user can perform ineligible acts.

Moreover, encryption/ decryption mechanisms are used to further secure users' passwords and patient's sensitive data. Data stored in an encrypted way can ensure the confidentiality in case that a third party breaches the database access. Users' credentials are stored in an encrypted unidirectional way. That means that passwords are not decryptable and thus cannot be recovered. On the other hand, all patients' sensitive data (data that can be used for identifying the patient) are stored in an encrypted bidirectional way within the database, allowing them to be decrypted, since the identification of the patient is required.

Finally the Secure Socket Layer (SSL) [3] protocol is utilized in order to preserve the secure data exchanged through a public-and-private key encryption mechanism which includes the use of a digital certificate.

The data access sub-tier handles all the logic regarding data storage and management. That is achieved by providing an abstract interface by using Data Access Objects (DAO) and thus delivering specific data operations without exposing details of the database. Finally, data persistence is achieved by adopting the Object Relational Mapping (ORM), which solves object-relational impedance mismatch problems by replacing direct persistence-related database accesses with high-level object handling functions.

Intelligence tier

The intelligence tier basically corresponds to the knowledge-based system, described in section A, offering knowledge extraction from the existing patient information and concluding into clinical decision support through treatment recommendations and alerts.

Data tier

The bottom tier is the data tier, which constitutes the database server of the integrated platform to store all the information data. In that way, data is kept neutral and independent from the rest of the tiers offering improved scalability and performance. The design of the relational database model was based on HL7-RIM[3], which is the cornerstone of the HL7 Version 3 development process and provides to the database a flexible and extensible structure.

ALIGNMENT OF THE ONTOLOGICAL-BASED CDSS AND THE PATIENT-CENTRIC EHR

The main contribution of this paper is the assignment of the ontology entities to the EHR entities, in order to enable communication and connec-

[3] http://www.hl7.org/implement/standards/rim.cfm

Table 1

Relations between ontology and ehr entities

Ontology Classes/Subclasses	EHR Task Categories/Subcategories
Dynamic Entities	
PatientState: patient's current state (in euthymia or in an episode)	**Clinical Data** – Clinical Picture **Diagnosis** **Patient's Diagram**
Symptom: the symptom (type, severity)	**Clinical Data** – Clinical Picture
Therapy: the therapeutic approaches a patient may receive (medication, hospitalization, psychotherapy)	**Clinical Data** – Biological Therapy – Psycotherapy – Psychoeducation
Medicine: the substance administration of the patient	**Clinical Data** – Biological Therapy – Drug Information **Medicine** **Patient's Diagram**
Monitoring: **(i) FunctionTest** **the tests a patient is submitted to (imaging tests, laboratory tests etc.)** **(ii) Biosignal** **keeps the information of biosignals recorded from sensors applied on patient**	**Clinical Data** – Laboratory Testing Process – Longitudinal Monitoring
AssessmentTools (i) Interview (ii) Questionnaire (iii) RatingScale (iv)EvaluationTest	**Clinical Data** – Clinical Picture – Longitudinal Monitoring – Psychometric Approach **Diagnosis**
Static Entities	
Patient: patient's personal and demographic information	**General Information** **Contact**
Episode: the type (manic or depressive) and severity of an episode	**Clinical Data** – Clinical Picture **Patient's Diagnosis** **Patient's Diagram**
Diagnosis: the type of the disorder (Type I or Type II) and whether the patient suffers from rapid cycling	**Diagnosis** (according to DSM– IV or DSM– V criteria for bipolar disorder) **Clinical Data** – Past Psychiatric History **Patient's Diagram**
PatientHistory: patient's medical and past psychiatric history (age of onset, heredity, number of manic or depressive episodes, previous medication)	**Clinical Data** – Personal History – Medical History – Past Psychiatric History
FamilyHistory: patient's family history	**Clinical Data** – Family History
SideEffect: possible side effects of a medicine	**Clinical Data** – Drug Information – Longitudinal Monitoring
DifferentialDiagnosis: differential diagnosis for the diagnosis procedure. It is a combination of: **(i) ClinicalEvaluation** **(ii) SubstanceEvaluation** **(iii) DepressionCriteria**	**Clinical Data** – Clinical Picture – Psychometric Approach
MedicalCause: whether the clinical evaluation suggests other causes than bipolar disorder	**Clinical Data** – Clinical Picture – Psychometric Approach

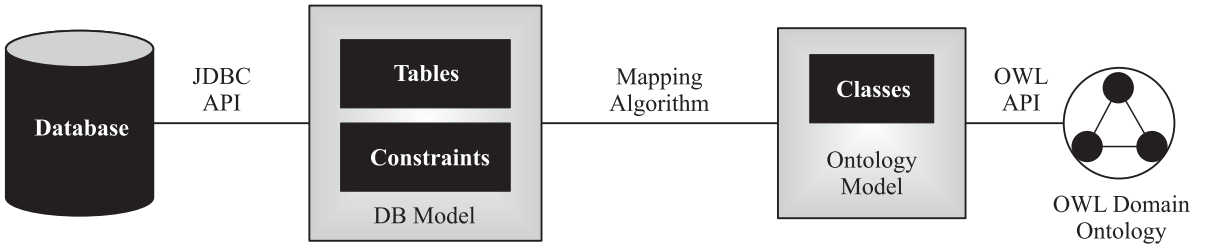

Fig. 4. *Mapping process*

Table 2

SQL tables

Table Name	Attributes
SubstanceAdministration	id, dosequantity, frequency, adm_r, startDate, endDate, actId, substanceAdministrationCodeId$_{[F K]}$
ActInstance	id, type, actId$_{[F K]}$, observationId$_{[F K]}$, reviewed, substanceAdministrationId$_{[F K]}$, diagnosisId$_{[F K]}$, consentFieldId$_{[F K]}$, signalFieldId$_{[F K]}$
Participation	id, actClass, actMood, code, title, desc, statusCode, roleInstanceId$_{[F K]}$, actInstanceId$_{[F K]}$
RoleInstance	id, statusCode,validForm, validUntil, personId$_{[F K]}$, roleCodeId$_{[F K]}$
Person	id, classCode, username, password, enabled

tivity among the ontological-based CDSS and the patient-centric EHR [18] (Table 1).

The EHR records longitudinally the patient health information, including demographics, contact information, clinical data (e.g. patient's personal, medical, and past psychiatric history, mental state examination, laboratory and data, and electronic diary mood reports, drug information), diagnosis, patient's diagram (visualization of the current and/or previous status of patients in terms of episodes/ disease state and drug administration over time), as well as an up-to-date drug database. The EHR supports indirectly the developed ontology-based DCSS leading to advanced health care quality.

Moreover, in order to achieve the integration between the ontology and the database, a mapping mechanism able to define the correspondences between the entities of the database and the ontology schema, is needed. Although relational databases are based on closed-world assumption whilst ontologies use open-world semantic, at a conceptual level, a database and an ontology are semantically related and correspondences are established between the database components and the ontology components. For instance, an attribute in a relational database schema may correspond to a property in an OWL ontology.

In our approach, a naïve mapping procedure is adopted retrieving data from SQL queries, through JDBC[4], applied over the source database and reformulates the results, in terms of the target ontology, through OWL API[5]. Such mapping specifies the ontology population from the data in the database.

Fig. 4 depicts a simplified conceptual view of the mapping process. As a simplified model, it does not show the complex nature of its components (e.g. database, tables, or ontology classes), rather the interaction between DB Model and Ontology Model, which is feasible through a mapping procedure with OWL API.

A query example retrieving the medicine information for a specific patient is presented. The database tables that relate with each other are the following, see Table 2. The sql query is presented in Table 3.

TEST AND VALIDATION OF THE AI-CARE MONITORING SYSTEM

The clinical use of the AI-CARE system is expected to provide answers to relevant questions related to the individualization of diagnosis, treatment approaches and effectiveness of treatment, transition hazard from major depressive episodes to manic, and malignant types of BD.

More specifically the monitoring system will be tested under the following issues in BDI regarding the knowledge residing in the ontology model and the patient information in the EHR model: (1) Diagnostic criteria of BD in terms of early and complete

[4] http://www.oracle.com/technetwork/java/javase/jdbc/index.html

[5] http://owlapi.sourceforge.net/

recognition of disease, (2) Evaluation of clinical effectiveness in terms of timely, and regular treatment, and acceptability of treatment dosage, (3) Evaluation of current patient's condition, (4) Identification of directly transition from depressive episodes to manic, and *vice versa* (5) Evaluation of treatment effectiveness in terms of quality of life, and improvement in symptoms, and (6) Identification of high risk patients (treatment non-response in BDI patients).

CONCLUSIONS

In our study, we align an ontological-based CDSS and a patient-centric EHR providing an on line monitoring tool, which seek to support psychiatrists and mental health professionals in tailor evidence-based practice in day-to-day clinical decision making for the longitudinal monitoring of each bipolar patient. Apart from the test and validation, the ontology population is an ongoing process. In the future, we aim to adjust the monitoring system for other types of BD and for epilepsy. The presented AI-CARE ontological-based monitoring system combines both personalized and evidence-based medicine in order to promote the care process for the patients suffering from bipolar I disorder.

ACKNOWLEDGEMENTS

This work is partially supported by the «AI-CARE» project of the «COOPERATION 2011» framework under the NSRF 2007-2013 Program of the Greek Ministry of Education, Lifelong Learning and Religious Affairs.

REFERENCES

1. *Hristoskova A., Sakkalis V., Zacharioudakis G., Tsiknakis M., De Turck F*. Ontology-Driven Monitoring of Patient's Vital Signs Enabling Personalized Medical Detection and Alert // Sensors. Vol. 14, N 1. P. 1598–1628, 2014.

2. http://www.fda.gov/downloads/ScienceResearch/SpecialTopics/PersonalizedMedicine/UCM372421.pdf

3. *Carmeli B., Casali P., Goldbraich A., Goldsteen A., Kent C., Licitra L. et al.* Evicase: an evidence-based case structuring approach for personalized healthcare // Stud. Health Technol. Inform. 2012. 180. 604–608,

4. *Sackett D.L., Rosenberg W.M., Gray J.A., Haynes R.B., Richardson W.S.* Evidence-based medicine: what it is and what it isn't,» [editorial] // BMJ. 1996. 312. 7023. 71–72,

5. https://healthit.ahrq.gov/sites/default/files/docs/page/09-0069-EF_1.pdf

6. *Maedche A., Staab S.* Ontology learning for the Semantic Web // IEEE Intelligent Systems. 2001. 16. 2. 72–79.

7. *Thase M.E.* Bipolar Depression: Issues in diagnosis and treatment // Harvard Rev. Psychiatry. 2005. 13. 257–271.

8. *Baader F., McGuinness D.L., Patel-Schneider P.F., and Nardi D.* The Description Logic Handbook: Theory, Implementation, and Applications, Cambridge University Press, 2nd ed., 2007.

9. *Gomez-Perez A., Corcho-Garcia O., Fernandez-Lopez M.* Ontological Engineering, Springer-Verlag New York, Inc., 1st ed., 2003.

10. *Heja G., Surja G., Varga P.* Ontological analysis of SNOMED CT // BMC Med. Inform. Decis. Mak. 2008. 8. S8.

11. *Schulz S., Stenzhorn H., Boeker M., Smith B.* Strengths and limitations of formal ontologies in the biomedical domain // Rev. Electron Comun. Inf. Inov. Saude. 2009. 3. 1. 31–45.

12. *Halland K., Britz K., Gerber A.* Investigations into the use of SNOMED CT to enhance an OpenMRS health information system // South African Computer Journal. 2011. 47. 33–46.

13. *Preventis A., Petrakis E., Batsakis S.* Chronos Ed: A tool for handling temporal ontologies in Protege // (IJAIT), 2014.

14. *Timmermans S., Mauck A.* The promises and pitfalls of evidence-based medicine // Health Aff (Millwood). 2005. 24. 1. 18–28.

15. *Connolly K.R., Thase M.E.* The Clinical Management of Bipolar Disorder: A Review of Evidence-Based Guidelines // Prim. Care. Companion CNS Disord. 2011. 13. 4. PCC.10r01097.

16. *Seckman C.* Electronic health records and applications for managing patient care // In: Elsevier and typesetter Toppan Bes. 2013. 87–105.

17. *Ferraiolo D., Cugini J., Kuhn D.R.* Role-based access control (RBAC): Features and motivations // 11th ACSAC, 1995.

18. *Bhiogade M.S.* Secure socket layer // Computer Science and Information Technology Education Conference, 2002.

19. *Thermolia C., Bei E.S., Petrakis E.G.M., Kritsotakis V., Tsiknakis M., Sakkalis V.* Designing A Patient Monitoring System for Bipolar Disorder Using Semantic Web Technologies // In Proc. IEEE EMBC, Milano. Italy, 2015.

СИСТЕМА МОНИТОРИНГА ПАЦИЕНТОВ С БИПОЛЯРНЫМ АФФЕКТИВНЫМ РАССТРОЙСТВОМ I ТИПА НА ОСНОВЕ ОНТОЛОГИЧЕСКОГО ПОДХОДА

Хриса Х. ТЕРМОЛИА[1], Екатерини С. БЕИ[1], Эврипидес Г. М. ПЕТРАКИС[1], Вангелис КРИТСОТАКИС[2], Вангелис САККАЛИС[2]

[1] *Школа электронной и вычислительной техники, Критский технический университет 73100, Греция, г. Ханья, кампус Акротири*

[2] *Институт компьютерных наук, Фонд исследований и технологий 71110, Греция, г. Гераклион, Н. Пластира, 100*

Цель исследования – обеспечение системы мониторинга пациентов, объединяющей систему поддержки принятия клинических решений (CDSS) и электронных медицинских карт (EHR) и помогающей психиатрам и врачам первичного звена в обеспечении существующих потребностей здравоохранения в области психических заболеваний, связанных с лечением и регулирование биполярным аффективным расстройством I типа (BDI). Предложенная система мониторинга состоит из системы EHR, основанной на эталонной информационной модели медицинского стандарта 7 уровня (HL7-RIM) и онтологической CDSS, использующей возможности семантической паутины. Система мониторинга разработана на основании руководств по доказательной медицине и медицинских карт пациентов и позволяет кодировать и обрабатывать эту информацию для последующего назначения рекомендаций выбора и оповещения клиницистов с целью улучшения оказания психиатрической помощи. Учитывая данные соответствующих клинических руководств, а также истории болезни пациента, система мониторинга может способствовать принятию персонализированных решений при длительно текущем BDI. В качестве *онлайн-инструмента мониторинга* мы предлагаем систему AI-CARE, которая может оказать большую помощь в клинической практике.

Ключевые слова: система поддержки принятия клинических решений, электронные медицинские карты, семантическая паутина, онтология, биполярное аффективное расстройство.

Термолиа Х.Х. *– студент, e-mail: cthermolia@ intelligence.tuc.gr*
Беи Е.С. *– кандидат технических наук, докторант, сотрудник лаборатории, e-mail: abei@isc.tuc.gr*
Петракис Э.Г.М. *– проф., зав. лабораторией , e-mail: petrakis@intelligence.tuc.gr*
Критсотакис В. *– инженер, e-mail: vkrits@ics.forth.gr*
Саккалис В. *– главный научный сотрудник лаборатории, e-mail: sakkalis@ics.forth.gr*

УДК 004.89

SOFTWARE SYSTEM FOR DIAGNOSING SPINAL DISEASES USING CASE-BASED REASONING

Dmitry Evgenyevich PALCHUNOV[1,2], Gulnara Erkinovna YAKHYAEVA[2], Olga Vladimirovna YASINSKAYA[2]

[1] *Sobolev Institute of Mathematics*
630090, Novosibirsk, Academician Koptyug av., 4

[2] *Novosibirsk State University*
630090, Novosibirsk, Pirogov str., 2

This paper describes the Diagnostic Panel Software System designed for the domain of spinal deformity and degenerative spinal disease. The work has been based on the logical methods of processing of the data obtained from natural language medical records. The software system is based on a patient's clinical and laboratory test results that help the physicians to determine an initial diagnosis and obtain immediate information for the necessary analysis for a final diagnosis and to select the optimal treatment plan. The Diagnostic Panel Software System uses a case-based approach to presenting the information from the variety of native language sources. The model theoretic methods of domain ontology construction has been used to develop the case-based approach. The Formal Concept Analysis methodology has been implemented to process the represented information/data in the system.

Keywords: diagnosis; spine diseases; case-based model; fuzzy model; ontology; formal context; formal concept.

Degenerative-dystrophic diseases of the spine are among the most pressing problems of the present time. This is the most common chronic disease characterized by limitation of physical activity and pain, which is experienced by almost every adult. Numerous literature data indicate a steady increase in the number of patients with diseases of the spine [1, 15].

Avoiding errors in diagnosis and timely treatment assignment require consistency in the conduct of examination of patients with diseases of the spine. Final diagnosis is made using clinical, laboratory and instrumental research methods.

Instrumental research methods play a decisive role in the diagnosis of the spine diseases [5]. For today there are many methods for the diagnosis of various deformations and degenerative diseases of the spine. However, doctors (especially outpatient care, as well as working in small towns and district hospitals) are daily confronted with the problem of diagnosis, determination of necessary diagnostic procedures and consultations of other specialists. The doctor needs to determine the preliminary (working) diagnosis based on clinical and laboratory studies and direct the patient to specific instrumental investigations.

Therefore, it is critical and economically feasible to develop such a software system that would allow doctors using the statistical data to determine a preliminary diagnosis and to quickly obtain information about the necessity of those or other instrumental diagnostic procedures for the staging the final diagnosis and selecting the optimal treatment strategy.

In this paper we describe the «Diagnostic Panel» software system designed for «spinal deformity and degenerative diseases of the spine» subject domain. The system is based on statistical processing of medical records of patients treated at the Novosibirsk Research Institute of Traumatology and Orthopedics (NRITO) n. a. Y.L. Tsivyan. The developed software system uses case-based approach for the representation of knowledge extracted from a variety of natural language texts (medical histories) [12, 17]. Case-based approach is based on model-theoretic methods of subject domain ontologies for-

Palchunov D. *– doctor of physical mathematical sciences, professor, head of the chair for general informatics, leading researcher, e-mail: palch@math.nsc.ru*
Yakhyaeva G.E. *– candidate of physical mathematical sciences, docent, e-mail: gul_nara@mail.ru*
Yasinskaya O.V. *– lecturer assistant, e-mail: yasinskaya.olga@gmail.com*

malization [8]. For the processing of the knowledge represented in system the formal concept analysis methodology is used [3].

MODEL-THEORETIC FORMALIZATION OF SUBJECT DOMAIN

With model-theoretic point of view, the description of the ontology is the description of the subject domain signature (i. e. describing the concept set of that subject domain) and setting the analytic theory of the subject domain (i.e. describing the implicit and explicit definitions of the subject domain) [9].

Seven classes of attributes were established to create the concept set of subject domain Δ = «Spinal deformity and degenerative diseases of the spine»:

1) $\mathbb{P}_1$: «Gender»;
2) $\mathbb{P}_2$: «Age group»;
3) $\mathbb{P}_3$: «Laboratory research»;
4) $\mathbb{P}_4$: «Complaints on admission»;
5) $\mathbb{P}_5$: «Clinical research»;
6) $\mathbb{Q}$: «Instrumental research»;
7) $\mathbb{D}$: «Diagnoses».

Attribute class «Gender» is composed of two concepts: «Male» and «Female» (Table). Attribute class «Age group» is composed of eight concepts: «0–9 years», «10–19 years», «20–29 years», «30–39 years», «40–49 years», «50–59 years», «60–69 years», «70 years and older». Class «Laboratory research» has a hierarchical structure and is divided into three subclasses: clinical tests, biochemical tests, genetic tests. Attribute set for the class «Laboratory research» was formed under the Ingerleib reference book [4]. Attribute sets for the classes «Complaints on admission» and «Clinical research» were formed as a result of parsing the medical histories of individual patients. Attribute set for the class «Instrumental research» is designed according to the National handbook of Orthopedics [6]. Attribute set for the class «Diagnoses» is selected in accordance with the 10th revision of the International Classification of Diseases (ICD-10) [14], class 13 (code M). This class also has a hierarchical structure and is divided into subclasses: M40-M43 Deforming dorsopathies, M45-M49 Spondylopathy, M50-M54 Other dorsopathies.

With the model-theoretic point of view, the above attributes are the one-place predicates and form a signature σ_Δ of considered in this work subject domain Δ. We will call them as ***signature predicates***. Thereby,

$$\sigma_\Delta = \mathbb{P}_1 \cup\bigcup \mathbb{P}_2 \bigcup \mathbb{P}_3 \bigcup \mathbb{P}_4 \bigcup \mathbb{P}_5 \bigcup \mathbb{Q} \bigcup \mathbb{D}.$$

Denote by $S(\sigma_\Delta)$ the set of all one-place predicates definable by quantifier-free formulas of signature σ_Δ. For simplicity, the elements of $S(\sigma_\Delta)$ will simply be called ***formula predicates***. Note that each formula predicate is a boolean combination of signature predicates. It's obvious that $\sigma_\Delta \subseteq S(\sigma_\Delta)$.

To describe the subject domain ontology, a finite set of axioms $\mathcal{A}x(\Delta) \subseteq S(\sigma_\Delta)$ is defined. For the given subject domain Δ introduce axioms of three types: general-private axioms, axioms of exclusion and the axioms of completeness.

General-private axioms. Hierarchical ordering of concept classes «Laboratory research» and «Diagnoses» should be reflected axiomatically. The scheme of such axioms is the following:

$$P_1(x) \to P_2(x).$$

For example: «If M48.0 Spinal stenosis, then M48 Stenosis».

Axioms of exclusion. The concepts of classes «Gender» and «Age group», as well as some groups of concepts from the class «Laboratory research», are mutually exclusive. The scheme of such axioms is the following:

$$P_1(x) \to P_2(x).$$

For example: «If Male, then not Female» or «If The level of hemoglobin in the blood exceeds the norm, then it is not true that The level of hemoglobin in the blood is normal».

Axioms of completeness. For the subject domain description we consider medical histories of the patients that passed the full cycle of diagnostics, for

Table

Examples of attributes for each of the above classes

Attribute class	Example of attribute
Gender	«Male»
Age group	«0–9 years»
Laboratory research	«The level of hemoglobin in the blood exceeds the norm»
Clinical research	«Palpation of the spinous process is painful in the projection L4-S1»
Complaints on admission	«Pain in the lumbar spine»
Instrumental research	«MRI of the cervical spine»
Diagnoses	«M48.0 Spinal stenosis»

which a final diagnosis is known and which treated appropriately. Therefore, we believe that at least one attribute of each of the seven classes is reflected in every considered medical history. Thus, we have seven axioms of completeness:

$$\bigvee_{\mathrm{P}\in\mathbb{Y}} P(x), \text{ where } \mathrm{Y} \in \{\mathbb{P}_1, \mathbb{P}_2, \mathbb{P}_3, \mathbb{P}_4, \mathbb{P}_5, \mathbb{Q}, \mathbb{D}\}.$$

Note that the ordered pair $\langle \sigma_\Delta, \mathrm{A}x(\Delta)\rangle$ forms an ***ontology*** of subject domain Δ.

Let us now consider a finite set $\{e_1, ..., e_n\}$ of medical histories, i.e. a set of semi-structured texts written in natural language. Note that each medical history clearly shows all performed diagnostic studies, their results and the final diagnosis for the patient. Therefore, for each medical history e_i we can describe a set of attributes (signature predicates) that is true on e_i. Thus, for each medical history e_i we build a singleton model $\langle \{e_i\}\sigma_\Delta\rangle$ which we call a ***case*** of subject domain Δ. Denote by $\mathbb{E} = \{e_1, ..., e_n\}$ the class of cases generated by a set of medical histories $\{e_1, ..., e_n\}$.

This, in turn, will allow us to build an ***ontological model*** $\mathfrak{A}_\Delta = \langle \mathbb{E}, \sigma_\Delta\rangle$ of subject domain Δ generated by the set of cases $\mathbb{E}$. In ontological model $\mathfrak{A}_\Delta$ for each signature predicate $P(x) \in \sigma_\Delta$ and for each case $e \in \mathbb{E}$ we have $\mathfrak{A}_\Delta \models P(e)$ if and only if the predicate $P(e)$ is true on case e.

Note that if the predicate $P(x) \in S(\sigma_\Delta)$ belongs to the axiom set of subject domain Δ (i. e. $P(x) \in \mathcal{A}x(\Delta)$, then for any $\mathrm{e} \in \mathbb{E}$ holds $\mathfrak{A}_\Delta \models P(e)$. Thus, the ontology of this subject domain is true on ontological model.

To solve the problems of statistical data processing we need both case-based and fuzzy models of considered subject domain [19]. These models are based on the ontological model.

For further consideration we need the concept of the case-based model which is a special case of a Boolean valued model.

Definition 1 [10]**.** *Let* $\mathbb{B}$ *be a full Boolean algebra and* τ: $S(\sigma_\mathrm{A}) \to \mathbb{B}$. *Then the ordered triple* $\mathfrak{A}_\tau = \langle A, \sigma, \tau\rangle$ *is called a* ***Boolean valued model*** *if truth function* τ *is closed under logical operations.*

Definition 2. The ordered triple $\mathfrak{A}_{\tau E} \leftrightharpoons \langle \{a\}, \sigma_\Delta, \tau_E\rangle$ is called a **case-based model** of subject domain Δ, generated by ontological model $\mathfrak{A}_\Delta = \langle \mathbb{E}, \sigma_\Delta\rangle$, if for any predicate $P(x) \in S(\sigma_\Delta)$ we have

$$\tau_E(P(a)) = \{\boldsymbol{e} \in E \mid \mathfrak{A}_\Delta P(\boldsymbol{e})\}.$$

In case-based model each predicate is associated with set of cases for which the predicate is true. Thus, by a set of cases $\mathbb{E}$ we define a Boolean valued model $\mathfrak{A}_\mathrm{E}$. In this Boolean valued model each sentence of signature $\sigma_\Delta \cup \{c_a\}$ is associated with the element of Boolean algebra $\rho(\mathbb{E})$.

This description is based on the following result.

Theorem of duality [10]. Let $\mathbb{B}$ be a complete atomic Boolean algebra, $\mathfrak{A}_\mathbb{B}$ – Boolean valued model, $E = \{\mathfrak{A}_b = \mid b \in At(\mathbb{B})\}$ and $\mathfrak{A}_E$ – case-based model. Then $\mathfrak{A}_\mathbb{B} \cong \mathfrak{A}_E$.

Most methods of statistical data processing use objective and/or subjective probabilities. The objective probability refers to the relative frequency of occurrence of any event in the total number of observations, or the ratio of favorable outcomes to the total number of observations. The subjective probability refers to a measure of confidence of some expert or group of experts that this event will actually take place. In this approach the concept of fuzzy model is used to describe the objective probabilities.

Definition 3. The ordered triple $\mathfrak{A}_{\mu E} \leftrightharpoons \langle \{a\}, \sigma_\Delta, \mu_E\rangle$ is called a **fuzzy model** of subject domain Δ, generated by ontological model $\mathfrak{A}_\Delta = \langle \mathbb{E}, \sigma_\Delta\rangle$, if for any predicate $P(x) \in S(\sigma_\Delta)$ we have

$$\mu_E(\varphi) = ||\{\boldsymbol{e} \in E \mid \mathfrak{A}_\Delta \models P(\boldsymbol{e})\}||/||\mathrm{E}||.$$

In the fuzzy model the truth values of the sentences (concepts) are numbers from the interval [0, 1], which reflect the objective probability that a randomly selected case has a particular concept. A more detailed description of the properties of both case-based and fuzzy models can be found in [16, 11, 12].

KNOWLEDGE PROCESSING ALGORITHMS

A formal description of the preliminary diagnosis

Formal concept analysis technique (FCA) was used for a formal description of the preliminary diagnosis. Formal concept analysis is an applied branch of the algebraic theory of lattices. For today the FCA is one of the most powerful data mining techniques. More information on this trend can be found in the works [3, 2, 13].

The central concept of the FCA is the notion of ***formal context***. With model-theoretic point of view, formal context is defined by the class of models $K \subseteq K(\sigma)$ of fixed signature σ and the set of sentences $S \subseteq S(\sigma)$ of the same signature and is an ordered triple $\langle K, S, \models\rangle$ [7].

In this paper we consider the formal context $\mathcal{K}_\Delta = \langle \mathbb{E}, \sigma_\Delta, \models\rangle$ generated by ontological model $\mathfrak{A}_\Delta$.

Let $\mathfrak{A}_\mathrm{E}$ и $\mathfrak{A}_{\mu E}$ be a case-based and fuzzy models generated by ontological model $\mathfrak{A}_\Delta$. Then the pair of sets (A, B), such that $A \subseteq \mathbb{E}$, $A \subseteq \sigma_\Delta$, is a ***formal concept*** of the context $\mathcal{K}_\Delta$, if the following conditions are met:

$$\mu_E(\&_{\varphi(x)\in B}\varphi(a)) > \mu_E(\psi(a) \,\&\, (\&_{\varphi(x)\in}\varphi(a))),$$

$$\text{for each } \psi(x) \in \frac{S(\sigma_\Delta)}{B};$$

$$A = \tau_E\,(\&_{\varphi(x)\in B}\varphi(a)),$$

where $\{a\}$ is a basic set of fuzzy model $\mathfrak{A}_{\mu E}$.

The set B is called the ***content*** of the formal concept (A, B). For convenience, we call the formula $(\&_{\varphi(x)\in B}\varphi(x))$ (instead of set B) as the content of the formal concept (A, B).

The formal concept (A_1, B_1) is called a **more general concept** than the concept (A_2, B_2) (denoted $(A_1, B_1) \sqsupseteq (A_2, B_2)$) if $A_2 \subseteq A_1$. Note that if $(A_1, B_1) \sqsupseteq (A_2, B_2)$, then $B_1 \subseteq B_2$.

Consider a subset of the set of signature predicates $\mathbb{P} = \mathbb{P}_1 \cup \mathbb{P}_2 \cup \mathbb{P}_3 \cup \mathbb{P}_4 \cup \mathbb{P}_5$. To get a preliminary diagnosis we will use formal context $\mathcal{K}_{\mathbb{P}}$ $(\mathbb{E}, \mathbb{P}, \vDash)$, which is a subcontext of context $\mathcal{K}_\Delta$.

The formal concept (A, B) of the context $\mathcal{K}_{\mathbb{P}}$ we call ***positive hypothesis*** for the diagnosis $D(x) \in \mathbb{D}$, if the condition is met

$$\mu_E\,(\&_{\varphi(x)\in B}\varphi(a) \to D(a)) = 1.$$

Proposition 1. If $\mu_E\,(\varphi_1(a) \to D(a)) = 1$ and $\mu_E\,(\varphi_2(a) \to D(a)) = 1$, then $\mu_E\,(\varphi_1(a) \vee \varphi_{2(a)}) \to \to D(a)) = 1$.

Proposition 2. Let (A_1, B_1) and (A_2, B_2) be a formal concepts of the context $\mathcal{K}_{\mathbb{P}}$ such that $(A_1, B_1) \sqsupseteq (A_2, B_2)$. Then if concept (A_1, B_1) is a positive hypothesis of a diagnosis $D(x) \in \mathbb{D}$, then (A_2, B_2) also is a positive hypothesis for the same diagnosis.

Let $G(D)$ be the set of all positive hypotheses for the diagnosis D. We define the set $G_{\max}(D) \subseteq \subseteq G(D)$ of maximal positive hypotheses for diagnosis $D(x)$, i. e. such that for all concepts $(A, B) \in \in G_{\max}(D)$ there is no more general concept that belongs to the set $G(D)$.

Then the formula

$$F_D(x) = \bigvee_{A,\, B\in G_{\max}(D)} \&_{\phi(x)\in B}\, \phi(x),$$

will be called a formula description of diagnosis $D(x)$.

The algorithm for determining the working diagnosis

Consider patient ***Pat***. Suppose that a partial diagnostics of the patient ***Pat*** was made and now we need to get a preliminary diagnosis. Consequently, there is information about the truth of some, but perhaps not all, predicates of the set $\mathbb{P}$. Denote by *True*(***Pat***) the set of signature predicates from the set $\mathbb{P}$, whose truth is known for patient ***Pat***. Denote by *Th*(***Pat***) closure with respect to deducibility of the set *True*(***Pat***) (i.e. the theory generated by the set *True*(***Pat***)). According to the theory *Th*(***Pat***) we will build a ***model of the patient Pat.***

Definition 4. The ordered triple $\mathfrak{A}_{Pat} = \langle \{Pat\}, \sigma_\Delta, \eta_{Pat} \rangle$ is called a ***fuzzy model of the patient Pat,*** if for any predicate $\varphi(x) \in S(\sigma_\Delta)$ truth function η_{Pat} is defined as follows:

$$\eta_{(\mathrm{Pat})}\left(\phi(\mathrm{Pat})\right) = \begin{cases} 1, & \phi(x) \in \mathrm{Th(Pat)}; \\ 0, & -\phi(x) \in \mathrm{Th(Pat)}; \\ [0,1], & \text{otherwise.} \end{cases}$$

Model $\mathfrak{A}_{Pat}$ is a generalized fuzzy model of signature σ_Δ. The formal definition and description of the properties of these models can be found in [18].

Further, to determine a preliminary diagnosis (or several preliminary diagnosis), we need to check on model $\mathfrak{A}_{Pat}$ the truth of formula descriptions $F_D(x)$ of all diagnoses D of the set $\mathbb{D}$. Diagnoses for which the condition $\eta_{Pat}(F_D(Pat)) = 1$ is met are declared a preliminary diagnosis for the patient.

However, there may be a situation where the working diagnosis is not defined, i.e. for any $D(x) \in \in \mathbb{D}$ we have $\eta_{Pat}(F_D(Pat)) \neq 1$. Then, if there is at least one diagnosis $D(x)$ such that $\eta_{Pat}(F_D(Pat)) = = [0, 1]$, then the system offers to make an additional examination of the patient. If there is a situation where for any $D(x) \in \mathbb{D}$ we have $\eta_{Pat}(F_D(Pat)) = = 0$, then we are dealing with unusual situation, i.e. it is impossible to diagnose this patient using the developed system.

Algorithm of appointment of additional diagnosing

Assume that during the initial examination of the patient ***Pat*** preliminary diagnoses $D_1(x)$, …, $D_k(x) \in \mathbb{D}$ were set. A further objective of the system is to select the most appropriate tools of instrumental research for setting final diagnosis.

Select a subset of cases $\mathbb{E}'$ from the set of cases $\mathbb{E}$ for which at least one of diagnoses $D_1(x)$, …, $D_k(x)$ was defined, i.e.

$$\mathbb{E}' = \{\boldsymbol{e} \in \mathbb{E} \mid \mathfrak{A}_\Delta \vDash D_1(\boldsymbol{e}) \vee \ldots \vee \mathfrak{A}_\Delta \vDash D_k(\boldsymbol{e})\}.$$

Consider the formal context $\mathcal{K}_{\mathbb{Q}} = (\mathbb{E}', \mathbb{Q}, \vDash)$ which is a subcontext of context $\mathcal{K}_\Delta$. The content of this context is the set of tools of instrumental research. In this context we seek the most general formal concept (A, B). The content of the concept B will be considered as optimal set of instrumental research tools based on working diagnoses $D_1(x)$, …, $D_k(x)$.

Note that the relation $\sqsupseteq$ – «*to be the most general notion*» is a partial order relation. Therefore, there may be not the only one largest concept, but the several maximal concepts. Let concepts (A_1, B_1), …, (A_l, B_l) be the maximal formal concepts of con-

text $\mathcal{K}_{\mathbb{Q}}$ with ordering $\sqsupseteq$. Then the system offers alternative solutions: $B_1, \ldots, B_l$.

It is obvious that the set of maximal formal concepts $(A_1, B_1), \ldots, (A_l, B_l)$ has the following properties:

$$A_1 \cup \ldots \cup A_l = \mathbb{E}';$$

For any formal concept (A, B) of context $\mathcal{K}_{\mathbb{Q}}$ there is $i = 1, \ldots, l$ such that $B_i \subseteq B$.

Thus, by offering a set of alternative solutions $B_1, \ldots, B_l$ on one hand we provide coverage of all considered cases, and on the other hand we minimize the amount of instrumental research tools required for setting the final diagnosis.

DESCRIPTION OF THE «DIAGNOSTIC PANEL» SYSTEM

In view of the anticipated program usage scenarios, it was decided to conduct the development in the form of a web application built on the ASP.NET platform. ASP.NET MVC framework was used as an architectural template of web application. Using the MS SQL Server (Express) database applies to be the best option in this case.

To describe the medical histories in the MS SQL Server 2014 database 12 tables were created and relationships between tables were organized. They describe the 7 categories of considered attributes of medical histories – Gender, Age group, Diagnosis, Complaints, Clinical research, Laboratory research, and Instrumental research tools. To replenish the database information on new medical histories and view existing in a web application the «List of medical histories» page was developed. On this page the standard operations on the data were implemented such as view, create, edit, and delete. The design of the page for editing the list of medical histories is shown in Figure 1.

The interface of the main page is a form to fill in the data of a new medical history. The user fills in five categories of attributes: Gender, Age group, Complaints, Clinical research, and Laboratory research. Attributes of Gender, Age group and Complaints filled via drop-down lists. Attributes of Clinical research and Laboratory research are filled with the help of checkbox-lists. The appearance of data input form is shown in Figure 2.

The button «Find working diagnoses» starts performing the main algorithm for a given information in the form. Building a hypothesis is based on medical histories stored in the MS SQL Server database.

The result of the main algorithm work is a list of preliminary (working) diagnoses. Under the list of working diagnoses the table of instrumental research tools needed for clarification of diagnosis is shown. An example of the results of the main algorithm work is shown in Figure 3.

CONCLUSIONS

The paper describes developed methods for identifying the need for additional diagnostic tests for definitive diagnosis of the patient. These methods are based on a combination of the two methodologies: a case-based approach of knowledge representation and formal concept analysis.

For the formalization of subject domain knowledge a finite set of medical histories of patients is used, i.e. set of semi-structured texts written in natural language. For each medical history a singleton

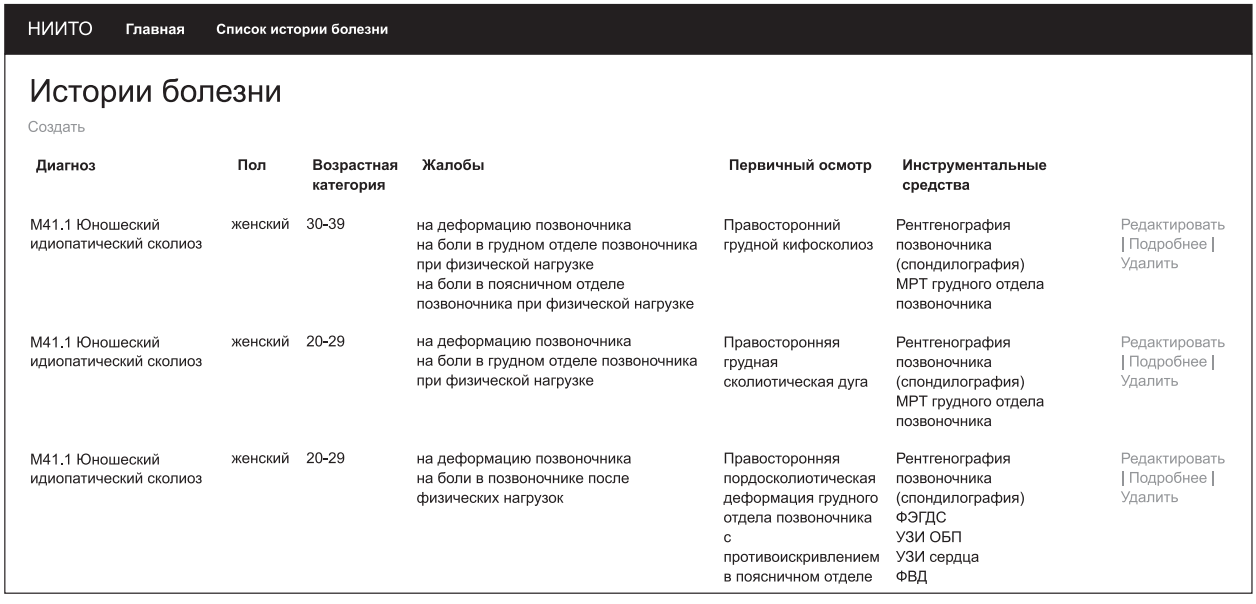

Fig. 1. *«List of medical histories» page*

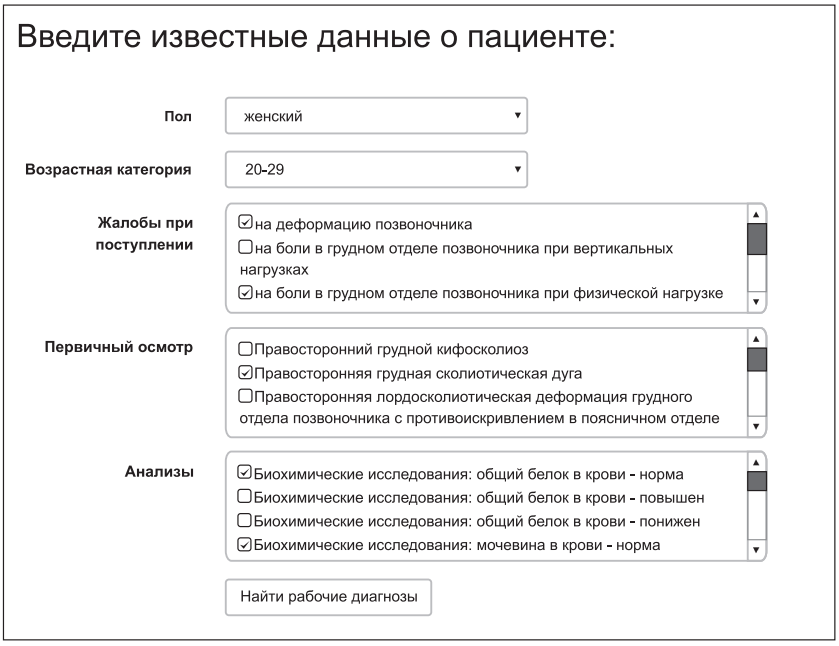

Fig. 2. *Data input form*

algebraic system – a case of subject domain is built. The class of all cases creates an ontological model of considered subject domain. Subject domain ontology is true on the ontological model.

Formal context is built on the basis of ontological model of the given subject domain. In constructed formal context a formal concepts is defined, confirming the one or the other diagnosis. Formula descriptions of diagnoses are built.

Then fuzzy model of the patient passed partial examination is constructed. Truth values of formula descriptions of various diagnoses are tested on this model, a set of preliminary diagnoses for the patient is formed. The formal context of diagnoses which is a subcontext of subject domain context is considered. In this context, the maximal formal concept, the content of which is declared as a set of needed additional instrumental research tools, is found.

The developed methods are implemented in «Diagnostic Panel» software system. The ontological model is the core of the program. The software system is tested on a «spinal deformity and degenerative diseases of the spine» subject domain. System returns a set of preliminary (working) diagnoses for the patient based on clinical and laboratory research of that patient with disease of the spine. On the basis of the preliminary diagnosis, the system helps the user (doctor) to select the minimum necessary set of instrumental diagnostic tools to determine the final diagnosis of the patient.

We express our gratitude to the staff of the Novosibirsk Research Institute of Traumatology and Orthopedics n. a. Y.L. Tsivyan, who kindly provided us with the necessary medical information.

ACKNOWLEDGMENTS

The reported study was supported by RFBR, research project No. 14-07-00903-a.

REFERENCES

1. *Alexander J.* Principles of spinal surgery. N. Y.: McGraw-Hill Comp., Health Professions Division, 1996.

Рабочие диагнозы:

- M41.1 Юношеский идиопатический сколиоз

Инструментальные средства для уточнения диагноза:

Инструментальное исследования	Диагнозы
Рентгенография позвоночника (спондилография) МРТ грудного отдела позвоночника	M41.1 Юношеский идиопатический сколиоз

Fig. 3. *Results of the main algorithm work*

2. *Ganter B., Stumme G., Wille R.* Formal concept analysis. Foundations and applications. Springer, 2005.

3. *Ganter B., Wille R.* Formal Concept Analysis: Mathematical Foundations // Heidelberg: Springer, 1999.

4. *Ingerleyb M.B.* Analyses. Full reference book. Moscow: Astral, 2011. [In Russian].

5. *Maigne J., Rime B., Delignet B.* Computed tomographic follow-up study of forty-eight cases of nonoperatively treated lumbar intervertebral disc herniation // Spine. 1992. 17. (9). 1071–1074.

6. *Mironov S., Kotelnikov G.* Orthopedics. National guidelines. Moscow: GEOTAR-Media, 2008.

7. *Palchunov D.* Lattices of relatively axiomatizable classes // Formal Concept Analysis. Eds. S. Kuznetsov, S. Schmidt. Berlin; Heidelberg: Springer, 2007. 4390. 221–239.

8. *Palchunov D.* Simulation of thinking and formalization of reflection: I. Model-theoretic formalization of the ontology and reflection // Filosofiya nauki = Phylosophy of science. 2006. 31. (4). 86–114. [In Russian].

9. *Palchunov D.* Simulation of thinking and formalization of reflection: II. Ontologies and formalization of concepts // Filosofiya nauki = Phylosophy of science. 2008. 37. (2). 62–99. [In Russian].

10. *Palchunov D., Yakhyaeva G.* Fuzzy algebraic systems // Vestnik Novosibirskogo gosudarstvennogo universiteta. Seriya: Matematika, mekhanika, informatika = Herald of Novosibirsk State University. Series: Mathematics, mechanics, informatics. 2010. 10. (3). 75–92. [In Russian].

11. *Palchunov D., Yakhyaeva G.* Fuzzy logics and fuzzy model theory // Algebra and Logic. 2015. 54. (1). 74–80.

12. *Palchunov D., Yakhyaeva G.* Interval fuzzy algebraic systems // 9th Asian Logic Conference: Proc. Novosibirsk, 2005. 23–37.

13. *Priss U.* Formal Concept Analysis in Information Science // Annu. Rev. Inf. Sci. Technol. 2006. 40. 521–543.

14. The international statistical classification of the diseases and related health problems; 10th revision. http://www.who.int/classifications/icd/en/.

15. *Umashev G., Backbone F.M.* Osteochondrosis, 2nd edition. Moscow: Meditsina, 1984. [In Russian].

16. *Yakhyaeva G.* Fuzzy model truth values // Aplimat': Proc. 6th Int. Conf. Bratislava, 2007.

17. *Yakhyaeva G.* Logic of fuzzifications // IICAI-09: Proc. 4th Int. Conf. Tumkur, 2009.

18. *Yakhyaeva G., Yasinskaya O.* An algorithm to compare computer-security knowledge from different sources // ICEIS: Proc. 17th Int. Conf. Barcelona, 2015.

19. *Yakhyaeva G., Yasinskaya O.* Application of case-based methodology for early diagnosis of computer attacks // J. Comput. Inf. Technol. 2014. 22. (3). 145–150.

ПРОГРАММНАЯ СИСТЕМА, ОСУЩЕСТВЛЯЮЩАЯ CASE-BASED REASONING ДЛЯ ДИАГНОСТИРОВАНИЯ ЗАБОЛЕВАНИЙ ПОЗВОНОЧНИКА

Дмитрий Евгеньевич Пальчунов[1,2], Гульнара Эркиновна Яхъяева[2], Ольга Владимировна Ясинская[2]

[1] Институт математики им. С.Л. Соболева СО РАН
630090, г. Новосибирск, пр. Академика Коптюга, 4

[2] Новосибирский национальный исследовательский государственный университет
630090, г. Новосибирск, ул. Пирогова, 2

В работе описывается программная система «Diagnostic Panel», разработанная для предметной области «деформации позвоночника и дегенеративные заболевания позвоночника». Работа основана на методах статистической обработки данных, извлекаемых из медицинских документов, написанных на естественном языке. Программная система помогает врачам на основе данных клинических и лабораторных исследований пациента определять предварительный диагноз и максимально быстро получать информацию о необходимости проведения тех или иных инструментальных диагностических процедур для постановки заключительного диагноза и выбора оптимальной стратегии лечения. В программной системе «Diagnostic Panel» для представления знаний, извлечённых из различных текстов естественного языка, используется прецедентный подход к представлению знаний. Разрабатываемый прецедентный подход основан на теоретико-модельных методах формализации онтологий предметных областей. Для обработки представленных в системе знаний используется методология анализа формальных понятий.

Ключевые слова: диагноз, заболевания позвоночника, прецедентная модель, нечеткая модель, онтология, формальный контекст, формальное понятие.

Пальчунов Д.Е. *– д.ф.-м.н., проф., зав. кафедрой общей информатики, в.н.с., e-mail: palch@math.nsc.ru*
Яхъяева Г.Э. *– к.ф.-м.н., доцент, e-mail: gul_nara@mail.ru*
Ясинская О.В. *– ассистент преподавателя, e-mail: yasinskaya.olga@gmail.com*

УДК 004.89

DEVELOPMENT OF AUTOMATED METHODS FOR REDUCING THE RISK OF CRITICAL CONDITIONS, BASED ON THE ANALYSIS OF MEDICAL RECORDS

Chimit Antonovich NAYDANOV[1], Dmitriy Evgenyevich PALCHUNOV[1,2], Polina Andreyevna SAZONOVA[1]

[1] *Novosibirsk National Research State University*
630090, Novosibirsk, Pirogov str., 2

[2] *Sobolev Institute of Mathematics of SB RAS*
630090, Novosibirsk, Koptyug av., 4

This paper describes the methods of development of ontologies and ontological modes in medicine. We present four-level structure of knowledge representation. Using the basics of ontological methods of presenting knowledge, we developed algorithms to prevent risks of critical conditions and complications. The work is based on the model-theoretic approach to represent medical knowledge, which is shown through partial atomic diagrams of algebraic systems and of a patients' cases data via Boolean-valued models. This data helped to develop ontology and ontological models of the «spinal deformity and spinal degenerative disease». The ontology model contains: a) general knowledge that is applicable for all patients, b) data on specific patients, and c) estimated knowledge that help doctors make recommendations. Estimated knowledge is a set of hypothetical possibilities that could lead to a patient's critical condition or complications. We also developed an algorithm generating the estimated (fuzzy) knowledge based on the analysis of medical records. A software system generating recommendations to help prevent and reduce the risk of a patient's critical condition (life threatening) was implemented. The results used in the study are from data of patients with spinal deformity or spinal degenerative diseases.

Keywords: risk management, critical conditions, ontology model, precedent model, Boolean-valued model, knowledge representation, spinal deformity, degenerative diseases of the spine.

This paper describes methods of ontology and ontological model development for the medical subject area. The ontology development was carried out for the subject domain of «Spinal deformity and degenerative diseases of the spine».

The given approach is based on the four-level knowledge representation: the ontological knowledge level in the subject domain ontology and three levels of knowledge representation contained in the ontological model. In particular, this knowledge representation is the basis for development of methods and algorithms of critical condition and complication risk prevention.

The developed methods are implemented in the software system MedOntoModel. In particular, this software helps predict the probability of occurrence of patient's critical condition and gives appropriate recommendations to doctors. The software system is designed for the subject domain of «Spinal deformity and degenerative diseases of the spine.»

A new approach to the development of the ontological model structure is presented. It is viewed as a four-level one with strict division of knowledge into ontology, general knowledge, specific knowledge and probabilistic knowledge.

Model theoretical approach is used for formal representation of knowledge. This approach allows describing knowledge with different degree of reliability and generality. General knowledge is represented in the model by $\forall$-sentences of the first order predicate language. Specific knowledge about the patients is presented in the form of fragments of atomic diagrams of algebraic systems. Probabilistic knowledge is represented by fuzzy models.

On the basis of ontological model we have developed critical condition risk prevention algorithms

Naydanov Ch.A. *– postgraduate student, e-mail: naydanov.fit@yandex.ru*
Palchunov D.E. *– doctor of physical mathematical sciences, leading researcher, e-mail: palch@math.nsc.ru*
Sazonova P.A. *– master student, e-mail: psazonova@gmail.com*

for finding drug contraindications and negative interactions, generation of estimated knowledge. These algorithms have been implemented in the software system MedOntoModel and tested on medical data obtained from patient medical records.

CLINICAL DECISION SUPPORT SYSTEM

This part provides a brief overview of Clinical Decision Support System (CDSS). The most interesting examples of Russian and foreign CDSS's have been considered.

A CDSS is an information technology system that helps doctors to estimate patient's condition, diagnose, choose a course of treatment or prescribe drugs [4]. The system works with patient's characteristics compared with information from a knowledge base. A CDSS outputs recommendations for patients or evaluation of a patient's condition using special algorithms contained in it.

Modern CDSS should automatically warn of critical condition onset, be able to present data in an easy-to-understand form, automate doctor's interaction with other computer systems, be able to verify the medical diagnostic solutions and build assumptions about patient's condition [4].

According to [10], the use of CDSS can reduce the number of medical errors, and improve the treatment process and its outcome. In particular, the work [17] shows a twofold reduction of negative drug interactions leading to serious consequences, due to CDSS.

The review conducted by researchers Jeffery et al. [9] shows that the CDSS use for tracking the status of diabetic patients reduces death rate among them. In another paper [15] the authors argue that CDSS use leads to increased performance of medical staff.

Let us consider the most known CDSS used in Russia and other countries.

System IBM Watson for Oncology

This system helps oncologists determine a diagnosis and select a treatment plan. Watson compares the patient data and the knowledge gained from experts and medical texts. The system offers a suitable means of treatment and provides evidence of their efficiency. IBM Watson can process patient information that is derived both from structured sources (electronic medical records) or unstructured (medical records in simple English).

IBM Watson system is able to automatically extract information from medical texts. Knowledge Base of the system is formed by processing more than 290 medical journals, 200 manuals and 12 million pages of text.

System Dxplain

Dxplain was developed in the Computer Science Laboratory at Massachusetts General Clinical Hospital. This system is one of the first CDSS's. Its development began in 1984, and the first version was released in 1986. The Dxplain knowledge base contains a description of 2400 diseases and 5000 different medical data (symptoms, signs, epidemiology, laboratory researches and other).

Input data for Dxplain are data on patients (signs, symptoms, laboratory tests). Output data of the system is a ranked list of presumptive diagnosis. For each of the suspected diagnoses the system provides its rationale in the form of relevant publications from the PubMed database.

Pharm Expert

One of the most interesting systems developed in Russia is Pharm Expert. The system helps doctors make decisions in the preparation of treatment. The main functions of Pharm Expert are:

- detecting drug interactions and contraindications based on the personal characteristics of patient and drug route;
- warning about exceeding the maximum daily dose of drug;
- recommendations for the replacement of a conflicting drug by an optimum one;
- automatic selection of dosages, dosage forms and ways of drug introduction.

There is the possibility of automatic creation of the prescription, collect statistics about the prescribing and reporting on medical errors. The system can be integrated into existing health information systems. Pharm Expert System can analyze the electronic medical records of all common formats.

The system uses the base of medical knowledge named United Medical Knowledge Base. Content of the database is managed by experts from well-known Russian institutions. The Pharm Expert System has been tested clinically.

APPLICATION OF THE ONTOLOGICAL APPROACH TO MEDICAL DIAGNOSTICS

Most of the existing medical decision support systems are based on formalization and conceptualization of subject area [1, 5, 11, 12, 25, 26]. This approach is called «ontology or ontological model» in scientific literature.

A group of specialists headed by A.S. Kleschev developed a series of approaches to the development of ontologies in medicine [2, 13]. Subsequently, they developed an ontology of medical diagnostics [11, 12], ontology of medication treatment [7],

filling the knowledge base approaches [3], formal description of a number of diseases, approach to the development of computer simulators in ophthalmology [8] and others.

A model of subject area, incl. the medicine, shall meet the following requirements:

- the knowledge base terms shall be clear to specialists of the subject area;
- the knowledge shall remain useful during the entire system operation;
- the knowledge base shall be available for enlargement;
- availability of automated result accumulation for the verification of decisions made.

The approach to formalization of medical diagnosis is based on the allocation of tasks in the doctor's everyday activity; on the control of decisions made; on management of knowledge bases, namely specification, extension and debugging of knowledge bases.

The daily work of doctor consists of task groups, such as diagnosis, treatment planning, forecasting, monitoring and examination. Each of these task groups was assigned its own domain ontology, which consists of a description of examined object (patient) and knowledge necessary to make a decision. The first description is called ontology, the second – the ontology of knowledge. They are linked together with ontological agreements.

Knowledge Bases are based on the tasks of doctor's everyday activity. These bases are filled up by experts and automatically, and later undergo an automated check. If the system detects a task, for the solution of which the knowledge is scarce, the task gets solved in any other way and added to the knowledge base. The newly added knowledge is checked by an expert in the subject area.

A group of specialists headed by A.S. Kleschev has developed a software system that solves the problem of determining a patient's diagnosis based on described approaches [16]. This system outputs a set of estimated diseases and explains the chosen solution. It based on the observed patient signs and symptoms.

THE STRUCTURE OF THE ONTOLOGICAL MODEL «DEGENERATIVE DISEASES OF THE SPINE AND SPINAL DEFORMITY»

Most of the modern ontological models describe the subject area in two levels. First is a meta-level, which describes the generalized concepts. Second level is a factual level, which describes the specific domain objects.

Our approach to the development of ontologies and ontological model is based on model-theoretic methods of knowledge representation [18–21]. The developed ontology and ontological model primarily intended for the generation of new knowledge and for the integration of knowledge obtained from different sources. In particular, the knowledge is generated by the evaluation of patent's critical condition probable risk.

The knowledge presented as four levels: the level of ontological knowledge represented in the domain ontology, and three levels of substantial knowledge represented in the ontology model of the subject area.

The first level is the ontology. The ontology presented knowledge about the key (specific) domain concepts. It describes definite specification of the meaning of key concepts. It presents a number of ontological relationships between concepts, such as «is-a», «part-of», different kinds of associative links between concepts and others.

These three levels of knowledge are included in the ontological model:

1. General knowledge that are true in all instances of a given subject area. This knowledge is extracted from regulations (e.g. Ministry of Health and others), monographs on medical topics, articles and other sources. Such knowledge is formally represented in the ontological model by using of universal sentences, i.e., ∀-sentences. ∀-sentence is a sentence of the first-order predicate logic that starts with universal quantifiers ∀. After quantifiers, there is a quantifier-free part of the sentence.

2. Knowledge about individual patient extracted from their medical reports. This knowledge is presented in the form of precedents. Precedent model consist of a set of precedents. This is purely empirical knowledge. It is true for quite specific situations limited in space and time. Formally, such knowledge is represented in the ontological model using quantifier-free sentences. We consider such sentence as fragments of atomic diagram of an algebraic system [14].

We use the previously developed methods at the stage of ontological model filling with the information on specific patients. Besides, we use previously developed software system designed for knowledge extraction from natural language texts and fragments of building atomic diagrams of algebraic systems [14, 24].

3. Probabilistic (estimated) knowledge. This knowledge is used for automated issuance of medical advice. For example, the doctor can get recommendations for the prevention of risks of patient critical conditions. Evaluative knowledge in ontological model replenished by analysis of precedents (patient records) using existing ontological and universal knowledge, as well as general knowledge.

Formally, the probability and evaluative knowledge is represented using fuzzy models [22, 23].

Thus, this paper presents a four-level structure of the ontology and ontological model. This structure allows formalizing the subject area on four levels of knowledge representation. Level of precedents and the level of estimated knowledge have particular importance in the context of this work.

The level of precedents is knowledge of the individual patient. Its level allows describing the subject area in terms of private facts. Each such fact contains only partial information. However, if we bring information from a huge amount of different patient's private data together, we can work out general knowledge. This knowledge is presented in the ontological model on the level of probabilistic (estimated) knowledge.

The level of evaluation knowledge describes the subject area in the terms of «generalized» precedent. The role of this knowledge is the generalization of previously gained experience. Precedents (the patient's medical report) represent this experience. Evaluation knowledge is inexact; any such statement is true only with a certain probability. As a matter of fact, we are dealing with fuzzy truth-values. Therefore, we use fuzzy model for evaluation of knowledge representation [22, 23].

Ontology

Ontology describes the key concepts of the subject area. It describes the types of objects, types of relationships between objects, object attributes. In developing our ontology, we used Kleschev's, Moskalenko's and Chernyakhovskaya's researches [11, 12].

Condition of patients is presented in the form of medical report in the ontological model (Fig. 1). Information on the results of analysis, surveys, any symptoms, some events, and anatomical and physiological characteristics of the patient are stored as true on this medical report statement. Each medical report has a time scale of non-negative integers representing the number of hours since the start of patient monitoring. All information on the results of analysis, surveys, any symptoms, occurred events is recorded in accordance with this scale.

Base of general knowledge

The database contains information of general knowledge, derived from medical regulatory documents, monographs and articles, as well as by experts of the subject area. In contrast to the ontological knowledge, these statements reflect the properties of the real world. Therefore, some of these statements can become unreliable later.

General knowledge describes the relationship between diseases and complications of critical conditions on the one hand, and the results of analysis and surveys of symptoms on the other hand. If the patient doesn't have a disease, complication or critical condition, the results of analysis and examinations are determined as the relationship between normal reactions and reactions to the impact of events.

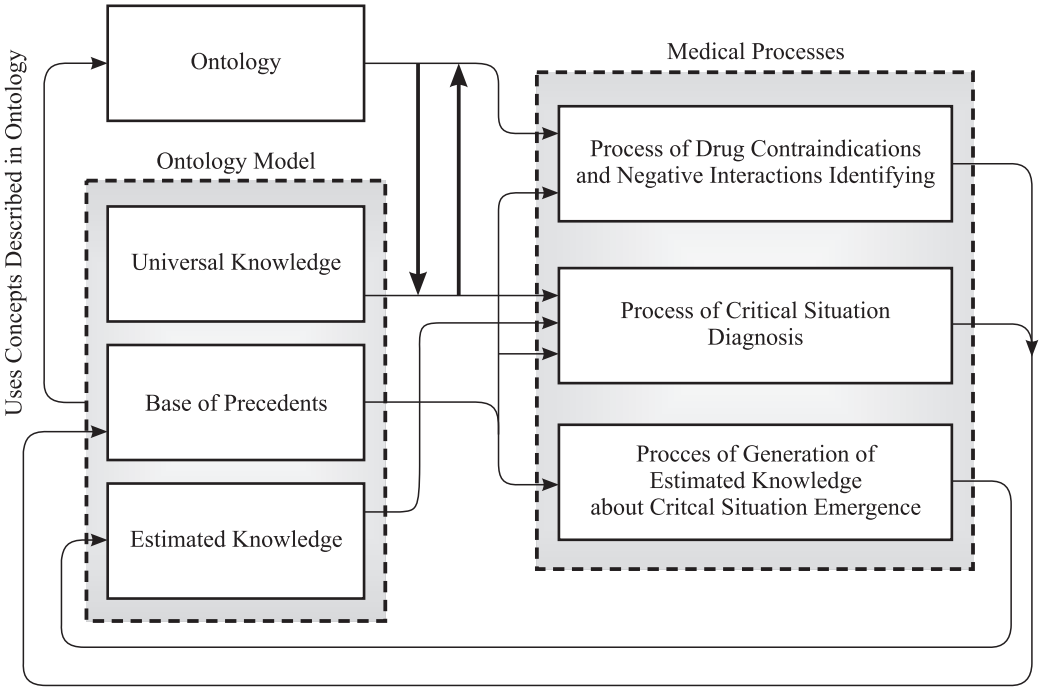

Fig. 1. *The structure of ontology model*

All links have several options of manifestation. Which of the options will take place in the situation depends on the anatomical and physiological characteristics of patient and the medical event occurred. Description of the negative drug interactions also refers to the general knowledge base. Negative drug interaction is presented as a cause-effect link where the causes are the use of several different drugs, and the consequence is a negative reaction.

Base of precedents

The base of precedents stores a lot of records of real patients. Each case record is presented as a precedent.

Let us introduce the concept of a formal precedent. Formal precedent is the description of a precedent in some formal language. It is a model containing a set of logical sentences that is true on that model. It describes the patient's condition during the disease.

The onset of symptoms, diseases or other events is recorded in the form of a logical statement where the predicate is the predicate that indicate an action, such as «Observed». The variables are appropriate terms of symptoms, diseases, and other concepts that reflect with the condition of patient.

The meaning of all symbols that are used as variables and predicates in logical sentences must be defined in ontology. Formally, logically precedent is described in the form of fragments of atomic diagrams of algebraic systems.

Base of probabilistic knowledge

Knowledge stored at the base of probabilistic knowledge generated by the set of precedents (case records of patients). It is generated using algorithms implemented in the functional part of system. In particular, the probabilistic knowledge base contains a set of hypotheses on the probability of patient's critical conditions or complications (Fig. 2).

FUNCTION PART OF PROGRAM SYSTEM MEDONTOMODEL

The functional part of the ontological model implements the algorithms of knowledge integration and new knowledge generation. It includes algorithms to detect the risks of critical conditions, finding drug contraindications and negative interactions, algorithms of probabilistic knowledge generation.

In the context of this work, we use the following definition of critical situation, critical states and complications. The critical situation is a situation in which there is a sharp deterioration of patient's condition or the risk of such deterioration is increased. In particular, it's an event of critical condition or complication.

Critical condition is an extreme degree of pathology, which requires artificial replacement or support of vital functions.

Complication is a pathological process joined to the main disease. It aggravates the typical course of the disease. This process is not due to the cause of disease, but the additional changes arising in the body in the course of disease.

Developed algorithms are aimed at minimization of the risk of critical situations. They function as follows. First, for all base of precedents (it consist of medical records of patients) an algorithm of generation of evaluating knowledge about the critical condition onset risk is used. The result of the algorithm is a set of hypotheses about the possible critical conditions. Then, for a given individual pa-

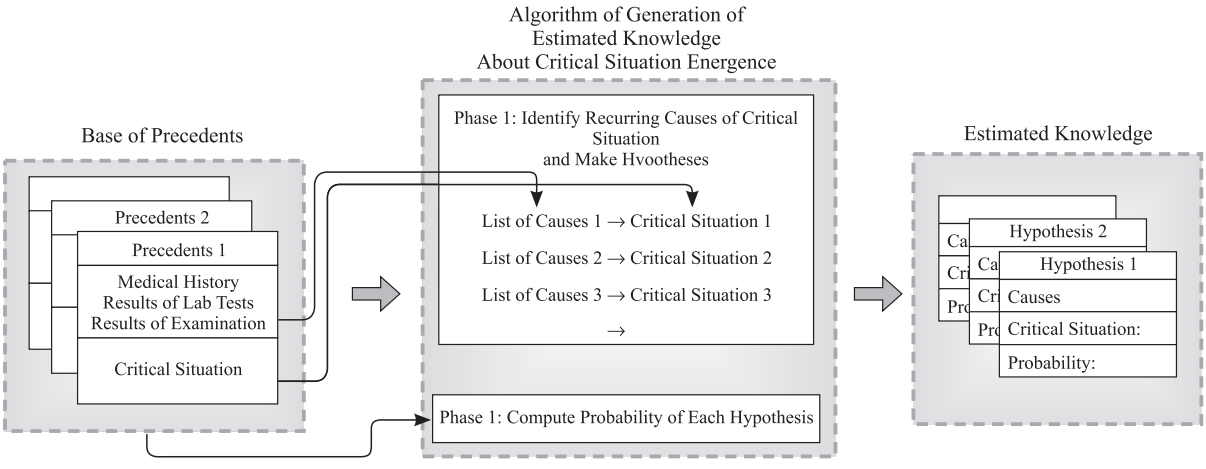

Fig. 2. *Refilling of the base of probabilistic knowledge*

tient's medical record the algorithm for identifying the risks of critical situations and algorithm for finding drug contraindications and negative interactions are applied. The results of these algorithms is a list of warnings to the doctor about potential negative effects of drug for the individual patient, a list of potential critical situations in this patient and, if necessary, a list of recommended further examination of the patient (Fig. 3).

Let us consider each of these algorithms in detail.

1) Algorithm of generation of evaluating knowledge about the critical condition onset risk.

The algorithm accepts for input a base of precedents, namely the medical records of different patients with critical situations set for them. The algorithm looks for repeated combinations of reasons for each critical situation and thus creates a hypothesis. Hypotheses can be positive (a critical situation occurs) and negative (a critical situation does not occur).

The output of algorithm is a set of hypotheses of cause and effect. For every critical situation, it describes a set of causes. A set of hypotheses forms a base of evaluation knowledge.

2) The algorithm for identifying the risks of critical situations.

This algorithm is based on the algorithm given in [16]. It defines a list of possible critical situations for a particular patient. In addition, algorithm recommends a list of additional surveys to find the risk of critical situations.

The algorithm uses a medical record of individual patient. For each event in the medical record a time of the event is indicated. Also, the algorithm uses ontological model and the base of probabilistic knowledge obtained after application of algorithm of generation of evaluation knowledge about the critical condition onset risks.

3) The algorithm for finding drug contraindications and negative interactions.

One of the most common causes of critical situations [6] and later mortality is prescribing contraindicative drugs to patient. In particular, the combination of drugs can be dangerous if it includes incompatible substances.

To prevent such cases we have developed an algorithm for finding drug contraindications and negative interactions.

Whenever a doctor prescribes a new medication to a patient, the algorithm checks the correctness of choice using the knowledge from ontology and ontological model.

For example, if contraindications read «liver disorder», the system concludes that the drug is also contraindicated to patients with hepatitis, cirrhosis

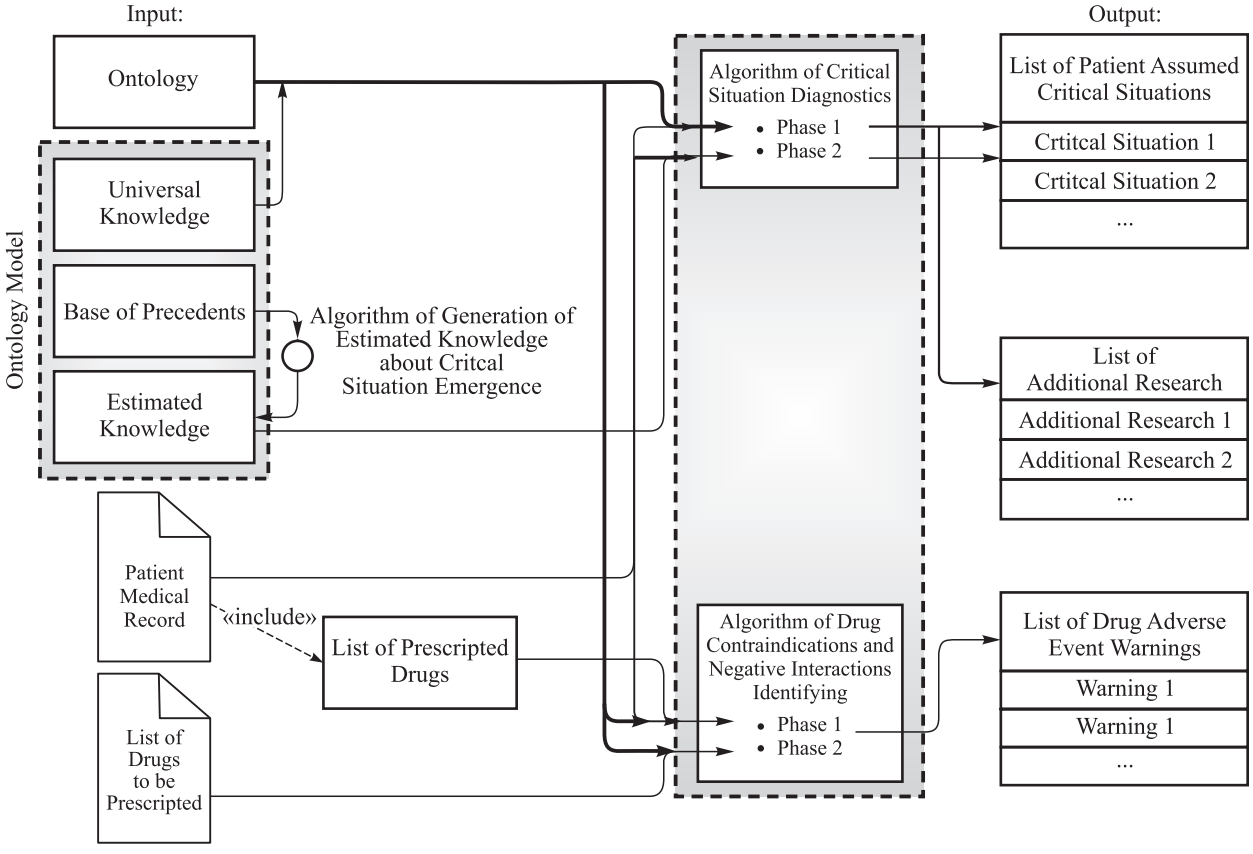

Fig. 3. *Functional part of the system*

and other, because hepatitis and cirrhosis are certain cases of liver disorder.

RESULTS

The software system MedOntoModel has been tested on clinical data – medical records of more than 250 patients. As a result, the system has revealed possibility of occurring of neurological and inflammatory complications in about half of the patients. On this basis, appropriate warnings have been issued for doctors.

Approximately in one fourth of medical records system could not accurately determine whether there was a probability of critical situations or not, and requested additional information. With additional information, these patients were identified for the probability of critical situations and appropriate warnings for physicians were given.

In all cases where the possibility of occurrence of critical situations was found, the actual existence of critical situation was confirmed by the information from the patient's medical record.

In particular, clinical data of patient with a preliminary diagnosis of «osteochondrosis of the lumbar spine» were entered into the system. There were patient personal information (date of birth, sex, etc.), characteristics of the patient's body (intolerance, height, weight, etc.), medical record, results of examination and blood tests among the entry data.

On the basis of knowledge about infectious endotoxicosis the system MedOntoModel has found symptoms of occurrence of post-operative complications in clinical data. This result has been confirmed by the presence of infectious endotoxicosis in the patient's medical record.

In some patient prescriptions the system found contraindicated drugs and drugs with a negative interaction of active ingredients. The system issued a list of warnings to physicians in form of enumeration of drugs and whether conflicting drug or patient's contraindications to it from the medical record.

With the help of a separate sample of patient medical records the system MedOntoModel generated hypotheses about the causes of neurological complications. Generated hypotheses were added to the estimated knowledge and were used in the following work of the system. In particular, the added knowledge was used to identify the risks of neurological complications that are not described in the general knowledge.

CONCLUSION

We present methods for developing ontologies and ontological models based on the four-level model of knowledge representation. The subject domain knowledge is represented on the following levels: ontology, general knowledge, specific knowledge (precedents) and estimated (probabilistic) knowledge. On the basis of this representation the ontological model of the «Spinal deformity and degenerative diseases of the spine» subject domain has been developed.

We have developed specific algorithms for identifying the risks of critical situations, finding drug contraindications and negative interactions. These algorithms have been implemented in the software system MedOntoModel. This system helps predict critical conditions of patients and provides recommendations for doctors. It has been tested on the data from medical records of patients with spinal deformity and degenerative diseases of the spine.

ACKNOWLEDGMENTS

The reported study was partially supported by RFBR, research project No. 14-07-00903-a.

REFERENCES

1. *Abas H., Yusof M., Noah S.* The application of ontology in a clinical decision support system for acute postoperative pain management // STAIR: Proc. Int. Conf. Semantic Technology and Information Retrieval. Putrajaya, 2011. 106–112.

2. *Artemyeva I.L.* Multilevel models of complex structured subject domains and their use in the development of the systems based on knowledge: abstract of thesis … doctor of technical sciences. Vladivostok, 2008. [In Russian].

3. *Chernyakhovskaya M.Yu.* Formation of observation database on the basis of medicine ontology // Informatika i sistemy upravleniya = Information science and control systems. 2009. (4). 198–200. [In Russian].

4. *Clinical* Decision Support Systems / Ed. Eta S. Berner. N. Y.: Springer, 2007.

5. *Denysenko S.V.* Diagnosis and prognosis of states in invitro fertilization based on the ontology knowledge // Zaporozhskiy meditinskiy zhurnal = Zaporozhye medical journal. 2014. 2. 137–140. [In Russian].

6. *FAERS* Reporting by Patient Outcomes by Year // U.S. Food and Drug Administration. URL: http://www.fda.gov/Drugs/GuidanceComplianceRegulatoryInformation/Surveillance/AdverseDrugEffects/ucm070461.htm (Accessed: 15.09.2015).

7. *Gribova V.V., Okun D.B., Chernyakhovskaya M.Yu.* Ontology and ontology model of «Medication treatment» domain // Informatika i sistemy upravleniya = Information science and control systems. 2015. (2). 70–79. [In Russian].

8. *Gribova V.V., Petryaeva M.V., Fedorischev L.A.* Formalization of examination method in ophthalmology for computer diagnostic simulators // High Technologies, Basic and Applied Researches in Physiology and Medicine: Abstr. III Int. Conf. St. Petersburg, 2012. 2. 191–195. [In Russian].

9. *Jeffery R., Iserman E., Haynes R.* Can computerized clinical decision support systems improve diabetes management? A systematic review and meta-analysis // Diabet. Med. 2013. 30. (6). 739–745.

10. *Jia P., Zhang P., Li H. et al.* Literature review on clinical decision support system reducing medical error // J. Evid. Based Med. 2014. 7. (3). 219–226.

11. *Kleschev A.S., Moskalenko F.M. Chernyakhovskaya M.Yu.* Ontology model of Medical diagnostics» domain. Part 1. Informal description and definition of basic terms // Nauchno-tekhnicheskaya informatsiya. Seriya 2 = Automatic Documentation and Mathematical Linguistics. Series 2. 2005. (12). 1–7. [In Russian].

12. *Kleschev A.S., Moskalenko F.M. Chernyakhovskaya M.Yu.* Ontology model of «Medical diagnostics» domain. Part 2. Formal description of causal links, reasons of feature values and reasons of diseases // Nauchno-tehnicheskaya informatsiya. Seriya 2 = Automatic Documentation and Mathematical Linguistics. Series 2. 2006. (2). 19–30. [In Russian].

13. *Kleschev A.S., Shalfeyeva E.A.* System analysis contents for intelligent activity automation at branch level // OSTIS-2014: Abstr. Int. conf. Minsk, 2014. 285–290.

14. *Makhasoeva O.G., Palchunov D.E.* Semi-automatic methods of construction of the atomic diagrams from natural language texts // Vestnik Novosibirskogo gosudartsvennogo universiteta. Seriya: Informatsionnye tekhnologii = Novosibirsk State University Journal of Information Technologies. 2014. 12. (2). 64–73. [In Russian].

15. *Mickan S., Tilson J., Atherton H. et al.* Evidence of effectiveness of health care professionals using handheld computers: A scoping review of systematic reviews // J. Med. Internet Res. 2013. 15. (10). e212.

16. *Moskalenko F.M.* Methods for solving the problem of medical diagnostics on the basis of a mathematical model of the subject domain: abstract of thesis … candidate of technical sciences. Vladivostok, 2010. [In Russian].

17. *Nuckols T., Smith-Spangler C., Morton S. et al.* The effectiveness of computerized order entry at reducing preventable adverse drug events and medication errors in hospital settings: a systematic review and meta-analysis // Syst. Rev. 2014. 3. (1). ID 56.

18. *Palchunov D.E.* Knowledge search and production: creation of new knowledge on the basis of natural language text analysis // Filosofiya nauki = Philosophy of Science. 2009. (4). 70–90. [In Russian].

19. *Palchunov D.E.* Solution for Information Retrieval Problem Based on Ontologies // Biznes-informatika = Business informatics. 2008. (1). 3–13. [In Russian].

20. *Palchunov D.E.* Virtual catalogue: the ontology-based technology for information retrieval // Knowledge Processing and Data Analysis: Coll. Sci. Art. Eds. K. Wolff, D. Palchunov, N. Zagoruiko, U. Andelfinger. Berlin; Heidelberg: Springer-Verlag, 2011. 164–183.

21. *Palchunov D.E., Stepanov P.A.* Use of model-theoretic methods of extraction of ontological knowledge in the domain of information security // Programmnaya inzheneriya = Program engineering. 2013. (11). 8–16. [In Russian].

22. *Palchunov D.E., Yakhyaeva G.E.* Fuzzy logics and fuzzy model theory // Algebra Logic. 2015. 54. (1). 74–80.

23. *Palchunov D.E., Yakhyaeva G.E., Hamutskaya A.A.* Software system RiskPanel for management of information risks // Programmnaya inzheneriya = Program engineering. 2011. (7). 29–36.

24. *Patent* N 2014619198 RF. Software system for building atomic diagram of model from natural language texts / Makhasoyeva O.G., Palchunov D.E.; published 11.07.2014.

25. *Phalakornkule K., Jones J., Finnell J.* Ontological model for CDSS in knee injury management // Universal Access in Human-Computer Interaction. Applications and Services for Quality of Life: Coll. Sci. Art. Eds. C. Stephanidis, M. Antona. Berlin; Heidelberg: Springer-Verlag, 2013. 526–535.

26. *Seo D., Jung H., Sung W. et al.* Development of Korean spine database and ontology for realizing e-Spine // Cluster Comput. 2014. 17. (3). 1069–1080.

РАЗРАБОТКА АВТОМАТИЗИРОВАННЫХ МЕТОДОВ ПРЕДУПРЕЖДЕНИЯ РИСКОВ ВОЗНИКНОВЕНИЯ КРИТИЧЕСКИХ СОСТОЯНИЙ, ОСНОВАННЫХ НА АНАЛИЗЕ ЗНАНИЙ, ИЗВЛЕЧЁННЫХ ИЗ ИСТОРИЙ БОЛЕЗНЕЙ ПАЦИЕНТОВ

Чимит Антонович НАЙДАНОВ[1], Дмитрий Евгеньевич ПАЛЬЧУНОВ[1,2], Полина Андреевна САЗОНОВА[1]

[1] Новосибирский государственный университет
630090, г. Новосибирск, ул. Пирогова, д. 2.

[2] Институт математики им. С. Л. Соболева СО РАН
630090, г. Новосибирск, пр. Академика Коптюга, д. 4.

Статья посвящена методам разработки онтологий и онтологических моделей предметных областей в медицине. Предложена четырёхуровневая модель представления знаний. На основе онтологических методов представления знаний разрабатываются алгоритмы предупреждения рисков возникновения у пациентов критических состояний и осложнений. Работа основана на теоретико-модельном подходе к представлению медицинских знаний. Используется представление знаний при помощи фрагментов атомарных диаграмм алгебраических систем, а также представление знаний о пациентах в виде булевозначной прецедентной модели. Разработаны онтология и онтологическая модель предметной области «Деформации позвоночника и дегенеративные заболевания позвоночника». Онтологическая модель содержит универсальные знания, истинные для всех пациентов, данные о конкретных пациентах и оценочные знания, служащие для выдачи рекомендаций врачу. Оценочные знания являются вероятностными гипотезами о возможности возникновения критического состояния или осложнения у пациента. Разработан алгоритм порождения оценочных знаний на основе анализа историй болезней. Реализована программная система, предназначенная для выдачи рекомендаций по предупреждению и уменьшению риска возникновения критических состояний и осложнений у пациентов. Программная система была протестирована на данных о пациентах, имеющих деформации позвоночника и дегенеративные заболевания позвоночника.

Ключевые слова: управление рисками, критические состояния, осложнения, онтологическая модель, прецедентная модель, булевозначная модель, деформации позвоночника, дегенеративные заболевания позвоночника.

Найданов Ч.А. *– аспирант, e-mail: naydanov.fit@yandex.ru*
Пальчунов Д.Е. *– д.ф.-м.н., в.н.с., e-mail: palch@math.nsc.ru*
Сазонова П.А. *– магистрант, e-mail: psazonova@gmail.com*

УДК: 612.13.001.573: 616.13.002.2-007.64-001.5

PERSONALIZED MATHEMATICAL MODELING OF CEREBRAL ARTERIAL ANEURYSMS

Aleksandr Kancherovich KHE[1,2], Aleksandr Pavlovich CHUPAKHIN[1,2], Aleksandr Aleksandrovich CHEREVKO[1,2], Daniil Vasilevich PARSHIN[1], Aleksey Leonidovich KRIVOSHAPKIN[3], Kirill Yurevich ORLOV[3]

[1] *Lavrentyev Institute of Hydrodynamics*
630090, Novosibirsk, Lavrentyev av., 15

[2] *Novosibirsk State University*
630090, Novosibirsk, Pirogov str., 2

[3] *Meshalkin Novosibirsk Research Institute of Circulation Pathology*
630055, Novosibirsk, Rechkunovskaya str., 15

The mathematical and computational framework for personalized modeling of the cerebral hemodynamics in the presence of arterial aneurysms has been described. As an example we study nonlocal hydrodynamic properties of cerebral arterial aneurysms. The area of the vessel aneurysm influence on the surrounding blood flow and the changes caused by pressure increase and decrease have been determined using numerical simulations, as well as the flow features in the case of multiple aneurysms presence have been investigated. The personalized clinical data obtained during intraoperative endovascular measurements have been used for computations.

Keywords: hemodynamics, arterial aneurysm, aneurysm rupture factor, liquid 3D-flow modeling.

Cerebral aneurysms are local enlargement of the arterial wall due to the wall damage and weakening. In most cases aneurysms occur in the places of anatomic variations and pathological conditions or high-flow arteriovenous malformations which cause locally increased flow in the cerebral circulation, and, at points of flow bifurcation [7]. Aneurysm is one of the most frequent and dangerous diseases of the cerebral arteries. The most serious consequences of the presence of the aneurysm are their rupture and intracranial hemorrhage which could be lethal. According to statistics, up to 5 % of all deceased people being in autopsy have cerebral aneurysms. Treatment of aneurysms is a challenging task, as often there are no visible symptoms of aneurysms before its rupture. At the same time, treatment carries a risk which often exceeds a risk of having an aneurysm rupture on the early stage. So, at the moment when neurosurgeon recognizes that patient has aneurysm, he meets a problem of determining the time when it is better to treat the patient. To start a surgery on time, a surgeon must know how aneurysm is growing and when it will rupture. Despite an aneurysm is a frequent disease, mechanisms of its formation, evolution, and rupture are not well understood yet. Thus, the planning of an effective surgery is a very difficult task for neurosurgeons.

There are several factors involved in the aneurysm formation, growth, and rupture, such as histological, hemodynamic, and genetic factors. Modeling of aneurysms is a complex multi-parametric problem. There are several theories of aneurysm

Khe A.K. *– candidate of physical mathematical sciences, senior researcher of laboratory for differential equation, e-mail: alekhe@hydro.nsc.ru*
Chupakhin A.P. *– doctor of physical mathematical sciences, head of laboratory for differential equation*
Cherevko A.A. *– candidate of physical mathematical sciences, senior researcher of laboratory for differential equation*
Parshin D.V. *– candidate of physical mathematical sciences, junior researcher of laboratory for differential equation, e-mail: danilo.skiman@gmail.com*
Krivoshapkin A.L. *– corresponding member of RAS, chief researcher, neurosurgeon*
Orlov K.Yu. *– candidate of medical sciences, neurosurgeon, head of the center for angioneurology and neurosurgery*

formation and growth. For example, in [7] it is stated that the main factor influencing a dynamics of the aneurysm is the wall shear stress (WSS) provoked by the blood flow. It is considered that endothelium could sense WSS and effect the wall structure. At the same time, Sforza et al. doesn't assert that it is exactly the WSS increase that leads to aneurysm, or to its growth, or rupture. According to them, there are two main hypothesis: «low-flow» and «high-flow» theories (low and high velocities of the blood flow). We are not able to decide which of these theories is correct, as each of them has its pros and cons.

Treating an aneurysm requires a surgery. There are several types of endovascular surgery that could be used. The main idea of such treatment is to cut off an aneurysm from the blood flow by an introduction of the agents provoking thrombosis inside aneurysm, or, in other words, to do embolisation of the aneurysm.

The main difficulty of the endovascular treatment is coming from a wide-neck aneurysm, as it is often too difficult to occlude an entire aneurysm sac. In that case, neurosurgeons usually resort to put a stent either to redirect flow and reduce cross-neck flow into the aneurysm or to bring a vessel geometry to its initial state. Usually neurosurgeons don't try to coil such aneurysms because of the risk of the coil falling out after a surgery even with the stent support.

In our previous papers [8, 9] we studied local characteristics of flow in the vicinity of aneurysm (both hydrodynamic and mechanical parameters). Our focus was on the analysis of the main hemodynamic parameters and elastic stresses for the clinical data analysis of a specific patient. To understand how the fluid flows in the aneurysmal sac and how the flow changes after a surgery, we examined streamlines' behavior. Furthermore, we examined pressure distribution, its gradient, and wall shear stresses.

In this work our goal is to determine how far the aneurysm affects the hemodynamics in the circulation network. We carried out several numerical experiments for different case studies: effect of the presence of the aneurysm, influence of the pressure change, presence of the multiple aneurysms.

Real-world data play crucial role in mathematical modeling and it is the main ingredient for verification and justification of the theory being developed. Designing an experimental setup and a measurement system is a challenging task in engineering sciences. And it is even more difficult in natural and medical sciences. In this work we describe a measurement system we use in the framework of mathematical modeling of cerebral hemodynamics. Clinical data are collected during endovascular neurosurgical treatments of cerebral blood vessel diseases (arteriovenous malformations or aneurysms).

A widely used method to assess cerebral blood flow is the transcranial Doppler ultrasonography [3]. However it is applicable only for relatively large vessels–carotid arteries and their first level branches: a., m., and p. cerebral arteries. Moreover this method does not allow one to measure the pressure. In our work we use endovascular flow and pressure measurement system Volcano ComboMap (Volcano Corp., USA). Measurements are performed using a 0.36 mm diameter wire ComboWire. In Fig. 1, 2 an example of the blood flow monitoring is shown.

Using analog-to-digital convertor we collect the data being measured in real time. The data is being processed and displayed with a home-made software (Fig. 3). The software displays real-time velocity–pressure and flow rate–energy flow rate diagrams which can be used to evaluate the operation [0, 4, 5].

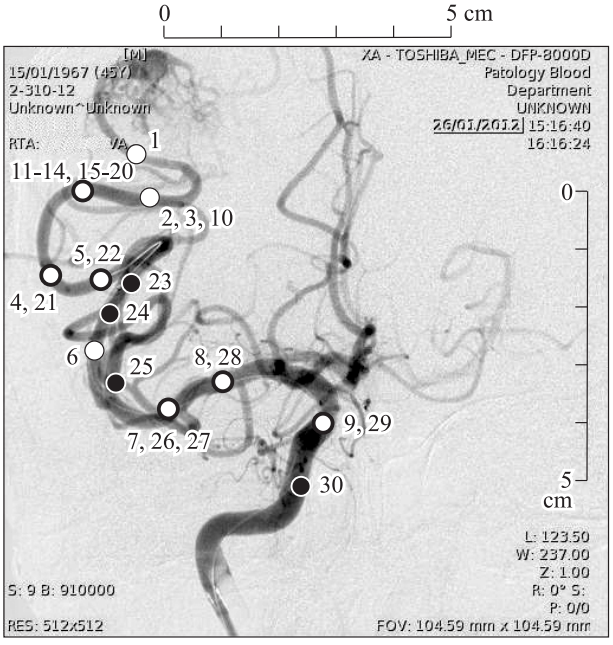

Fig. 1. *Measurement locations*

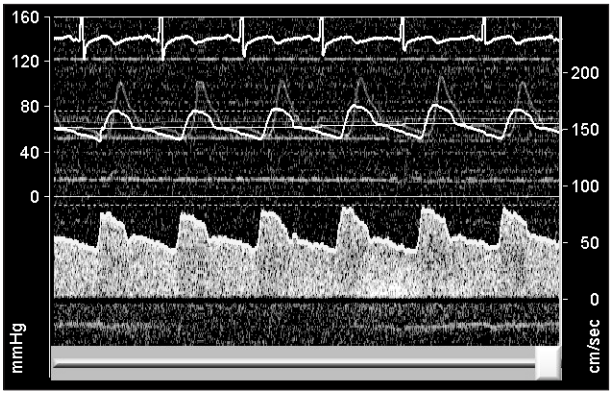

Fig. 2. *ComboMap screen showing pressure and velocity*

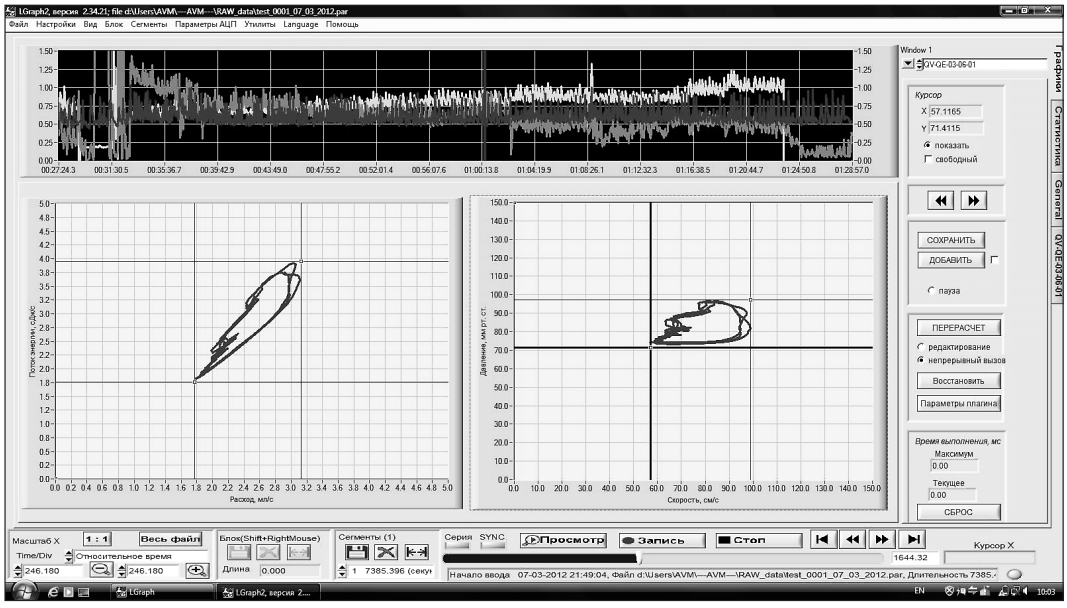

Fig. 3. *Clinical data acquisition and real-time diagrams*

Data post-processing includes noise filtering, extraction of the signal segments and mapping it to a measurement location. After that, the data can be used for patient-specific numerical modeling.

The measurement system presented in this work can be used as an additional instrument used in endovascular surgery for assessment and monitoring of the operation [6].

MATERIAL AND METHODS

In this work we perform nonstationary 3D numerical simulations of relatively large cerebral arterial circulation areas with aneurysms (Fig. 4). Computations are carried out at the Informational and Computational Center of the Novosibirsk State University using the ANSYS commercial software. Hydrodynamic properties of the flow are simulated using the ANSYS CFX solver, while the deformations and stresses in the vessel wall are computed with the ANSYS Mechanical.

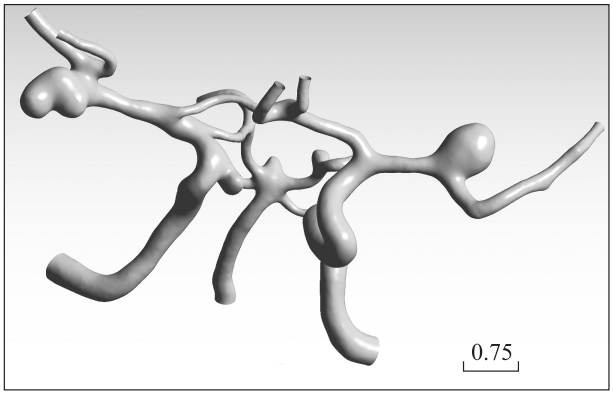

Fig. 4*. Computational geometry with multiple aneurysms*

For our simulations we use patient specific MRI and CT data obtained at the Meshalkin Novosibirsk Research Institute of Circulation Pathology and the Burdenko Research Institute of Neurosurgery. The patients underwent minimally invasive (endovascular) or open surgery. To reconstruct the flow domains preoperative scans are used. The segmentation was performed with ITK-SNAP [10] and VMTK [1].

Blood flow parameters (velocity and pressure) are taken from intraoperative monitoring with Volcano ComboMap endovascular blood flow measurement system [0].

When modeling such complex and multifactorial objects one always has to find a balance between a mathematical model describing the phenomenon the most accurately, however being computationally very expensive, and a simpler one, but describing the main features of the case. In our work we consider blood as a viscous incompressible Newtonian fluid governed by the Navier–Stokes equations. The vessel wall is considered a linearly elastic isotropic material. However the elasticity parameters of the healthy vessel wall and the one of the aneurysms can be different.

RESULTS

In our first series of numerical simulations we studied the effect of the presence of the aneurysm of the flow. The «treatment» of the aneurysm was performed numerically with an appropriate software surface editor. The calculations show the localness of such an influence. The influence area spreads out no far than several diameters of the aneurysm. In Fig. 5 a comparison of the pressure distribution is

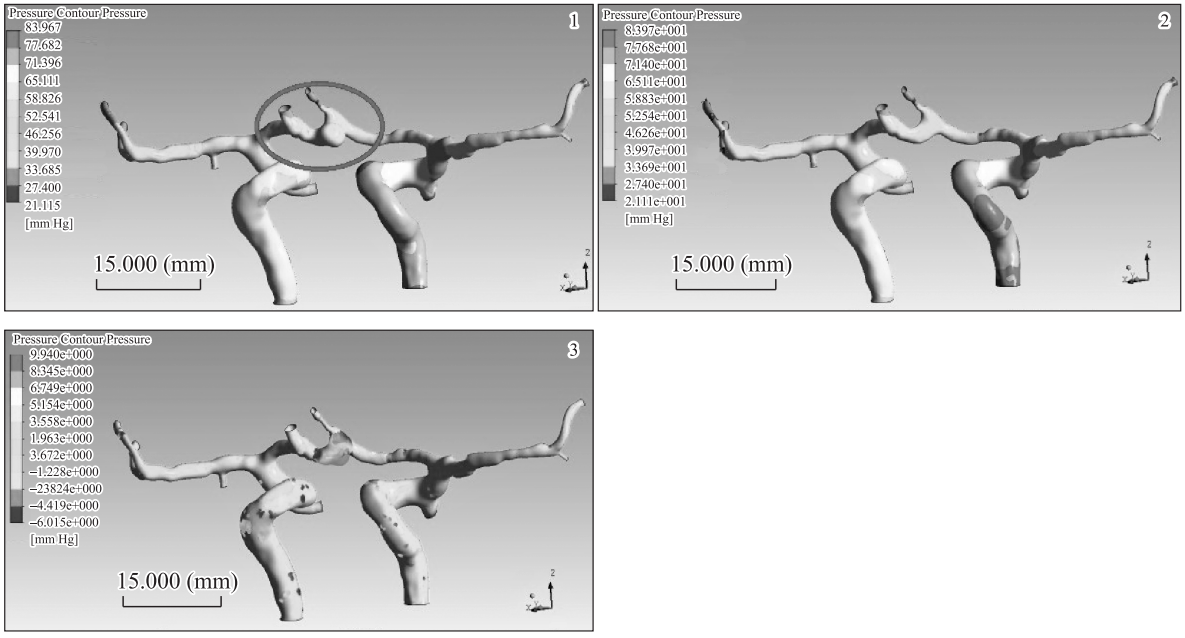

Fig. 5. *Comparison of the pressure distribution on the vessel walls*

shown: 1 – original configuration with aneurysm, 2 – with aneurysm numerically removed, 3 – the pressure difference between the two calculation (where applicable) is shown.

In the second series of the experiments we gradually increased and decreased pressure at the outlet of the flow domain. These changes can be considered as hypertension (high blood pressure) and hypotension (low blood pressure). In Fig. 6 a diagram of relative change in velocity and pressure is shown. The computations show localness of the changes in flow structure and linear quantitative changes of flow parameters.

In the last series of our work we studied hemodynamic properties of the blood flow in a vessel net with multiple aneurysms. The purpose of these simulations was to determine if there is an influence of the aneurysms on each other. An example of the numerical simulations is shown in Fig. 7.

ACKNOWLEDGMENTS

This work was financially supported by the Russian Foundation for Basic Research (Project No. 14-01-00036).

REFERENCES

1. *Antiga L., Steinman D.* The vascular modeling toolkit. URL: http://www.vmtk.org/

2. *Chupakhin A.P., Cherevko A.A., Khe A.K. et al.* Measurement and analysis of cerebral hemodynamic parameters in the presence of brain vascular anomalies // Patologiya krovoobrashcheniya i kardiokhirurgiya [Circulation Pathology and Cardiac Surgery]. 2012. 4. 27–31. [In Russian].

3. *Gaidar B.V., Semenyutin V.B., Parfenov V.E., Svistov D.V.* Transcranial Doppler ultrasonography in

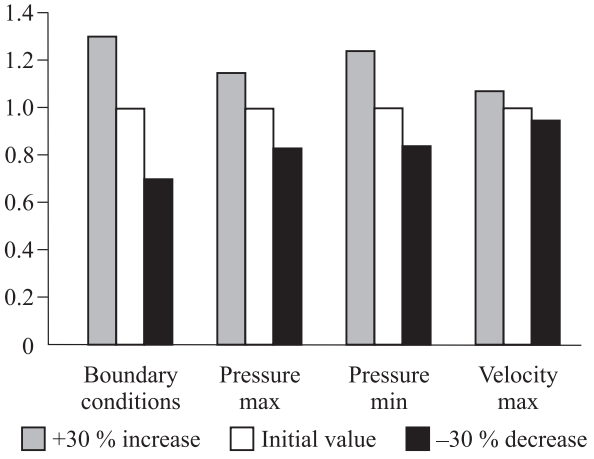

Fig. 6. *Relative velocity and pressure changes*

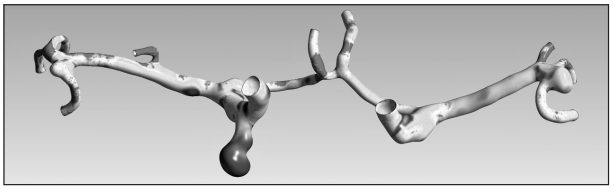

Fig. 7. *Wall shear stress*

neurosurgery. Saint-Petersburg: ELBI-SPb, 2008. 288 p. [In Russian].

4. *Krivoshapkin A.L., Panarin V.A., Orlov K.Yu. et al.* Hemodynamic hemorrhage prevention algorithm during cerebral arteriovenous malformations embolization. Byulleten' Sibirskogo otdeleniya Rossiyskoy akademii meditsinskikh nauk [Bulletin of Siberian Branch of Russian academy of medical sciences]. 2013. (6). 65–73. [In Russian].

5. *Panarin V.A., Orlov K.Yu., Krivoshapkin A.L. et al.* Hydrodynamic calculations for embolization strategy of cerebral arteriovenous malformations with fistulous component. Patologiya krovoobrashcheniya i kardiokhirurgiya [Circulation Pathology and Cardiac Surgery]. 2012. 3. 39–43. [In Russian].

6. *Patent* 2511235 RF. Method for intraoperative Doppler control of radicality of arteriovenous malformation embolisation / Orlov K.Yu., Panarin V.A., Berestov V.V. et al; published 10.04.2014. [In Russian].

7. *Sforza D.M., Putman C.M., Cebral J.R.* Hemodynamics of Cerebral Aneurysms // Annu Rev Fluid Mech. 2009. 41. 91–107.

8. *Vorobtsova N.A., Yanchenko A.A., Cherevko A.A. et al*. Modelling of cerebral aneurysm parameters under stent installation // Rus. J. Numer. Anal. Math. Model. 2013. 28. 505–516.

9. *Yanchenko A.A., Cherevko A.A., Chupakhin A.P. et al.* Nonstationary hemodynamics modelling in a cerebral aneurysm of a blood vessel // Rus. J. Numer. Anal. Math. Model. 2014. 29. 307–317.

10. *Yushkevich P.A., Piven J., Hazlett H.C. et al.* User-guided 3D active contour segmentation of anatomical structures: Significantly improved efficiency and reliability // Neuroimage. 2006. 31. (3). 1116–1128.

ПЕРСОНАЛИЗИРОВАННОЕ МАТЕМАТИЧЕСКОЕ МОДЕЛИРОВАНИЕ ЦЕРЕБРАЛЬНЫХ АРТЕРИАЛЬНЫХ АНЕВРИЗМ

Александр Канчерович ХЕ[1,2], Александр Павлович ЧУПАХИН[1,2], Александр Александрович ЧЕРЕВКО[1,2], Даниил Васильевич ПАРШИН[1], Алексей Леонидович КРИВОШАПКИН[3], Кирилл Юрьевич ОРЛОВ[3]

[1] *Институт гидродинамики им. М.А. Лаврентьева СО РАН*
630090, г. Новосибирск, пр. Академика Лаврентьева, 15

[2] *Новосибирский государственный университет*
630090, г. Новосибирск, ул. Пирогова, 2.

[3] *Новосибирский НИИ патологии кровообращения им. Е.Н. Мешалкина*
630055, г. Новосибирск, ул. Речкуновская, 15

В работе представлен математический и компьютерный подход к моделированию церебральной гемодинамики при наличии артериальной аневризмы. С использованием численного моделирования определяются: воздействие аневризмы на окружающий ее поток крови, изменения, обусловленные ростом или падением давления в сосуде, а также исследуются характеристики потока крови в случае наличия множественных аневризм. Для численных расчетов были использованы клинические данные, собранные в ходе проведения эндоваскулярного вмешательства.

Ключевые слова: гемодинамика, артериальная аневризма, критерий разрыва аневризмы, моделирование трехмерного потока жидкости.

Хе А.К. *– к.ф.-м.н., лаборатория дифференциальных уравнений, старший научный сотрудник, e-mail: alekhe@hydro.nsc.ru*
Чупахин А.П. *– д.ф.-м.н., лаборатория дифференциальных уравнений, заведующий лабораторией*
Черевко А.А. *– к.ф.-м.н., лаборатория дифференциальных уравнений, старший научный сотрудник*
Паршин Д.В. *– к.ф.-м.н., лаборатория дифференциальных уравнений, младший научный сотрудник, e-mail: danilo.skiman@gmail.com*
Кривошапкин А.Л. *– чл.-корр. РАН, д.м.н., главный научный сотрудник, врач-нейрохирургч*
Орлов К.Ю. *– к.м.н., врач-нейрохирург, руководитель Центра ангионеврологии и нейрохирургии*